

University of Southampton Research Repository
ePrints Soton

Copyright © and Moral Rights for this thesis are retained by the author and/or other copyright owners. A copy can be downloaded for personal non-commercial research or study, without prior permission or charge. This thesis cannot be reproduced or quoted extensively from without first obtaining permission in writing from the copyright holder/s. The content must not be changed in any way or sold commercially in any format or medium without the formal permission of the copyright holders.

When referring to this work, full bibliographic details including the author, title, awarding institution and date of the thesis must be given e.g.

AUTHOR (year of submission) "Full thesis title", University of Southampton, name of the University School or Department, PhD Thesis, pagination

UNIVERSITY OF SOUTHAMPTON

PHYSICAL CONSTRAINTS ON PHYTOPLANKTON IN ESTUARIES

AND SHALLOW COASTAL WATERS

using management information, the different types of information from the supply to the demand markets, specific where the production was located in the environment of production, transportation, and distribution in a multi-level decentralized environment. The major and minor regional markets are distributed in a number of locations, both rural and urban.

MARY LOUISE LAURIA

During our 12-hour flights, passengers reported seeing bright meteors and observed several meteoroids passing within the next few minutes of each other. One fellow was struck by a falling meteorite which he took out of his pocket. He was very lucky. During the 12 hours of the trans-Pacific flight, 100 meteors were sighted with certainty and 100 more were suspected.

The *mesocarp* (that is, the middle layer) of the fruit is composed of a mass of small, rounded, yellowish-green, fleshy, *mesocarp cells* (Fig. 10), which are separated by a thin, yellowish, *mesocarp tissue* (Fig. 11).

A thesis submitted to the Faculty of Science in fulfilment of the requirements for the

Degree of Doctor of Philosophy.

contrasting properties of field settings in the regulation of these processes and their effects on coastal and shelf waters through time and space. **SCOTTISH OCEANOGRAPHY CENTRE**

SOUTHAMPTON OCEANOGRAPHY CENTRE

SEPTEMBER 1998

SEPTEMBER 1998

ABSTRACT

Faculty of Science

Oceanography

Doctor of Philosophy**PHYSICAL CONSTRAINTS ON PHYTOPLANKTON IN
ESTUARIES AND SHALLOW COASTAL WATERS**

by

Mary Louise Lauria

Highly dynamic aquatic systems have often been reported to support actively growing populations of phytoplankton. The partially-mixed, macrotidal, temperate estuary Southampton Water is no exception, with reports of frequent temporal patterns of spring and summer maxima in algal biomass. During this study, the close coupling between the estuarine hydrology and the phytoplankton community was confirmed by the results from an intensive sampling strategy, spanning various temporal scales. Using high frequency data, collected from acoustic Doppler current profilers (ADCP) and CTDs, the physical mixing processes within the estuary were determined and combined with high resolution phytoplankton species data to assess the physical pressures on the microalgal community. Initial surveys were conducted to provide snapshots of the estuary during productive periods, followed by more intensive, longer term monitoring to observe population growth and succession.

Through seasonal investigations, the aggregation of algal biomass (quantified by chlorophyll *a* concentration) at differing vertical heights in the water column was realised. On closer examination using microscopic identification, the different vertical profiles were shown to be due to phytoplankton succession from the spring to the summer months. Diatoms (Rhizosolenia delicatula) proliferated in the spring, where the population was localised in the near-bottom layers, whilst the summer bloom was dominated by autotrophic dinoflagellates (Prorocentrum micans and Peridinium trochoideum), manifesting in a sub-surface chlorophyll *a* maximum. The vertical position of diatom species, both pelagic and benthic, suggested no dependence on incident irradiance, but seemed solely governed by current velocities, shear and wind mixing events. Other passive constituents of the water column, such as suspended particulate matter, were also closely coupled with boundary shear and followed regular patterns of re-suspension similar to those shown by the diatom community. In the summer, apparent active vertical migration was observed for several species of dinoflagellate. Whilst this apparent migration was closely linked to the incident irradiance, the extent and timing of migration was highly dependent on the tidal state and the water column stability.

During one 25 hour Eulerian investigation, apparent positive vertical migration was observed in several dinoflagellate species, where the controlling factor was incident irradiance. Dinoflagellates were observed to descend during the dark periods when the water column was stable. However, the vertical distribution of the autotrophic ciliate Mesodinium rubrum suggested that migrations into the surface waters were linked with periods of water column stability and not triggered by surface irradiance.

The unique tidal régime that governs the physical mixing processes in Southampton Water translates into periods of stability separated in time by intermittent turbulence. This periodic stability within the water column during reduced tidal forcings permitted the surface aggregation of dinoflagellates, which became homogeneously distributed when turbulence intensified during the ebb and flood currents. Diatoms, conversely, relied on vertical mixing to enter the surface layers of the water column, and aggregated in the lower layers during times of water column stability. Data from the seasonal surveys suggested that diatoms and dinoflagellates were able to co-exist during the summer by utilising contrasting properties of tidal mixing to develop and reside within this partially mixed environment. The segregation of these two phytoplankton groups was not apparent from the chlorophyll concentrations alone, and was only made evident through the high resolution phytoplankton sampling through both time and space.

The close coupling between the phytoplankton community and physical forcings were also investigated in the usually well-mixed southern North Sea. During a 12 hour Lagrangian survey, the stabilising effect of the Rhine region of freshwater influence (ROFI) was recognised and provided the temporary stability necessary for apparent dinoflagellate (Prorocentrum micans and Gonyaulax sp) migration. Associated solely with this lower salinity plume was the diatom Rhizosolenia styliformis, which was not detected during other times of the survey. Very small changes in total algal biomass were detected through the use of chlorophyll *a* determinations (chlorophyll *a* < 2 mg m⁻³). The intermittency of the mixing forces proved to be an important physical characteristic which defines the species and distribution of the phytoplankton community.

In memory

ACKNOWLEDGEMENTS

We're always told we're on our own doing a PhD, it's not true. At the end of the day your PhD is not really your own, but a challenge aided by so many. Now that I have the chance to thank all those involved in 'mine', I apologise in advance to anyone I fail to mention.

I am indebted to my supervisor Duncan Purdie for giving me the opportunity to undertake a PhD within the Department. I am grateful not only for his advice throughout my research but also for the support through those unexpected moments. My gratitude also extends to the N.E.R.C. who not only provided my funding for three years, but gave me the opportunity to attend overseas courses and conferences. Thanks also to those I worked with during the *RV Challenger* cruises in the North Sea (*LOIS* and *ASGAMAGE*).

An enormous thank you to Paul Hardisty and to all at Komex, who not only employed me (!), but have also encouraged and supported me to finish this thesis. Particular thanks to Trudi James; and Simon Firth, Pat Monks and Sara Wright.

Advice (and distractions) were readily available from many within the Department of Oceanography, particularly from Simon Boxall, Dave Burden, Julia Cheftel, Margot Cronin, Patrick Holligan, Don Hutchinson, Greg Lane-Serff, Emma Matthey, Rhu Nash, Alex Nimmo-Smith, Debbie Oppenheim, Silke Severmann, Jill Schwarz, Amanda Tyler, Lauretta Wall and Paul Wright.

I'd especially like to thank Pete (Shaw) and Jen for the many discussions/dinners and drinks; Keith Weston for the ridiculous drinking games, acid jazz and for teaching me all I know about subculturing; Jonathan Sharples, for the encouragement and support; and Cathy Lucas, for letting me win (sometimes) at squash and for lots of support and friendship.

To my PhD buds- where do I begin? Thanks for the occasional distractions when we all deserved (?) a break; for the dinners, the music, the talking, the blading, the companionship, the jokes, the running, the coffee breaks, the Lagavulin and the cycling. To *Coniston*, Leonie, Jimmy, Phillippeee, Antonio, - thank you.

My gratitude extends to many treasured buds, of whom I've had the great fortune of knowing for many years and who have always been ready to make me get on with things. Thanks particularly to my travelling chums Debs and Liz, for encouraging words and making me continue; to Nikki and Al, for many laughs and hangovers; to Robert for much fun and encouragement; and to Ju, March, Mads, Mel and Jonnie - may many years of fun, skiing (boarding!) and friendship continue.

Finally, I'd like to thank my parents, for their continuous encouragement, love and for always being there -no matter what; my brother Paul, for always making me laugh and for taking the rap as the younger sibling (!); Uncle J, for endless tolerance and support.; and to '*Mairn*', who always knows the answer, has the best advice, and who's strength and love are endless.

TABLE OF CONTENTS

1. General Introduction	1
1.1 Oceanographic Scale	1
1.2 Descriptive Turbulence	2
1.3 Bio-Physical Coupling	3
1.4 Phytoplankton Cell Size	7
1.5 Sinking of Phytoplankton Cells	7
1.6 Phytoplankton Motility	8
1.7 Biological Effects Of Turbulence	10
1.7.1 General Theories: Indirect Effects	10
1.7.2 General Theories: Direct Effects	13
1.8 Turbulent Mixing in Estuaries	17
1.9 Coastal Phytoplankton Dynamics	19
1.10 Research Objectives	22
2. Methodology	23
2.1 General Sampling Strategy for Southampton Water	23
2.2 Instrument Specifications	23
2.2.1 Conductivity Temperature Density Sensor (CTD)	23
2.2.2 Fluorometer (Chelsea Instruments, Aquatracka III)	24
2.2.3 Transmissometer (Seatech, 25cm pathlength)	24
2.2.4 Acoustic Doppler Current Profiler (ADCP)	25
2.2.5 NBA current profiler	25
2.2.6 Li-COR Cosine Irradiance Sensor	26
2.3 Laboratory Analyses and Instrument Calibration	26
2.3.1 Chlorophyll a Determination	26
2.3.2 Total Suspended Particulate Matter	26
2.3.3 Current Velocity	27
2.3.4 Attenuation Coefficient	27
2.3.5 Phytoplankton Preservation, Identification and Enumeration	28
2.3.6 Data Manipulation and Plotting	29
2.4 Laboratory Experiments	29
2.4.1 Subculturing Techniques	29
2.5 Growth Rate Experiments	30
2.5.1 <i>Amphidinium carterae</i> (Small Volume)	30
2.5.2 <i>Rhizosolenia delicatula</i> (Small Volume)	31
2.5.3 <i>A. carterae</i> (Large Volume)	31
2.5.4 <i>R. delicatula</i> (Large Volume)	31
3. Southampton Water	32
3.1 General Introduction to Southampton Water	32
3.1.1 Phytoplankton Populations in Southampton Water	36
3.1.1.1 Spring-Neap Forcings	36

3.1.1.2 Recurrence of Red Tides and Flushing Rates	40
3.1.2 Summary	41
3.2 Horizontal Studies in Southampton Water	45
3.2.1 Sampling Strategy	45
3.2.2 Results	49
3.2.2.1 Along Estuary Transects	49
3.2.3 Discussion	57
3.2.3.1 Current Structure during a Neap Tide	57
3.2.3.2 Suspended Particulate Matter	58
3.2.3.3 Phytoplankton Population Dynamics	60
3.2.3.4 Phytoplankton Speciation	60
3.2.4 Conclusions	63
3.3 Seasonal Differences in the Vertical Distribution of Phytoplankton Populations in Southampton Water	64
3.3.1 Sampling Strategy	64
3.3.2 Results May 1995	66
3.3.2.1 Physical Structure	66
3.3.2.2 Phytoplankton Dynamics and Speciation	67
3.3.3 Results August 1995	71
3.3.3.1 Physical Parameters	71
3.3.3.2 Phytoplankton Dynamics and Speciation	72
3.3.4 Discussion	76
3.3.4.1 Tidal currents and SPM concentration	76
3.3.4.2 Phytoplankton Distribution	76
3.3.5 Conclusions	80
3.4 25 Hour Eulerian Survey in Southampton Water	81
3.4.1 Sampling Strategy	81
3.4.2 Results	82
3.4.2.1 CTD Data	82
3.4.2.2 ADCP Data	85
3.4.2.3 Irradiance PAR	88
3.4.2.4 Phytoplankton Dynamics	88
3.4.3 Discussion	95
3.4.3.1 CTD Data	95
3.4.3.2 Wind Driven Mixing	96
3.4.3.3 Estuarine Circulation	97
3.4.3.4 SPM Flux	98
3.4.3.5 Photosynthetic Available Radiation (PAR)	99
3.4.3.6 Phytoplankton Community	100
3.4.4 Conclusions	103
3.5 Spring-Neap Tidal Cycle: Physical Constraints on Phytoplankton Growth and Distribution.	104
3.5.1 Introduction	104
3.5.2 Sampling Strategy	104
3.5.3 Results	105
3.5.3.1 Current Velocity	105
3.5.3.2 CTD Data	108
3.5.3.3 SPM and Irradiance	108
3.5.3.4 Phytoplankton Dynamics	114
3.5.4 Discussion	120
3.5.4.1 Physical Consequences of a Spring-Neap Cycle	120
3.5.4.2 SPM Fluctuations over a Spring-Neap Cycle	123
3.5.4.3 Biological Consequences from Spring-Neap Forcings	125
3.5.5 Conclusions	129
3.6 General Conclusions from Southampton Water	130

4. North Sea	131
4.1 Introduction	131
4.2 General Introduction to the North Sea	131
4.3 Phytoplankton Dynamics	136
4.4 Regions of Freshwater Influence	137
4.5 Background to North Sea Study: Tracer Release	138
4.5.1 ASGAMAGE	138
4.5.2 Sampling Strategy for the North Sea (Dutch Coastal Waters)	140
4.5.3 Dual Tracer release and Underway Monitoring	140
4.5.4 Lagrangian survey	143
4.6 Results	143
4.6.1 Physical Parameters	144
4.6.2 Biological Parameters	148
4.7 Discussion	150
4.8 General Conclusions from the North Sea Study	152
5. General Discussion	153
5.1 Spring-Neap Tidal Mixing	153
5.2 Daily Tidal Influences	155
5.3 Concluding Remarks	163
6. References	165

APPENDICES

APPENDIX I	LABORATORY STUDIES.
APPENDIX II	PHOTOPLANKTON SUBCULTURING.
APPENDIX III	INSTRUMENT CALIBRATION.
APPENDIX IV	NORTH SEA PHOTOPLANKTON SPECIES.

LIST OF FIGURES

FIGURE 1.0	Schematic of size ranges and physical length scales.	1
FIGURE 1.1	Kolmogorov Spectrum and Inertial Sub-range.	4

FIGURE 1.2	Boundary layers.	6
FIGURE 1.3	Conceptual model of external energy and phytoplankton	11
FIGURE 1.4	Schematic of phytoplankton production and respiration.	12
FIGURE 2.1	Location of Southampton Water.	13
FIGURE 3.0	Southampton Water	35
FIGURE 3.1	Predicted tidal ranges for Southampton Water during years of exceptional phytoplankton blooms.	38
FIGURE 3.2	Southampton Water, location of sampling stations.	42
FIGURE 3.3	Average monthly River Test flow rates.	43
FIGURE 3.4	Average monthly Residence Times for Southampton Water	44
FIGURE 3.5A, B, C	Phytoplankton Species	46
FIGURE 3.5 D, E	Phytoplankton Species	47
FIGURE 3.5 F, G, H, I	Phytoplankton Species	48
FIGURE 3.6 A, B, C	Physical measurements during a Neap Tide.	51
FIGURE 3.7A-E	Horizontal salinity structure from NW Netley to Hamble Jetty.	52
FIGURE 3.8 A-E	Horizontal SPM structure from NW Netley to Hamble Jetty.	54
FIGURE 3.9 A-E	Horizontal Chlorophyll <i>a</i> structure from NW Netley to Hamble Jetty.	55
FIGURE 3.10 A-E	Horizontal distribution of various phytoplankton species.	56
FIGURE 3.11	May and August 1995 - Tidal Ranges.	65
FIGURE 3.12 A-E	May 1995; Physical Parameters.	69
FIGURE 3.13 A, B	May 1995; Chlorophyll <i>a</i> concentration and <i>Rhizosolenia delicatula</i> distribution.	70
FIGURE 3.14	August 1995; Physical Parameters.	73
FIGURE 3.15	Vertical distribution of Chlorophyll <i>a</i> .	74
FIGURE 3.16	Vertical distribution of Phytoplankton Species.	75
FIGURE 3.17	Time series. 25 hr Survey; Physical Parameters.	83
FIGURE 3.18	25 hr Survey; CTD data.	84
FIGURE 3.19	25 hr Survey; ADCP data.	86
FIGURE 3.20	25 hr Survey; PAR data.	87
FIGURE 3.21	25 hr Survey; Benthic Diatom Distribution.	89
FIGURE 3.22	25 hr Survey; Pelagic Diatom Distribution.	91
FIGURE 3.23	25 hr Survey; Motile Phytoplankton Distribution.	93
FIGURE 3.24	Spring-Neap Tidal Cycles; Survey Days.	106
FIGURE 3.25	Residual Circulation.	107

FIGURE 3.26	Spring-Neap cycle; SPM Time Series.	109
FIGURE 3.27	Spring-Neap cycle; Variation in SPM.	110
FIGURE 3.28	Spring-Neap cycle; PAR Time Series.	112
FIGURE 3.29	Spring-Neap cycle; Chlorophyll <i>a</i> Time Series.	113
FIGURE 3.30	Phytoplankton Populations during a Neap Tide.	116
FIGURE 3.31	Benthic Diatoms during a Neap Tide.	117
FIGURE 3.32	Phytoplankton Populations during a Spring Tide.	118
FIGURE 3.33	Benthic Diatoms during a Spring Tide.	119
<hr/>		
FIGURE 4.1	North Sea.	131
FIGURE 4.2	Residual Currents in the North Sea.	132
FIGURE 4.3	North Sea Cruise Track.	133
FIGURE 4.4	Met Data during the "Lagrangian Survey".	134
FIGURE 4.5	Tidal Range for the Hook van Holland.	136
FIGURE 4.6	CTD data from the southern North Sea	139
FIGURE 4.7	ADCP data from the southern North Sea	140
FIGURE 4.8	Diatom distributions in the southern North Sea	143
FIGURE 4.9	Dinoflagellate species in the southern North Sea	144
<hr/>		
TABLE 5.0	Richardson Numbers for Southampton Water	152

LIST OF TABLES

TABLE 1.0	Summary of studies on Phytoplankton and Turbulence.
TABLE 2.0	Rates of Turbulent Energy (ε).
TABLE 3.0	Calibration parameters for Aquatracka III.
TABLE 4.0	Phytoplankton Species Succession in Southampton Water.
TABLE 5.0	Phytoplankton monitoring in Southampton 1973-1994.

TABLE 6.0 Re-suspension velocities.

TABLE 7.0 *Rhizosolenia delicatula* chain length.

TABLE 8.0 List of Phytoplankton cell volumes.

TABLE 9.0 Residual currents in Southampton Water.

TABLE 10.0 Mean velocity currents over a Spring-Neap cycle.

TABLE 11.0 Mean suspended particulate matter (SPM) concentration over a Spring-Neap cycle.

TABLE 12.0 Average PAR over a Spring-Neap cycle.

TABLE 13.0 Periods and Amplitudes for Tidal Harmonics.

TABLE 14.0 Maximum surface current velocities over a Spring-Neap cycle.

TABLE 15.0 Maximum bottom current velocities over a Spring-Neap cycle.

TABLE 16.0 Distance travelled per day in the surface and bottom waters.

TABLE 17.0 Division rates (per day) for *Asterionella japonica*.

TABLE 18.0 Percentage of *Peridinium trochoideum* in the surface and bottom layers of the water column.

TABLE 19.0 Percentage of *Coscinodiscus spp* in the surface and bottom layers of the water column.

GLOSSARY

ϵ	dissipation rate ($\text{cm}^{-2} \text{ s}^{-3}$ / W m s^{-3}).
η	Kolmogorov scale.
μ	division rate for phytoplankton.
ρ	density.
σ_t	density of seawater at atmospheric pressure determined from observed salinity and <i>in situ</i> temperature. σ_t = potential density (kg m^{-3}) - 10^3 .
τ	shear stress.
v	velocity.
ψ	potential energy anomaly.
Δ	gradient.
k	wavenumber ($=2\pi/\lambda$).
π	pi.
λ	wavelength.
p	pressure.

ABBREVIATED ACRONYMS

ADCP	acoustic Doppler current profiler.
CTD	conductivity, temperature and depth sensor.
DVM	diel vertical migration.
FSW	filtered ($0.45\mu\text{m}$) seawater.
L:D	light: dark cycle.
PAR	photosynthetic available (active) radiation, 350-700 nm.
Re	Reynolds number.
Ri	Richardson number, dimensionless measure of turbulence.
ROFI	region of freshwater influence.
SONUS	southern nutrient study.
SPM	suspended particulate matter (mg litre^{-1}).
TKE	turbulent kinetic energy.

CHAPTER ONE

GENERAL INTRODUCTION

1. GENERAL INTRODUCTION

1.1 OCEANOGRAPHIC SCALE

The motion of water influences phytoplankton on many spatial and temporal scales in the sea. At the largest oceanic spatial scales, phytoplankton production may be strongly associated with regions of oceanic upwelling, where the combination of nutrient rich water, irradiance and the presence of organisms provide the fundamental factors necessary for net production. At the mesoscale, bio-physical coupling occurs at the scales of ocean eddies, jets and fronts, where nutrient injections stimulate production in the upper layers. At the smallest scales, however, relative to phytoplankton, turbulence is the dominant mixing process. Turbulence influences nutrient diffusion at a molecular level and may also have direct effects on fundamental processes such as cell division (Berdalet 1992; Savidge 1981) and herbivorous grazing (Kiørboe and Saiz 1995; Costello *et al.* 1990).

Over the past decade, there has been a growing appreciation of the interactions between biology and fluid flow at the scales of individuals (Denman and Gargett 1995), where fluid motion is turbulent, intermittent and the velocity field is isotropic. At these small scales intermittency is a general feature of turbulent flows, related to the presence of strong coherent vortices, with long lengths and diameters of the order of ten times the smallest (Kolmogorov) scale (Estrada and Berdalet 1997). Phytoplankton cells are typically smaller than the Kolmogorov length (described in section 1.3), creating a micro-environment which may have a linear velocity gradient or shear varying randomly in time (Lazier and Mann 1989).

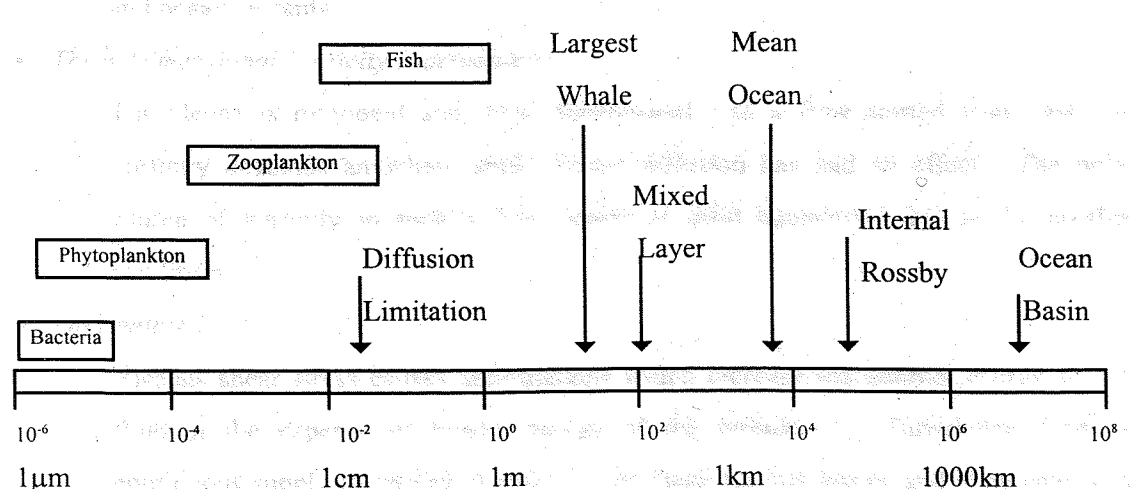


Figure 1.0. Schematic of the size scale from $1\mu\text{m}$ to $100\ 000\text{km}$, showing the characteristic size ranges and physical length scales. (Re-drawn from Mann and Lazier, 1996).

Coriolis and gravitational forces give rise to other mesoscale features such as the Rossby deformation scale or radius. This scale is the typical width of ocean currents such as the Gulf Stream, the width of the coastal upwelling systems or the radius of ocean eddies.

Viscous losses occur only at very small scales of motion, where viscous drag forces convert velocity fluctuations into heat (intermolecular motion). The intermediate scales are generally assumed to be part of an energy cascade first hypothesised by Kolmogorov (1941), in which energy is moved progressively from larger to smaller scales: there is no energy supply or loss directly to scales within this cascade range, merely a transfer of energy which ends at the smallest scale of velocity variance. So the questions arise, what is the smallest scale and how does it influence the phytoplankton?

1.2 DESCRIPTIVE TURBULENCE

Turbulence is not a property of the fluid, but of its state of motion. Turbulent flows are highly individualistic, but share a number of characteristics (Tennekes and Lumley 1972) including:

- *Irregularity:*

Turbulent motion is unpredictably variable in instantaneous speed and direction, and is often characterised by values of averaged quantities.

- *Diffusivity:*

The diffusivity of turbulence is the single most important feature as far as applications are concerned: it increases heat transfer rates in machinery, it is the source of the resistance of flow in pipelines, and it increases momentum transfer between winds and ocean currents.

- *Three Dimensional Vorticity Fluctuations:*

Turbulence is rotational and three dimensional. In a flow started from rest, no vorticity develops anywhere until viscous diffusion has had an effect. The only source of vorticity in such a flow occurs at solid boundaries due to the no-slip condition.

- *Dissipative :*

Viscous shear stress causes deformations which increase the internal energy of the fluid at the expense of kinetic energy of the turbulence. Turbulence needs a continuous supply of energy to make up for these viscous losses, and if no energy is supplied the turbulence decays rapidly.

In flows which are originally laminar, turbulence arises from instabilities. Early experiments conducted by Osborne Reynolds (1842-1912), who introduced a dye stream into a pipe of flowing liquid, discovered that in some cases the resulting straight streak indicated laminar flow, or the dispersal of the streak signalled turbulent flow. The transition was fairly sudden, both in location along the pipe and as the parameters of the flow were altered. He found that the fluid could be persuaded to shift from laminar to turbulent flow in several ways:

- by increasing speed;
- by increasing the diameter of the pipe;
- by increasing the density of the liquid; and,
- by decreasing the viscosity.

Reynolds developed a dimensionless parameter which describes turbulence arising from instabilities. The Reynolds number is defined as:

$$Re = \frac{\rho l U}{\nu} \quad (1)$$

where ρ is density; l is a length factor, U is velocity and ν is viscosity. The Reynolds number is a scaling parameter which makes order of a diverse set of physical phenomena. Turbulence occurs at large Reynolds numbers, where $Re > 2000$.

1.3 BIO-PHYSICAL COUPLING

Turbulence cannot maintain itself, but depends on the surrounding flow to obtain energy, making steady-state turbulence non-existent in nature. A common source of energy is the shear in the mean flow, which can be free-shear, due to velocity differences across fluid layers, or it can be boundary-generated shear (wall friction). Turbulence exists at all scales, from the largest eddies to the dissipative scales, where fluid molecular viscosity acts to erase gradients of velocity more rapidly than they are produced. While turbulent kinetic energy (TKE) is carried by the large scales, the shear field is concentrated at the dissipation range, where the size of the smallest shear before dissipation is referred to as the Kolmogorov length scale (η) which is defined as:

$$\eta = (\nu^3 / \epsilon)^{0.25} \quad (2)$$

where ν is the kinematic viscosity and ϵ is the dissipation rate of TKE per unit mass.

Kolmogorov (1941) sought a theory of turbulent eddies of a size intermediate between the large scale (where energy is added) and small-scale (dissipation). This intermediate scale is the inertial range. Kolmogorov suggested that within this range, eddies transmit their energy from larger scales to smaller scales in such a way that the power spectral density $S_{(k)}$ (velocity variance per unit wave number) depends only on the wave number itself and the rate ε at which energy is dissipated at fine scales by viscosity. The prediction is that the distribution of velocity variance over length scale (wave number, $2\pi / \text{wavelength}$) in this turbulent field should vary as $-5/3$ power of the wave number (Figure 1.1).

$$S_{(k)} \simeq \varepsilon^{2/3} k^{-5/3} \quad (3)$$

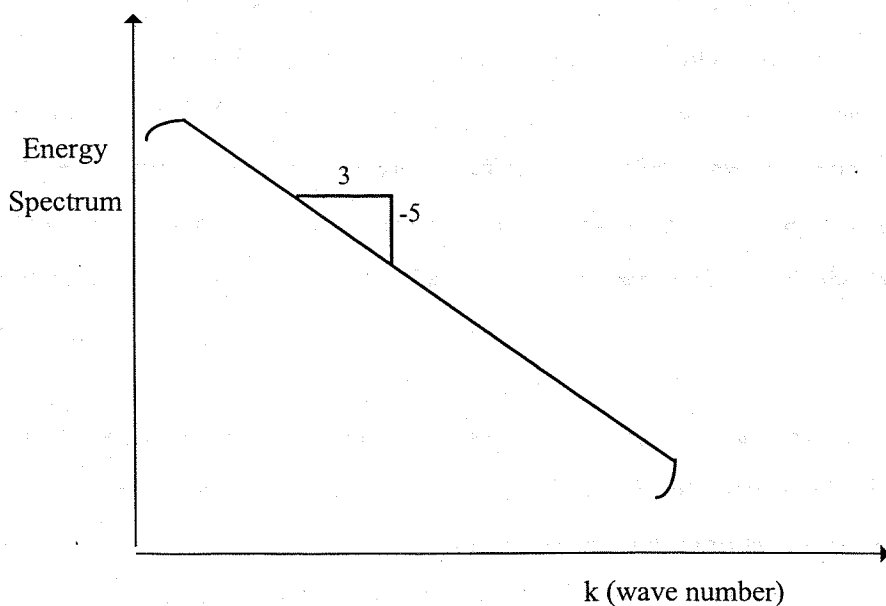


Figure 1.1. The Kolmogorov Spectrum and Inertial Sub-range.

While turbulent velocity spectra have a degree of common properties, this is much more controversial for the scalar properties of fluid. These may be passive in the sense that their presence does not significantly affect the dynamics of the flow: others such as temperature and salinity may be active scalars affecting flow dynamics through their effect on fluid density.

For the ocean environment of plankton, temperature and salinity are important scalars. In a turbulent field, scalar variance occurs at much higher wavenumbers (smaller scales) than velocity variance - a fact that may hold further biological implications (Gargett 1997).

If $\varepsilon = 10^{-1} \text{ cm}^2 \text{ s}^{-3}$ (a reasonably large scale typical of the upper surface mixed layer under moderate wind forcing), the shear mean is at higher wave numbers, i.e. scales smaller than 1 cm.

If $\varepsilon = 10^{-4} \text{ cm}^2 \text{ s}^{-3}$ (typical of the lower mixed layer, or sporadically the stratified region at the oceanic mixed layer base) the shear is at lower wavenumbers, i.e. the shear is contained in scales greater than 1 cm.

The shear environment, therefore, at the scale of a biological particle will depend not only on its size but on the strength of the turbulence in its environment. The gradients in scalar fields such as temperature and nutrient concentration both extend to smaller scales than Kolmogorov. The length scale of the smallest fluctuation in any property of diffusion is referred to as the Batchelor scale. For example, if ε varies from 10^{-6} to $10^{-9} \text{ cm}^2 \text{ s}^{-3}$ the smallest scale for temperature fluctuations is 2 to 13 mm and the smallest scale for salinity fluctuations is 0.2 to 1.0 mm (Mann and Lazier, 1996). The possibility of interaction between gradients produced by turbulence and biological organisms therefore, depends upon an overlap in their spatial scales. Since the smallest gradient scales depend on ε , and decrease when ε increases, the degree of overlap is a complex function of organism size and all the factors driving the turbulence.

As described above, turbulent energy is passed from large to small eddies and the viscosity of the water limits the size of the smallest eddies to a few millimetres (Mann and Lazier 1996, Gargett 1997). Such turbulence is ineffective in transporting nutrients and wastes for organisms less than 1mm diameter (which make up more than half the total biomass of the oceans, Sheldon 1972). Smaller organisms must therefore, rely on the flux due to molecular diffusion. This process can be very slow, requiring ~ 10 s to produce an effect over a distance of $100\mu\text{m}$ (Mann and Lazier 1996). This flux of some constituent through the water due to molecular diffusion is given by Fick's first law of diffusion, where the coefficient of molecular diffusion of large molecules (i.e. salt) is $\sim 1.5 \times 10^{-9} \text{ m}^2 \text{ s}^{-1}$.

The surfaces of organisms have associated with them a boundary layer in which water movement is reduced, thus reducing the rate of exchange between the external environment and the cell. A boundary layer is also associated with the water above the sea floor where the fundamental property to be considered is the 'no-slip' condition. Water molecules in contact with the solid surface are in essence stationary.

As distance increases away from the boundary layer, velocity increases to a free stream velocity. This schematic diagram, shown as Figure 1.2, is simplified by suggesting constant laminar flows, whereas in reality flows are turbulent and fluctuating. However, these fluctuations from the mean flow decrease toward the boundary layer. This decrease in magnitude is caused by stress (τ) or drag exerted on the water by a solid boundary. The transmission of this stress across the layer of water is accomplished, in turbulent flows, by eddy diffusion. For sedentary organisms, rapidly flowing water will cause a thinning of the boundary layer, and rapid swimming (or sinking) of phytoplankton is expected to have the same effect.

The thickness of the boundary layer surrounding an object moving through water increases with increasing distance from its leading edge. This concept led to the findings that:

- the larger the organism, the thicker the boundary layer; and,
- the boundary layer becomes thinner as the velocity of the water relative to the organism increases.

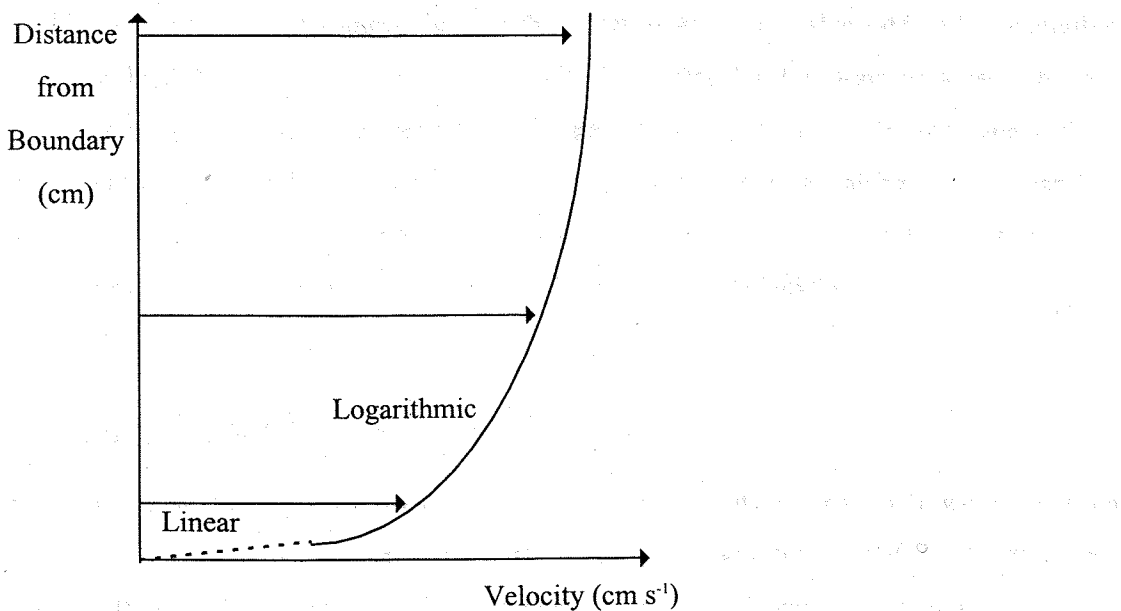


Figure 1.2. Vertical profile of the mean water velocity through the boundary layer above a smooth surface. Note the linear sublayer where viscous stresses dominate and the logarithmic layer where Reynolds stresses dominate.

1.4 PHYTOPLANKTON CELL SIZE

It is frequently assumed that nutrient uptake rate by phytoplankton cells depends on the cell surface area, and that nutrient uptake is most efficient in small cells due to their higher specific surface area. However, this is only true in highly eutrophic environments. In oligotrophic environments, uptake is limited to the rate at which molecules can diffuse to the cell, and this has already been shown to be a slow process (Section 1.3). One way to overcome this limitation is to generate movement in the water to replenish the depleted microzone, but the size range in which benefits exist is debatable. Munk and Riley (1952) suggested that benefits only occurred for organisms $>20\mu\text{m}$; smaller than this size and the effect of turbulence was negligible. Lazier and Mann (1989) demonstrated that turbulent motion across small distances is simply a linear shear, due to the damping effect of viscosity, and calculated that even the most energetic turbulence had no effect on the microzones of organisms $< 100\mu\text{m}$. Kiørboe (1993), on the other hand, suggested $10\mu\text{m}$ in diameter, below which the advective contribution of sinking or swimming will have no effect on the rate of molecular diffusion, whereas for cells $\sim 100\mu\text{m}$ relative motion will have a significant increase on the diffusive flux, which can be explained by Stoke's law (section 1.5). Berg and Purcell (1977) calculated that swimming through the water at any reasonable rate had a negligible effect on the diffusive flux of organisms $< 5\mu\text{m}$ in diameter, but for larger organisms the rate increases rapidly. Reviewing the literature suggests that $5\text{--}100\mu\text{m}$ is the size range where movement (whether sinking, swimming or turbulence) will be an advantage to an organism, with the lowest limits remaining controversial. This controversy stems from the inherent difficulties of monitoring turbulence at the size scales of phytoplankton.

1.5 SINKING OF PHYTOPLANKTON CELLS

Most phytoplankton cells are denser than water. The density of sea water varies between 1,021 to 1.028 g cm^{-3} , but the density of cytoplasm ranges from 1.030 to 1.100 g cm^{-3} (Kamykowski 1995). Diatoms have a hydrated silicon dioxide cell wall with a density of $\sim 2.6\text{ g cm}^{-3}$ and coccolithophorids have plates of calcite, aragonite, or vaterite with densities between 2.60 to 2.95 g cm^{-3} . Therefore, many non-swimming phytoplankton will sink except when an upward movement of water causes re-suspension. The rate at which cells fall can be estimated using Stokes' equation when the Reynolds number is <1.0 and if the cells are approximately spherical. Stokes defined that a fluid slows a falling sphere by exerting a

resisting force. This force must be equal to the weight of the sphere less the upward push due to buoyancy.

For a given excess density and viscosity, a sphere will increase its sinking speed in proportion to the square of its radius. Few phytoplankton are spherical, but for $Re < 0.5$ Stokes' law may still be applied to non-spherical bodies without significant error. Another factor influencing the sinking rate of cells is their life history. Smayda (1970) showed through laboratory culture experiments that senescent cells sink faster than actively growing cells. It has also been shown that preserved cells sink faster than living cells and that natural blooms of phytoplankton tend to sink in the water column as they approach senescence. Several other potential mechanisms may work together to cause increased sedimentation rates, particularly through the coagulation of cells into aggregates (Kiørboe *et al.* 1996; Alldredge and Gotschalk 1989; Jackson 1990), attachment to marine snow (Kiørboe 1993) buoyancy control (Villareal 1988) or spore formation. Turbulence has been linked to increasing the rate of aggregation in certain populations of phytoplankton depending and varying on the species present and their inherent "stickiness" (Kiørboe 1993). The subsequent increase in the settling velocity of marine aggregates, observed during exceptional phytoplankton blooms has been suggested as a potential accelerating factor in the rapid decline of populations at the termination of the bloom.

1.6 PHYTOPLANKTON MOTILITY

For small organisms that perform movements relatively slowly, the Reynolds number is low and viscous forces predominate. For example a picoplankton cell of ca. $1\mu\text{m}$ diameter moving at $30\mu\text{m s}^{-1}$, will generate inertial forces that are so small that movement will stop in 0.6×10^{-6} s, travelling only $10^{-4}\mu\text{m}$ once swimming has ceased. Dinoflagellates, in contrast have typical size ranges between $10 - 2000\mu\text{m}$ (Kamykowski 1995), and have been cited as the fastest phytoflagellate swimmers. Their swimming behaviour has been investigated intensely for many years particularly in terms of natural vertical migrations (Hasle 1950). Dinoflagellates have a distinctive dinokont or desmokont flagellar morphology. In dinokonts, the two flagellae (longitudinal and transverse) generally have a lateral insertion and occur in grooves (Taylor 1987b). The longitudinal flagellum is often rounded, but can be ribbon-like and can extend posteriorly behind the cell for over $200\mu\text{m}$. The transverse flagellum is ribbon-like with many inherent bends (3-4 waves per $10\mu\text{m}$) and typically extends around the cell. Although desmokont flagellae can be morphologically similar to those of the dinokonts,

they are inserted anteriorly and do not occur in grooves. In Prorocentrales for example, one free flagellum extends away from the cell, while the other flagellum is coiled and is attached to the cell body for most of its length. In *Prorocentrum micans*, for example, the free flagellum beats with an unusual tip-to-base motion that pulls the cell through the water. The coiled flagellum exhibits a rotational motion that provides a whip-like result at the unattached tip.

The combined propulsive effect of the two dinoflagellate flagellae results in a characteristic swimming speed and direction. Average swimming speeds of individual cells determined through laboratory observations or *in situ* population diel vertical migrations, estimate ranges between 0.2-2.0 m h⁻¹, but some speeds of greater than 5.0 m h⁻¹ have been reported (Lombardi and Capon 1971). Swimming speed dependence on salinity and temperature have been well documented (Hand *et al.* 1965). Kamykowski and McCollum (1986) surveyed the swimming speeds of 14 dinoflagellate clones representing 11 species. Mean maximum swimming speeds ranged from 0.4-2.0 m hr⁻¹ within a temperature optima that ranged from 9.1 to 33.5°C but generally exceeded 25°C. This range suggests a varying metabolic effect in different species because changes in the characteristics of the external medium, such as viscosity, influence all species in a similar way. For example, *Gyrodinium dorsum* swam at an average speed of 1.5 m h⁻¹ at 20°C compared to 2.0 m h⁻¹ at its optimum temperature of 29°C.

Diel vertical migration (DVM) of autotrophic dinoflagellates is classically modelled as ascent during daylight hours and descent during the dark (Kamykowski 1987). However in some cases (Eppley *et al.* 1978; Kamykowski 1981b) this pattern deviates from that expected from phototaxis alone. These observations range from dusk ascents (Hasle 1950; Forward 1976) to a field population of *Gymnodinium sanguineum* that ascended between 23:00 and 04:00 hr (Kiefer and Lasker 1975). Circadian rhythm has been suggested as a plausible explanation for such deviations from the main daylight phase. Passive orientation has also been suggested, defined as the orientation of a swimming cell in a velocity gradient resulting from compensating torques due to gravity and shear (Pedley and Kessler 1992). For example, a posteriorly weighted cell (i.e. unbalanced mass distribution of cell organelles) with anterior flagella pulling the cell, contributes to negative geotaxis. Swimming velocity determines an organism's vertical progress in a stationary water column, however vertical water motions combine with the biological vector to determine their actual trajectory in natural water columns. Dinoflagellate swimming speeds at irradiance values above 200 µE m⁻² s⁻¹ has been

shown to exceed those in the dark by 20% (Kamykowski 1995). The ascents aided by phototaxis during the day may compensate for descents aided by cell sinking in the dark. Natural dinoflagellate populations often aggregate in discrete layers in the water column (Levandowsky and Kaneta 1987), which requires that the individual cells direct their swimming ability to maintain a chosen position.

1.7 BIOLOGICAL EFFECTS OF TURBULENCE

1.7.1 GENERAL THEORIES: INDIRECT EFFECTS

At the size-scale of the individual organism, fluid motion is due to turbulence and the velocity field has become isotropic, making irrelevant any distinction between horizontal and vertical components (Denman and Gargett 1995). Since an organism's swimming speed increases with size, larger organisms (mature fish for example) may be considered free agents in the sense that swimming speeds exceed typical fluid velocities. However, as size decreases organisms become increasingly susceptible to ambient fluid velocities. Considering the importance of external energy, Margalef (1978) proposed a systematic functional morphology for phytoplankton on the basis of two environmental factors: nutrient supply and intensity of turbulence. This conceptual model is expressed schematically in Figure 1.3. Major taxonomic groups of phytoplankton occupy different niches within the model. Diatoms, usually non-motile and with fast potential growth rates thrive in relatively turbulent, nutrient-rich waters. Under these conditions, lack of motility is compensated by re-suspension of cells due to vertical mixing. Dinoflagellates, in contrast can regulate their position actively. This allows for survival in stratified waters, where motility and migration behaviour can override sedimentation. In terms of Margalef's conceptual model, a typical phytoplankton succession would follow a trend from the high turbulence-high nutrient corner to the opposite low turbulence-low nutrient corner. Red tides and exceptional blooms tend to occur in the anomalous situation of high nutrients and low turbulence.

Nutrient supply to the surface layer is dependent on the larger scale mesoscale mixing processes such as eddies and upwelling as well as the turbulent diffusive processes across the pycnocline. Net primary production in the surface layer is essentially a balance between the rate of nutrient supply, the timescale of cell division, the timescale of mixing processes and the availability of the sufficient irradiance.

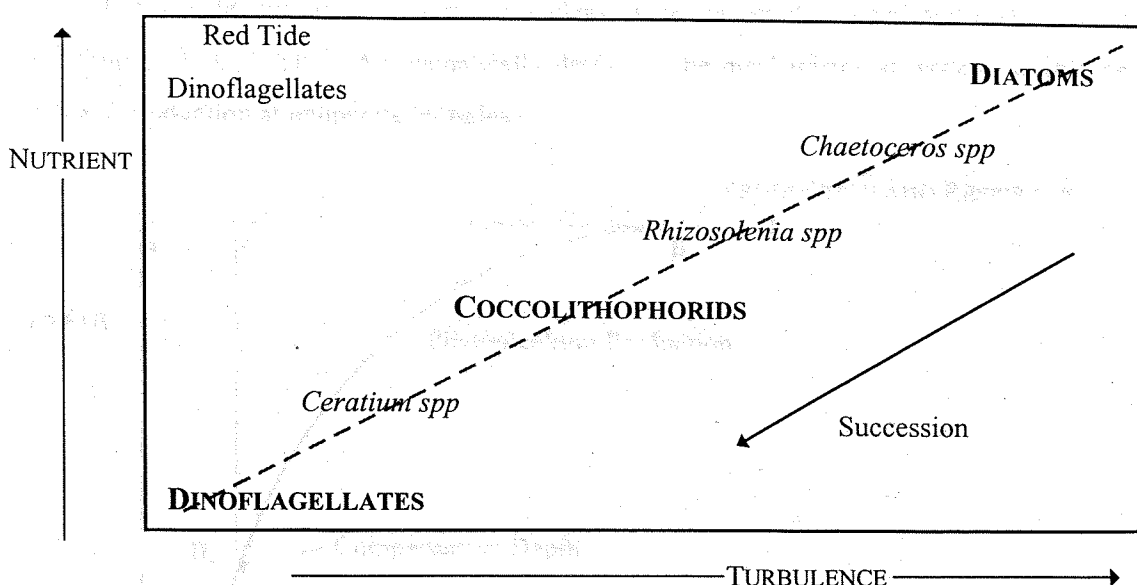


Figure 1.3. A schematic representation of the main phytoplankton life forms in an ecological space defined by nutrient concentration and turbulence (Margalef 1978).

The vertical structure of the water column involves a delicate balance between destabilising forces (for example, wind stress, heat loss and shear) and stabilising effects (buoyancy). The typical vertical profile of the upper ocean, with a surface mixed layer overlying a sharp pycnocline, is associated with large variations in the intensity of turbulent energy dissipation and has important effects in controlling nutrient supply and vertical phytoplankton distribution. The entrainment of phytoplankton by water motion exposes the organisms to continuously varying irradiance. In temperate regions, these fundamental features of the upper ocean, including increased TKE, the depth of the mixed layer and variable irradiance have served to represent the governing factors of the spring phytoplankton (diatomous) bloom. Gran and Braarud (1935) suggested that stabilisation of the water column by thermal stratification could have the effect of greatly stimulating primary production. These early ideas were further developed by Riley (1942), Sverdrup (1953) and Platt *et al.* (1991), who concluded that *“Incipient stabilisation of the water column by surface heating can then be seen as the fundamental process that promotes the rapid growth of phytoplankton that leads to the incidence of a bloom.”*

Throughout the temperate winter months, phytoplankton are circulated to the full depth of the mixed layer, and the average irradiance received is not adequate to sustain net production. As the mixed layer reduces through spring, average irradiance received by the phytoplankton increases as the organisms are retained within the photic zone, and positive net primary

production can be sustained. These early ideas, were further developed and quantified by Sverdrup (1953). Figure 1.4 schematically describes the mechanisms at work to enable net primary production at temperate latitudes.

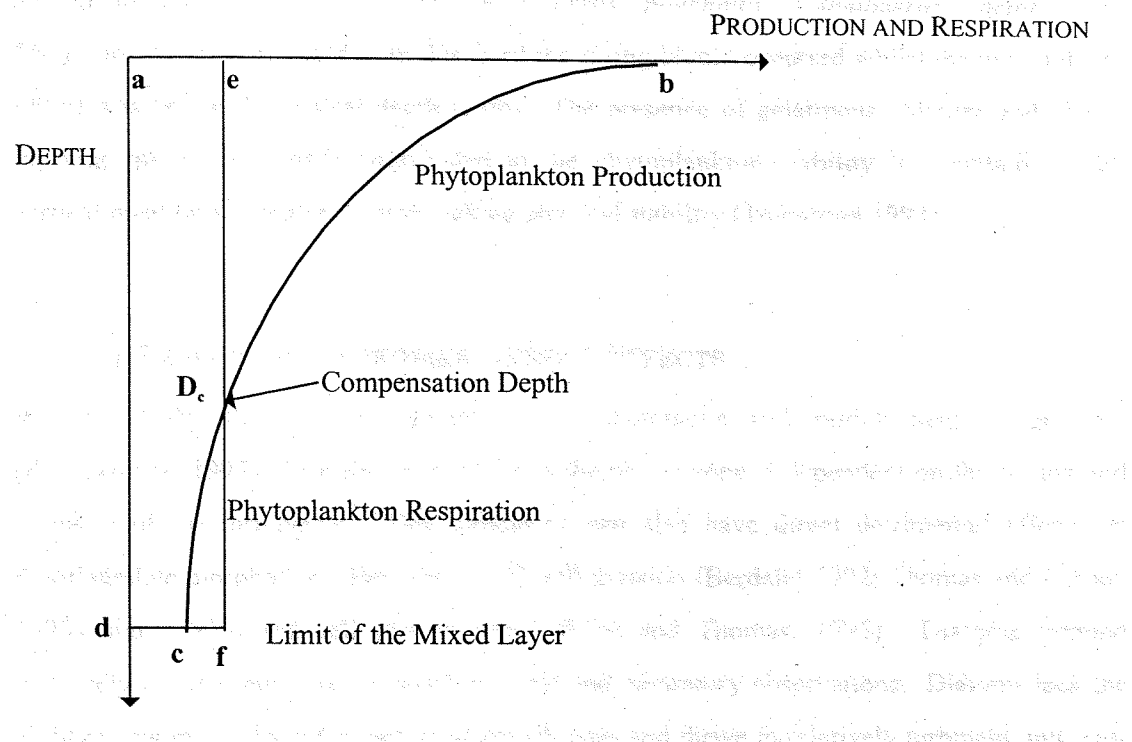


Figure 1.4. Schematic diagram describing the theoretical distribution of phytoplankton production and respiration. (After Sverdrup 1953).

A phytoplankton cell circulating randomly throughout the mixed layer will have a continuously varying photosynthetic rate depending on its vertical position in terms of the amount of photosynthetically available radiation (PAR). Net production will occur in the photic zone, whilst below the compensation depth (lower limit of the photic zone), respiration will dominate. The condition, however, for net positive population growth is that the integrated production (represented by the area $abcd$) be greater than the integrated respiration (represented by the area $aefd$). As the depth of the mixed layer increases, respiration increases proportionally but production increases are negligible. There is, therefore, a critical depth of the mixed layer at which integrated production equals integrated respiration. As the mixed depth reduces net phytoplankton production occurs. However, exceptions do occur, for example Townsend (1992) observed in the offshore waters of the Gulf of Maine, that a spring bloom occurred in the absence of thermal stratification. It was further implied that the early bloom of diatoms was a contributing factor to the development of the thermocline by virtue of the light scattering and absorption properties of the phytoplankton. Eilertson (1993) confirmed Townsend's (1992) observations, through surveys in a Norwegian fjord. Fresh water run-off

from melt water increased in early May and peaked in June, although no thermal stratification occurred. The spring bloom began in mid March and culminated at the end of April, following the annual increase in irradiance, but in the absence of stratification. The dominant phytoplankton in this case were *Phaeocystis pouchettii*, *Chaetoceros socialis* and *Thalassiosira nordenskioeldii*. In this fjord the spring bloom occurred whilst the mixed depth (90m) was below the critical depth (55m). The presence of gelatinous colonies and chain-forming species may have contributed to the phytoplankton's ability to maintain a high vertical position in a water column lacking physical stability (Townsend 1992).

1.7.2 GENERAL THEORIES: DIRECT EFFECTS

Whilst dinoflagellate species remain motile, phototactic and exhibit negative geotaxis (Kamykowski 1995), their ability to return to the photic zone is dependent on the timing and intensity of the turbulence. This turbulence can also have direct detrimental effects on dinoflagellate morphology (Berdalet 1992), cell division (Berdalet 1992; Thomas and Gibson 1990a and 1990b) and cell growth rate (Gibson and Thomas, 1995). Diatoms respond positively to turbulence, as supported by field and laboratory observations. Diatoms lack the ability to swim, but have fast potential growth rates and thrive in relatively turbulent, nutrient-rich waters (Estrada and Berdalet 1997), but lack the behavioural responses necessary to avoid removal beyond a critical depth when turbulence is intense. Exceptions to this have been shown by Villareal (1988), where individual chains of the oceanic diatom *Rhizosolenia debyana* were seen to exhibit positive buoyancy in the surface waters off Miami, the Bahamas and the Sargasso Sea. The average ascension rates were measured as 112m d^{-1} , thus providing an effective solution to the problem of suspension for oceanic diatoms. This positive buoyancy characteristic is thought to be due to the modification of the internal cell density.

The indirect and direct effects of turbulence are inseparable in the field. As a result, well defined laboratory experiments have targeted turbulence as a 'controllable' variable influencing phytoplankton at the scale of the individual. Table 1.0 summarises laboratory studies which used turbulence and focused on the direct effect upon phytoplankton. Many other laboratory turbulence studies have been performed, but these have tended to focus on zooplankton, in relation to predator-prey contact rates (Saiz and Kiørboe 1995) and metabolic rates (Alcaraz *et al.* 1988) rather than on the phytoplankton community. Very few studies have determined a quantified turbulent measurement comparable to field values - an area initially targeted by the research presented in this thesis. In recent years, video

techniques (Marassé *et al.* 1990) have been incorporated to produce a quantitative analysis, based on the work of Dickey and Mellor (1980), which allowed a measurement to be made of the turbulent dissipation rate (ε), comparable to real values.

Most of these laboratory studies involving phytoplankton have concentrated on dinoflagellates, which are known to bloom in calmer water conditions. Direct turbulent effects have been demonstrated, such as the very low growth rate of *Gonyaulax excavata* (White 1976) with increasing agitation, and, for *Peridinium cinctum*, growth inhibition depending on the timing of turbulence (Pollinger and Zemel, 1981). When turbulence was applied in the dark period, i.e. during cell division, a strong inhibitory effect occurred. This was also the case for *Gymnodinium nelsonii*, where Berdalet (1992), and Berdalet and Estrada (1993) suggested physiological damage at the organelle level causing a blockage in the process of chromosome division after the duplication of DNA. Cell volumes increased and cellular concentrations of RNA and DNA increased up to ten times those of controls (i.e. non-turbulent). Similar results were reported for *Alexandrium minutum*, *Prorocentrum micans* and *Prorocentrum triestinum*, but it was found that a small *Gymnodinium* sp. (10 μm diameter) was not affected by shaking at 100 rpm (Estrada and Berdalet, 1998). This suggested that deleterious effects appear to be stronger for larger organisms and for smaller culture vessels (Estrada and Berdalet, 1998), a finding that ties in with the early theories of Munk and Riley (1952) which suggested no turbulent effects on organisms $<20\mu\text{m}$ (Section 1.6). The overall effect of turbulence on dinoflagellates appears to be generally negative, with the deleterious effects of water motion including disturbances of cell division, morphological changes, cell disruption and interference with organism behaviour.

YEAR AND AUTHOR	PHYTOPLANKTON SPECIES	METHOD	CONCLUSION
Fogg and Than-Tun (1960)	<i>Anabaena cylindrica</i>	Shaking at 90 oscillations per minute and higher	Increased growth up to 90 osc. min^{-1} , decreased when shaking increased
White (1976)	<i>Gonyaulax excavata</i>	Continuous rotary shakers ($>125\text{rpm}$) 125ml	Degree of growth inhibition dependent on the rate of agitation.
Pollinger and Zemel (1981)	<i>Peridinium cinctum</i>	Continuous intermittent and zero shaking on a rotary shaker	Cont.-cell death Inter.-inhibits division rate
Oviatt (1981)	Phytoplankton spp. (+ Zooplankton)	Vertical plunger in tank	Enhanced nutrient uptake + contact rates
Savidge (1981)	<i>Phaeodactylum tricornutum</i> <i>Brachiomonas submarina</i>	25 litre cultures Oscillating grid	Increased lag when nutrient (P) limited. Aeration had a shearing effect
Estrada <i>et al.</i> (1987) Alcaraz <i>et al.</i> (1988)	Seawater taken from Masnou, 20km N of Spain	30dm ³ microcosms. oscillating net grids and elliptical 'plungers'	Phytoplankton biomass increased when copepods and turbulence interact.
Thomas and Gibson (1990)	<i>Gonyaulax polyedra</i>	Couette devices.	Turbulence inhibits dinoflagellate growth
Kiørboe <i>et al.</i> (1990)	Phytoplankton spp.	Oscillating grid	Quantified coagulation
Berdalet (1992)	<i>Gymnodinium nelsonii</i>	5mm oscillating grid	Inhibition of growth
Howarth <i>et al.</i> (1993)	N-fixing cyanobacteria	3m ³ volume tanks, reciprocating grid	N-fixation not prevented by turbulence
Berdalet and Estrada (1993)	Various dinoflagellates e.g. <i>P. micans</i>	Rotary shaking	Cell volume increase (RNA and DNA increases)
Thomas <i>et al.</i> (1995)	<i>Gonyaulax polyedra</i>	Couette devices	Photosynthetic activity less sensitive to turbulence

Table 1. Summary of studies investigating the direct effect of turbulence on phytoplankton.

One important and controversial feature of these laboratory studies is that the methods for creating and measuring 'turbulence' are many and varied ranging from rotary shaking, and Couette devices to grid stirred turbulence (which is the most documented form of laboratory turbulence). In most cases it has proven very difficult to reconstruct 'typical' natural levels of turbulence in small enclosed chambers. Table 2 shows a comparison of typical ε values for natural and experimental turbulence.

	ε ($\text{cm}^{-2} \text{s}^{-3}$)
NATURAL SYSTEMS	
Lakes (Reynolds 1994)	$0.014 \times 10^{-2} - 4 \times 10^{-2}$
Open Ocean (Kiørboe and Saiz 1995)	$10^{-6} - 10^{-2}$
Shelf (Kiørboe and Saiz 1995)	$10^{-3} - 10^{-2}$
Coastal Zone (Kiørboe and Saiz 1995)	$10^{-3} - 10^0$
Tidal Front (Kiørboe and Saiz 1995)	10^{-1}
Tidal Estuary: Severn (Reynolds 1994)	$2.2 - 8 \times 10^{-2}$
EXPERIMENTAL SYSTEMS	
Animal Cell Cultures (Lakhota and Papoutsakis 1992)	0.6 - 1.0
Couette Cylinders (Thomas and Gibson 1995)	<ul style="list-style-type: none"> Range Effect Threshold
Paddle Stirrer (Dempsey 1982)	<ul style="list-style-type: none"> 0.045 - 164 0.18 0.096 - 0.14

Table 2. Turbulence dissipation rates (ε) from various environments. (Redrawn from Estrada and Berdalet 1997)

This summary of ε for natural and experimental systems suggests that dissipation rates used in laboratory studies have been much higher than levels that occur within the natural environment. Thomas and Gibson (1990b) have suggested that negative effects of turbulence are observed on phytoplankton growth rates when $\varepsilon > 0.1 \text{ cm}^{-2} \text{ s}^{-3}$. This corresponds to levels above those found typically in marine waters, although higher ε values have been recorded in estuaries or at tidal fronts. Gibson and Thomas (1995) further proposed that the action of intermittent wave breaking could be sufficient to cause cellular effects on dinoflagellates. These observations lead to the hypothesis that direct effects of turbulence on phytoplankton cells could be important, for example, in shallow estuarine areas (Estrada and Berdalet, 1997).

In addition to disturbances at a cellular level, several studies have suggested the possibility of more subtle effects on dinoflagellate swimming, migration and other behavioural

characteristics (White 1976). Estrada *et al.* (1987a) found that in 30 litre microcosms a diverse dinoflagellate community thrived in cylindrical containers agitated by oscillating grids at 20 rpm, while all dinoflagellates crashed in vessels with stagnant water or at higher turbulence levels. In a following study (Estrada *et al.*, 1987b), dinoflagellates did not grow in containers that were illuminated only in the lower region. It was suggested that this unusual irradiance régime interfered with the migration behaviour of the dinoflagellates.

Another interesting direct effect of turbulence on phytoplankton is that it stimulates bioluminescence in many dinoflagellates. Anderson *et al.* (1988) measured the luminescent response of *Gonyaulax sp.* using a laminar flow in a capillary tube and found that bioluminescence occurred at the transition from laminar to turbulent flow. In many cases of bioluminescence reported through turbulent stimulation (Rohr *et al.* 1990) the value of ϵ involved was much higher than typical oceanic values.

1.8 TURBULENT MIXING IN ESTUARIES

Estuaries can be described as bays, parts of a bay or a narrow inlet in which freshwater flow from the land has reduced the salinity of the ocean water (Boynton *et al.* 1982). The flow of freshwater causes a characteristic circulation pattern within the estuary, in which the less dense fresh water flows out of the estuary in the surface layer and a deeper bottom current intrudes from the sea generating a residual estuarine circulation. In estuarine environments, tides are usually recognised as the principal source of mechanical energy for vertical mixing. Estuaries regularly oscillate between conditions of vertical homogeneity and stratification in conjunction with the monthly spring-neap cycle (Haas 1977). The increased turbulent mixing associated with increased tidal currents and prism during spring tides causes a shift from a stratified to a well-mixed water column. Conversely, decreased turbulent mixing during neap tides permits stratification, often due to the influx of higher salinity bottom water (Haas 1977). Superimposed on this fortnightly cycle, is the daily tidal cycle which may be unique to one particular area, e.g. Southampton Water exhibits a semi-diurnal, asymmetric cycle of rapid ebb currents which can be double the velocity of the flood (Webber 1980). This tidal influence can often be of such intensity as to overcome the stabilising properties of a neap tide, for example, and cause temporary vertical homogeneity.

Early measurements of vertical mixing in estuaries (Bowden and Fairbairn 1956; Gardner and Smith 1978) focused on determining the energetic scales of motion, and it is only

in recent years that the smallest viscous scales of turbulent microstructure have been investigated (historical review by Gregg 1991). Peters (1997) analysed the variability patterns and magnitude of turbulent mixing in the Hudson River using the Shallow Water Microprofiler (SWAMP) and a 600kHz acoustic Doppler current profiler (ADCP). The asymmetry in vertical current structure between the flood and ebb is an important feature of this system, which has been related to the longitudinal straining of the estuarine density field by the superposition of tidal and residual flow (Simpson *et al.* 1990). The reduced shear during the slack after the flood, compared to the larger shear during the transition from the ebb to the flood, is a major feature of ebb-flood asymmetry.

Estuarine environments have a source of buoyancy derived from fresh water riverine inflow coupled with the mechanical energy from the tides. The river discharge into estuaries varies seasonally and this is reflected in the fluxes within the estuary and in the salinity distribution. At low river discharge the amount of river water accumulated in the estuary is relatively small, but the salinity intrudes well into the estuary. As river discharge increases, the saline water is pushed seawards, the stratification is increased and the river flows out in a surface layer more efficiently, with less mixing (Dyer, 1997). Internal mixing within estuaries is caused by the turbulence produced by the velocity shear resulting from both bottom friction and by internal current shear.

In a partially-mixed estuary, the specific tidal intermittency and the rapid timescales involved allow stratification and vertical mixing to occur over a short timescale i.e. a few hours. The important feature of natural turbulence, particularly when considering biological entities, is its intermittency, where irregularity occurs over a range of timescales, caused by surface breaking waves, wind events, internal wave instabilities or tidally-induced motions. Changes in phytoplankton populations in estuarine systems can result from seasonal and inter-annual variations in river flow (Demers *et al.* 1986), but more pronounced variations result from fluctuations in tidal-stirring. Cloern (1991), working in South San Francisco Bay, showed that phytoplankton populations are strongly influenced by daily fluctuations in vertical mixing, with blooms occurring during periods of low mixing. Predictions of biological responses to physical variability in these environments are inherently difficult due to the recurrent seasonal patterns of mixing, complicated by aperiodic fluctuations in river discharge, and the high frequency components of tidal variability (Simpson *et al.* 1991).

Other distinctions between the physical régimes of the open and coastal oceans, directly influence the observed differences in phytoplankton dynamics. Shallow coastal waters have high concentrations of suspended particulate matter (SPM) that originate from wind-wave or tidal re-suspension of bed sediments as well as riverine inputs of terrigenous particulates (Koseff *et al.* 1993). Coastal systems are characterised by a large spatial variability in turbidity and a temporal variability from hours to seasons (Cloern *et al.* 1989). Light attenuation by SPM acts as a major control on phytoplankton photosynthesis in shallow marine systems, to the extent that primary production is associated with variability in SPM concentration (Cloern 1987). On the semi-diurnal scale, SPM concentrations are closely related to current velocities. For example in the near bottom waters of the Forth estuary, Scotland, the current velocities required to make re-suspension and deposition evident are 0.6 and 0.3 m s⁻¹ respectively (Lindsay *et al.* 1996). Within the semi-diurnal cycle, these velocities are exceeded for longer periods when the tidal range is large, thus spring tidal cycles are the dominant influence in controlling the transport of SPM within the estuary.

The spring-neap tidal cycle has been identified as an important factor for influencing phytoplankton growth in estuaries and shallow coastal seas. For example, variations in algal biomass have been correlated to this cycle at two stations on the coast of Connemara, Ireland (Roden, 1994), with a chlorophyll *a* maxima occurring on the neap tides (see chapter three for further details).

1.9 COASTAL PHYTOPLANKTON DYNAMICS

Irradiance can be a primary limiting factor for phytoplankton growth in estuarine systems. Riley (1967) estimated that a threshold surface mixed layer photon flux density of 196 W m⁻² was necessary to allow a positive net growth of phytoplankton, attained when the mixed layer primary production sufficiently exceeds respiration. The onset of the spring bloom, for example, has been observed to be triggered by thermal and/or salinity stratification in a number of estuaries (Hitchcock and Smayda 1977; Radach and Moll 1990), however the concentration of suspended sediment can be high and reduce the levels of PAR. In the Bristol Channel, for example, the rate of primary production in the inner turbid areas (where the photic depth was reduced to 0.5 m) was 7 gC m⁻² yr⁻¹, compared to 165 gC m⁻² yr⁻¹ in the clearer zones where photic depth was 10m (Joint and Pomroy 1981). In highly turbid estuaries, primary production tends to peak in the summer during times of reduced rainfall and maximum irradiance (Randall and Day 1987; Cole and Cloern 1984).

The mixing of varying volumes of seawater and freshwater determine the estuarine salinity. Phytoplankton may be subjected, over timescales of hours, to large variations in salinity due to movements along the longitudinal axis with tidal currents or may vertically migrate across large salinity gradients. Estuarine phytoplankton are the most euryhaline of species (Brand 1984), surviving large fluctuations in salinity without osmotic shock.

Estuaries are systems with high nutrient loading from rivers and often anthropogenic sources. Excessive nutrient concentration can give rise to eutrophication, although in estuaries where river flow is high (leading to a decreased residence time), large nutrient accumulations are prevented (for example, the Thames and Delaware estuaries). This concept of estuarine residence time is not only important for nutrient dynamics, but has also been shown to be vital for the accumulation of phytoplankton (Ketchum 1954) and general contaminants. Investigations in the lower Hudson estuary showed that phytoplankton were washed out of the estuary by surface layer flow during the autumn, winter and spring when growth rates were low relative to surface dilution rates, and tended to accumulate during the summer when growth rates exceeded dilution rates (Malone 1977). This suggests that estuaries with very high flushing rates (i.e. less than one day) can not retain the phytoplankton population. Garcon and Anderson (1986) observed the tidal flushing of Perch Pond, a Cape Cod embayment subject to recurrent dinoflagellate blooms of *Gonyaulax tamarensis*. This estuary exhibits a density-driven circulation pattern, which ensures a relatively high tidal-flushing efficiency, becoming even stronger when vertical mixing is minimised (i.e. low wind stress) and when the gravitational residual circulation is established (Barlow 1956). The effective tidal flushing rate of 0.36 d^{-1} in Perch Pond, is approximately equivalent to the maximum specific growth rate of *G. tamarensis* (Watras *et al.* 1982). Theoretically, motile cells liberated from germinated cysts would be advected from the pond as fast as they could divide, resulting in no net population accumulation under the best growth conditions. However, substantial blooms do occur, suggesting that these cells must actively regulate their distribution and so reduce advective losses.

A decade of investigations in the South San Francisco Bay has demonstrated that estuarine phytoplankton biomass fluctuates in the time scale of days to weeks, and that much of this variability is associated with fluctuations in the tidal forcings (Cloern 1991). The occurrence of blooms only during the spring was presumed to be a consequence of the enhanced water column stability that occurs following freshwater inflow during the wet season. Although the duration and magnitude of the spring bloom varied from year to year, it was a persistent

feature that occurred every year from 1980-1990 (period of investigation). However, this feature was not sustained for the shorter timescales associated with the daily evolution of individual bloom events. Other observations from this and other (Haas *et al.* 1981, Roden 1984) estuaries have shown that rapid population growth often occurs during periods of low tidal energy (neap tides). For South San Francisco Bay, phytoplankton blooms always occurred during sustained weak tides where tidal energy was low, with bloom declines following periods of strong currents.

The spring bloom in the Straits of Georgia, which lies between the Vancouver Island and the lower mainland of British Columbia was investigated in April 1991 (Yin *et al.* 1996). They observed that the Fraser river inputs during March had been sufficient to counteract wind and tidal mixing. The stability of the water column allowed phytoplankton to bloom, with algal biomass and production higher at the more stratified sites. An average wind speed of approximately 5 m s^{-1} over 7 days destroyed the stratification and chlorophyll *a* concentrations reduced by half. The magnitude of the early spring bloom was never again achieved, and it was postulated that this wind event had altered the phasing between phytoplankton and zooplankton in the Strait.

A common feature connecting research on phytoplankton blooming in highly dynamic estuaries appears to be the necessity for initial water column stability in the form of stratification (salinity and/or thermal). The intensity of these blooms thereafter, depends on a wide array of variables controlling the bloom dynamics, such as the availability of light, nutrients and the prevailing flushing rate. The investigations presented in this thesis targeted tidal turbulence which acts to control the proliferation of phytoplankton populations in estuarine and coastal temperate waters.

1.10 RESEARCH OBJECTIVES

The main objective of this research was to investigate the physical mixing processes that combine to control the growth, distribution and succession of the phytoplankton community in coastal temperate waters. The following hypotheses were tested using results from a number of intensive field surveys undertaken in a partially-mixed, macrotidal estuary (Southampton Water) and in the shallow coastal southern North Sea.

1. Intermittency of turbulence is fundamental for the proliferation of phytoplankton.
2. Extended water column stability is not a prerequisite to an abundant phytoplankton community in a partially mixed estuary.
3. Certain motile phytoplankton species can respond to short lived, intermittent stabilising events and apparent behavioural migrations by motile species are ultimately constrained by vertical mixing.
4. Boundary shear generated by tidal forcings within an estuary causes re-suspension of both the bottom sediments and the phytobenthic community, permitting the organisms to be intermittent members of the pelagic microalgal community.

2. METHODOLOGY

2.1. CHAPTER TWO: SUMMARY OF METHODOLOGICAL APPROACH

This chapter presents the methodology adopted in this research. It is divided into two parts: (i) the research design and (ii) the data collection and analysis. The research design is discussed in the first part, while the second part discusses the data collection and analysis.

Methodology is the systematic way of conducting research. It is concerned with the design and execution of research activities. The methodology adopted in this research is qualitative research, which involves the collection of data through interviews, case studies, and document analysis. The research design is based on the principles of qualitative research, which include the following:

CHAPTER TWO

METHODOLOGY

The research design in this study is qualitative research with a focus on descriptive research. The data collection methods used in this study include interviews, case studies, and document analysis. The data collection process involved the following steps:

2.2. CHAPTER TWO: SUMMARY OF METHODOLOGICAL APPROACH

This chapter presents the methodology adopted in this research. It is divided into two parts: (i) the research design and (ii) the data collection and analysis. The research design is discussed in the first part, while the second part discusses the data collection and analysis.

Methodology is the systematic way of conducting research. It is concerned with the design and execution of research activities. The methodology adopted in this research is qualitative research, which involves the collection of data through interviews, case studies, and document analysis. The research design is based on the principles of qualitative research, which include the following:

2. METHODOLOGY

2.1 GENERAL SAMPLING STRATEGY FOR SOUTHAMPTON WATER

The Southampton University Department of Oceanography research vessel (*Bill Conway*) was used for all studies in Southampton Water estuary, during the spring-summer months from 1995-1997.

Conductivity, temperature and depth (CTD) profiles were recorded using a Falmouth Scientific CTD with attached Aquatracka III fluorometer and Seatech 25cm pathlength transmissometer. A Niskin water bottle (6 x 1.6 litre, bottle length ~50cm) rosette fixed to the CTD frame provided simultaneous discrete water samples, with instruments and water samples at the same vertical position, but separated by 0.5m horizontally. A downward facing ADCP (Acoustic Doppler Current Profiler) was deployed on the port-side of the vessel recording data at 1-5 minute intervals with 0.5-1.0 m depth resolution. On the days when the ADCP was unavailable, an NBA current profiler was deployed to measure velocity magnitude and direction. For surveys during summer 1996 and 1997, a profiling Li-COR submersible cosine sensor was deployed, measuring downwelling irradiance over the photosynthetically active radiation (PAR) wavelengths (350-700 nm), with a second sensor recording surface incident PAR. Both sensors were logged simultaneously with time into a Li-COR data logger. Discrete water samples for instrument calibration (fluorometer and transmissometer) and for phytoplankton identification and enumeration were taken from the Niskin bottles, closed at 3, 4 or 5 depths.

2.2 INSTRUMENT SPECIFICATIONS

2.2.1 CONDUCTIVITY TEMPERATURE DENSITY SENSOR (CTD)

The CTD unit consisted of a Falmouth Scientific Inductive Conductivity Sensor with a range of 0-65 mho cm^{-1} set at a sampling frequency of 6 Hz; a Falmouth Scientific titanium pressure sensor with a range of 0-2000 psi, set at a sampling frequency of 6 Hz; and a Falmouth Scientific pressure protected stabilised thermistor (glass) with a range of -2 to 32 °C set at a sampling frequency of 6 Hz. Depth correction was applied to all raw data to amend changes in the diameter/length of the sensor measurement volume as a function of bulk

compressibility. The cell changes size due to the thermal expansion coefficient of the alumina.

A FORTRAN programme, written by Dr L Nash, was used to offset the depth, calculate salinity (UNESCO tech paper 44) and also convert the logarithmic fluorometer signal to fluorescence units and the transmissometer to attenuation.

2.2.2 FLUOROMETER (CHELSEA INSTRUMENTS, AQUATRACKA III)

The measurement of red light emitted from photosynthetic pigments when excited by blue light, forms the basis of the fluorometric method for measuring chlorophyll *a* and hence algal biomass in sea water. The Aquatracka III measured the fluorescence through a 2-beam ratiometric method, in which the intensity of a beam of light from the water sample was compared to a reference beam. The light was directed onto a photo-diode and was converted into a logarithmic voltage signal. Sampling rate was 0.5Hz. Examples of calibration parameters are listed in Table 3.0.

FLUOROMETER CALIBRATION

DAY	R ²	Intercept	Slope
Late May	0.663	-32.970	19.137
August	0.867	-41.941	21.283

Table 3.0. Calibration parameters of the Aquatracka III.

2.2.3 TRANSMISSOMETER (SEATECH, 25CM PATHLENGTH)

A transmissometer measures the ratio of transmitted light flux (E_T) and incident light flux (E_0) at both ends of a narrow beam of fixed length (25cm). When all light entering the near end of the beam also exits the far end, transmission is 100% (0% attenuation). This is an optical method used to quantify suspended particulate material (SPM) which relies on the inherent properties of light transmission in water, i.e. attenuation due to the scattering-deflection of water molecules, dissolved solids, suspended particles and absorption which convert light to heat or energy with a different wavelength. The sampling rate was 0.5Hz.

2.2.4 ACOUSTIC DOPPLER CURRENT PROFILER (ADCP)

The RD Instruments ADCP is based on the Doppler shift, and transmits sound at a fixed frequency and 'listens' to the echoes returning from sound scatterers in the water. These scatterers are small particles or plankton that reflect sound back to the ADCP and in general move at the same horizontal velocity as the water. The Doppler shift is a measure of the relative radial velocity between different objects and is the change in the observed sound pitch, resulting from relative motion which is directly proportional to velocity. An ADCP senses different velocity components using multiple beams pointed at different directions. This four beam ADCP generates two horizontal velocities and two estimates of vertical velocity for the three components of the flow (horizontal, perpendicular horizontal and vertical). The velocity profile is broken into uniform bins (depth cells) where each bin is comparable to a single current meter. The bin depth used was 0.5 - 1.0 m, depending on the ADCP frequency. Profiles are produced by range-gating the echo signal, which breaks up the signal into successive segments and processes each separately. Echoes from hard surfaces (e.g. surface or bottom) are so much stronger than from scatterers, that suppression of the transducer side-lobe occurs. This causes echoes from the side-lobe facing the surface, to return to the ADCP at the same time as the echo from the main lobe, thus a percentage of the data is usually contaminated. However, the percentage of 'bad' data is dependent on the angle of the transducers and the use of narrow or broad band ADCP. The ADCP also produces binned data for beam intensity, which can be averaged (over the 4 beams) to provide a measurement of the relative backscatter. In 1995, the instrument used in the Southampton Water studies was an RD Instruments 1200kHz, narrow band ADCP (% bad data =15). In 1996 and 1997, the instrument used was an RD Instruments 600kHz, broad band ADCP (% bad data =20). During the North Sea, CH129 cruise, a vessel mounted RD Instruments 150kHz, narrow band ADCP was used (% bad data = 10).

2.2.5 NBA CURRENT PROFILER

The NBA current meter, unlike the ADCP, gives velocity magnitude and direction readings at one depth only, but can provide data from the near bottom and near surface waters. During 1995 and 1996, vertical profiles were performed every 0.5hr, with 0.5-1.0 m depth resolution. The instrument relies on the physical motion of the water to rotate a paddle which translates this movement into a velocity measurement (ms^{-1}). An internal compass determined direction (degrees).

2.2.6 LI-COR COSINE IRRADIANCE SENSOR

This sensor is cosine-corrected to allow measurement of irradiance flux densities through a given plane. When a parallel beam of radiation of given cross-sectional area spreads over a flat surface, the area that it covers is inversely proportional to the cosine of the angle between the beam and a plane normal to the surface. Therefore, the irradiance due to this beam is proportional to the cosine of the angle. This instrument also has an immersion effect when profiling in water, where correction factors need to be applied to normalise the measurement to a typical air reading. Final values are given as photon irradiance (i.e. the rate of arrival of visible quanta per unit area) in units of $\mu\text{E m}^{-2} \text{ s}^{-1}$ ($\equiv \mu\text{mol m}^{-2} \text{ s}^{-1}$).

2.3 LABORATORY ANALYSES AND INSTRUMENT CALIBRATION

2.3.1 CHLOROPHYLL *a* DETERMINATION

Chlorophyll *a* and phaeopigment concentration were determined by filtering between 100-200ml water (collected in Niskin bottles at known depth) through 25mm diameter Whatman GF/F filters. Filters were stored frozen, in the dark until analysis. 5ml of 90% acetone was added to each filter and ground using an ultra-turrax mixer for ~3 minutes (or until fully pulped). This mixture was centrifuged for 5 minutes at 3000rpm and the supernatant removed and mixed (to destroy any pigment concentration gradients). This supernatant was measured in an Aminco fluorometer, before and after acidification (a reading was taken after the addition of 2 drops of 10% (v/v) HCl to allow the calculation of total phaeopigment concentration). Pigment concentrations were calculated using equations based on the methods of Lorenzen (1967). The Aminco fluorometer was calibrated with a standard solution of chlorophyll *a* (Sigma chemicals), assayed using a spectrophotometer, as described by Parsons *et al.* (1984).

2.3.2 TOTAL SUSPENDED PARTICULATE MATTER

The conversion of beam attenuation to total SPM concentration was gravimetrically processed using the discrete water samples. Total SPM in the water samples was determined by filtering 100-200ml water through pre-weighed and dried 25mm diameter Whatman GF/F filters (pore size 0.7 μm). Before storage, ~10ml distilled water was passed through the filter to prevent the formation of salt crystals. All filters were dried overnight at 80°C and re-weighed.

$$\text{Total SPM concentration (g l}^{-1}\text{)} = \frac{(Wt_2 - Wt_1)}{V} \quad (4)$$

where: Wt_1 = initial weight of filter after drying (g); Wt_2 = weight of sample + filter after drying (g); V = sample volume filtered (litre).

2.3.3 CURRENT VELOCITY

ADCP data were further analysed to provide velocity shear (τ , s^{-2}) and gradient Richardson number (Ri). Where:

$$\tau (s^{-2}) = \left(\frac{\delta u}{\delta z} \right)^2 \quad (5)$$

where z = depth; u = velocity magnitude.

$$Ri = - \frac{g}{\rho} \frac{\delta \rho}{\delta z} \left/ \left(\frac{\delta u}{\delta z} \right)^2 \right. \quad (6)$$

where g = acceleration due to gravity; ρ = density.

2.3.4 ATTENUATION COEFFICIENT

The diffuse attenuation (=extinction) coefficient for a water sample was calculated from two PAR measurements at different depths:

$$k (m^{-1}) = \frac{\log_e I_1 - \log_e I_2}{d_2 - d_1} \quad (7)$$

where I_1, I_2 = irradiance at depths 1 and 2; d_1, d_2 = depths at two measurements ($d_2 > d_1$) in metres.

2.3.5 PHYTOPLANKTON PRESERVATION, IDENTIFICATION AND ENUMERATION

All whole water samples were preserved with Lugol's iodine solution for storage until microscopic examination. A stock solution of 200 g KI, 100 g I₂ in 2000 ml H₂O with 190 ml glacial acetic acid was prepared (Parsons *et al.* 1984). To each 200 ml whole water sample, 0.2 ml Lugol's Iodine was added.

In 1995, species identification and cell counts involved a 2-stage sampling process:

- i. Primary sub-samples for concentration through sedimentation
- ii. Secondary sub-samples (1 ml) from the concentrate for identification and counting in a Sedgewick-Rafter chamber.

Using 10-20 ml sedimentation chambers, samples were settled for at least 12 hours, allowing for a sedimentation rate of 4 cm d⁻¹ (Kifle 1992). The surface volume was removed using a pipette and the remaining 1 ml (allowing for ~0.5 ml evaporation) was mixed and removed to a Sedgewick-Rafter chamber and left to stand for 5 minutes. Species identification was performed using an inverted Leica microscope with 100-400 x magnification.

Cell counts were calculated using:

$$\text{Cells litre}^{-1} = \frac{(10^6 \times C)}{(15 \times F)} \quad (8)$$

where: C= number of cells counted in 15 squares (1 square=1 μl); F= concentration factor (volume primary sub-sample/ volume secondary sub-sample).

During 1996 and 1997, cells were identified and enumerated on the base plate of the sedimentation chambers. Samples were left to settle overnight. The total area of each base plate was 490.87 mm², and the actual area counted was determined by the number of transects viewed. 1-4 whole transects were counted, depending on cell density.

Counting error was calculated on the basis of triplicate sampling of one Sedgewick-Rafter or sedimentation chamber. Standard deviations were related to the concentration of cells per sample (i.e. high cell densities = reduced error). Sub-sampling and counting error was calculated as a % coefficient of variation (%CV) determined by the standard deviation divided

by the mean. In all cases $\%CV < 15$.

During the North Sea CH129 cruise, whole water samples were counted live, as few motile species were present. Samples were concentrated by filtering 0.5-1.0 litre through a 20 μm nylon mesh. The mesh was washed and then re-suspended in 10 ml filtered seawater and 1 ml was transferred to a Sedgewick-Rafter chamber, where 30-50 squares were counted, depending on cell density.

Species identification was determined through the use of identification keys including Drebes (1974).

2.3.6 DATA MANIPULATION AND PLOTTING

Data from the ADCP were filtered and averaged at 5 minute intervals, using the *Transect* software supplied by RD Instruments. As these data were collected using a downward facing ADCP, the data were normalised to the sea surface and blanking files were created to eliminate "bad" data. This information is presented using the surface mapping package *Surfer* (Win32) v. 6.02. The gridding method used was Kriging, with grid sizes determined by the sampling frequency. In all cases the data were normalised to the sea bed, with blanking files added to each diagram to highlight the varying water column height due to the tidal influence.

The CTD data were filtered to remove any above water sampling collected during the deployment, and both the up and down cast are presented in the figures. The same mapping (*Surfer*) programme as for the ADCP data was used for these plots.

X-Y plots were produced using the graphical options in *Excel* (version 7.0) and *Quattro Pro* (version 6.0 for windows).

2.4 LABORATORY EXPERIMENTS

2.4.1 SUBCULTURING TECHNIQUES

12 species of phytoplankton (Appendix II) were routinely maintained in the laboratory, in 200ml batch cultures, each species in duplicate. The growth media used was a modified Keller's recipe (see Appendix II) in filtered seawater (salinity >31). Borosilicate glass and

polycarbonate conical flasks were used, with cotton bungs covered with muslin. 200 ml filtered sea water (FSW) was added to each glass conical flask and sterilised in a Rodwell autoclave. The sterilisation period was 30 minutes at 120 °C at a pressure of 2.2 bar. All species were subcultured at two week intervals.

From this culture collection, species were chosen to carry out experiments investigating the effect of turbulence on growth rate. In each case turbulence was created by bubbling air into a batch culture of varying volume.

2.5 GROWTH RATE EXPERIMENTS

2.5.1 AMPHIDINIUM CARTERAE (SMALL VOLUME)

Growth rates were determined for the dinoflagellate *Amphidinium carterae* grown in varying turbulent conditions. 3 x 1 litre Duran bottles were autoclaved with 800ml FSW and enriched with Full Keller's nutrient recipe (no added NH₄Cl). Two bottles simulated a turbulent regime in which air was pumped into the culture at varying flow rates (i.e. low turbulence, 50-100 cc min⁻¹; a high turbulence, 200-300 cc min⁻¹) quantified using a flow gauge. The third culture was left as a control with no bubbling, although stirring did occur before each sampling period to ensure a representative sample. Temperature was kept constant at 15°C with the use of a water bath, set on a light bank providing irradiance of ~100μE m⁻² s⁻¹, on a 16:8hr L:D cycle. Cultures were covered with aluminium foil leaving only the base open to the light source. Cultures were inoculated to give an initial cell count of 200 cells ml⁻¹ (± 30). Cell counts were taken daily and observed using an inverted Leica microscope with 100-400 x magnification. Growth rates were calculated using:

$$k_e = \frac{\ln(N_1 - N_0)}{t_1 - t_0} \quad (9)$$

where N is number or concentration of cells in the culture, t is time, and k_e is the number of 'logarithm-to-base-e' units of increase per day. Subscripts denote values at two times and \ln indicates natural (base e) logarithms.

2.5.2 *RHIZOSOLENIA DELICATULA* (SMALL VOLUME)

Growth rates were determined for the chain-forming diatom *Rhizosolenia delicatula* grown in varying turbulent conditions. The experimental design followed that of the first culture experiment, with some modifications. Na_2SiO_3 (10 μM) was added along with Keller's nutrients and 500 cells ml^{-1} was the initial inoculum. As well as cell numbers, the actual number of cells per chain were counted. Growth rates were calculated using equation (9). Cell and chain counts were taken daily until the culture entered stationary phase.

2.5.3 *A. CARTERAE* (LARGE VOLUME)

Using a square tank (internal dimensions 282 x 268 x 339mm) growth rates of *A. carterae* were determined in a 15 litre culture. Due to the structure of the tank it cannot be autoclaved, so prior to use it was cleaned with a sterilisation solution (Presept disinfectant tablets ~2.5g sodium dichloroisocyanurate in 2 litres) and rinsed. Autoclaved FSW enriched with Keller's nutrient recipe provided the growth media. This was left to equilibrate in the constant temperature room (15 °C) before inoculation. A novel sampling technique was used to prevent any movement within the tank, in order to establish the optimum growth rate achievable in a non-turbulent environment. Three silicon rubber tubes set in a silicon bung were placed through a side wall sampling port and held at different vertical heights within the chamber. Samples were extracted daily to determine the homogeneity within the culture. Before inoculation, a siphoning system was set up, so future sampling aliquots flowed freely through the tubes. Sampling in this way prevented daily intrusion into the tank. As such a large culture volume was used, the initial inoculum was 1060 cells ml^{-1} (\pm 60). Temperature was kept constant at 15°C, with irradiance at 100 $\mu\text{E m}^{-2} \text{ s}^{-1}$ set on a 16:8 hr L:D cycle. Sampling occurred daily from each position.

2.5.4 *R. DELICATULA* (LARGE VOLUME)

Using the experimental set up as for the third culture experiment, growth rates for *Rhizosolenia delicatula* were determined. Two initial trials using this diatom with this experimental design proved unsuccessful, (which used Keller's nutrient recipe with the extra addition of Silica). The initial inoculum was 530 cells ml^{-1} (\pm 35). Temperature was kept constant at 15°C, with irradiance at 100 $\mu\text{E m}^{-2} \text{ s}^{-1}$ set on a 16:8 hr L:D cycle. Sampling occurred daily from each position until the stationary phase. Chain length was also determined.

— 1 —

CHAPTER THREE

SOUTHAMPTON WATER

3. SOUTHAMPTON WATER

3.1 GENERAL INTRODUCTION TO SOUTHAMPTON WATER

Southampton Water forms the north-westerly extension of the Solent System on the south coast of England, and includes the estuaries of three chalk-derived rivers: - Test, Itchen and Hamble (Figure 3.0). The Test and the Itchen, enter at the head of Southampton Water and account for 45% of the total river flow into the Solent. In a typical year, the Test has a discharge of 25 cumecs in mid-winter, diminishing exponentially during the summer to 6 cumecs the following October. The flow from the Itchen is approximately half that of the Test.

Southampton Water is a partially-mixed estuary, with an active central shipping lane, where the main channel is dredged to a depth of 15m from the mouth to the upper reaches of the Test estuary. This dredging from 12-15 m occurred during September 1996 - May 1997. Southampton Water is 10km in length, with a maximum width of 2 km and is bordered by the urbanised area of Southampton with major industrial and chemical sites such as the Calshot power station and the Esso oil refinery at Fawley. Limited intertidal mudflats remain along the western shore at Hythe.

The salinity structure along Southampton Water, very much depends on the tidal state and the seasonal cycle of freshwater flow (Phillips, 1980). At high water a weak stratification occurs, with surface salinities usually exceeding 30 at Dock Head (at the confluence of the Test and Itchen rivers) during the summer and autumn. The vertical salinity difference at the mouth of Southampton Water, typically ranges from 0.5 to 3, with a seasonal range in temperature between 3.0 - 21°C. A seaward decrease in water temperature generally exists.

The area has an unusual tidal pattern, first described by Airy (1843), where the interaction of the M_4 and M_6 tidal constituents (particularly prominent during a spring tide) creates a double high water, making their combined amplitude significant when compared to the principal lunar tide (M_2). This high water stand can last up to three hours, reducing the time available for the ebb phase. The resulting tidal asymmetry leads to six hours of moderate flood currents and four hours of rapid ebb velocities up to 1.5 ms^{-1} . The flood has a normal duration (6 hours), but there is an intermediate near stand (1 hour) which commences 2 hours after low water (Webber, 1980) where tidal current velocities are temporarily reduced. Maximum currents for the ebb occur 2 hours before low water at neap tide and 1 hour before at spring

tide; whilst during the flood period, maximum currents occur 2 hours and 1 hour after low water for the neap and spring tides respectively. This cyclicity of tidal energy and slack water generates semi-diurnal periods of strong mixing, with intensity being greatest during the ebb phase and increasing from a neap to a spring tide. Spring currents are twice those of neaps, displaying a tidal prism volume ratio of 2:1.

Williams (1980) suggested that photosynthetic processes in Southampton Water are mainly controlled by planktonic rather than benthic species. This however, was based on both a low frequency temporal sampling programme and little data of microphytobenthic community production. Estimates by Iriarte (1992) of total water column primary production (POC and DOC) showed Southampton Water to be a moderately productive estuary, with rates of 207 g C m⁻² yr⁻¹ measured at Netley (mid-estuary) and 162 g C m⁻² yr⁻¹ calculated for Calshot (mouth). Temperature and salinity stratification is seen at Netley in the summer months, with maximum chlorophyll *a* concentration reaching 350 mg m⁻² in mid June (Iriarte 1992). Calshot remains vertically homogenous throughout the year, with a chlorophyll *a* maximum of 160 mg m⁻² at the end of April. Chlorophyll *a* levels are reported to decrease from the mid-estuary region, longitudinally down toward the mouth (Bryan 1979; Antai 1990; Kifle 1992).

Kifle (1992) described the spatial and seasonal distribution of phytoplankton at two stations in Southampton Water from intensive studies conducted during 1988-1990. He observed that phytoplankton populations were established on the low neap tides and were then apparently flushed from the system during spring tides. Individual species tended to develop on the neap tides when water stability was enhanced, with a succession of species dominating between May and August. In years of exceptional red tides, dominated by the phototrophic ciliate *Mesodinium rubrum*, this physical-biological association may be further aligned with a modulation of the spring tide due to the N₂ tidal constituent. A review of the tidal data and literature indicates that the spring tide associated with the full moon exhibits a reduced tidal range compared to the new moon and in some years produces a range close to the mean. This extends the period of reduced tidal mixing, enhancing dynamic stability and permitting sustained net growth of the population within the estuary. *M. rubrum* blooms were often associated with these reduced spring tides, and during the summers of 1985 and 1986 reached concentrations of 3×10^5 cells litre⁻¹, corresponding to chlorophyll *a* concentrations of >100mg m⁻³ (Crawford and Lindholm 1997). This association between *M. rubrum* and the dynamic stability of the water column was further explained by Crawford and Purdie (1992) who examined the vertical distribution of the organism in relation to a tidal cycle. Apparent

vertical migration was observed, suggesting that the photosynthetic ciliate population aggregates in the surface layers during the high water stand, and at the onset of the ebb flow, moved down in the water column. However, when vertical mixing becomes intense, the population can no longer occupy a 'suitable' position in the water column.

From several studies conducted in Southampton Water, a typical pattern of phytoplankton succession occurring over the spring and summer months can be described, as summarised in the Table 4.0.

SEASON	SPECIES	PHYTOPLANKTON GROUP
Mid April- May	<i>Skeletonema costatum</i> <i>Thalassiosira spp</i>	Diatoms
Apr/ May - June	<i>Rhizosolenia delicatula</i>	
Late August	<i>Chaetoceros spp.</i>	
Mid-Late May	<i>Eutreptiella marina</i>	Euglenoids
End May - Late August	<i>Mesodinium rubrum</i>	Ciliate (autotroph)
Mid June	<i>Peridinium trochoideum</i>	Dinoflagellate

Table 4.0. Phytoplankton Species Succession in Southampton Water (Kifle, 1992).

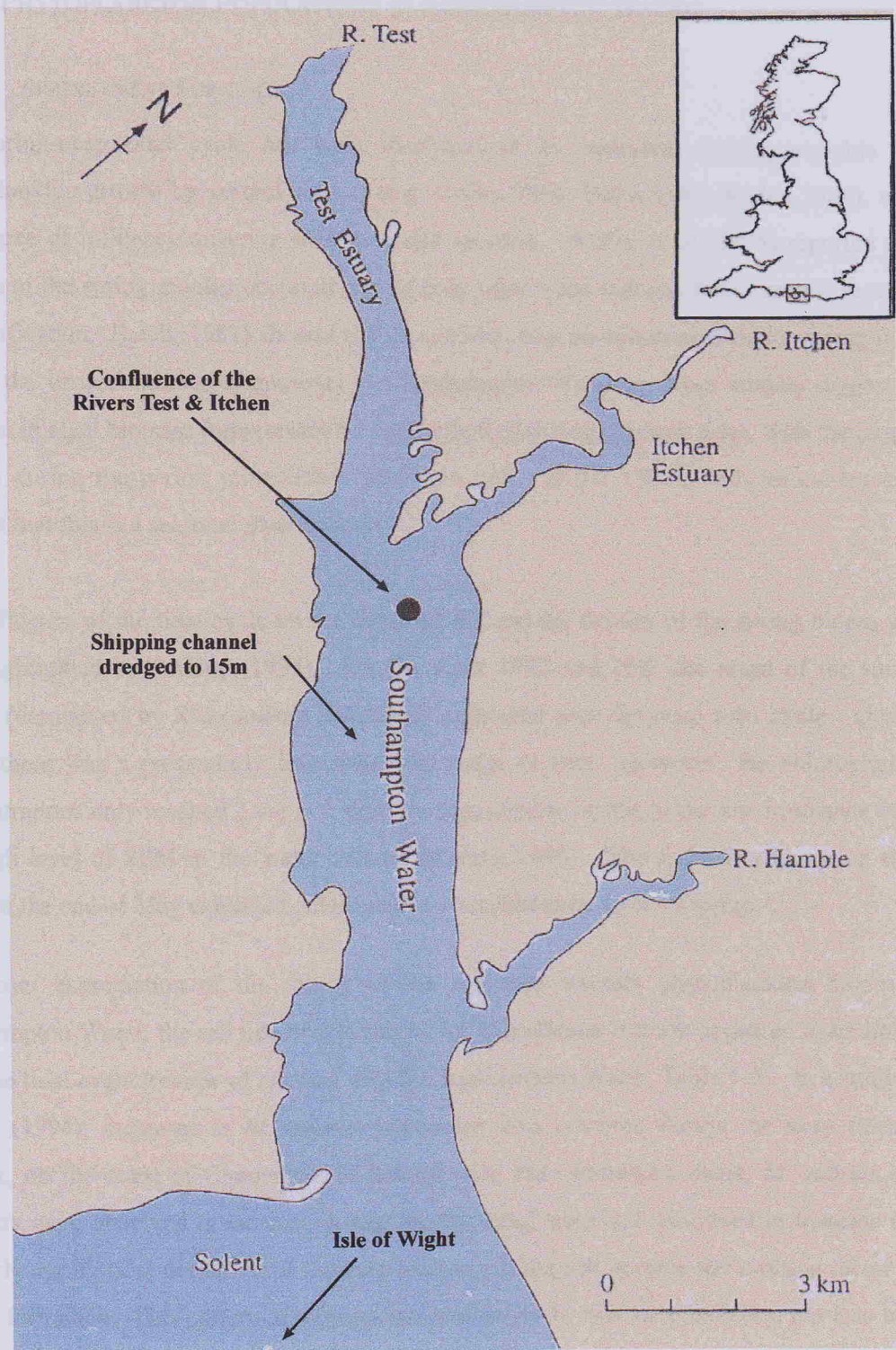


Figure 3.0 - Southampton Water estuary, highlighting the major fresh water rivers entering from the north.

3.1.1 PHYTOPLANKTON POPULATIONS IN SOUTHAMPTON WATER

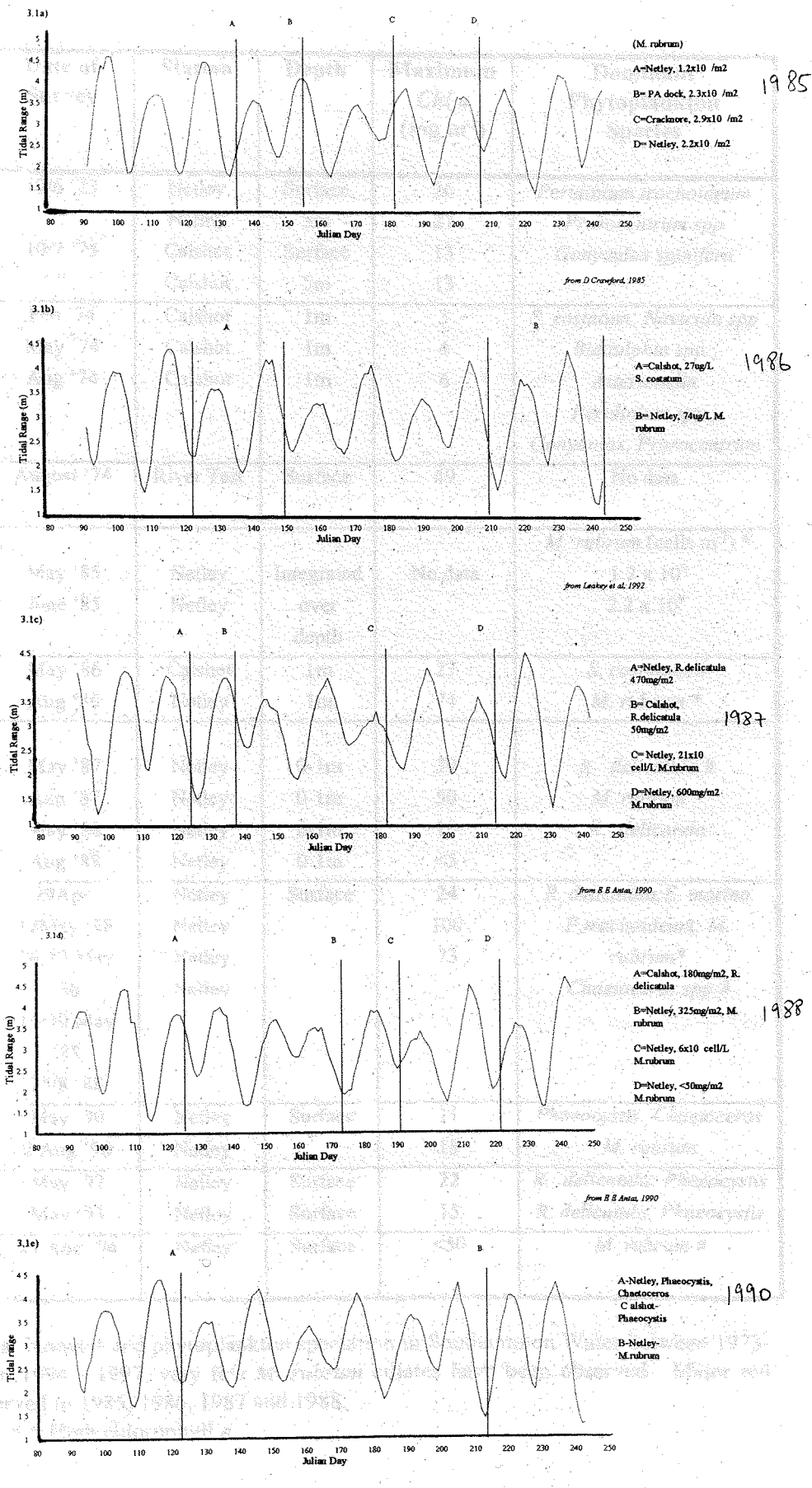
3.1.1.1 SPRING-NEAP FORCINGS

The spring-neap tidal cycle has been identified as an important driving variable for phytoplankton growth by several authors (e.g. Cloern 1991; Balch 1981; Roden 1984), with the degree of influence differing with time and location. Winter *et al* (1975) reported that blooms in the spring months occurred during neap tides when reduced tidal currents resulted in stratification. Balch (1981) showed that in summer, blooms occurred at major spring tides due to the vertical mixing of nutrients. In Southampton Water, previous studies suggest an increase in algal biomass (represented by chlorophyll *a*) during the neap tides, with the largest growth during the period immediately after low neaps (Kifle 1992), with no evidence to suggest that this is a seasonal phenomenon.

The influence of the tidal cycle on the development and the demise of the spring bloom was also highlighted by Anning (1995). For the years 1992 and 1993 the onset of the spring bloom (dominated by *Rhizosolenia delicatula*) coincided with the neap tidal cycle. During 1992, there was a particularly low neap tidal range (1.5m). However, the chlorophyll *a* concentrations only reached 2 mg m^{-3} , this was suggested to be due to the low irradiance from the high level of SPM in the water column (Anning 1995). The following low neap tidal range at the end of May exhibited chlorophyll *a* concentrations up to 22 mg m^{-3} .

On closer examination of the timing of the recurrent summer phytoplankton bloom in Southampton Water, the red tide events caused by *Mesodinium rubrum* appeared to be linked with the tidal cycle (review of existing data for Southampton Water, Table 5.0). In a study by Roden (1994), increases in *M. rubrum* population also occurred during the neap tides at Glynsk, on the coast of Connemara in Ireland. On the Connemara coast, *M. rubrum* cell numbers were observed to increase during the low neap tides and continued to increase into the early spring tidal period, until flushing rates amplified and became the limiting factor for bloom formation. This pattern of biomass increase in the *M. rubrum* population has also been observed in Southampton Water. High frequency temporal studies, over a daily tidal cycle, have shown this autotrophic ciliate to vertically migrate through the water column, presenting the opportunity to increase its residence time in the estuary by reducing the flushing losses (Crawford and Purdie 1992). However, during spring tides, where flushing rates are enhanced, individuals are removed from the estuary. In 1985, 1986, 1987 and 1988 when exceptional blooms of *M. rubrum* occurred, the tidal pattern prior to blooming took on a

similar pattern (Figure 3.1). Usually, the second spring tide of each lunar month repeatedly has a smaller tidal range than the first, but in the above years this second spring was exceptionally small. This suggests that tidal flushing rates were reduced, allowing a larger population to remain in the estuary. In conjunction with the neap tides, this provided a prolonged period during which tidal energy was low, extending the time during which rapid growth could occur. This asymmetry in tidal range is the result of the orbit of the moon around the earth-moon centre of mass: it is not circular, but elliptical. The variation in distance from earth to moon results in corresponding variations in the tide-producing forces. When the moon is closest to earth, it is said to be in perigee, and the moon's tide producing force is increased by up to 20 % above the average value. When the moon is furthest from the earth, it is in apogee, where the tide producing force is reduced by 20 % below the average. The interval between successive perigrees is 27.5 days. Figure 3.1 shows the spring and summer predicted tidal ranges for the years when exceptional red tides of *M. rubrum* occurred. Phytoplankton blooms occurred during the neap to spring tidal period, and formed exceptional concentrations when the flushing rates (freshwater fraction method) were reduced, during periods of a double low spring tidal range. The instigation of the phytoplankton increase at the start of the spring bloom is likely to be irradiance dependent (general observation of the timing of blooms in 1997).

Figure 3.1 - Predicted tidal ranges for years when exceptional blooms of *M. rubrum* occurred.

Year and Author	Date of Survey	Station	Depth	Maximum Chl a (mg m ⁻³)	Dominant Phytoplankton Species
Diwan 1978	19/6 '73	Netley	Surface	26	<i>Peridinium trochoideum</i>
	"	Netley	5m	27	<i>Prorocentrum spp</i>
	10/7 '73	Calshot	Surface	13	<i>Gonyaulax spinifera</i>
	"	Calshot	5m	13	
Burkhill 1978	Feb '74	Calshot	1m	3	<i>S. costatum; Navicula spp</i>
	May '74	Calshot	1m	4	<i>Biddulphia spp.;</i>
	Aug '74	Calshot	1m	6	<i>Asterionella</i> <i>Peridinium spp.;</i> <i>Gonyaulax, Prorocentrum</i>
Bryan 1979	August '74	River Test	Surface	49	No data
Crawford 1992	May '85	Netley	Integrated over depth	No data	<i>M. rubrum</i> (cells m ⁻²) *
	June '85	Netley			1.2 x 10 ⁹
					2.2 x 10 ⁹
Leakey 1986	May '86	Calshot	1m	27	<i>S. costatum</i> #
	Aug '86	Netley	1m	74	<i>M. rubrum</i> *
Antai 1989	May '87	Netley	0-1m	39	<i>R. delicatula</i> #
	Aug '87	Netley	0-1m	50	<i>M. rubrum</i> *
	May '88	Netley	0-1m	10	<i>R. delicatula</i>
	Aug '88	Netley	0-1m	<5	-
Kifle 1992	29Apr- 12May '88	Netley	Surface	24	<i>R. delicatula; E. marina</i>
	16-19 May '88	Netley		100	<i>P. trochoideum; M.</i>
	14-30 May '88	Netley		73	<i>rubrum</i> *
	25/8 '88				<i>Chaetoceros spp</i> #
Iriarte 1992	May '90	Netley	Surface	11	<i>Phaeocystis; Chaetoceros</i>
	2 Aug '90	Netley		18	<i>M. rubrum</i>
Anning 1995	May '92	Netley	Surface	22	<i>R. delicatula; Phaeocystis</i>
	May '93	Netley	Surface	15	<i>R. delicatula; Phaeocystis</i>
Ryan 1994	25 Aug '94	Netley	Surface	<50	<i>M. rubrum</i> #

Table 5.0. Algal biomass and phytoplankton speciation in Southampton Water between 1973-1994. Between 1994 - 1997, very few *M. rubrum* ciliates have been observed. Major red tides were observed in 1985, 1986, 1987 and 1988.

* = Red Tides: # = High chlorophyll *a*.

3.1.1.2 RECCURRENCE OF RED TIDES AND FLUSHING RATES

Southampton Water receives fresh water from two main tributaries at its head, the River Test on the western side and the River Itchen from the east (Figure 3.2). Both these rivers contribute to 45% of the total inflow into the Solent and to 1/75 of the mean tidal prism of Southampton Water. Average monthly Test river flows were obtained from the Environment Agency (formerly NRA) from their flow gauge at the top of the Test, during the period of 1987-1995 (Figure 3.3), no data were collected for the Itchen. February, March and April typically show highest river flows, with February 1990 proving the highest over the period 1987-1995, reaching a monthly average of 30 cumecs. In 1990, January, February and March accounted for 66.6% of the annual Test river inputs. This would have caused increased estuarine flushing rates, nearing the levels quoted by Zinger (1989), of 3-5 days (compared to summer flushing rates of ~20 days). The increased river flow during certain months in the year causes both a downstream movement of the salinity intrusion from the Solent and a more rapid circulation of water, whilst at the same time increasing the buoyancy input into the estuary. Based on the fresh water flows (cumecs), residence times (Figure 3.4) within the estuary were estimated using the fresh water fraction method (Dyer 1996).

Flushing time is the time required to replace the existing fresh water in the estuary at a rate equal to the river discharge. This concept is also known as the residence time.

$$\text{Flushing time (T)} = \frac{Vf}{R} \quad (10)$$

where Vf is the total amount of river water accumulated in the section of the estuary from Netley to Calshot, and R is the river flow (based on EA values).

The mean fractional fresh water concentration over any segment is therefore:

$$f = \frac{Ss - Sn}{Ss} \quad (11)$$

where Ss is the salinity of the undiluted sea water and Sn is the mean salinity in a given segment of the estuary. The total volume of fresh water Vf is found by multiplying the fractional fresh water concentration (f) by the volume of the estuary segment.

The red-water appearance caused by *Mesodinium rubrum* was a typical feature of the recurrent, exceptional summer blooms during 1985, 1986, 1987 and 1988 (Table 5.0). During the time period of this study, exceptional red-tides were not observed, and over the period 1995-1997, *M. rubrum* has provided a small contribution to the total algal biomass, with comparatively low numbers of individuals observed. Crawford and Lindholm (1997) have suggested that the main 'triggers' governing *M. rubrum* growth are increased temperature and water column stability (from fresh water input). Combining the previous studies in Southampton Water by incorporating bloom timing, tidal régime and fresh water data, suggest that this ciliate proliferated during the neap periods (of low tidal energy) and formed red tide events during periods of a reduced spring tidal prism (i.e. the intertidal volume), which would prevent flushing losses from the estuary. Referring to Figure 3.1, the years when red-tide events occurred in Southampton Water have lower than average spring tidal ranges followed by greater neaps, suggesting that these summer periods would exhibit lower TKE and coupled with average summer riverine inputs (6 cumecs) would suggest the occurrence of a salinity stratification. For years such as 1990, where although *M. rubrum* (18 mg m⁻³ chlorophyll a) was present, a red-tide did not occur, the predicted tidal data did not suggest periods of low tidal energy (through consecutive reduced spring tides) and with the reduction in summer fresh water inputs (3 cumecs), the prerequisite of water column stability may not have been achieved.

The decline of these red-tides did not suggest an instantaneous collapse (phaeopigments did not increase, Crawford and Lindholm 1997). As with the bloom initiation, the decline of the population may have been due to tidal dynamics. The greater tidal prism of spring tides may have increased flushing rates beyond a limit that the population could sustain through growth (Ketchum 1954) or vertical migration (Crawford and Purdie 1992).

3.1.2 SUMMARY

These previous studies describing the occurrence and duration of blooms within Southampton Water were used to devise a sampling strategy for Southampton Water between 1995-1997. The timing of blooms seems to occur after neap tides, with exceptional blooms more frequent after reduced spring tidal ranges. Phytoplankton species succession suggest that diatom blooms occur in the spring months, whilst motile species seem to bloom in the summer. This background information was used as a basis for the sampling protocol implemented in Southampton Water for the period 1995-1997.

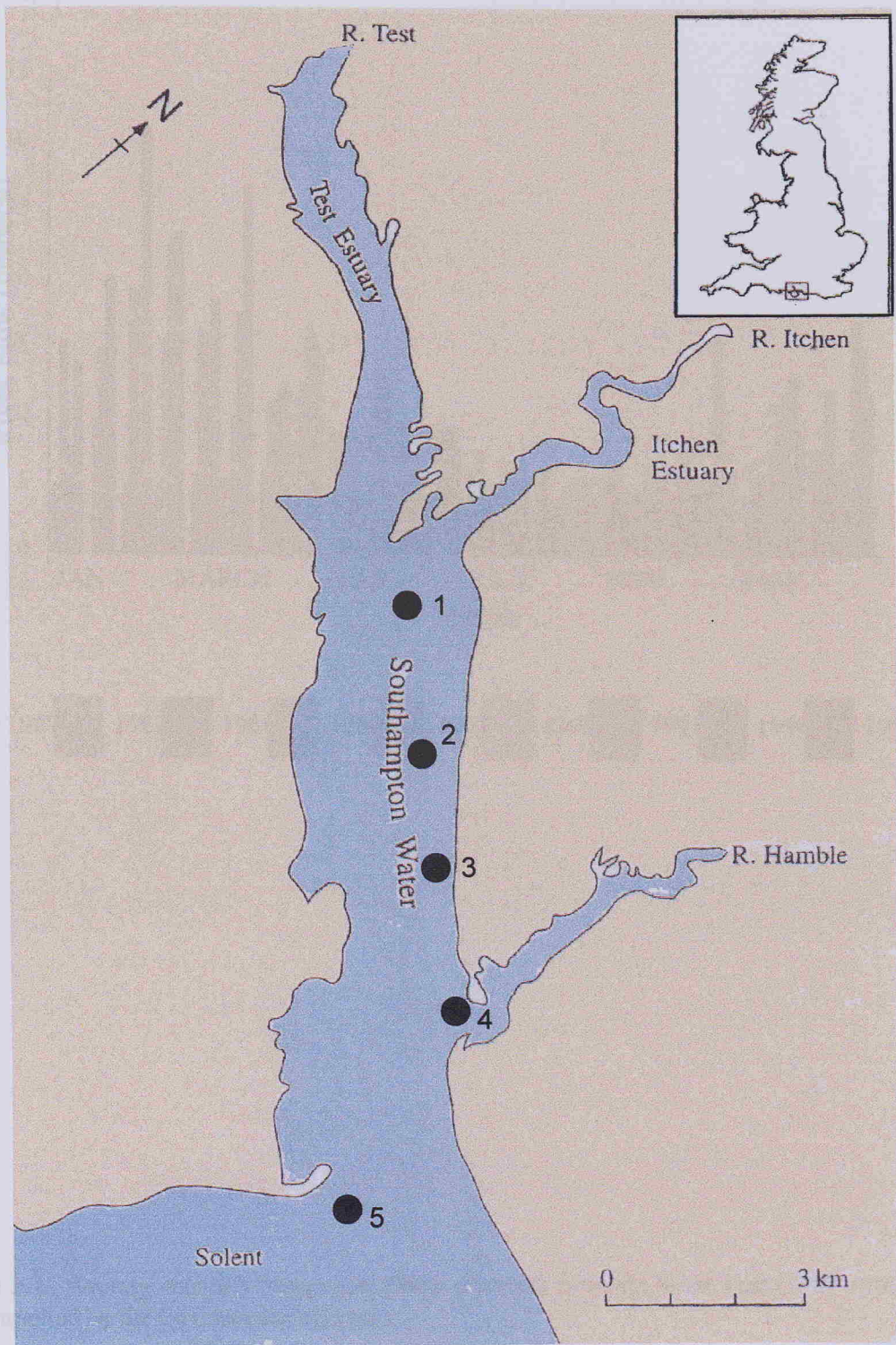


Fig 3.2 - Southampton Water estuary. Location of sampling stations used during the surveys between 1995 - 1997. 1) NW Netley. 2) Hound Navigational Buoy. 3) Greenland Buoy. 4) Hamble Jetty. 5) Calshot.

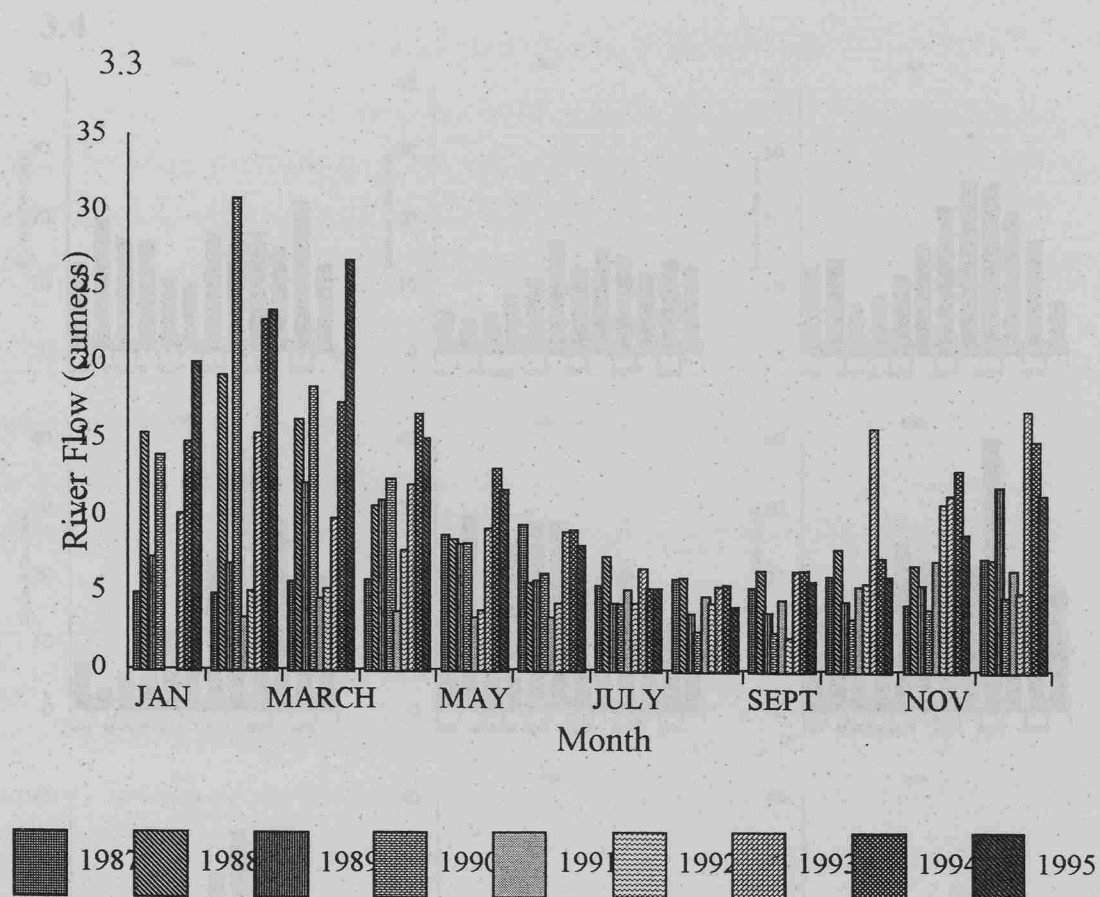


Figure 3.3. Average monthly fresh water flows (cumecs) from the River Test (1987 - 1995). Data supplied by the Environment Agency.

3.4

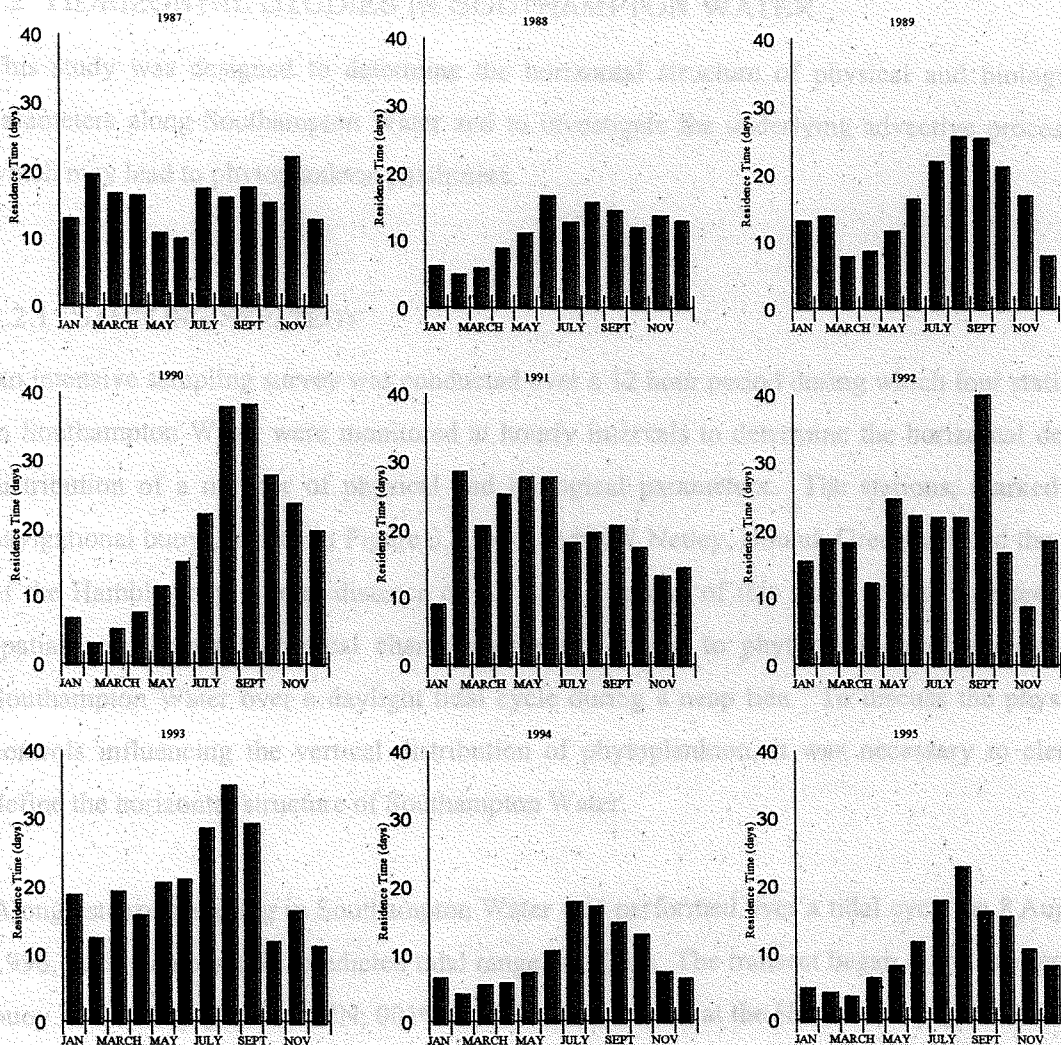


Figure 3.4. Average monthly residence times for Southampton Water (from Netley to Calshot), based on the fresh water fraction method. All time in days.

3.2 HORIZONTAL STUDIES IN SOUTHAMPTON WATER

This study was designed to determine the horizontal structure of physical and biological parameters along Southampton Water and to investigate the underlying advective processes which may lead to phytoplankton patchiness.

3.2.1 SAMPLING STRATEGY

An intensive sampling survey was conducted over a 12 hour period during which four stations in Southampton Water were monitored at hourly intervals to determine the horizontal depth distribution of a number of physical and biological parameters. The stations, marked by navigational buoys, shown in Figure 3.2, included NW Netley, Hound, Greenland and the site of the Hamble jetty, a total distance of 6.0 km. The aim of this study was to interpret the spatial and temporal physical characteristics in relation to phytoplankton populations in Southampton Water over a daylight tidal cycle during a neap tide. To discuss the physical controls influencing the vertical distribution of phytoplankton, it was necessary to clearly define the horizontal structure of Southampton Water.

Along estuary sampling in Southampton Water was performed over a tidal cycle on 8 August 1996, during a neap tide (predicted tidal range = 1.8 m). The transect began at the navigation buoy NW Netley ($50^{\circ} 51.972N$; $001^{\circ} 21.789E$), terminating at the Hamble Jetty ($50^{\circ} 50.828N$; $001^{\circ} 19.448E$). CTD casts (with attached fluorometer and transmissometer) were profiled on the hour at NW Netley beginning at 05:00 (GMT), with the last cast at 17:15 (GMT). Subsamples from Niskin bottles (5 depths) were taken for instrument calibration and phytoplankton preservation.

Profiling at the Hamble Jetty began at 05:30 (GMT), with the last cast at 17:00 (GMT). Water samples were collected and filtered through GF/F filters for chlorophyll *a* determination and gravimetric measurement of total suspended particulate matter (SPM). Phytoplankton samples were preserved from two depths. Intermediary CTD casts were deployed along the transect at Hound buoy ($50^{\circ} 51.652N$; $001^{\circ} 21.476E$) and Greenland buoy ($50^{\circ} 51.652N$; $001^{\circ} 20.324E$). Water samples were not collected at these sites. The typical current structure during a neap tide was provided from a 13hour anchor survey conducted in May 1997, when the tidal range was 2.7 m. This data was collected using a 600 kHz broad band ADCP, whilst anchored at Hound navigational buoy.

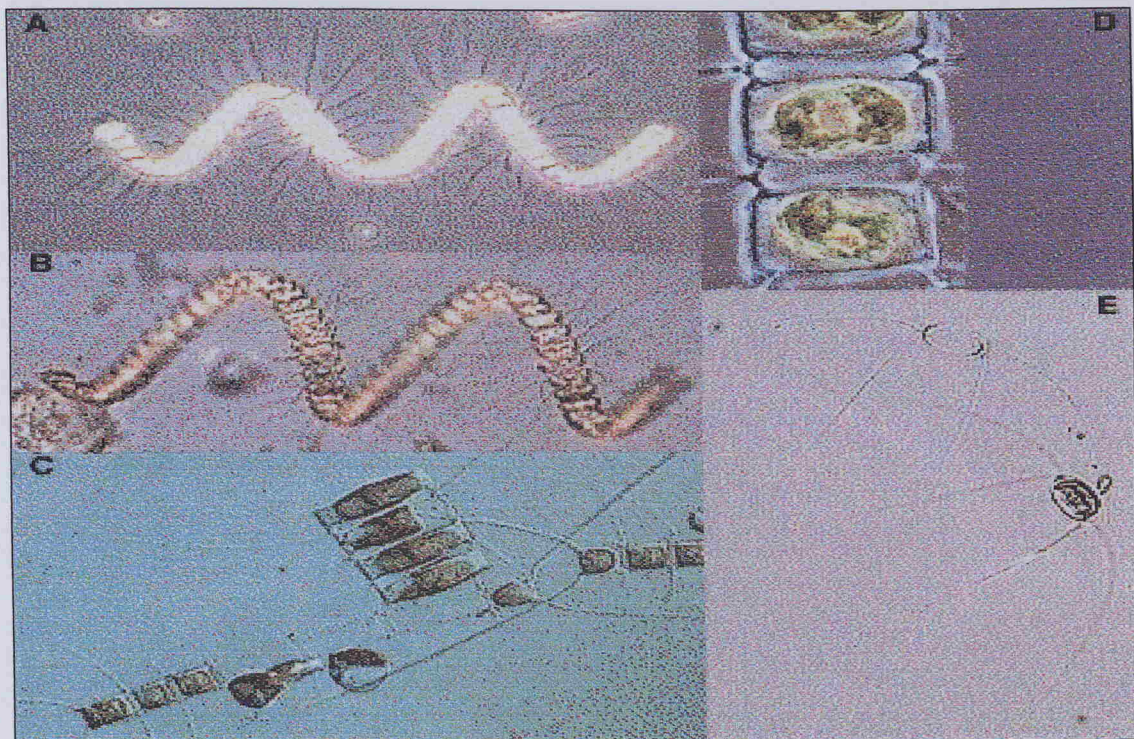


Figure 3.5 a) *Chaetoceros debilis*. Size range 10-40 μ m. A & B = spirally twisted chain; C = production of auxospores; D = frustules; E= valve view.

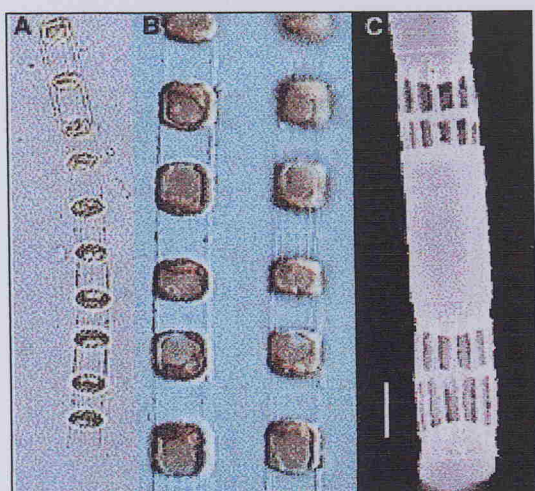


Figure 3.5 b). *Skeletonema costatum*. Size range ~5-25 μ m. A-C varying magnification.

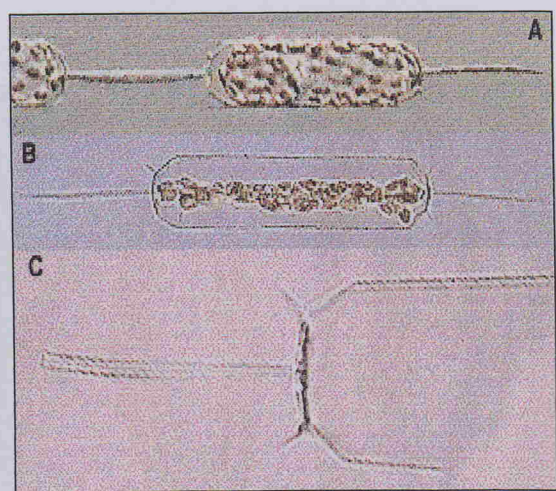


Figure 3.5 c) *Ditylum brightwelli*. Size range ~25-100 μ m. A = 2 live cells; B = whole frustule; C = part of frustule.

Figure 3.5 e) *Navicula* sp.

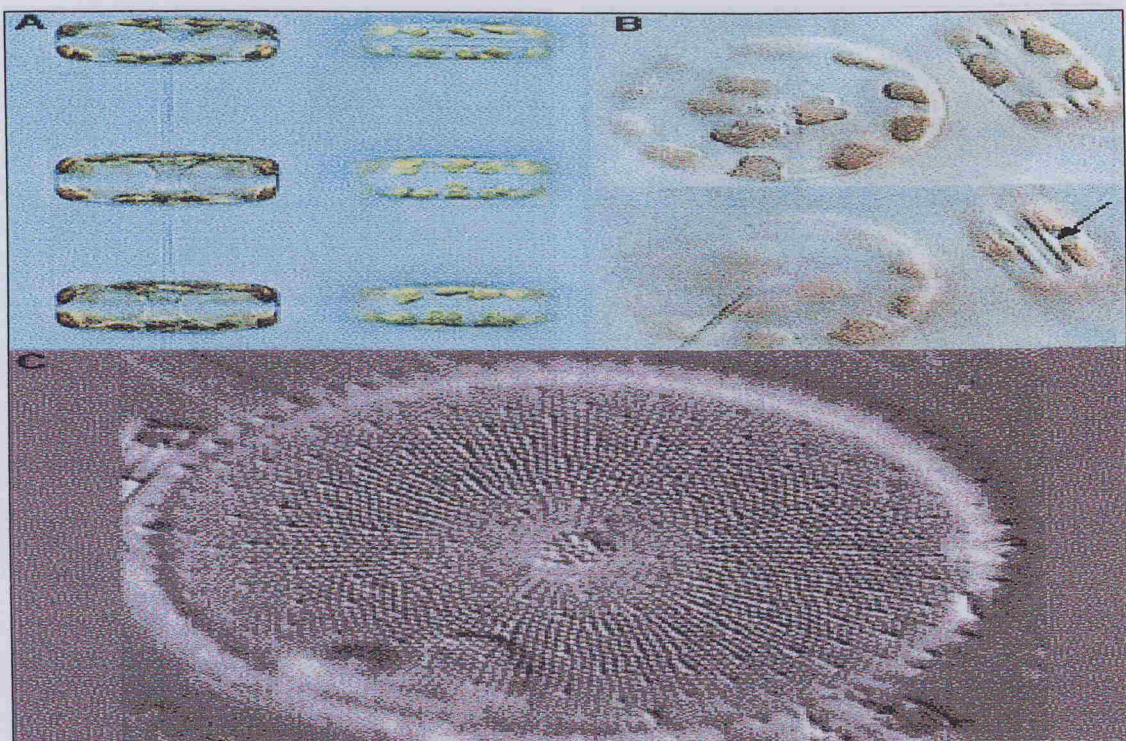


Figure 3.5 d) *Thalassiosira* sp.

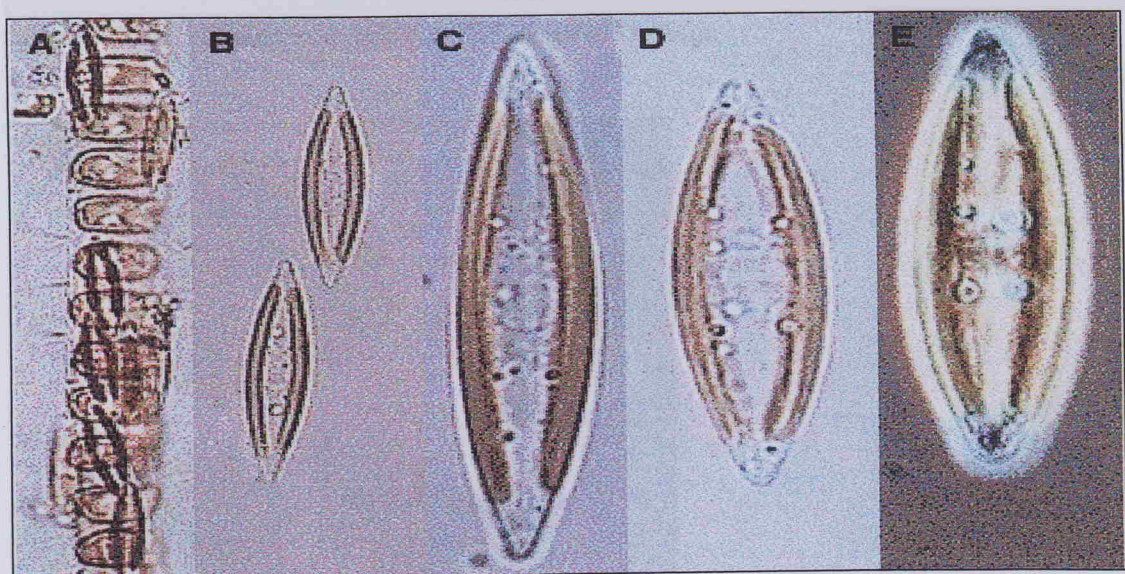


Figure 3.5 e) *Navicula* sp.

Figure 3.5 f) *Leptocylindrus* sp.

Figures 3.5 are taken from the British Diatom Collection, Department of Marine Biology, Clothing University, St Andrews (www.marine.bios.ed.ac.uk).

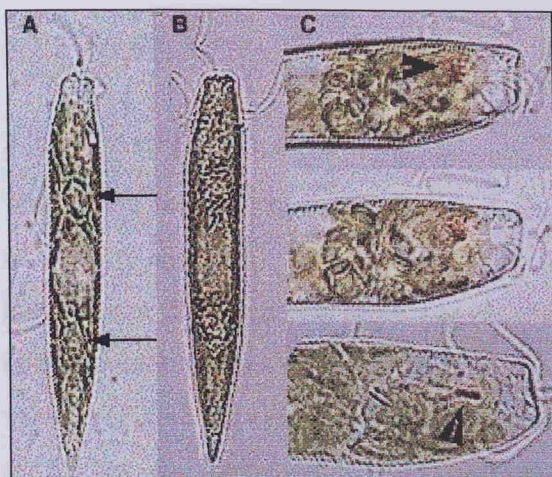


Figure 3.5 f) *Eutreptiella* sp. Size range 10-80 μ m.

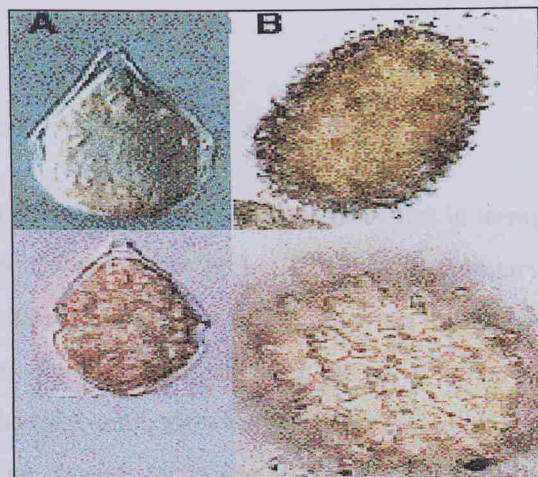


Figure 3.5 g) *Peridinium* (=*Scripsiella*) *trochoideum*. Size range ~20-100 μ m.



Figure 3.5 h) *Prorocentrum micans*. Size range = 35-70 μ m.

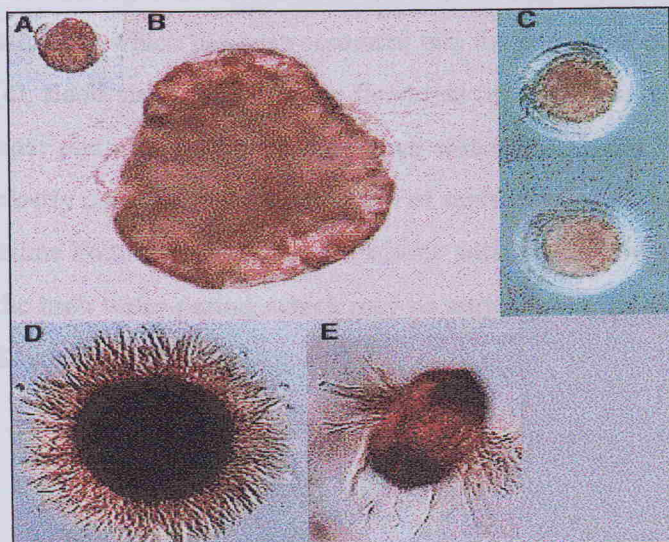


Figure 3.5 i) *Mesodinium rubrum*.

Figures 3.5 are taken from the Baltic Sea database. Department of Marine Botany, Göteborg University, Sweden (www.marbot.gu.se/sss/ssshome.htm).

the estuary, with the flow being driven by tidal water intrusion from the confluence of the Rivers Test and

3.2.2 RESULTS

The flow extended beyond Mount Pleasant and the vertical salinity gradient at Netley had

3.2.2.1 ALONG ESTUARY TRANSECTS

The current structure during a neap tide (Figures 3.6 a, b, c) depicts typical velocities in terms of velocity magnitude (cm s^{-1}), u-velocity (cm s^{-1}) and shear (s^{-2}). The tidal asymmetry between the flood and ebb flows was clearly highlighted (Figure 3.6b), showing maximum ebb velocities $>45 \text{ cm s}^{-1}$ compared to maximum flood currents reaching 30 cm s^{-1} . The u-velocity (Figure 3.6 b) indicated the periods of the tidal state, showing the flood period lasting for 5.5 hrs, and the period of flood stand reducing currents to $<5 \text{ cm s}^{-1}$ for 2 hrs. The high water stand highlights the estuarine circulation, with a surface seaward current, overlying a landward bottom flow. The surface current extends to 2m depth, and occurred approximately 0.5 hrs after the first high water. The difference in current velocities between the velocity magnitude (Figure 3.6a) and the u-velocity (Figure 3.6b) suggested that v-velocity contributes significantly to the tidal asymmetry. Frictional boundary shear (Figure 3.6c) was determined from the velocity magnitude and highlighted the regions of increased mixing, caused by the benthic boundary during the flood and ebb periods, but also from the free-flow estuarine circulation in the upper water column during high water. It is clear that this is a highly dynamic system, with periods of mixing followed by temporary stability.

Data derived from CTD profiles (Figure 3.7), SPM (Figure 3.8), chlorophyll *a* (Figure 3.9) and velocity were combined to produce a longitudinal view of the estuary, presenting a time sequence which has been separated into the periods of high water (a), ebb flow (b), low water (c), flood stand (d) and latter flood tide (e). One transect was chosen as an example of each tidal phase. Even during the high water period, the horizontal and vertical structure was clearly dynamic, with the removal of surface waters down estuary and the intrusion of a more saline bottom current. Lower salinity surface water was observed at the Hamble jetty during the high water period, which may be attributed to the influence of the Hamble river entering Southampton Water.

During the ebb flow, the fresher water intrusion from the confluence of the rivers Test and Itchen had extended beyond Hound Buoy and the vertical salinity gradient at Netley had reduced from 2 to 1.5. By low water, this gradient of 1.5 was a notable feature throughout the transect. During the young flood stand, the vertical gradient of salinity had reduced to ~ 1, with the 33.5 isohaline extending to 10m at Netley, and rising to a depth of 5m at the Hamble jetty. This suggests that the higher salinity coastal water was re-entering the estuary. During the latter stage of the flood, this higher salinity near-bottom flow had extended to Hound buoy. An accelerated north-westerly surface current existed at 2m, indicating that the seaward low salinity freshwater current was still prevailing and reducing the surface flood flow. At all times, a degree of salinity stratification existed along the estuary, being strongest during the high water stand, with intermittent vertical mixing during the ebb and flood phases.

SPM concentrations were highest in the bottom layers, and became intensified during the ebb tide (Figure 3.8b). During the flood tide, higher surface SPM concentrations were observed, suggesting higher SPM loading related to the intrusion of a tongue of higher salinity water entering the estuary from the coastal waters. This higher sediment load may have arisen from re-suspension events occurring in the well-mixed region of Calshot.

The chlorophyll *a* distribution along the transect (Figure 3.9) suggested that during high water a near-surface patch of higher concentration existed along the transect, showing a vertical gradient of 4 mg m^{-3} . There was little change during the ebb tide, with highest concentrations aggregated in the surface layers (maximum concentrations were 10 mg m^{-3}). The advection of the sub-surface chlorophyll *a* aggregation was clearly shown to move down estuary with the ebb tide. At low water, chlorophyll *a* was horizontally well mixed, but the vertical gradient was reduced to 3 mg m^{-3} , and the maximum concentrations of 8 mg m^{-3} became vertically mixed to 10 m depth. During the flood period chlorophyll *a* reached a maximum of 11 mg m^{-3} and vertical variation showed a maximum of 9 mg m^{-3} . Maximum levels were found in the near-surface zone at all the sites sampled.

The distribution of chlorophyll *a* however, although homogenous throughout the transect, does not allow conclusions to be drawn concerning the nature of the phytoplankton community. Phytoplankton cell counts from the whole water Lugol's preserved samples highlighted the interspecific vertical variance between groups of phytoplankton and presented further information into phytoplankton patchiness.

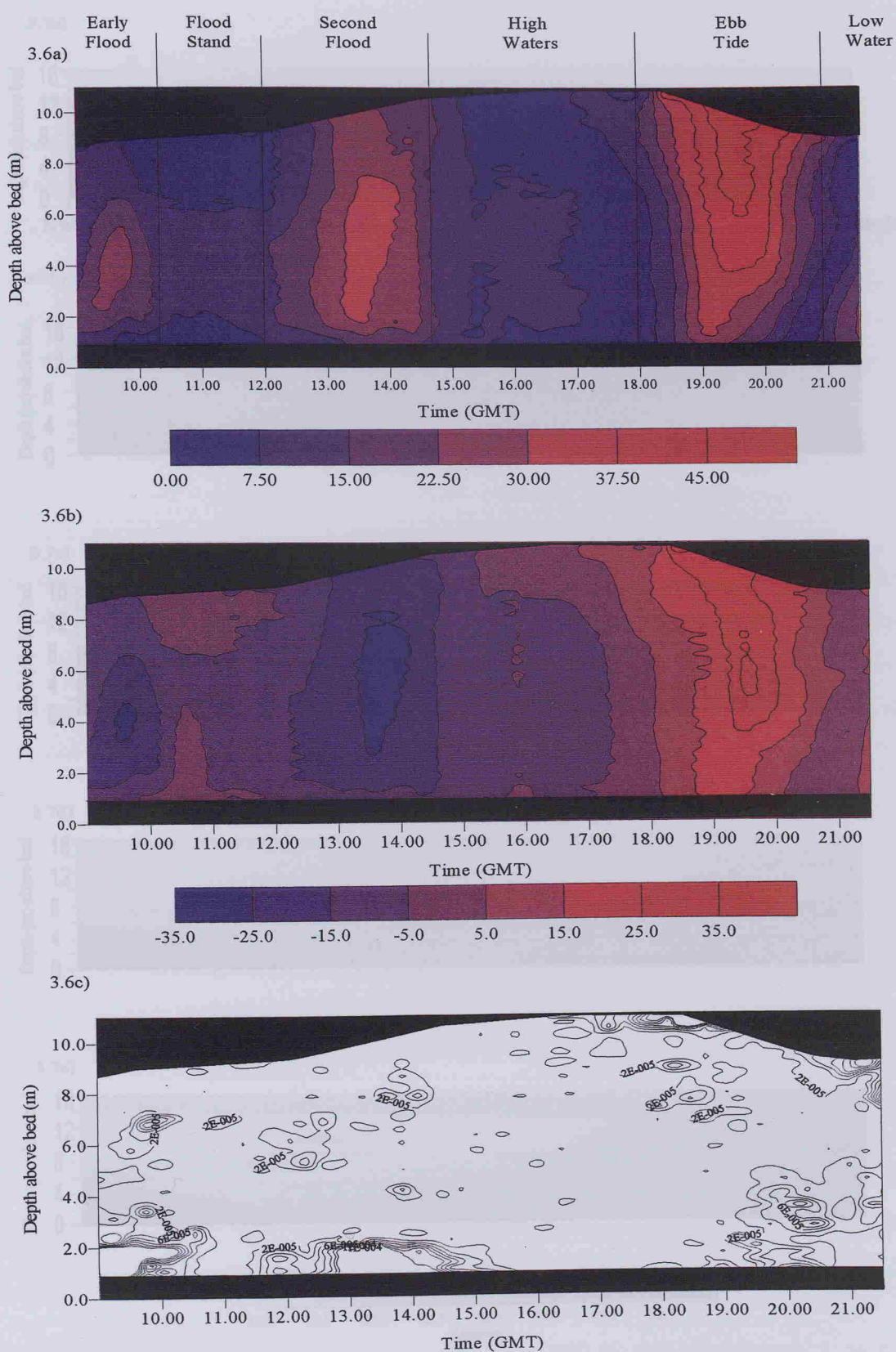


Figure 3.6. ADCP data from a neap tide survey in May 1997, where the predicted tidal range was 2.7m. Data collected during an anchor station survey at Hound navigation buoy. a) velocity magnitude (cm s^{-1}); b) u-velocity (cm s^{-1}); c) velocity shear (s^{-2}). The tidal state is annotated.

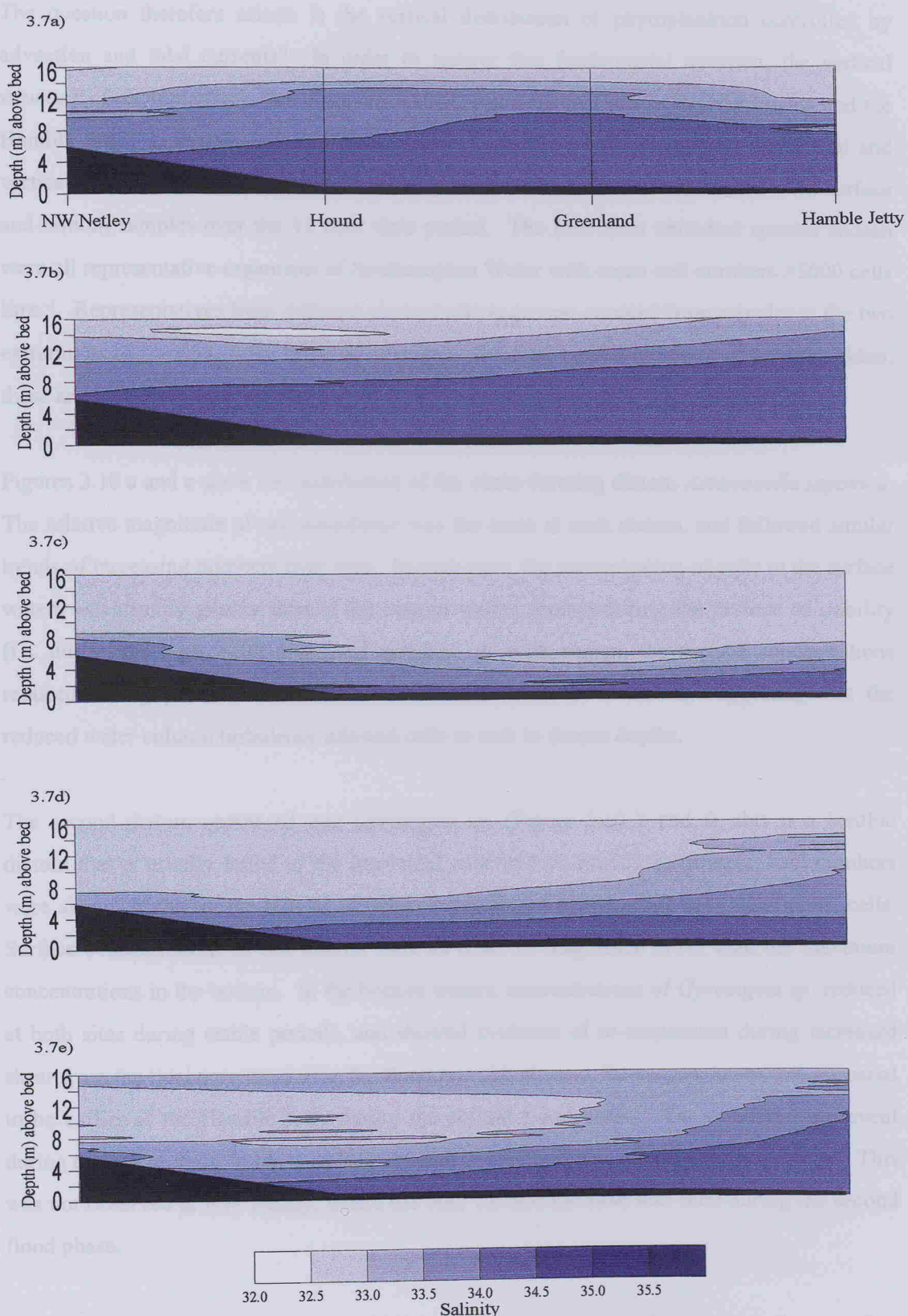


Figure 3.7 a-e. Horizontal salinity structure from NW Netley to the Hamble Jetty at varying tidal states. a) high water; b) ebb phase; c) low water; d) young flood stand; e) flood phase. Vertical lines on figure a) represent CTD stations. Data were normalised to the sea bed. Water column depth at Netley is ~5 m shallower than other sampling stations, thus bottom blanking.

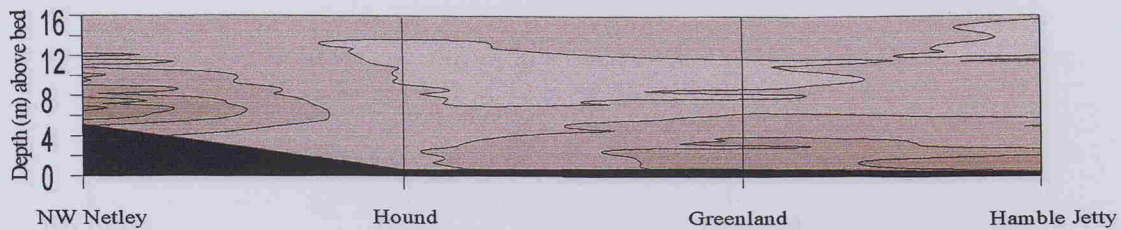
The question therefore arises: is the vertical distribution of phytoplankton controlled by advection and tidal currents? In order to answer this fundamental question, the vertical structure of phytoplankton was observed at different horizontal locations (NW Netley and the Hamble Jetty) during this survey. Four species were chosen to examine the horizontal and vertical distribution (Figures 3.10a-d). Phytoplankton populations were counted from surface and bottom samples over the 12 hour time period. The four most abundant species chosen were all representative organisms of Southampton Water with mean cell numbers >5000 cells litre $^{-1}$. Representatives from different phytoplankton groups, counted from samples at the two extremities of transect, were taken as examples of the horizontal structure of phytoplankton, these are shown in Figures 3.10a-d (NW Netley) and Figures 3.10 e-h (Hamble Jetty).

Figures 3.10 a and e show the distribution of the chain-forming diatom *Asterionella japonica*. The relative magnitude of cell abundance was the same at each station, and followed similar trends of increasing numbers over time. In each case, the concentration of cells in the surface waters was usually greater than in the bottom waters, except during the periods of stability (i.e. during the high water and flood stands). At each station, the surface concentrations reduced during periods of stability and the bottom levels increased, suggesting that the reduced water column turbulence allowed cells to sink to deeper depths.

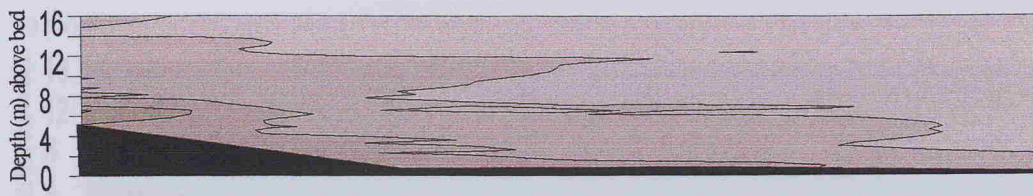
The second diatom compared was *Gyrosigma* sp. (Figure 3.10 b and f), this is a benthic diatom that is usually found in the inter-tidal zone and on muddy substrates. Cell numbers were always higher in the bottom samples, suggesting a near-benthic accumulation of cells. Surface concentrations of this diatom were an order of magnitude lower than the maximum concentrations in the bottom. In the bottom waters, concentrations of *Gyrosigma* sp. reduced at both sites during stable periods, and showed evidence of re-suspension during increased shear from the tidal currents during the flood and ebb phases. Re-suspension events appeared to be earlier at the Hamble Jetty during the second flood phase. The re-suspension event during the ebb currents led to a surface increase in cell numbers, after a lag phase of 1hr. This was not observed at NW Netley, where the only surface increase was seen during the second flood phase.

The dinoflagellate *Prorocentrum micans* (Figures 3.10 c and g), showed a surface accumulation in the afternoon, after the ebb phase. The distribution of this phototrophic, naked dinoflagellate suggested a well-mixed vertical profile during the first half of this

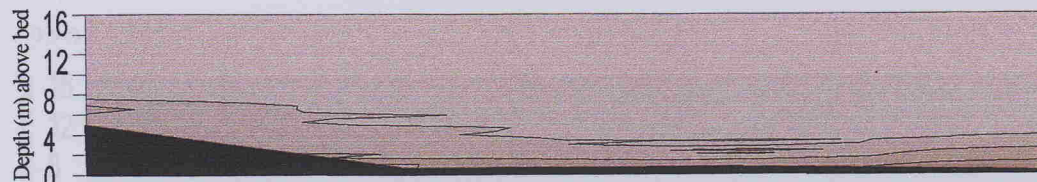
3.8a)



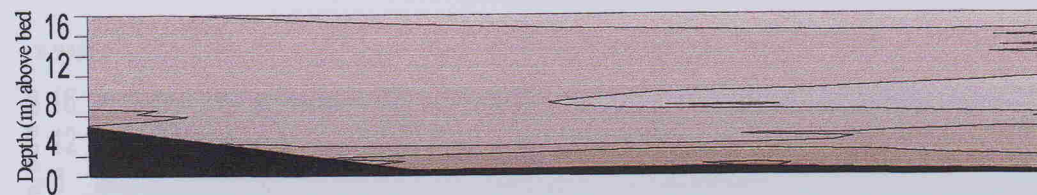
3.8 b)



3.8 c)



3.8d)



3.8e)

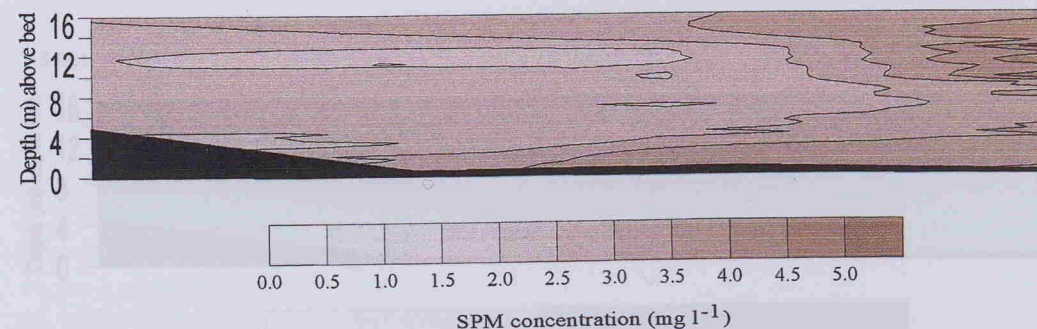
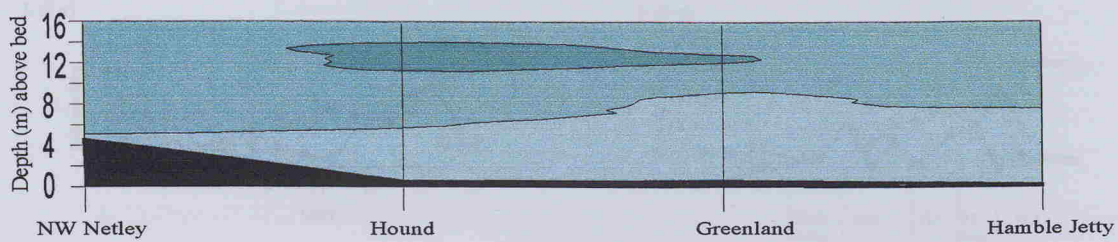
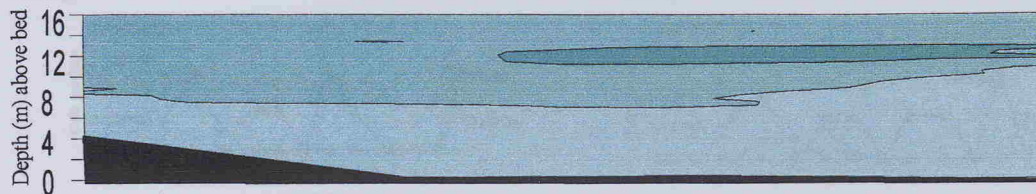


Figure 3.8 a-e. Horizontal SPM concentrations from NW Netley to the Hamble Jetty at varying tidal states. a) high water; b) ebb phase; c) low water; d) young flood stand; e) flood phase. Vertical lines on figure a) represent CTD stations.

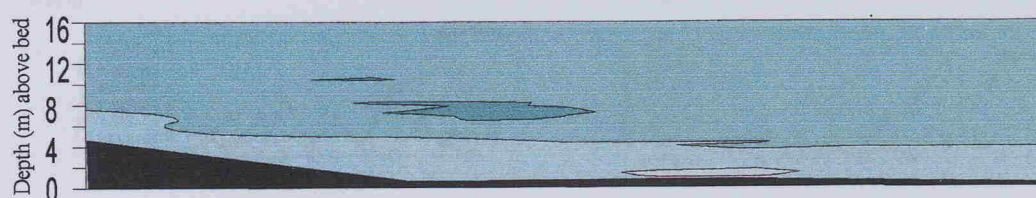
3.9a)



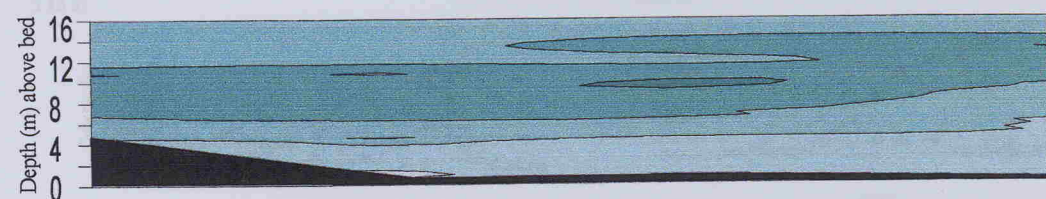
3.9b)



3.9c)



3.9d)



3.9e)

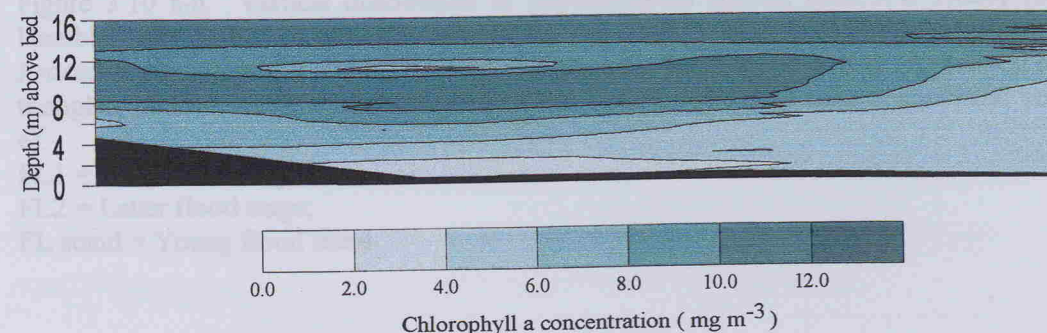
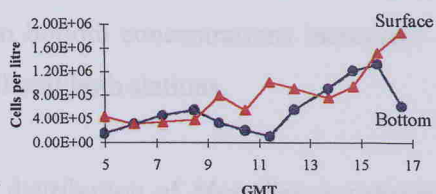
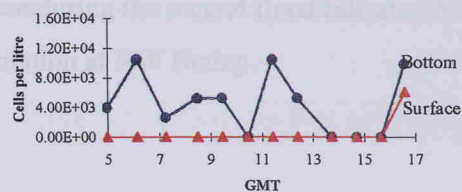


Figure 3.9 a-e. Horizontal chlorophyll *a* concentrations from NW Netley to the Hamble Jetty at varying tidal states. a) high water; b) ebb phase; c) low water; d) young flood stand; e) flood phase. Vertical lines on figure a) represent CTD stations.

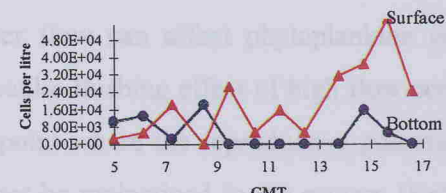
3.10 a)



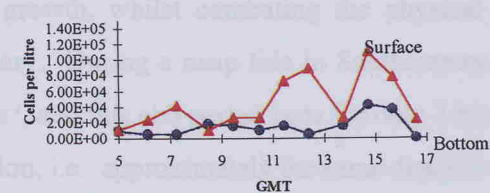
3.10 b)



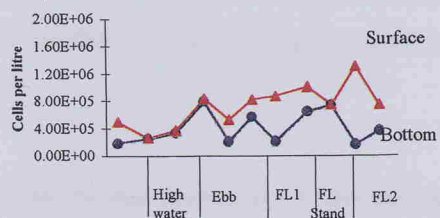
3.10 c)



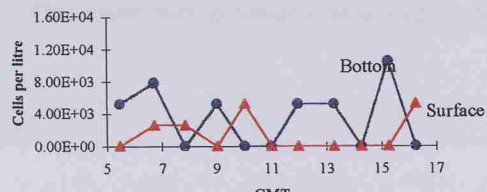
3.10 d)



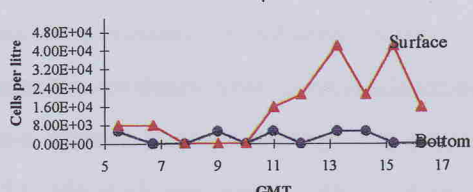
3.10 e)



3.10 f)



3.10 g)



3.10 h)

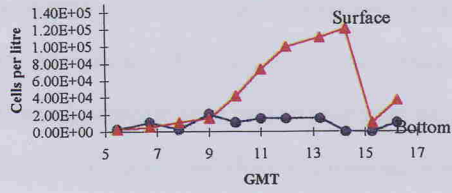


Figure 3.10 a-h. Vertical distribution of phytoplankton species from NW Netley (a-d) and Hamble Jetty (e-h). a and e) *Asterionella japonica*; b and f) *Gyrosigma* sp.; c and g) *Prorocentrum micans*; d and h) *Mesodinium rubrum*. Surface cell counts represented by filled triangles, bottom samples represented by filled circles. The tidal state is annotated on Figure e).

FL1 = Early flood stage;

FL2 = Latter flood stage;

FL stand = Young flood stand.

survey. Throughout the day, there was very little variance in the concentration of cells in the bottom layers. Some variance occurred at NW Netley, during high water and the flood stand, when bottom concentrations increased. The absolute numbers of the population were very similar at both stations.

The distribution of *Mesodinium rubrum* was very similar to that shown by *P. micans*, with surface accumulations building up throughout the survey. This was particularly prominent at the Hamble Jetty. Surface accumulation seemed to begin at the start of the ebb tide, and reduce during the second flood tide at ~15:30 GMT. This trend was generally followed by the population at NW Netley.

3.2.3 DISCUSSION

3.2.3.1 CURRENT STRUCTURE DURING A NEAP TIDE

Water flow can affect phytoplankton communities in a number of different ways. The hydraulic flushing effect of high flow periods reduces the residence time of phytoplankton to the point where the reproductive potential of certain species is never attained and densities cannot be maintained in the estuary (Ketchum 1954; Marshall and Alden 1997). However, increased riverine inputs may stimulate primary production through enhanced nutrient loading and salinity stratification. A fine balance must exist between the necessary inputs to sustain net growth, whilst combating the physical forces which act to remove species from the estuary. During a neap tide in Southampton Water, maximum ebb velocities can reach ~45 cm s⁻¹, and this ebb period lasts for only 3 hrs. This would equate to a tidal excursion of up to 4.9 km, i.e. approximately the same distance of this transect, and therefore organisms initially in the NW Netley region would still be retained within the main body of Southampton Water. During the flood tide, which lasts for up to 6 hours with a 1 hour stand, maximum velocities reach ~33cm s⁻¹, for a period of 4hrs. This equates to a tidal incursion of 4.7 km. This suggests that tidally, the net transport during a neap tide will be out of the estuary, at a rate of 0.48km d⁻¹. Thus a population of pelagic diatoms at NW Netley would take approximately 17 days to enter the Solent if this rate of 0.48 km day⁻¹ was sustained. However, in reality, this net transport may be greatly increased under a spring tide régime where maximum ebb flows reach >100cm s⁻¹, with the flood currents approximately half this value.

An important assumption in this investigation was that the current structure is the same at all sites along the transect as it is at Hound navigation buoy (the site of ADCP data collection). This was a reasonable consideration based on the estuarine geometry, i.e. it is narrow, rectilinear and shallow.

The salinity values show clearly that this is a partially-mixed estuary, although the salinity structure depends greatly on the tidal stage, as was emphasised by the longitudinal transects. Westwood and Webber (1977) estimated that during a 13 hour neap tide, new water entering the estuary constituted 32% of the flood tidal prism, which reflects a significant degree of flushing. Using the river flow data supplied by the Environment Agency 1987-1995 (section 3.1.1.2), the fresh water fraction was calculated as 33.5%, representing a fresh water volume of $1.6 \times 10^7 \text{ m}^3$, in Southampton water from Dockhead to the estuary mouth (based on equation 11).

3.2.3.2 SUSPENDED PARTICULATE MATTER

The sediment concentrations were low during this survey, with maximum values reaching only 5 mg l^{-1} . This was to be expected, as SPM levels are reported as lowest during a neap tide, a feature shown for many estuarine systems, where the tidal mixing is greatly reduced during periods of low tidal range. For example, surveys conducted in the Forth estuary, Scotland (Lindsay *et al.* 1996), showed a relationship between SPM and tidal range, where maximum SPM concentrations were 150 mg l^{-1} during a neap tide and 300 mg l^{-1} during a spring tide. For the varying tidal ranges, sharp increases in SPM were observed in the Forth estuary due to re-suspension which occurred at approximately the same current velocity for different tidal ranges and observed heights. The re-suspension velocity mentioned is the 'effective' re-suspension velocity that is related to a detectable increase in SPM concentrations above the background level. Table 6 shows a summary of re-suspension velocities over a spring and neap period for the Forth Estuary.

Concentrations are lower than those of the other estuaries for which concentrations for Southampton Water have been calculated by Houghton and Munn (1997). A partially mixed estuary, such as Southampton, may have a flow that is different to fully mixed estuaries, and it is often the case that this may cause the concentration to be greater in the upper reaches during a neap tide, for example. This occurs due to the mixing with freshwater plumes, which is of great significance for the development of the estuary.

Tidal Range (m)	Tidal State	Re-suspension Velocity m s ⁻¹	Max SPM mg l ⁻¹	Maximum Velocity m s ⁻¹
3.0 Neap	Flood	>0.60	33	0.65
3.0 Neap	Ebb	>0.65	47	0.66
5.1 Spring	Flood	>0.70	213	1.24
5.1 Spring	Ebb	>0.80	178	1.36

Table 6. Re-suspension velocities related to a detectable increase in SPM in the Forth Estuary, Scotland (Redrawn from Lindsay *et al.* 1996). A comparison to Southampton Water is described in the text.

On the flood tide in the Forth estuary, the re-suspension velocity described by Lindsay *et al.* (1996) was approximately 0.6 m s^{-1} at 5cm from the bed, and was associated with a 4-70 fold increase in SPM. During the ebb tide, re-suspension was evident when current velocities exceeded approximately 0.65 m s^{-1} . When the tidal range was $< 2.5\text{m}$, no distinct peak in SPM was apparent, which was attributed to the current velocities being of insufficient magnitude to re-suspend sediments. This can be directly compared to the re-suspension velocities in Southampton Water, which is approximately half that of the Forth estuary. The difference in the re-suspension velocities between the two estuaries is likely to be due to the different sediment types. The re-suspension of sediment is discussed in further detail in section 3.5.4.2.

The ebb-flood asymmetry apparent in Southampton Water may lead to a tidal pumping of sediment. This suggests that the higher suspension occurring during the rapid currents of the ebb tide (due to the large frictional bed shear), would cause a net flux of SPM down estuary, with a short period of deposition during the low water period, when the current velocities were less than 0.2 m s^{-1} and a small percentage returning on the following flood, when current velocities are less than those of the ebb. Net sedimentation rates for Southampton Water have been calculated to be between 2 and 6 mm yr^{-1} (Dyer 1997). In partially-mixed estuaries, the landward-moving bottom flow may be sufficient to push sediment up-estuary, and in some cases this may cause the concentration to be greater in the upper reaches causing a distinct turbidity maximum. The riverine input from three rivers into Southampton Water is also of great significance for the sediment load of the estuary.

The vertical patterns of SPM distribution were similar along the estuarine transect, with maximum concentrations generally observed in the near-bottom waters. The highest concentrations were clearly seen during the ebb phase which was closely associated to the boundary shear generated during the ebb tide which was seen to propagate up through the water column. Near surface SPM increases were also measured at the Hamble jetty, which was possibly due to mixing events at the estuary mouth.

3.2.3.3 PHYTOPLANKTON POPULATION DYNAMICS

The horizontal distribution of chlorophyll *a* showed little variation during the transect, suggesting an along estuary homogeneity, with less chlorophyll *a* at the extremities of the transect. Earlier investigations along Southampton Water, of the surface phytoplankton community (Iriarte 1992; Bryan 1979) suggested that the lowest chlorophyll *a* concentrations exist in less saline waters, and reached maximum estuarine values in Southampton Water between salinities of 29-34. The down-estuary decrease in chlorophyll *a*, (also observed by Bryan (1979), Kifle (1992) and Antai (1989)) has been associated with a seaward increase in the rate of exchange of estuarine and Solent water on each tidal cycle. The finding during this study that algal biomass was horizontally homogenous over a tidal cycle within the transect area was of fundamental importance for defining the future sampling strategy implemented in Southampton Water.

The vertical distribution of the chlorophyll *a* concentration at the four stations varied during the day and with the state of the tide. The increase in algal biomass during the day was expected, due to *in situ* growth after exposure to enhanced PAR, but the overall increase was greater than expected (i.e. from 9 mg m⁻³ in the early hours during high water to 12 mg m⁻³ in the late afternoon during the flood period), suggesting other factors may be acting to enhance the local biomass, such as the presence of an estuarine frontal barrier (J. Sharples pers. comm.).

3.2.3.4 PHYTOPLANKTON SPECIATION

Clearly the great variation in the vertical distribution of different phytoplankton species detected during this survey was not highlighted directly from the chlorophyll *a* data. This stresses the importance of intensive sampling to determine changes in phytoplankton species abundance, even in environments as dynamic as an estuary. One important feature to arise

from this investigation was the fact that all the species examined showed a homogeneity along the transect. Species numbers were of the same order at NW Netley and the Hamble Jetty, with their distributions following very similar trends (Figure 3.10).

The planktonic diatom, *A. japonica* is common in Southampton Water throughout the spring and summer months and was the most abundant species found during this survey in August 1996. It is a chain-forming diatom, reaching maximum cell numbers of 2.0×10^5 cells litre⁻¹. The vertical distribution of this species showed very little aggregation, but consistently increased in total biomass throughout the day. If the observed increase in total biomass was due to growth alone, μ_e (division rate) would have to be in the order of 0.49 hr⁻¹, which translates into 12 doublings per day. This growth rate unlikely to be achievable in laboratory cultures. Maximum laboratory growth rates for *A. japonica* are quoted as ~ 1.97 d⁻¹ under super-saturated nutrient conditions (Eppley and Thomas 1969). This implies that factors other than *in situ* growth were causing the increase in cell numbers. One explanation may be re-suspension events occurring during the ebb tide, which can sweep previously settled cells into the surface layers (surface cell numbers increased by a factor of 3 after a high shear event), and progressively increase the number of cells throughout the day due to the continued bottom stresses during low water and the following flood. However, the vertical distributions do not suggest major increases in the population after increased benthic shear. This species is planktonic, and thus does not accumulate in the bottom waters, but relies on turbulence to ensure suspension, coupled with a cell shape (spirals and long chains) and a structure (low weight frustule) to enable a reduction in the sinking rate. Another possibility may include the accumulation of cells down estuary, after flushing by the ebb tide. These organisms may not have been entirely removed from the system, due to the reduced tidal excursion (neap tide) and the probable presence of an estuarine front identified at Calshot Spit and as far up-estuary as the Esso terminal (Sharples pers. comm.). This may act as a barrier to mass transport between the estuary and the well mixed coastal waters.

Gyrosigma sp. is predominantly a benthic, pennate diatom which is capable of a gliding movement when on the surface of the sediment. This movement is caused by a streaming motion of the cytoplasm along the raphe (sigmoid canals), often supplemented by the extrusion of mucilage. It is a common species observed in the inter-tidal areas along Southampton Water. For example, on Hythe mud flats benthic diatoms have been found down to the sub-littoral zone in the surface millimetres of the substrate, where water column depth was > 4 m at high tide (Dransfeld pers. comm.). The vertical distribution of this species

in the water column showed population maximums in the bottom samples at both NW Netley and at the Hamble Jetty, which was expected due to the benthic history of this organism. However, at certain stages over the survey period, *Gyrosigma sp.* was observed in the surface samples, particularly at the Hamble Jetty. The appearance of this benthic organism at the surface was associated with periods of strong mixing and increased bed shear, suggesting that the population became re-suspended into the main water column. The data from the Hamble Jetty, clearly indicated a lag phase of approximately 1 hour (the following sampling interval) between bottom re-suspension and surface increase in cell numbers. The re-suspension of these benthic diatoms from the sediment and into the water column can cause enhanced primary productivity (Roman and Tenore 1978), particularly during low phytoplankton periods where self-shading is minimal and benthic phytoplankton communities are able to contribute substantially to the overall water column productivity.

The population distribution of two motile species, *P. micans* and *M. rubrum*, showed very similar vertical distributions at two stations over a distance of ~ 6 km along the estuary. The overall increase in biomass of the two species was clearly shown during the sampling survey, coupled with a surface accumulation in the late afternoon. This suggested that the apparent diel vertical migration, (DVM) of the two species observed, was triggered by the increasing irradiance measured over the survey, however other variables such as tidal phase may have been a governing force. "Normal" DVM of autotrophic motile phytoplankton is modelled as ascent during daylight and descent at night (Kamykowski 1974). However, dinoflagellates in particular, frequently exhibit variable phase relationships with daylight (Sournia 1982). In most of the literature reviewed, dinoflagellate migrations have been observed in oceanic environments, where vertical mixing is dominated by wind stress and tidal straining is minimal. For estuarine systems, the highly dynamic nature of the environment presents changes over relatively short time scales with vertical mixing dominated by the tides, and, for Southampton Water, on a semi-diurnal cycle. During this survey to define the horizontal structure, surface aggregation of both *P. micans* and *M. rubrum* occurred throughout the transect, with total cell concentrations of the same order at each site (Figure 3.10). It was interesting to note the timing of these ascents, which correlate to a period after the rapid ebb currents, and the vertical homogeneity of each species during the second stage of the flood tide. These observations were further investigated, and are discussed in section 3.4.3.6.

3.2.4 CONCLUSIONS

Although Southampton Water is a highly dynamic, unique environment, this along estuary transect has shown that fundamental properties, such as salinity, SPM and chlorophyll *a* distributions can follow the same horizontal patterns over the small spatial scale of the transect.

An important observation from this study was that although the patterns of chlorophyll *a* indicate a subsurface maximum throughout the day at all stations, using this measure of algal biomass alone masks the distributions of individual phytoplankton species. Individual species distributions at all the stations sampled clearly showed the vertical variation of phytoplankton, and highlighted that the populations were following similar patterns over the 6 km transect. The biological parameters show a close coupling with the fundamental physical mixing processes (i.e. tides) and possibly diel irradiance changes in this partially-mixed estuary, combining to have a controlling influence on the vertical distribution of different phytoplankton species.

3.3 SEASONAL DIFFERENCES IN THE VERTICAL DISTRIBUTION OF PHYTOPLANKTON POPULATIONS IN SOUTHAMPTON WATER

Surveys during May and August 1995 formed the basis of Eulerian investigations to determine the biological and physical vertical structure of Southampton Water, at one representative station, NW Netley. The predicted tidal cycle based on the Admiralty Tide Tables indicates the time over which daytime studies were conducted (Figures 3.11).

3.3.1 SAMPLING STRATEGY

Sampling was performed within the vicinity of the navigation buoy NW Netley (Figure 3.2) during the spring and summer in 1995. These surveys took place during daylight hours. A downward facing ADCP (Narrow Band 1200kHz) was used to determine current speed and direction every 3 minutes with a 0.5m depth resolution. CTD casts, with attached fluorometer and transmissometer, were made at intervals of 0.5hour. Discrete subsamples (100-200 ml) were collected from the Niskin bottles every 0.5hr and filtered through GF/F filters for instrument calibration, (for chlorophyll α and SPM conversions). Whole water samples (150-200ml) were collected from 3 depths at hourly intervals and preserved with Lugol's iodine for subsequent laboratory phytoplankton analysis.

Figure 3.11 Predicted tidal regime for the May and August 1995 surveys in Southampton Water. Depicts a typical 24 hour tidal regime in May/June

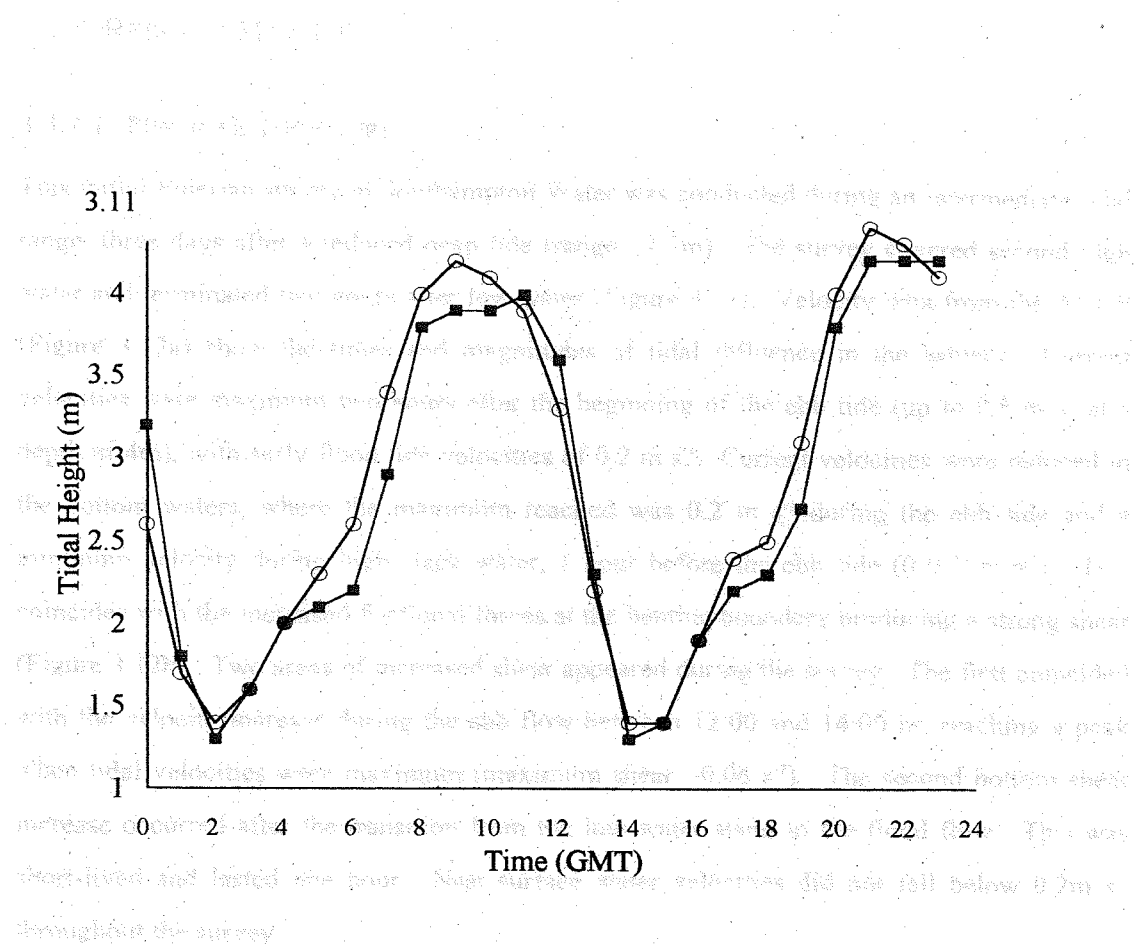


Figure 3.11. Predicted tidal ranges for the May and August 1995 surveys in Southampton Water. Squares represent 8 August 1995, circles represent 26 May 1995.

Figure 3.11 shows the predicted tidal ranges for the May and August 1995 surveys in Southampton Water. The graph plots Tidal Height (m) on the y-axis (1 to 4) against Time (GMT) on the x-axis (00 to 24). Two sets of curves are shown: one for 8 August 1995 (squares) and one for 26 May 1995 (circles). Both sets show two major tidal cycles. The May 1995 curves peak at approximately 3.8m and 3.5m, while the August 1995 curves peak at approximately 3.6m and 3.4m. The May curves start at a higher tide around 2.8m at 00:00, while the August curves start at 1.5m at 00:00. The May curves also show a small secondary peak around 2.2m at 06:00.

The tidal ranges for the May 1995 survey were similar to the predicted ranges shown in Figure 3.11. The highest tide was recorded at approximately 3.8m at 06:00 on 26 May 1995. The lowest tide was recorded at approximately 1.5m at 00:00 on 26 May 1995. The predicted ranges for the August 1995 survey were similar to the predicted ranges shown in Figure 3.11. The highest tide was recorded at approximately 3.6m at 06:00 on 8 August 1995. The lowest tide was recorded at approximately 1.5m at 00:00 on 8 August 1995.

3.3.2 RESULTS MAY 1995

3.3.2.1 PHYSICAL STRUCTURE

This initial Eulerian survey in Southampton Water was conducted during an intermediate tidal range, three days after a reduced neap tide (range ~2.5m). The survey covered second high water and terminated two hours after low water (Figure 3.11). Velocity data from the ADCP (Figure 3.12a) show the times and magnitudes of tidal influence in the estuary. Current velocities were maximum two hours after the beginning of the ebb tide (up to 0.5 m s^{-1} at a depth of 4m), with early flood tide velocities of 0.2 m s^{-1} . Current velocities were reduced in the bottom waters, where the maximum reached was 0.2 m s^{-1} during the ebb tide and a minimum velocity during high slack water, 1 hour before the ebb tide ($0-0.05 \text{ m s}^{-1}$). This coincides with the increased frictional forces at the benthic boundary producing a strong shear (Figure 3.12b). Two areas of increased shear appeared during the survey. The first coincided with the velocity increase during the ebb flow between 12:00 and 14:00 hr, reaching a peak when tidal velocities were maximum (maximum shear $\sim 0.06 \text{ s}^{-2}$). The second bottom shear increase occurred after the transition from the low water stand to the flood flow. This was short-lived and lasted one hour. Near-surface water velocities did not fall below 0.2 m s^{-1} throughout the survey.

Time series data (between 11:00 - 16:00 GMT) for salinity (Figure 3.12c), density and temperature (not shown) indicated vertical and temporal variations, with salinity the most stable parameter over time. Salinity stratification was apparent, with 'fresher' (29.4) water overlying denser, more saline water (33), which was a characteristic feature of the first survey (section 3.2). This stratification remained intact during the ebb tide. The highest salinity water (~33) occurred at the time of the first CTD profile (~11:00) at a depth of 8-10m, immediately after high slack water. The vertical temperature profiles suggested stratification, leading to a combination of salinity and thermal stratification. The temperature range was between 13.8 and 15.2°C , with warmer water at the surface and maximum temperatures (15.2°C) at the start of the flood tide. Density profiles confirmed the salinity driven gradients.

The SPM concentration showed a daily range of 4-34 mg l⁻¹ (Figure 3.12d). The maximum SPM concentration occurred at the benthic boundary corresponding to the region of maximum shear (Figure 3.12b). The regions of increased SPM were closely linked to the times of increased shear during the ebb and flood flow. SPM concentrations appeared as plumes into

the water column suggesting re-suspension events which occurred during increased benthic boundary shear. The plume during the ebb flow was marked by the transition from the minimal current velocities of the high water stand to the rapid ebb velocities (up to 0.5 m s^{-1}). The low water 'plume' corresponded to an increased current velocity, suggesting a vertical input of turbulent energy into the benthos, approximately 20 minutes after the maximum mid-water ebb velocities.

3.3.2.2 PHYTOPLANKTON DYNAMICS AND SPECIATION

The concentration of chlorophyll *a* (Figure 3.13a) indicated a high algal biomass (confirmed by phytoplankton cell counts), due to a diatom bloom. Low water represented a time when chlorophyll *a* variance was maximum throughout the water column (gradient $\sim 2-17 \text{ mg m}^{-3}$), with lowest chlorophyll *a* concentrations in the less saline surface waters. Microscopic examination confirmed that the chain forming diatom *Rhizosolenia delicatula* was the dominant bloom species during this survey, with maximum cell numbers reaching $4.3 \times 10^6 \text{ cells litre}^{-1}$. This species has previously been reported in Southampton Water (section 3.1), forming blooms during May and June (Kifle and Purdie 1993; Anning 1995).

The vertical distribution of this chain-forming diatom (Figure 3.13b) suggests that maximum concentrations occur at a depth, which coincides with the maximum chlorophyll *a* concentrations. The actual cell numbers in relation to current velocity showed that the population aggregated in the bottom waters and became entrained into the water column during increased boundary shear as tidal velocities increased. As velocity increased at 11:00 hr and 14:00 hr, cell numbers increased in the near bottom waters suggesting a turbulent mixing (re-suspension) of the sediment. These patterns of re-suspension were highlighted by the SPM distribution (Figure 3.12d), with peak concentrations occurring during maximum mixing.

Table 7 outlines the mean number of cells per chain of *R. delicatula*; values are depth averaged. From microscopic observation it was noticed that diatom chains in the surface waters had longer average chain lengths than organisms collected near the bottom. Cell volumes were not determined.

SAMPLE DEPTH	NO. CELLS PER CHAIN (MEAN)	n	COEFFICIENT OF VARIATION (%)
Surface	3.86	10	15
Mid	3.27	12	21
Bottom	3.63	13	21

Table 7. *Rhizosolenia delicatula* chain lengths (number of cells per chain).

Whole water samples from a transect on 23 May 1995 provided species and chlorophyll *a* information prior to the 'bloom' period of *R. delicatula* during this survey. Surface chlorophyll *a* concentrations 3 days before the intensive sampling were approximately 1.5 mg m⁻³. This would suggest that chlorophyll *a* concentrations increased from 2-20 mg m⁻³ in 72 hours. This is highly unlikely and it should be noted that the chlorophyll *a* data on 23 May 1995 was based only on surface samples.

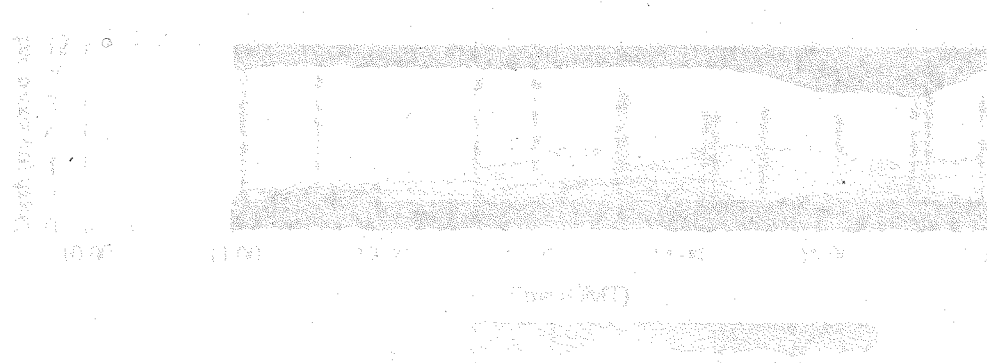


Figure 3.1, 3.2 & 3.3. Phytoplankton measured in May 1995 at A1W (electricity transect) (see Fig. 1) for diatom (3.1), dinoflagellate (3.2) and green algae (3.3).

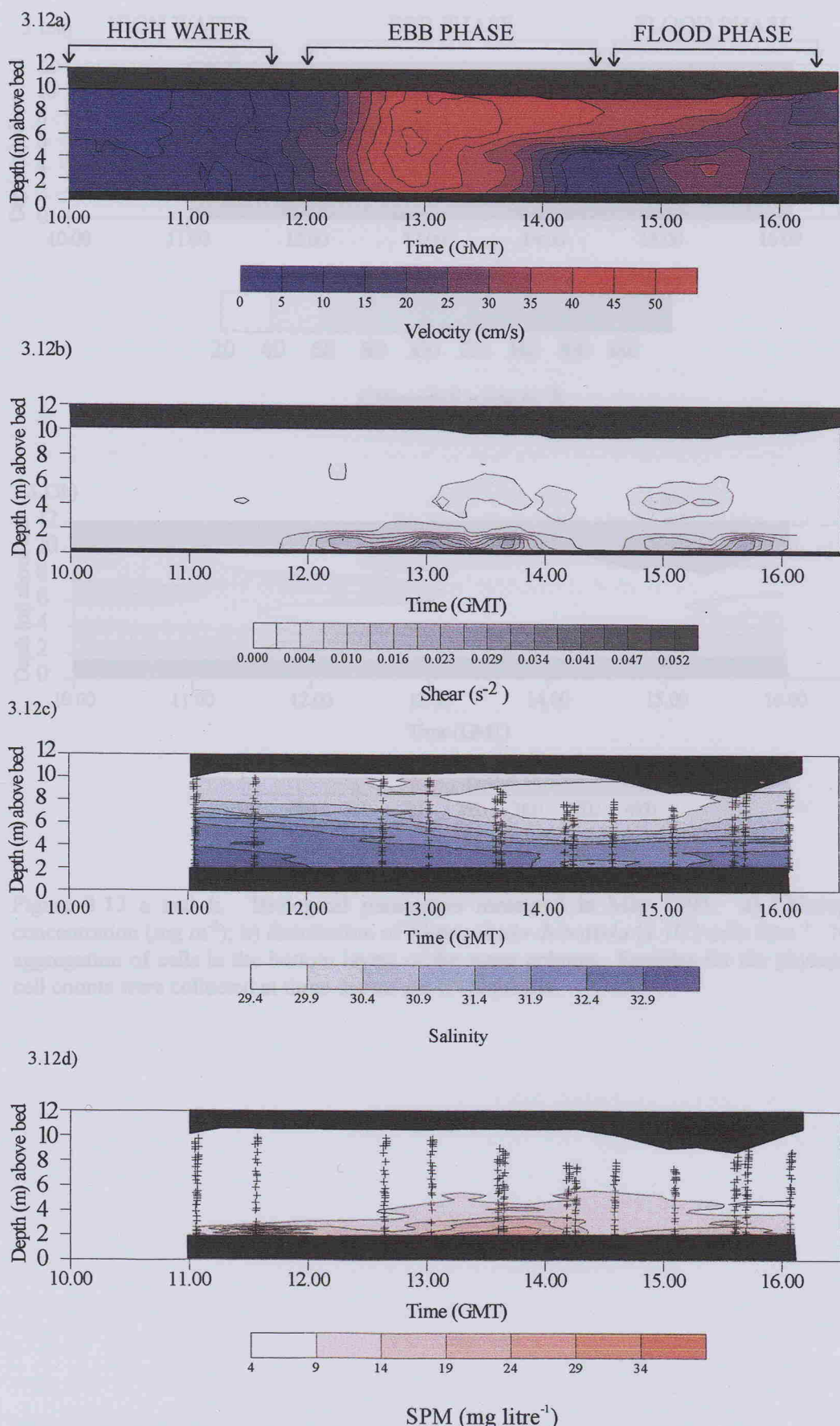


Figure 3.12 a-d. Physical parameters measured in May 1995. a) ADCP velocity magnitude (cm s^{-1}); b) shear (s^{-2}); c) salinity; and d) SPM (mg l^{-1}). Vertical lines represent CTD casts.

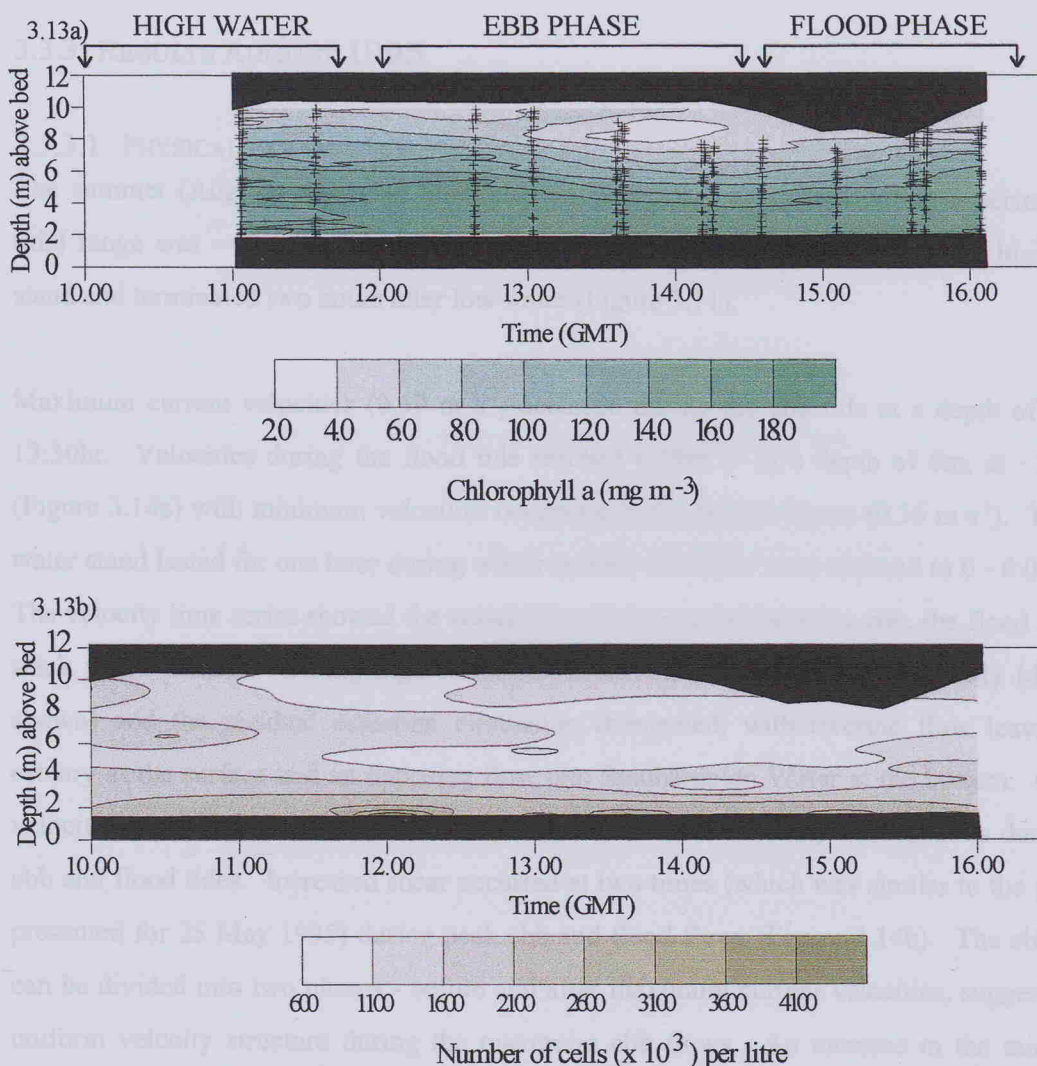


Figure 3.13 a and b. Biological parameters measured in May 1995. a) Chlorophyll *a* concentration (mg m^{-3}); b) distribution of *Rhizosolenia delicatula* ($\times 10^3$) cells litre $^{-1}$. Note the aggregation of cells in the bottom layers of the water column. Samples for the phytoplankton cell counts were collected at three depths per CTD profile.

The vertical salinity gradient for sample 1995 was ~ 1.3 (compared to ~ 4 in May 1995), suggesting the expected (Section 3.1) reduction in riverine input (Figure 3.14c). At the time of the ebb flow a mixing event was detected, where surface and bottom salinities were reduced, and the vertical salinity gradient decreased to ~ 0.5 . This was short lived and rapidly reformed following the maximum current velocities. Temperature showed very little vertical variation, but increased with time during the survey (range $\sim 0.5^\circ\text{C}$), and due to the timing of the tides the maximum occurred during the low water periods (plots not shown). A direct comparison of the vertical salinity profiles is shown in Figure 3.15d and 3.15h. The halocline is clearly shown in Figure 3.15d

3.3.3 RESULTS AUGUST 1995

3.3.3.1 PHYSICAL PARAMETERS

The summer (August) survey in Southampton Water was conducted during a period when tidal range was ~4m, three days before a spring tide. This survey covered the high water stand and terminated two hours after low water (Figure 3.11).

Maximum current velocities (0.59 m s^{-1}) occurred during the ebb tide at a depth of 4m, at 13:30hr. Velocities during the flood tide reached 0.29 m s^{-1} at a depth of 6m, at ~16:00hr (Figure 3.14a) with minimum velocities occurring in the bottom layers (0.36 m s^{-1}). The low water stand lasted for one hour during which current velocities were reduced to $0 - 0.06 \text{ m s}^{-1}$. The velocity time series showed the variability of currents between the ebb, the flood and the slack water periods. During high water slack, current direction varied vertically (data not shown) and the residual estuarine circulation dominated, with riverine flow leaving the estuary at the surface and an opposing flow into Southampton Water at the bottom. Current velocities were low ($> 18 \text{ cm s}^{-1}$). Current direction was vertically homogenous during the ebb and flood tides. Increased shear occurred at two times (which was similar to the profiles presented for 25 May 1995) during peak ebb and flood flows (Figure 3.14b). The ebb shear can be divided into two phases:- before and after maximum current velocities, suggesting an uniform velocity structure during the maximum ebb flows. An increase in the mid-water column free shear occurred during the maximum ebb currents at ~13:45hr.

Salinity

The vertical salinity gradient for August 1995 was ~1.5 (compared to 4 in May 1995), suggesting the expected (Section 3.1) reduction in riverine input (Figure 3.14c). At the time of the ebb flow a mixing event was detected, where surface and bottom salinities were reduced, and the vertical salinity gradient decreased to ~0.5. This was short-lived and rapidly reformed following the maximum current velocities. Temperature showed very little vertical variation, but increased with time during the survey (range = 0.5°C), and due to the timing of the tides the maximum occurred during the low water periods (data not shown). A direct comparison of the vertical salinity profiles is shown in Figure 3.15d and 3.15h. The halocline is clearly shown in Figure 3.15d.

SPM

On both surveys, the pattern of SPM through the water column followed a similar trend, with bottom concentrations up to five times greater than the surface values (Figure 3.15b and 3.15f). This can be compared to the time series profiles in May and August 1995 (Figure 3.12d and 3.14d), where the bottom concentrations of SPM were usually the highest values, coupled with the timing of the greatest shear events during the ebb currents.

Temperature

The vertical profiles of temperature (Figures 3.15c and 3.15g) highlight the seasonal variance in temperature. A change of up to 6°C occurred over the two month period. A weak thermocline is suggested by the vertical profile of temperature in May 1995. The water column appeared to be vertically mixed in August 1995 (enhanced by the salinity profile).

3.3.3.2 PHYTOPLANKTON DYNAMICS AND SPECIATION

The vertical distribution of chlorophyll *a* (Figure 3.15a, e) showed a very different pattern to the distribution observed in May 1995. Figures 3.15 highlight the variance in vertical parameters over time. Maximum algal biomass (chlorophyll *a*) occurred in the surface layers and increased over the survey period. Whole water cell counts confirmed the presence of many dinoflagellates and motile species during this survey. The distribution of *Mesodinium rubrum* (Figure 3.16d) and *Peridinium trochoideum* (Figure 3.16b) followed similar patterns adding to the sub-surface chlorophyll *a* maximum (Figure 3.15 e). Although cell numbers of *Chaetoceros* sp. (Figure 3.16a) were extremely high (maximum 1.2×10^6 cells litre⁻¹) the small size of this species suggests that it did not contribute greatly to the total chlorophyll *a* concentration. In the surface layers, *Eutreptiella marina* (Figure 3.16c) had a maximum concentration of 1.6×10^5 cells litre⁻¹ at 13:00hr. *Peridinium trochoideum* followed a similar pattern to *E. marina*, showing a maximum concentration of 9×10^3 cells litre⁻¹. The maximum chlorophyll *a* found during the day was ca. 18 mg m⁻³ at ~16:00hr in the surface layers, as the flood tide began (data not shown). At this time, *M. rubrum* had migrated into the surface waters, *Eutreptiella marina* was mixed vertically, and *P. trochoideum* accumulated at 5 m (at half the previous maximum numbers). *Chaetoceros* sp. cell numbers had declined.

Figure 3.15a and 3.15e. Vertical profiles of chlorophyll *a* measured in August 1995. (a) ATWF waterbody sample, (e) TSPF waterbody sample. The x-axis represents depth in metres and the y-axis represents concentration in mg m⁻³.

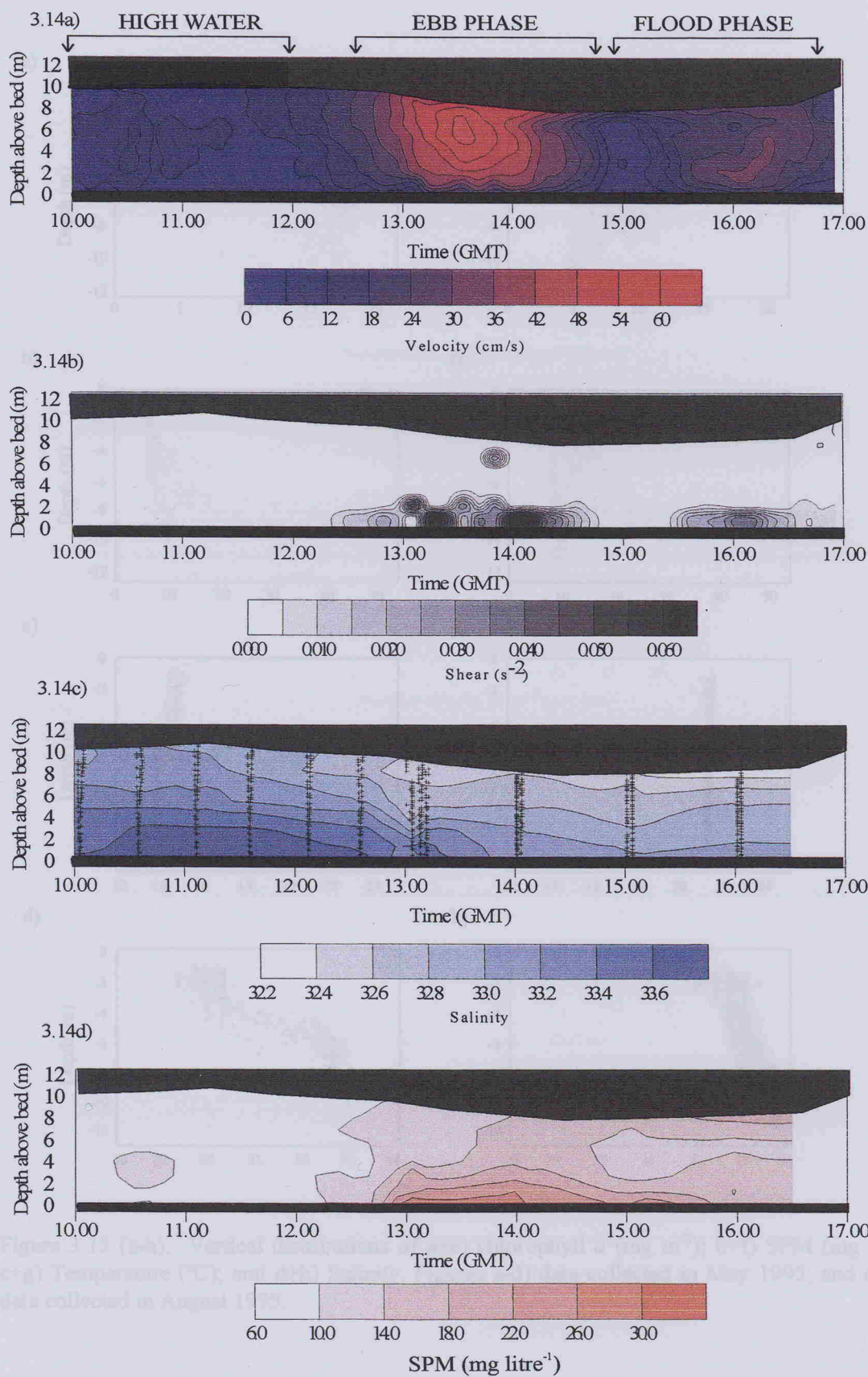


Figure 3.14 a-d. Physical parameters measured in August 1995. a) ADCP velocity magnitude (cm s^{-1}); b) shear (s^{-2}); c) Salinity; and d) SPM concentration (mg l^{-1}).

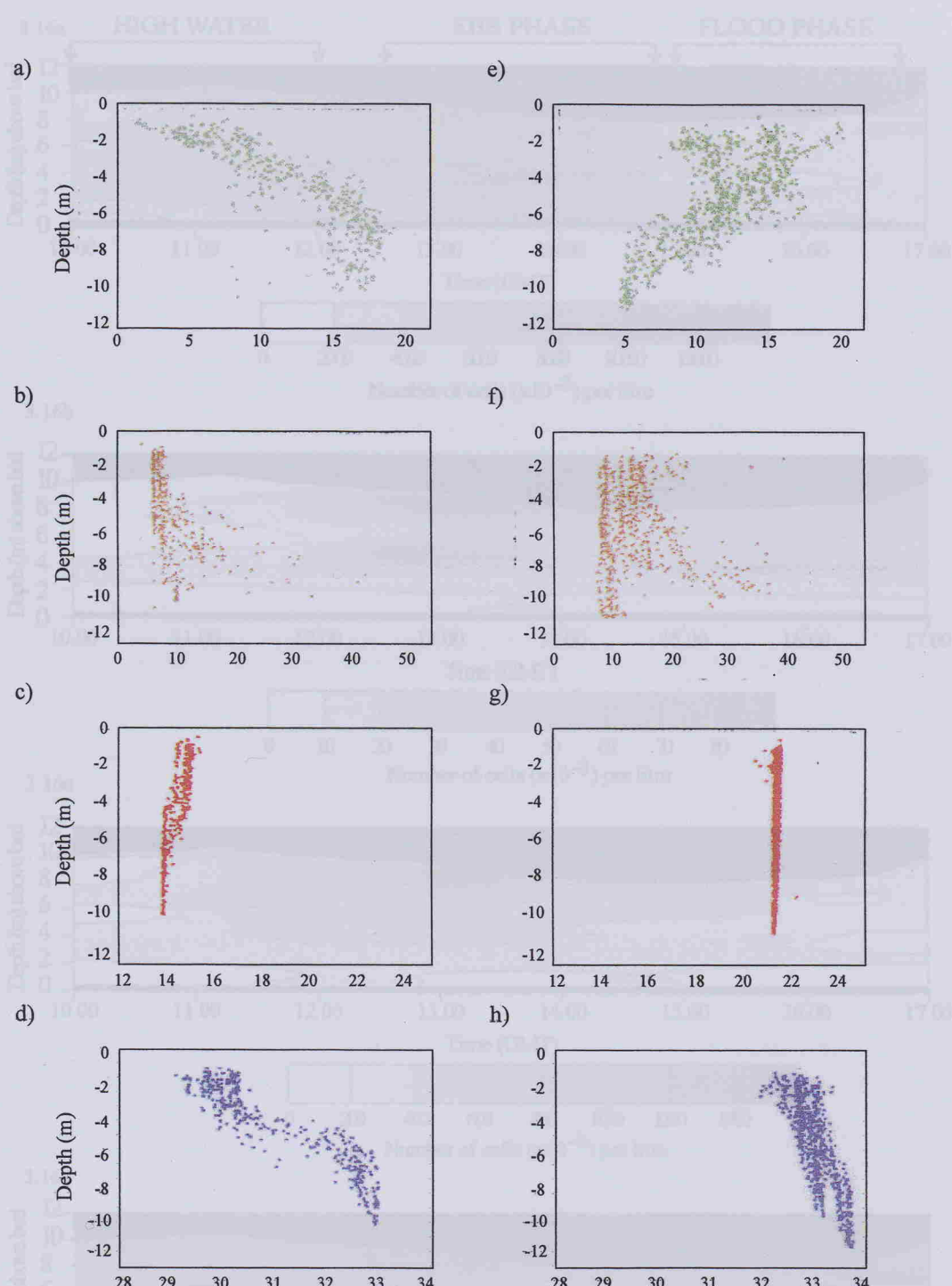


Figure 3.15 (a-h). Vertical distributions of a+e) chlorophyll *a* (mg m^{-3}); b+f) SPM (mg l^{-1}); c+g) Temperature ($^{\circ}\text{C}$); and d+h) Salinity. Figures a-d) data collected in May 1995; and e-h) data collected in August 1995.



Figure 3.16 a-d. Vertical distributions of several phytoplankton species in August 1995. a) *Chlorococcus* sp. b) *Peridinium erithrodiscum*. c) *Eukeratella marina*. and d) *Monoraphia rufum*. Crosses represent water sample collection for all diagrams.

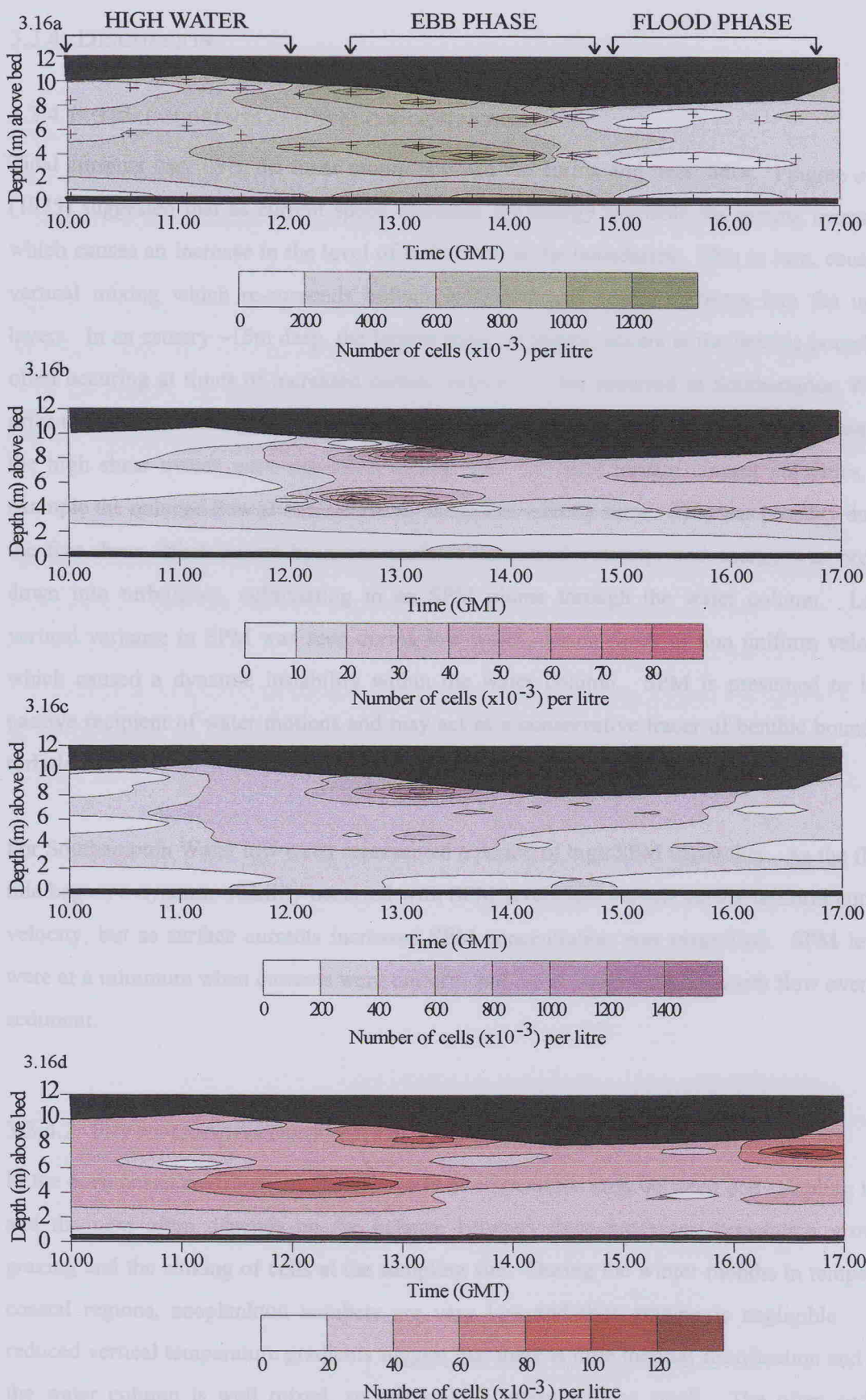


Figure 3.16 a-d. Vertical distribution of several phytoplankton species in August 1995. a) *Chaetoceros sp*; b) *Peridinium trochoideum*; c) *Eutreptiella marina*; and d) *Mesodinium rubrum*. Crosses represent water sample collection for all diagrams.

3.3.4 DISCUSSION

3.3.4.1 TIDAL CURRENTS AND SPM CONCENTRATION

Tidal currents vary over the lunar month between the spring and neap tides. Pingree *et al.* (1975) suggested that as current speed increases the energy available for mixing increases, which causes an increase in the level of turbulence at the boundaries. This in turn, causes a vertical mixing which re-suspends bottom sediments and brings nutrients into the upper layers. In an estuary ~15m deep, the largest shear, in theory, occurs at the benthic boundary, often occurring at times of increased current velocity. This occurred in Southampton Water prior to low water during the surveys in May and August 1995. In certain situations however, the high shear events were not solely linked with the most intense current velocities, for example the reduced flow at 8 m caused an increase in velocity shear. This was possibly due to the free-shear effect caused by a non-uniform horizontal velocity, and energy was broken down into turbulence, culminating in an SPM plume through the water column. Large vertical variance in SPM was seen during low water, during times of non uniform velocity which caused a dynamic instability within the water column. SPM is presumed to be a passive recipient of water motions and may act as a conservative tracer of benthic boundary turbulence.

For Southampton Water low water represented a period of high SPM variability. As the flood tide began, a dynamic stability occurred with SPM levels less variant during uniform current velocity, but as surface currents increased SPM concentration was magnified. SPM levels were at a minimum when currents were uniform and rapid, suggesting a smooth flow over the sediment.

3.3.4.2 PHYTOPLANKTON DISTRIBUTION

In the open ocean environment, the change in phytoplankton crop between one sampling time and the next often depends on the balance between three processes: population growth, grazing and the sinking of cells at the sampling site. During the winter months in temperate coastal regions, zooplankton numbers are very low and thus grazing is negligible. The reduced vertical temperature gradients suggest that there is little thermal stratification and that the water column is well mixed, so cell sinking losses will be small. The often sudden outburst of cell numbers in the early spring has been attributed to the phenomenon of the

critical depth (see Introduction, section 1.7), and the later progression to dinoflagellate species attributed to water column stability, increased daylength and lower nutrient concentration. In an estuarine environment these fundamental conditions are not applicable, due to the highly dynamic nature of these often continuously mixed systems. The seasonal climatic processes are a common feature for both systems, i.e. increased daylength and warmer temperatures. It is unlikely in an estuarine system such as Southampton Water that nutrient levels would be sufficiently reduced to be a limiting factor. Nutrient concentrations have been shown to be depleted over the summer period, but would still not be limiting (Kifle and Purdie 1992). Although there are many differences between the characteristics of an open ocean and an estuarine system, the seasonality of phytoplankton succession follows a similar pattern: a diatom bloom in the spring followed by an increase in the dinoflagellate and motile phytoplankton population.

Another prerequisite for phytoplankton blooms has been the presence of water column stratification. However, Townsend (1992) found, in the offshore waters of the Gulf of Maine, that a spring bloom can precede the onset of stability, and that by virtue of the light scattering and absorption properties of these organisms, stability can occur. Thus, the formation of a thermocline may be initiated by, rather than act as a prerequisite to, the spring bloom. These findings have also been shown by Eilertson (1993) in the Norwegian fjords where a spring bloom began in mid March following a yearly increase in radiation, but in the absence of stratification. Stratification in Southampton Water is often only temporary and does not seem to form a prerequisite for phytoplankton increase, especially during the later spring and summer months.

Algal biomass during the 1995 surveys varied in vertical distribution and intensity, highlighting the dynamic nature of phytoplankton populations. Maximum chlorophyll α was observed in the lower waters at 6m, during May. The dominant species during this bloom (chlorophyll α >10 mg m $^{-3}$) was *Rhizosolenia delicatula*, which is also a chain-forming diatom. The stratification of *R. delicatula* has been observed previously in the estuary (Kifle 1992, Anning 1995) and is a probable explanation for the large increase in cell numbers during 23 May 95 - 26 May 95, where the surface survey did not detect the presence of a bottom water bloom (section 3.3.3.2). An interesting observation made from the microscopic examination of the Lugol's samples was that *R. delicatula* chains found in the surface layers had a longer average chain length than those observed in the near bottom waters. This feature has been observed for other *Rhizosolenia* species (Villareal 1988, Richardson *et al.*

1996), where the chain and mat-forming species have been shown to alter their buoyancy through changes in their cytoplasmic density and through their size. Another explanation for shorter chain length in the bottom layers may be due to the disruptive effect of inhabiting a high shear environment. Laboratory studies (Thomas and Gibson 1990) have shown that dinoflagellates can have total cell destruction i.e. flagellar damage and complete removal, under high stress and shear. There appears to be a critical threshold where turbulence can be an advantage, i.e. in increased zooplankton contact rates (Peters and Gross 1994; Kiørboe 1993) and encounter rates (Marrasé *et al.* 1990), but adverse effects can cause reduced contact and encounter and can destroy mats and chains of phytoplankton.

One possible advantage to a population forming maximum numbers in the bottom zone is the reduced flushing from the estuary, as the mean flow at these depths will be landward. During the May survey salinity stratification did exist, and may have acted as a barrier to the *R. delicatula* population from appearing in the surface waters, thus suggesting that turbulent kinetic energy (TKE) lacked the intensity necessary to vertically mix the water column. This fact was highlighted through the salinity profiles, showing stratification over the survey period.

Cell numbers increased in the bottom waters at the times of increased SPM in the water column. When flow was uniform and rapid (dynamically stable), cell numbers remained low, with maximum cell numbers occurring when shear was intensified and currents non-uniform. This suggests that turbulence lifts cells from the benthos and re-suspends them into the water column, but not above the weak thermocline that existed in May. This further explains the low chlorophyll *a* concentration recorded during a surface survey three days prior to these vertical investigations.

Chaetoceros sp. was the most abundant species during the August survey. The species found was possibly *C. compressus* with a cell size range 7-26 μm . This small chain-forming diatom showed a chlorophyll *a* distribution opposite to the patterns seen in May, highlighting the enormous variation in phytoplankton water column structure. Although many cells were counted (maximum 14×10^6 cells litre $^{-1}$), it was not reflected by the chlorophyll *a* concentrations due to the small size of this species. The distribution of the motile euglenoid, *Eutreptiella marina*, suggested an active maintenance of position, with an upward vertical migration at 13:00 hr (GMT) forming a surface maximum, during maximum currents of the ebb tide. This surface aggregation of *E. marina* was also observed by Kifle (1992).

Peridinium trochoideum also followed this pattern forming a maximum of 9×10^3 cells litre⁻¹ with a mid water column aggregation at approximately 7 m. The phototrophic ciliate, *Mesodinium rubrum*, followed a similar pattern of mid-water aggregation during the rapid ebb flow. This pattern had been observed previously for *M. rubrum*, where Crawford and Purdie (1992) determined the vertical distribution of *M. rubrum* during a red tide event over a tidal cycle in Southampton Water. In their study, the population maximum of *M. rubrum* was deeper and more dispersed on the ebb than on the flood or during slack water. This behaviour was explained using the theory that a distribution governed solely by phototactic surface aggregation, would result in population losses on each daytime ebb period (a distance ~ 5 km). In contrast, *M. rubrum* maintained itself at the head of the estuary for several weeks without evidence for extensive flushing losses. These *in situ* observations were further supported by data obtained using an airborne thematic mapper to determine the spatial distribution of the bloom (Garcia *et al.* 1993), where surface chlorophyll *a* concentration throughout the upper estuary was shown to significantly reduce during the ebb tide. *M. rubrum* is an unusual member of the phytoplankton in that it is an obligate, functional phototroph due to the presence of an algal (cryptomonad) endosymbiont, and has been responsible for some of the highest recorded rates of planktonic primary production (Taylor 1982). Another unusual feature of this ciliate is its phenomenal swimming speeds (~ 8 mm s⁻¹) (Lindholm 1985), making it a difficult organism to isolate in the laboratory, where it has been seen to swim away from Pasteur pipettes. Such swimming speeds enable this species to perform diurnal migrations of ~ 40 m in the Peru upwelling zone (Smith and Barber, 1979). *In situ* observations of *M. rubrum* have been well documented, but the similar patterns shown by other motile organisms (euglenoids and dinoflagellates) have not been previously reported.

Phototaxis has been cited as a trigger for vertical migration (Kamykowski 1974), and as these experiments were not conducted over a 24 hour period, PAR may be a major factor instigating phytoplankton vertical migration. Theoretically, however, motile photosynthetic organisms should ascend in the daylight hours and descend prior to sunset (Kamykowski 1974). Alternative suggestions are that organisms descend the water column to collect nutrients and then return to the surface layers to photosynthesise, but as this is an estuarine system it is unlikely that nutrients are a limiting factor. The distributions of *M. rubrum*, *Eutreptiella* sp. and *P. trochoideum* showed similar patterns in vertical migration, which can be related to the aggregation of cells during the maximum ebb velocities, either as a passive effect due to the entrainment properties of the rapid flow, or as an active accumulation to a more 'suitable' vertical position.

3.3.5 CONCLUSIONS

The reduced riverine inputs during the summer survey, reduced the vertical salinity gradient, causing only a very weak salinity stratification, which was destroyed during maximum shear events. These shear events correlated with the timings of SPM re-suspension which were closely coupled to the increased boundary shear caused by non-uniform velocity gradients in the overlying water. For both the spring and summer surveys these re-suspension events were related to the increased velocities during the ebb flow. Opposing chlorophyll *a* patterns were clearly observed for each survey, with a bottom dwelling diatom dominating the spring bloom, followed by the bio-diverse phytoplankton population in summer, which was dominated by motile species aggregating in surface waters. During the summer survey, motile phytoplankton exhibited a vertical migration pattern causing species to aggregate in the surface and mid-water column during the ebb tide, at 13:00hr (GMT). To further investigate this apparent vertical migration, longer surveys were conducted in 1996 and 1997.

3.4 25 HOUR EULERIAN SURVEY IN SOUTHAMPTON WATER

A longer term investigation was implemented to determine the physical structure over two tidal cycles, during periods of wind driven and tidal mixing. This 25 hour survey had the advantage of allowing an assessment of the phytoplankton population (diatoms, dinoflagellates and phototrophic ciliates) during both daylight and dark hours.

During the first high water slack period (07:30-08:30) downwelling PAR decreased between 2200-1400 lux. During the first high water period, the very strong winds (20 m/s)

had been blowing for 12 hours, mixing the water column, preventing

3.4.1 SAMPLING STRATEGY

One station (Hound Buoy on Figure 3.2) was the focus of a 25 hour intensive monitoring programme to determine the physical parameters controlling phytoplankton vertical distribution over two tidal cycles under light and dark conditions. This experimental design marks the first of its type for Southampton Water investigations, permitting a large suite of parameters to be measured.

Sampling was performed over a 25 hour period, within the vicinity of Hound navigation buoy

(Figure 3.2) three days after a neap tide (tidal range ~ 3m). This experiment took place between 07:30 (GMT) 19 June- 08:30 (GMT) 20 June 1997. A downward facing ADCP (Broad Band 600kHz) was used to determine current speed every 5 minutes with a 0.5m depth resolution. CTD casts, with interfaced fluorometer and transmissometer, were profiled at intervals of 0.5hour. Subsamples (100-200 ml) were collected from the Niskin bottles (surface and bottom), from every odd numbered cast, and filtered through pre-weighed GF/F filters for transmissometer calibration (see calibration protocol chapter two). Water samples (150-200 ml) were filtered onto GF/F filters and collected from 5 depths at hourly intervals from every even numbered cast. Whole water sub-samples were preserved with Lugol's iodine for laboratory phytoplankton analysis, whilst the GF/F filters were frozen and stored for laboratory analysis (chlorophyll *a*). The Li-COR submersible irradiance sensor was deployed at 0.5hour intervals to monitor downwelling irradiance at 0.5m intervals throughout the water column, with the second sensor recording surface PAR situated above the cabin.

During the second high water slack period (07:30-08:30) downwelling PAR decreased between 2200-1400 lux. A very strong wind (20 m/s) was experienced throughout the second high water slack period of the 25 hour survey. It was just before 08:30 that the wind subsided, returning the wind speed to near zero. The decrease in the wind speed was accompanied by a strong high with an overcast sky.

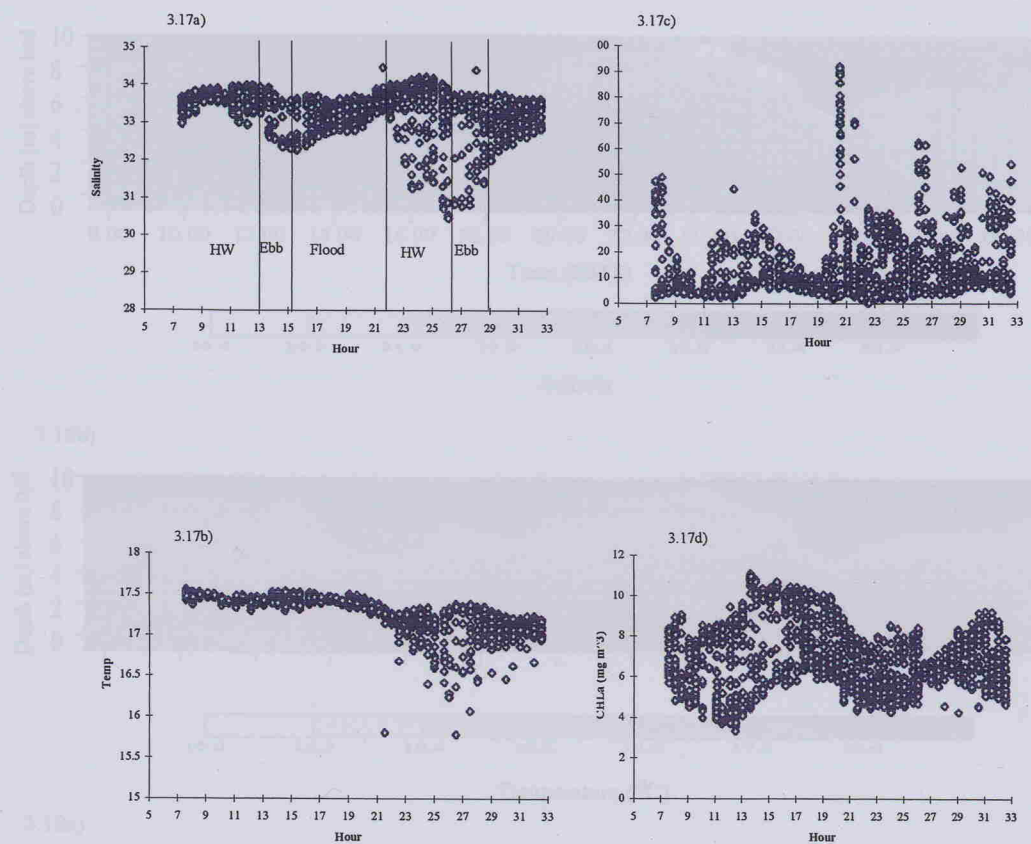
3.4.2 RESULTS

3.4.2.1 CTD DATA

The differences between the two tidal cycles were clearly indicated in the salinity time series (Figure 3.17a) over the period of the survey. The greatest vertical variation in salinity was during the second high water slack period ($\Delta \sim 3.5$), occurring in the dark hours between 22:00-04:00 GMT. During the first high water period, the very strong winds ($\sim 20 \text{ ms}^{-1}$, Meteorological Office data) may have acted to vertically mix the water column, preventing the salinity stratification which is usually governed by the dominant estuarine currents during slack waters. The contours of salinity (Figure 3.18a) highlight the lack of stratification during the first high water period ($\Delta \sim 0.5$). Salinity reduced rapidly during the ebb flow, beginning at 13:00 GMT, with an apparent halocline at $\sim 2\text{m}$ above the estuary bed. The salinity gradient approached zero as the early flood flow began at 16:30 GMT. The salinity structure of the second high water continued through the ebb flow. During this second ebb, the surface salinity reduced further, reaching a minimum of 30 (bottom values ~ 34). This stratification was destroyed during the second early flood at 05:00 GMT, although this vertical mixing was not as intense as the early mixing on 19 June 1997. As the later flood started, the salinity gradient approached zero and the near complete mixing of the first flood stage was again achieved.

The difference in the two tidal cycles was clearly apparent, with the strongest stratification occurring during the high water period of the second tidal cycle. Mixing was most intense during the daytime high water period.

The temperature time series (Figure 3.17b) followed a similar pattern to that observed for salinity, with the largest variance occurring over the high water and ebb of the second tidal cycle. Temperature was uniform throughout the water column until the second high water of the dark period (Figure 3.18b), where vertical variance was $\sim 2.5 \text{ }^{\circ}\text{C}$. The lowest temperature occurred at the second low water period, where values of $15 \text{ }^{\circ}\text{C}$ were recorded, overlying bottom values of $17.5 \text{ }^{\circ}\text{C}$. A weak thermal stratification continued through the second flood water until the end of the surveying period at 09:00 GMT. It was interesting to observe the cool water overlying the bottom warmer water. The patterns of the temperature time series suggested a strong link with salinity.



Figures 3.17 a-d. Time Series during the 25 hour Southampton Water survey in June 1997. 3.17a) Salinity; b) Temperature ($^{\circ}\text{C}$); c) SPM concentration (mg l^{-1}); d) Chlorophyll *a* concentration (mg m^{-3}). All data points used.



Figure 3.18 a-d. CTD information during the 25 hour survey in Southampton Water (June 1997). a) Salinity; b) Temperature ($^{\circ}\text{C}$); c) Chlorophyll *a* concentration (mg m^{-3}). Crosses represent data points.

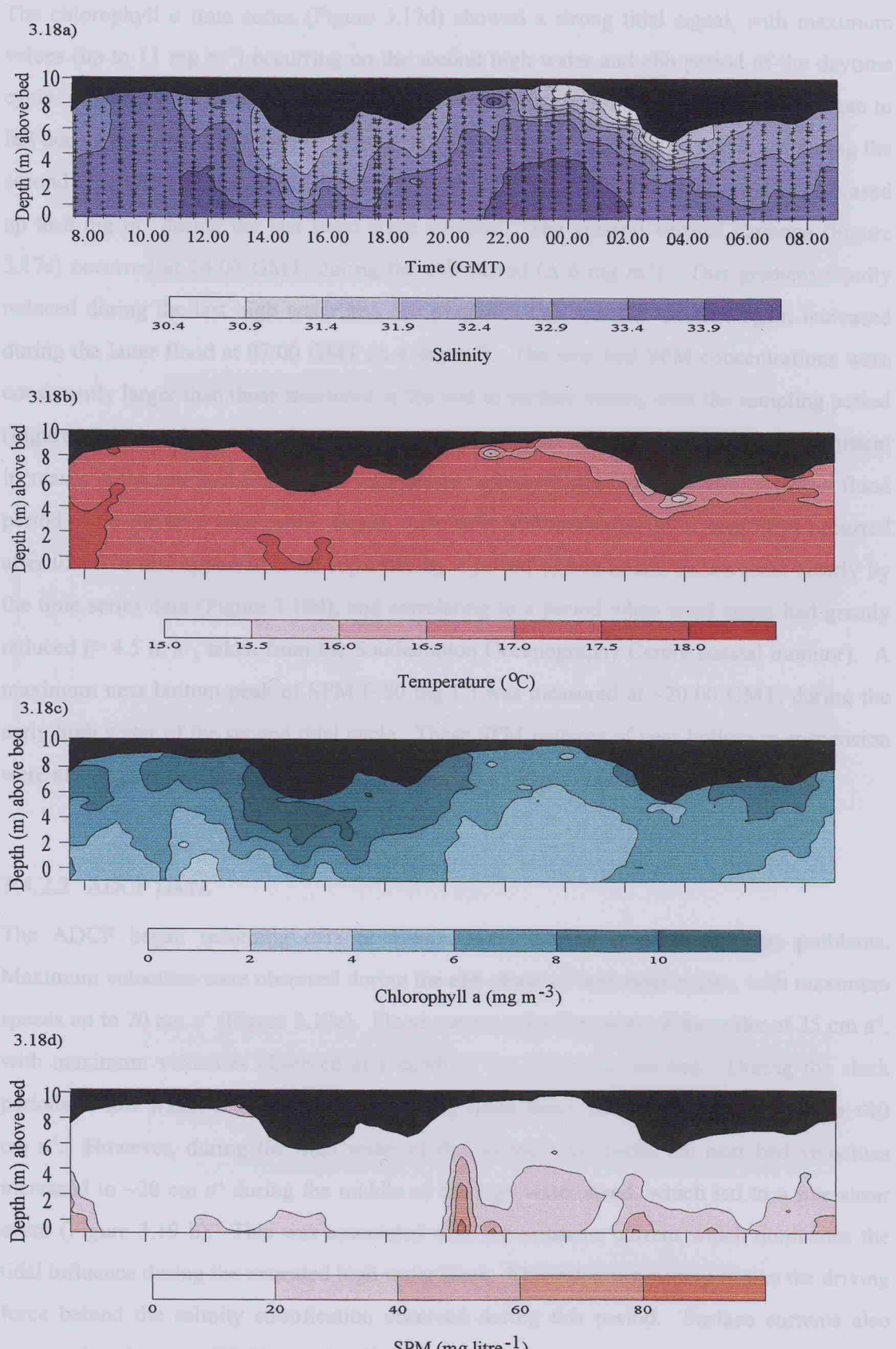


Figure 3.18 a-d. CTD information from the 25 hour survey in Southampton Water (Hound Buoy) June 1997. a) Salinity; b) Temperature ($^{\circ}\text{C}$); c) Chlorophyll a (mg m^{-3}); and d) SPM (mg litre^{-1}). Crosses represent data points.

The chlorophyll α time series (Figure 3.17d) showed a strong tidal signal, with maximum values (up to 11 mg m^{-3}) occurring on the second high water and ebb period of the daytime cycle. This peak concentration formed a near-surface maximum (Figure 3.18c), and began to fall during the second flood stage of the first tidal cycle, then marginally decreased during the second high water period of the dark tidal cycle at 21:00 GMT. The chlorophyll α increased up to 8 mg m^{-3} during the last flood stage sampled. The greatest vertical variance (Figure 3.17c) occurred at 14:00 GMT, during the ebb period ($\Delta 6 \text{ mg m}^{-3}$). This gradient rapidly reduced during the last high water and ebb periods. This vertical variance again increased during the latter flood at 07:00 GMT ($\Delta 4 \text{ mg m}^{-3}$). The near bed SPM concentrations were consistently larger than those measured in the mid to surface waters, over the sampling period (Figures 3.17c and 3.18d). Surface concentrations were always $<20 \text{ mg l}^{-1}$. Intermittent increases in the near bed SPM levels were clearly apparent, particularly during the latter flood period of the daytime tidal cycle. Peaks in the near bed concentration of total SPM occurred after 02:00 hr and appeared to be separated by a period of two hours, shown most clearly by the time series data (Figure 3.18d), and correlating to a period when wind stress had greatly reduced ($> 4.5 \text{ m s}^{-1}$, taken from the Southampton Oceanography Centre coastal monitor). A maximum near bottom peak of SPM ($\sim 80 \text{ mg l}^{-1}$) was measured at $\sim 20:00$ GMT, during the early high water of the second tidal cycle. These SPM patterns of near bottom re-suspension were also highlighted through the ADCP backscatter signal (Figure 3.19c).

3.4.2.2 ADCP DATA

The ADCP began recording data at 10:00 GMT, due to initial instrument problems. Maximum velocities were observed during the ebb phase of both tidal cycles, with maximum speeds up to 70 cm s^{-1} (Figure 3.19a). Flood current velocities were of the order of 35 cm s^{-1} , with maximum velocities observed at a depth of 4m above the sea-bed. During the slack periods of low water, high water and the young flood stand, current velocity reduced to $<10 \text{ cm s}^{-1}$. However, during the high water of the second tidal cycle, the near bed velocities increased to $\sim 20 \text{ cm s}^{-1}$ during the middle of the high water stand, which led to a free-shear event (Figure 3.19 b). This was associated with the estuarine current which dominates the tidal influence during the extended high water slack. This estuarine current is also the driving force behind the salinity stratification observed during this period. Surface currents also increased at this time ($10-20 \text{ cm s}^{-1}$). The tidal mixing intensity was maximum during the ebb currents (2 m cm s^{-3} ; Tinton 1997), with reduced mixing during the slack periods.

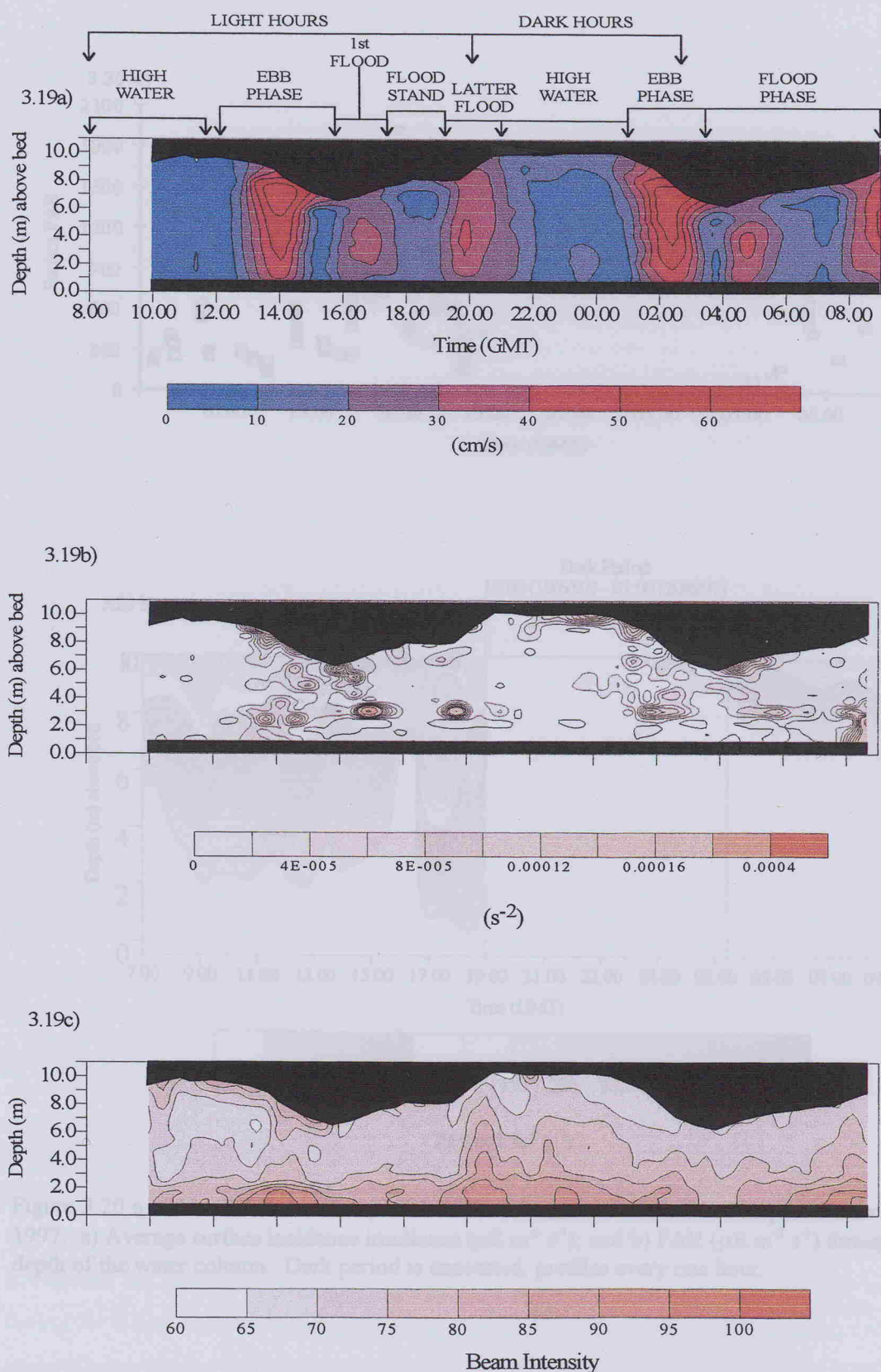
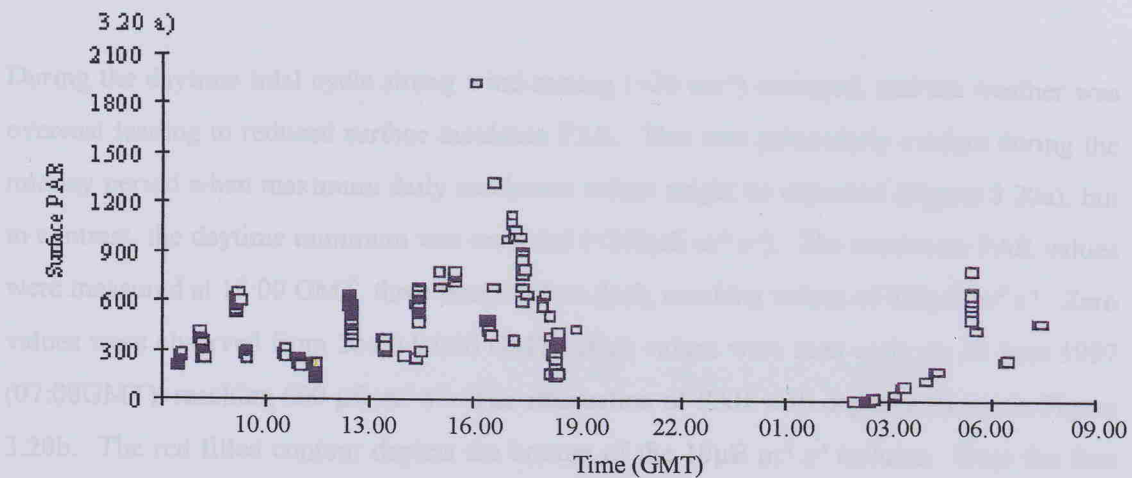


Figure 3.19 a-c. ADCP derived information from the 25 hour survey in Southampton Water, June 1997. a) current velocity (cm s^{-1}); b) shear (s^{-2}); and c) average beam intensity. Early data are missing due to instrument failure. Tidal state is annotated.

3.4.2.3 ILLUMINANCE PAR



3.20 b)

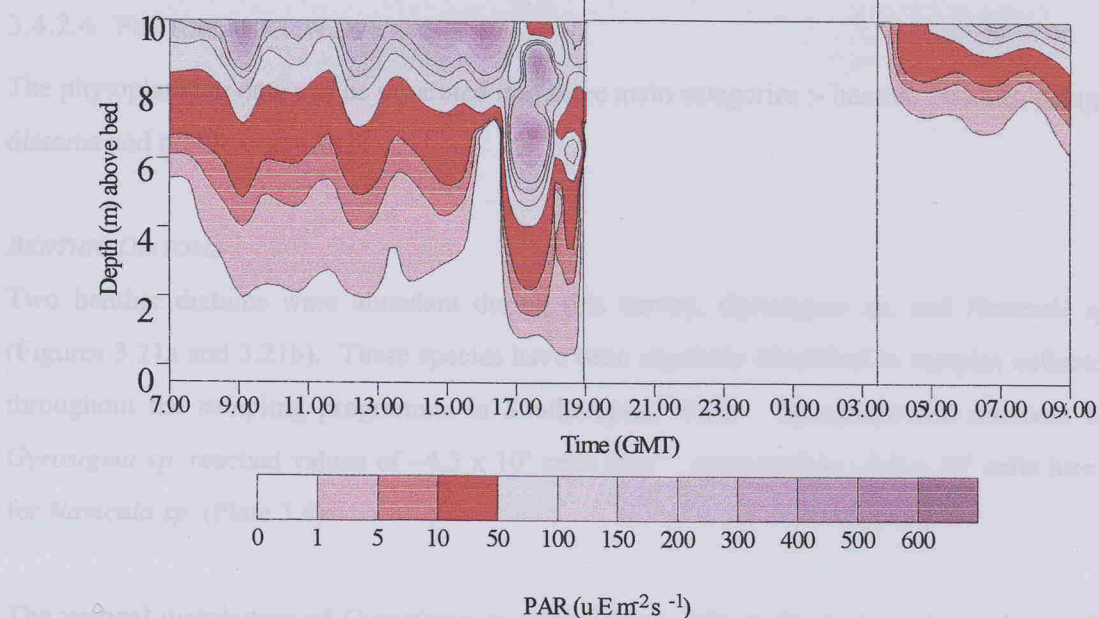
Dark Period
19:00 (19/6/97) - 03:00 (20/6/97)

Figure 3.20 a and b. PAR over the period of the 25 hour survey in Southampton Water, June 1997. a) Average surface incidence irradiance ($\mu\text{E m}^{-2} \text{s}^{-1}$); and b) PAR ($\mu\text{E m}^{-2} \text{s}^{-1}$) through the depth of the water column. Dark period is annotated, profiles every one hour.

during the initial flood flow, this mixing was associated with a period of greater water column shear (Tandon 1971). After high water during the second tidal cycle, and especially before the second low water at 05:00 hr, an increase in the numbers of the turbid organisms detected suspended in the mid water column.

3.4.2.3 IRRADIANCE PAR

During the daytime tidal cycle strong wind mixing ($\sim 20 \text{ ms}^{-1}$) occurred, and the weather was overcast leading to reduced surface incidence PAR. This was particularly evident during the midday period when maximum daily irradiance values might be expected (Figure 3.20a), but in contrast, the daytime minimum was recorded ($< 200 \mu\text{E m}^{-2} \text{ s}^{-1}$). The maximum PAR values were measured at 17:00 GMT, three hours before dusk, reaching values of $820 \mu\text{E m}^{-2} \text{ s}^{-1}$. Zero values were observed from 20:00-04:00 GMT. High values were seen early on 20 June 1997 (07:00GMT), reaching $600 \mu\text{E m}^{-2} \text{ s}^{-1}$. The attenuation of PAR with depth is shown in Figure 3.20b. The red filled contour depicts the bottom of the $10 \mu\text{E m}^{-2} \text{ s}^{-1}$ isolume. Over the first tidal cycle, the average depth of this $10 \mu\text{E m}^{-2} \text{ s}^{-1}$ isolume was $\sim 4\text{m}$, but at 17:00 GMT the depth increased to $\sim 8\text{m}$, corresponding to the maximum surface incident irradiance.

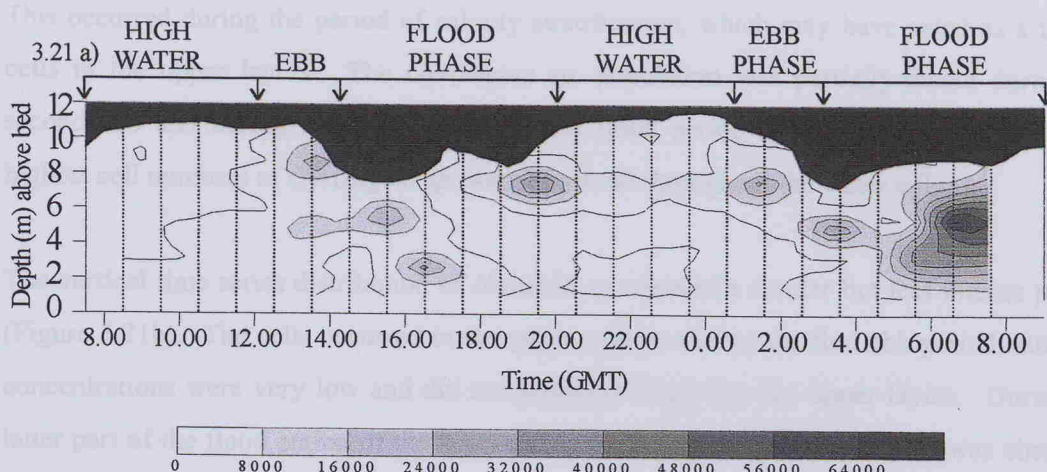
3.4.2.4 PHYTOPLANKTON DYNAMICS

The phytoplankton data can be separated into three main categories :- benthic diatoms, pelagic diatoms and motile organisms:

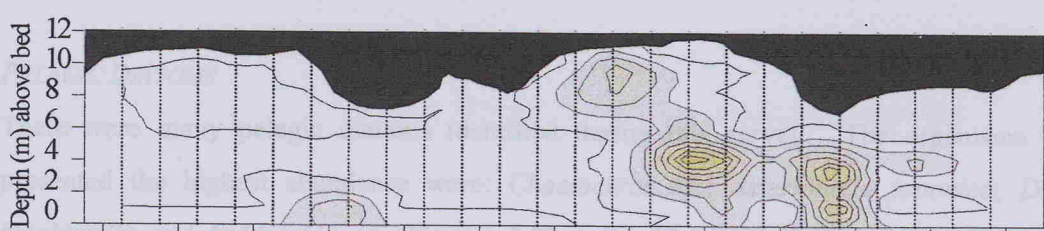
BENTHIC DIATOMS

Two benthic diatoms were abundant during this survey, *Gyrosigma sp.* and *Navicula sp.* (Figures 3.21a and 3.21b). These species have been regularly identified in samples collected throughout the sampling programme in Southampton Water. Maximum cell numbers for *Gyrosigma sp.* reached values of $\sim 4.5 \times 10^3 \text{ cells litre}^{-1}$, compared to $\sim 3.0 \times 10^3 \text{ cells litre}^{-1}$ for *Navicula sp.* (Plate 3.4).

The vertical distribution of *Gyrosigma sp.* showed few cells in the water column during the daytime high water period ($< 4.5 \times 10^3 \text{ cells litre}^{-1}$), with localised population increases during the first ebb flow from $\sim 12:00$ GMT. This population remained in the water column throughout the low water period, and showed evidence of becoming homogeneously mixed during the initial flood flow, this mixing was associated with a period of greater water column shear (Tinton 1997). Over high water during the second tidal cycle, and especially following the second low water at 05:00 hr, an increase in the numbers of this benthic diatom was detected suspended in the mid-water column.



concentrations were very low and did not exceed 1000 cells litre⁻¹ throughout the survey period. During the latter part of the survey, a marked increase in cell numbers was observed, and was particularly apparent during the second flood phase (20.00–22.00 GMT). High water which (2) 2000 (GMT). At 20.00 GMT, the population density, after the initial migration, cell numbers (~3.8 x 10⁴ cells litre⁻¹) were observed. During the low water of the second high water, the population appeared to increase (up to the next contour, and as the flood started again), the population was observed at the next high water.



diatoms exhibited a similar pattern, in terms of time and position of distribution with numbers. The most abundant diatom was *Chadwickia compressum* reaching cell numbers of 2.60 x 10⁶ cells litre⁻¹ (Figure 3.21 b). The distribution of *Chadwickia compressum* throughout the water column during the early high water period, when tidal mixing was greatest, with a maximum in numbers during

Figure 3.21 a and b. Benthic phytoplankton distribution during the 25 hour survey in Southampton Water, June 1997. a) *Gyrosigma sp.*; and b) *Navicula sp.* Cell numbers per litre, 5 water samples collected with depth every hour. Lines represent CTD profiles. Tidal state is annotated.

the high water period the concentration of cells decreased, although a small peak equal to the upper layers at ~3m at 20.00 (GMT), the time of the maximum currents during the latter flood. The surface accumulation extended through the high water period and followed a similar pattern of distribution to the benthic diatom *Gyrosigma sp.* The *Chadwickia compressum* population was again vertically mixed during the second tide phase (following the tides apparent over the first ebb), and formed a marked distribution during the first flood phase of the second tidal cycle.

This occurred during the period of salinity stratification, which may have acted as a trap to cells in the upper layers. The *Gyrosigma* sp. population was partially-mixed during the second ebb and during the flood. During this flood period of the second tidal cycle the highest cell numbers of *Gyrosigma* sp. were observed throughout the water column.

The vertical time series distribution of *Navicula* sp. showed a similar but less intense pattern (Figure 3.21b). The cells occurred in the water column during the first ebb period, although concentrations were very low and did not propagate high into the upper layers. During the latter part of the flood period of the first tidal cycle, a surface increase in cells was observed, and was particularly apparent during the first high water period of dark, high water slack (21:00 GMT). At 00:00 GMT, the *Navicula* sp. population exhibited maximum cell numbers ($\sim 2.8 \times 10^3$ cells litre⁻¹). During the low water of the second tidal cycle, the population appeared to sediment from the water column, and as the flood currents began, the population was only detected in the near bed zone.

PELAGIC DIATOMS

There were many pelagic diatoms identified during this survey. The organisms which presented the highest abundance were: *Chaetoceros* sp.; *Asterionella japonica*; *Ditylum brightwelli*; and *Biddulphia* sp. (Figures 3.22 a-d). The vertical time series for all these diatoms exhibited a similar pattern, in terms of time and position of maximum cell numbers. The most abundant diatom was *Chaetoceros* sp. reaching cell numbers of $> 10 \times 10^5$ cells litre⁻¹ (Figure 3.22a). This was a very small species (ca. 10µm diameter) possibly *Chaetoceros compressum*. This organism was mixed throughout the water column during the early high water period, when wind mixing was intense, with a reduction in numbers during the second high water at 12:00 GMT. The ebb period was also represented by a period of homogeneity. During the first flood phase (16:00 GMT) the population exhibited a peak in cell numbers which extended through the low water stand. During the second flood phase and the high water period the concentration of cells decreased, although a small patch existed in the upper layers at ~2m at 20:00 GMT, the time of the maximum currents during the latter flood. This surface accumulation extended through the high water period, and followed a similar relative distribution to the benthic diatom *Gyrosigma* sp. The *Chaetoceros* sp. population was again vertically mixed during the second ebb phase (following the trend apparent over the first ebb), and formed a maximum concentration during the first flood phase of the second tidal cycle.

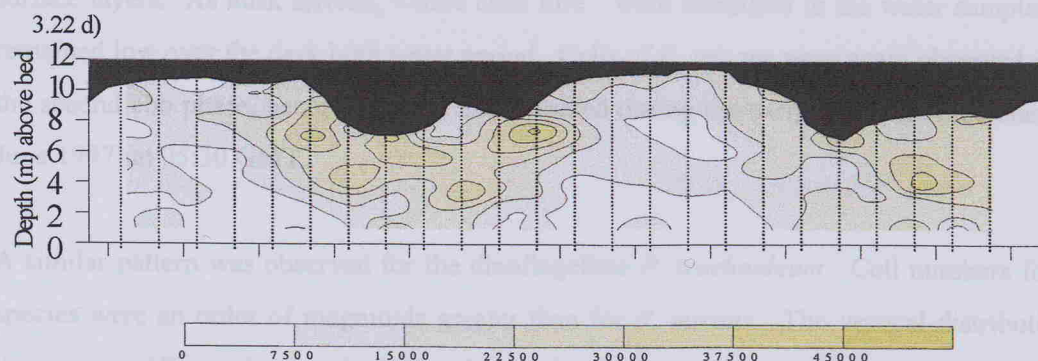
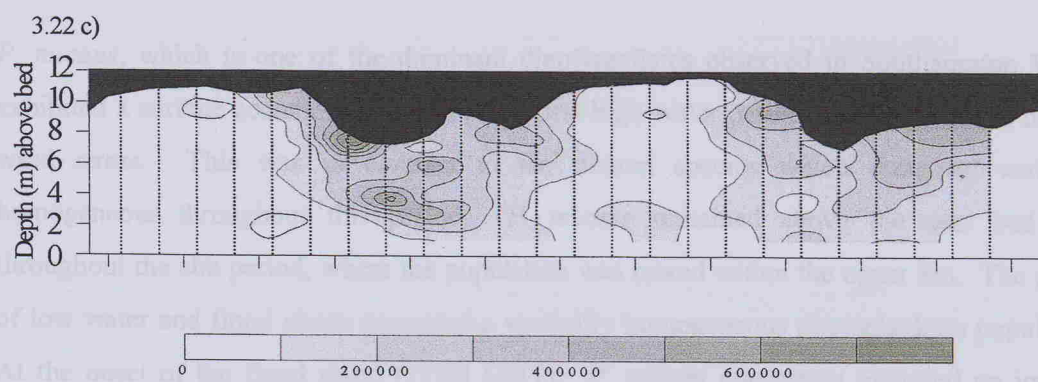
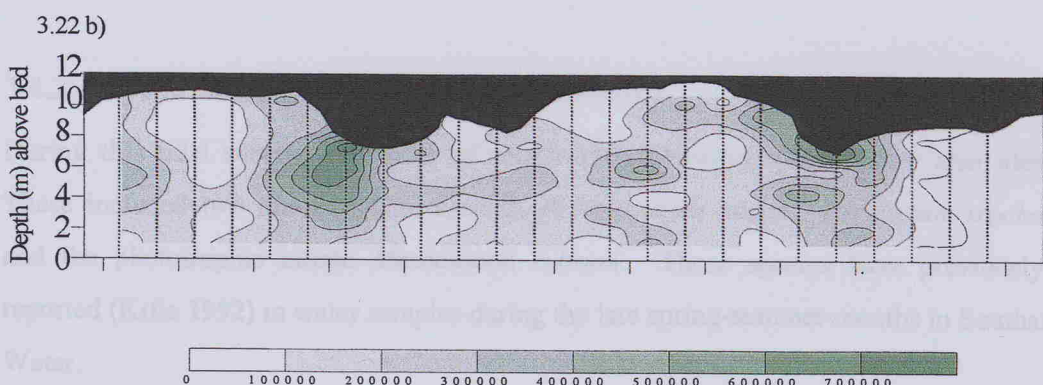
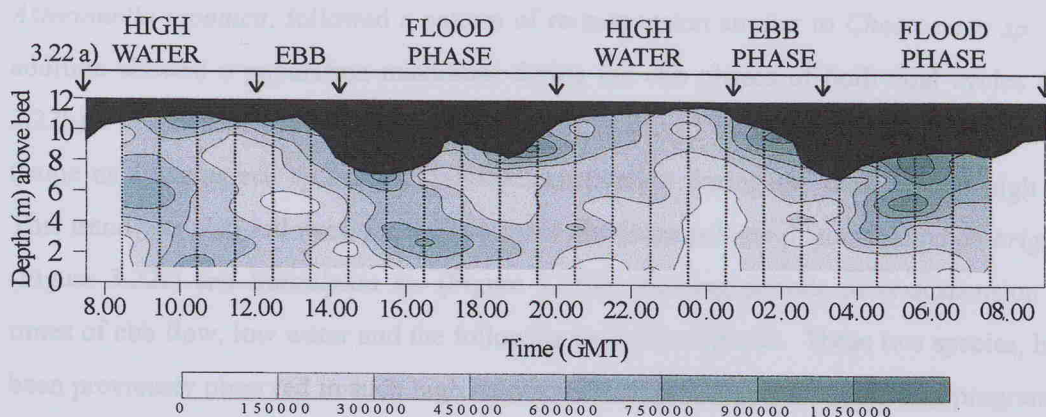


Figure 3.22 a-d. Pelagic diatom distribution during the 25 hour survey in Southampton Water, June 1997. a) *Chaetoceros* sp.; b) *Asterionella japonica*; c) *Ditylum brightwelli*; and d) *Biddulphia* sp. Cell numbers per litre.

Asterionella japonica, followed a pattern of re-suspension similar to *Chaetoceros sp.*, but in addition showed a population maximum during the ebb phases of both tidal cycles (Figure 3.22b). The cell distribution was again vertically mixed during the first high water period (same as *Chaetoceros sp.*) and exhibited stratification during the dark second high water. This trend was also followed for the two other dominant pelagic diatoms, *Ditylum brightwelli* (Figure 3.22c) and *Biddulphia sp.* (Figure 3.22d), showing periods of re-suspension at the times of ebb flow, low water and the following early flood phase. These two species, had not been previously observed in such high numbers throughout the entire sampling programme of 1995-1997 in Southampton Water.

3.4.2.4.1 THE MOTILE PHYTOPLANKTON COMMUNITY

During this tidal survey, a number of motile phytoplankton species were also identified. These included two dinoflagellate species, *Prorocentrum micans*, *Peridinium trochoideum* and the phototrophic ciliate *Mesodinium rubrum*. These species have previously been reported (Kifle 1992) in water samples during the late spring-summer months in Southampton Water.

P. micans, which is one of the dominant dinoflagellates observed in Southampton Water, exhibited a surface accumulation during the first high water period under conditions of high wind stress. This was in contrast to the diatom species which remained vertically homogeneous throughout this period. *P. micans* remained above the near bed zone throughout the ebb period, where the population was mixed within the upper 8m. The period of low water and flood phase presented a vertically homogeneous phytoplankton population. At the onset of the flood stand (17:30 GMT), *P. micans* apparently migrated up into the surface layers. As dusk arrived, <4000 cells litre⁻¹ were identified in the water samples, and remained low over the dark high water period. Cells of *P. micans* were again observed during the second ebb phase, becoming more concentrated during the early morning flood stand (20 June 1997) at 05:30 GMT.

A similar pattern was observed for the dinoflagellate *P. trochoideum*. Cell numbers for this species were an order of magnitude greater than for *P. micans*. The vertical distribution of this species (*P. trochoideum*) exhibited a surface aggregation during the initial high water period, although before 10:00 GMT this species was essentially vertically homogeneous, becoming

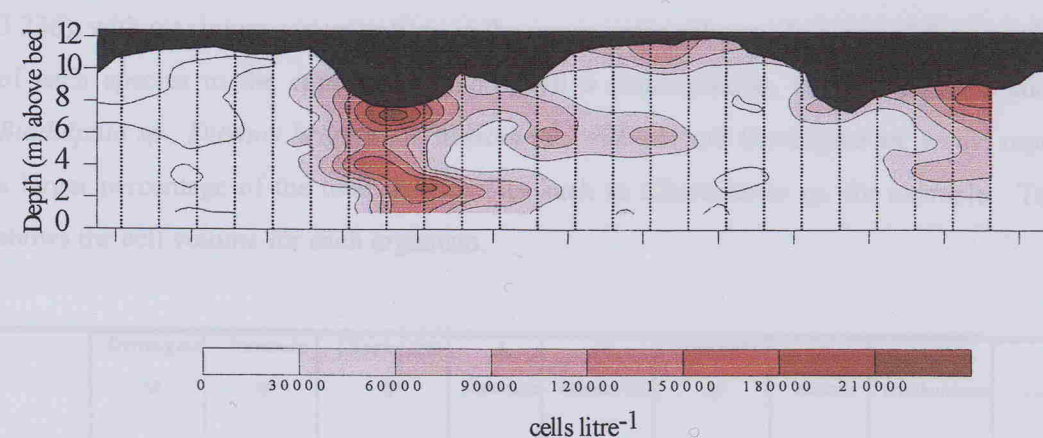
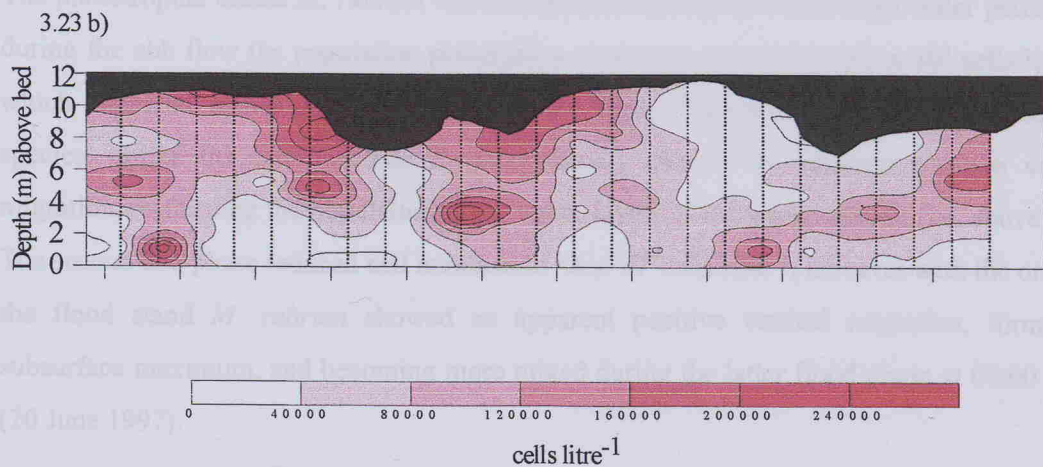
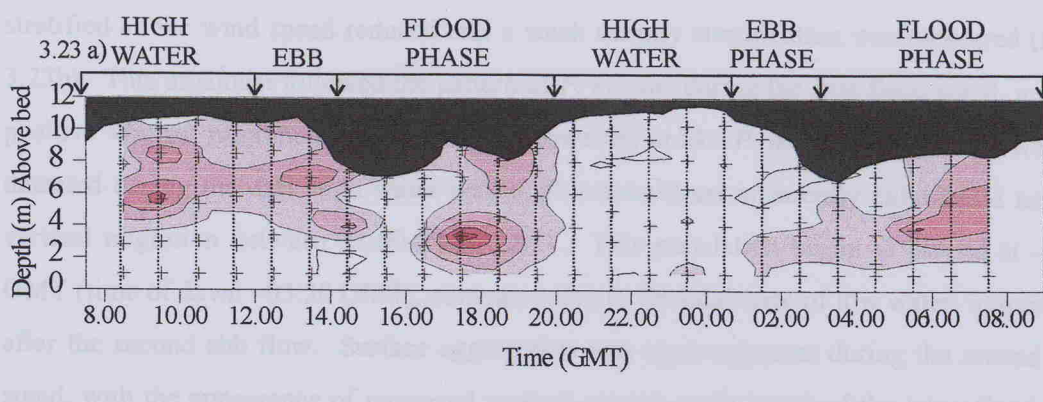


Figure 3.23 a-c. Motile phytoplankton distribution during the 25 hour survey in Southampton Water, June 1997. a) *Prorocentrum micans*; b) *Peridinium trochoideum*; and c) *Mesodinium rubrum*. Cell numbers per litre, crosses represent water samples collected.

stratified as the wind speed reduced and a weak salinity stratification was measured (Figure 3.23b). This organism followed the pattern of *P. micans* during the first flood stand, in which positive vertical migration was observed. However, unlike *P. micans* where cells were not detected during the dark high water period, *P. trochoideum* apparently exhibited a negative vertical migration between 21:00-24:00 GMT. This population began to ascend at ~03:00 GMT (time of dawn ~03:30 GMT), corresponding to the tidal state of low water, immediately after the second ebb flow. Surface aggregation was again apparent during the second flood stand, with the appearance of increased vertical mixing at the onset of the latter flood phase (08:00 GMT 20 June 1997).

The phototrophic ciliate *M. rubrum* was not detected during the initial high water period, but during the ebb flow the population presented a maximum population ($<3 \times 10^5$ cells litre⁻¹), which appeared vertically homogeneous at this time. During the high water period, this species, unlike the dinoflagellate *P. trochoideum*, showed an apparent positive vertical migration, re-forming the population in the upper layers of the water column (i.e. above 6 m). The second ebb phase reduced cell numbers to $<6 \times 10^3$ cells litre⁻¹, however with the onset of the flood stand *M. rubrum* showed an apparent positive vertical migration, forming a subsurface maximum, and becoming more mixed during the latter flood phase at 08:00 GMT (20 June 1997).

In general, maximum cell numbers for most species were observed approximately the period of ebb flow. This was clearly shown by the vertical time series for chlorophyll *a* (Figure 3.23d), with maximum concentrations in the upper water column. In terms of the contribution of each species to the cumulative chlorophyll *a* concentration, larger organisms such as:

Biddulphia sp., *Ditylum brightwelli*, *Mesodinium rubrum* and *Gyrosigma* sp. would represent a larger percentage of the total than species such as *Chaetoceros* sp. for example. Table 8 shows the cell volume for each organism.

	<i>Gyrosigma</i> sp.	<i>Navicula</i> sp.	<i>Chaetoceros</i> sp.	<i>A.</i> <i>japonica</i>	<i>D.</i> <i>brightwelli</i>	<i>Biddulphia</i> sp.	<i>P.</i> <i>micans</i>	<i>P.</i> <i>trochoideum</i>	<i>M.</i> <i>rubrum</i>
Cell Vol.	4189	2133	1795	2550	27245	280686	11781	2927	14137

Table 8. List of cell volumes (μm^3). Taken from Harbour 1988- cell volume program.

Biddulphia sp. has the largest cell volume by an order of magnitude, with the second largest *D. brightwelli*. Comparing the patterns of chlorophyll *a* distribution and the individual diatom species cell numbers showed a close association, however without species identification and enumeration data the apparent behavioural patterns would have remained undetected.

~~Appendix 3~~

3.4.3 DISCUSSION

3.4.3.1 CTD DATA

It is competition between the various stratifying and mixing influences which determines the character of stratification within an estuary (Nunes Vaz *et al.* 1989). The most fundamental of estuarine characteristics is the longitudinal density (salinity) gradient which drives a circulation in the longitudinal-vertical plane (estuarine circulation). The strength of this residual force is not specified by the magnitude of this density current, but it is governed by the intensity of the ambient turbulence. In highly turbulent conditions, which exist in Southampton Water during times of high current shear (i.e. ebb and latter flood phases), much of the energy allocated to residual circulation is diffused vertically. This slows down the circulation by orders of magnitude when compared to the calm situation. The role of turbulence has, to some extent, been resolved through laboratory investigations (Ippen and Harleman, 1961; Harleman and Ippen 1967). These earlier experiments identified that in a uniform density fluid, the horizontal diffusive mass flux increased with increasing tidal range (i.e. higher TKE). When a salinity gradient was introduced, the flux decreased with increasing turbulence. In all the experiments conducted, the horizontal flux of a passive contaminant was appreciably larger in trials with a buoyancy force than in those without.

The principal causes of mixing in the coastal environment relate to the mechanical stirring effects of tidal stress on the benthos and wind stress at the surface. The ability of boundary-generated turbulence to mix the interior of a vertical fluid column depends on: (a) the diffusion of turbulence into the region of stratification; (b) the efficiency of conversion of kinetic energy in the turbulence to potential energy (Nunes Vaz *et al.* 1989).

The decay of turbulence after the source is removed, and the gravitational overturning of a vertically mixed, horizontally stratified fluid, both suggest that stratification can be expected to develop within a period of 10 minutes (Nunes Vaz *et al.* 1989). Southampton Water consistently exhibits a high water slack of the order of 2.5 hours, twice daily, during which

time tidal forcings are minimal. During this time the residual circulation becomes the main source of kinetic energy through the water column, which often emerges as a period of salinity stratification, as shown by the second tidal cycle surveyed. The first tidal cycle allowed the opportunity to determine the efficiency of wind mixing on this shallow partially-mixed estuary.

3.4.3.2 WIND DRIVEN MIXING

Wind stress is often regarded as the major cause of the eddy flux of momentum across the air-water interface in coastal plain estuaries (Pritchard 1956). The vertical profile of wind induced flow is usually parabolic in form, with surface and upper layer flow in the direction of the wind, lower layer in the opposite direction and no flow at the bottom. Southampton Water is a relatively shallow estuary (~15m dredged depth) and clearly became vertically mixed (salinity $\Delta \sim$ zero) during the high winds ($\sim 20 \text{ m s}^{-1}$) encountered during the first high water of the initial tidal cycle. During the second high water (12:00 GMT) the residual estuarine circulation began to dominate, over-riding the wind-driven mixing. The potential energy anomaly (ϕ) remained relatively low during the first high water ($1-5 \text{ J m}^{-3}$), reaching 20 J m^{-3} throughout the second high water, where the strongest residual circulation is often observed. The potential energy anomaly (ϕ) is defined as the amount of work required per unit volume to bring about complete vertical mixing.

$$\Psi = \frac{1}{h} \int_h^0 (\hat{\rho} - \rho) gz dz; \quad \hat{\rho} = \frac{1}{h} \int_h^0 \rho dz \quad (12)$$

where $\rho(z)$ is the density profile over the water column of depth h (after Simpson *et al.* 1990).

The ϕ of the high waters of the daytime cycle can be compared to ϕ during the high water of the second tidal cycle which ranged between $2-20 \text{ J m}^{-3}$, suggesting a greater TKE demand to mix the water column (Tinton 1997). The halocline of weak stratification measured on the second high water was apparent at a depth of $\sim 8.5\text{m}$, suggesting that the wind-driven vertical mixing did not propagate through the whole water column at this time, allowing the tidal straining to act at a point removed from the source of turbulence.

3.4.3.3 ESTUARINE CIRCULATION

Significant salinity stratification developed during the second high water of the dark tidal cycle. The difference in the potential energy anomaly between the two high waters was $\sim 15 \text{ J m}^{-3}$, which emphasised the intensity of the wind stress energy of the initial high water period. Maximum current velocities were recorded during the ebb phases, and minimum velocities during the slack periods, as was expected. Although wind stress was an important source of turbulence during the early hours of the survey, current velocities did not appear to be influenced ($< 10 \text{ cm s}^{-1}$). During this time, velocities were uniform throughout the water column. The high water period of the second tidal cycle clearly showed a non-uniform current structure, with accelerated flows in the near-surface and near-bed zones. This occurred under conditions of little wind stress, allowing the estuarine circulation to dominate. Surface currents were strongest during the ebb flow where a combination of the residual outflow coupled with the ebb tide acted to accelerate the currents. In contrast, the vertical velocity structure during the flood phases highlights the zone of maximum currents in the middle of the water column. In this case, the incoming flood tide acted against the residual surface outflow and thus decelerated the current. The flood stand periods also highlighted this conflict between the tidal forces and the residual flow, with surface velocities reduced by a factor of 2 compared to the incoming bottom waters.

Residual currents (based on a simple advection equation) were calculated during the high water period 20 June 1997 (Tinton 1997). Surface and bottom currents are shown in Table 9.

	SURFACE (0-4M) VELOCITIES (CM S ⁻¹)	BOTTOM (4-11M) VELOCITIES (CM S ⁻¹)
1 ST HIGH WATER	-20	10
2 ND HIGH WATER	-30	8

Table 9. Residual current values taken from Tinton (1997). Average velocities are presented. Negatives represent flow out of the estuary.

The depth of 4m represented the location of the current reversal, with the excursion of the surface water overlying the more saline incursion. Clearly, this residual flow has further implications on mass transport, not only of particulate matter and pollutants, but on the biological community.

The vertical time series of temperature highlighted the more stable conditions observed during the high water period of the second tidal cycle. It was unusual to note the cooler, fresher water overlying the warmer, saline lower layer, although this emphasises the importance of the stabilising salinity driven gradient acting during this period. The vertical temperature gradient, however was small ($\Delta 1^{\circ}\text{C}$).

The strong tidal signature of the chlorophyll *a* distribution was clear, particularly from the time series data (Figure 3.17d). This correlation has also been observed in Southampton Water through the Southern Nutrient Study (SONUS). Using a moored, data collection buoy (stationed at the Hamble Jetty) continuous measurements of temperature, salinity, oxygen, fluorescence, transmission and nitrate were collected at fifteen minute intervals throughout a period of 100 days, beginning 5 April 1996 (Wright *et al.* 1997). The spring-neap signature was clearly apparent over the time period, but shorter term trends were also highlighted. Chlorophyll *a* concentrations were shown to peak twice daily immediately before low water during a spring tide (tidal range $\sim 4\text{m}$). Little variation in the chlorophyll *a* concentrations were observed over the two tidal cycles (i.e. day and night) which suggested that the phytoplankton governing these peaks were re-suspended phytoplankton. Harmonic analysis was performed on these data which revealed a significant harmonic in the chlorophyll *a* data at a period of a day, regardless of a spring or neap tide. The periods of the semi-diurnal M_2 and S_2 tides were also clear at a period of 0.5 days - governing the chlorophyll *a* peak every 12 hours. A small harmonic at 0.25 day was also observed. This is a period associated with shallow water tides, suggesting re-suspension four times daily due to the greater shear during the flood and ebb phases. These data are comparable to the 25 hour time series signal obtained from the chlorophyll *a* information (Figure 3.17d), which clearly showed two daily peaks in algal biomass.

The phytoplankton species enumeration data allowed the nature of the controlling factors governing the chlorophyll *a* dynamics during a tidal cycle to be investigated, and to assess the importance of re-suspension events and active vertical migration (section 3.4.3.6).

3.4.3.4 SPM FLUX

SPM is suspended in the water column in response to high energy in the near-bed zone (as described in section 3.2.3.3). However, the times of the large plumes of SPM propagating into the water column are not always associated with the times of maximum currents (when

shear is greatest, Figure 3.19b). This was the case for the plume observed at 20:30 GMT, during the first high water of the second tidal cycle. This peak reached SPM concentrations of $>80 \text{ mg l}^{-1}$, and was associated with the slowing down of the flood currents immediately before high water. This may have been due to a hysteresis effect, which has been noted for other estuaries (Schubel and Carter, 1984). The plume of SPM was short-lived, due to the dissipation of energy at the bed. The time series plot of SPM (Figure 3.17c) shows this peak clearly, followed by smaller peaks separated by approximately two hour intervals. These appear to be associated with the subsequent ebb, early flood and latter flood (possibly associated with the tidal harmonic at 0.25 day). It was unusual to note the lack of re-suspension during the first tidal cycle. This may have been caused by a suppression of bed-generated shear due to the wind stress, caused by the theoretical profile of wind induced flow (i.e. no bottom current).

Transport variations occur over a spring-neap cycle, with a reduction during the neap tides due to a decrease in velocity where the more stable water column becomes favourable for deposition (Proenca 1994). Net transport over different tidal states was calculated using the SPM concentration and the current velocity in the water column at given points in time and space (refer to Table 10 and Table 15). The ADCP data for this survey did not collect the direction component correctly, therefore velocity was only accurate as a magnitude measurement. Thus, transport fluxes can only be estimated during the ebb and flood periods, when direction was assumed uniform (for example, in the order of 400 kg m^{-1} , Tinton 1997).

3.4.3.5 PHOTOSYNTHETIC AVAILABLE RADIATION (PAR)

The low concentrations of SPM in the surface layers during the 25 hour survey, suggest that downwelling irradiance should not be influenced significantly by particle scattering. Indeed, the $10 \mu\text{E m}^{-2} \text{ s}^{-1}$ isolume extended through the water column, reaching a depth of $\sim 8\text{m}$ at 17:00 GMT. In this instance, PAR in the water column was less influenced by the SPM levels, than by the surface incidence irradiance which was very low throughout the daytime tidal cycle. The vertical time series of PAR with depth shows clearly that sufficient irradiance ($\sim 10 \mu\text{E m}^{-2} \text{ s}^{-1}$) to sustain net primary production was reaching depths of $\sim 4.5\text{m}$. This fact has major implications for the phytoplankton community, particularly those groups which rely on physical processes to enter the photic zone.

3.4.3.6 PHYTOPLANKTON COMMUNITY

The vertical time series of the benthic diatom *Gyrosigma sp.* was closely associated with the current shear. The importance of intermittent re-suspension of the phytobenthos has been a major focus of numerous investigations (e.g. Shaffer and Sullivan, 1988) and is described in further detail in section 3.2 of this thesis. The tidal signature is clearly indicated from the distribution of *Gyrosigma sp.*, with the patterns of re-suspension repeated during the second tidal cycle. However, this pattern was not so obvious for the second benthic diatom, *Navicula sp.* A major re-suspension event for this organism was not associated with an increase in boundary shear, but coincided with the increase in currents at the mid-point of the high water slack, a time associated with an accelerated residual current. The re-suspension at 03:00 GMT was, however, associated with the increased benthic shear of the second ebb phase. The timing of these re-suspension events is of great importance, particularly in a water column where PAR levels may be limiting algal growth.

The period of re-suspension for *Gyrosigma sp.* occurred during the highest surface PAR values recorded for the survey (i.e. between 15:00 - 18:00 GMT). The population reached cell numbers $>1.8 \times 10^3$ per litre at a depth of 3-6m, during the time of increased water column PAR. *Navicula sp.*, in contrast, entered the water column during the dark period, and thus did not receive the benefit of an intermittent increase in PAR. An important feature to note concerning this behaviour is that the timing of re-suspension will usually be coupled with an increase in total SPM, which will in turn decrease the PAR. However, following re-suspension events, *Gyrosigma sp.* occurs in the water column for a period of ~ 2 hours, which is in contrast to the short-lived SPM plumes which re-settle on a scale of 0.5hr.

The periods of re-suspension for the pelagic diatoms was closely coupled with the increased benthic shear. Patterns for all four species (*Chaetoceros sp.*, *A. japonica*, *D. brightwelli* and *Biddulphia sp.*) were very similar and all four species were mixed into the surface layers of the water column. These microalgae will achieve no benefit from the re-suspension event during the dark period, in terms of irradiance, but will be guaranteed at least one daytime stirring event, as Southampton Water is governed by semi-diurnal tides.

The motile species have the advantage of potentially controlling their vertical position through migration. The mechanisms triggering these migrations are a subject of much controversy (section 1.6). The vertical time series of the dominant motile dinoflagellates exhibited contrasting profiles to that of the diatom community. *P. micans* aggregated in the surface

waters during the first high waters and became entrained (or migrated) to the lower layers after the period of high shear during the first ebb phase. Throughout the dark period, this species was not found in the water samples, but re-appeared at dawn (~03:30 GMT) and moved up into the surface waters during the second flood stand. There appears to be a strong association with irradiance which acts to control the vertical position of this dinoflagellate, however this is dependent on the physical forcings, i.e. migration was only achievable during periods of low turbulence.

The vertical distribution of *P. trochoideum*, initially showed a similar pattern to that of *P. micans*, however its distribution during the dark period was very different. Downward migration was observed during the second high water between the dark hours of 21:00-23:00 GMT. These negative migrations have been observed for many dinoflagellate species, with the "normal" autotrophic dinoflagellate diel vertical migration modelled as ascent during daylight and descent at night (Kamykowski 1974; See section 3.2.3.4). For light responsiveness, however, no single type of dinoflagellate sensory structure has been found. In general, the location of the light-sensitive area for phototaxis is on the ventral side, beneath the sulcus near the base of the longitudinal flagellum. Different species respond to different light wavelengths, but blue (450-475 nm) sensitivity is most frequently observed; *P. micans* for example, responds to 570 nm (Kamykowski 1995). Only total PAR measurements were determined for Southampton Water estuary.

The strong diel migration observed in *P. trochoideum* has also been observed for *Gymnodinium pseudopalustre* in Chesapeake Bay (Tyler and Heinboekel 1985). This population was observed to migrate downwards just before sunset and remained within the lower few metres of the water column until sunrise. These migrations were shown to persist despite tidal changes and were coupled with PAR. Zooplankton grazing pressure was also suggested to be a probable factor in defining the distribution pattern of *G. pseudopalustre*. Zooplankton sampling was also conducted during the 25 hour survey in Southampton Water, and suggested a positive vertical migration of species during the dark period of high water, which may have exerted an added pressure on phytoplankton species to negatively migrate (pers. comm. Kostopoulou).

The fact that species migrate to the lower layers in the water column has further implications for mass transport of the population. Not only do these organisms gain the benefits of increased PAR during the daytime high water (dinoflagellates have a higher requirement for

PAR than diatoms, Holligan 1987), but also can selectively retain the population within the estuary. This has been suggested for other dinoflagellate species, where the migratory patterns ensure longer residence times than those calculated based on advective processes alone (Anderson and Stolzenbach 1985). The population's migration pattern for *P. trochoideum* in this study would suggest that through negative migration during the dark high water period, organisms would be carried landward by the bottom residual current. During this period the population could potentially travel 1.08 km up-estuary during the dark high water period, where the population remained at the near-bed zone until ~03:00 GMT (dawn). This was also the period of increased benthic shear which was associated with the second ebb phase. The population was vertically homogeneous during the ebb flow, and as water column turbulence reduced, it began to form a near-surface aggregation, during the flood flow.

The phototrophic ciliate, *M. rubrum*, has been the subject of many intensive behavioural studies not only in Southampton Water (Crawford and Purdie 1992), but also for many other locations such as the Baltic (Crawford and Lindholm 1997). This organism has been reported to cause recurrent red tides during the late 1980's in Southampton Water (section 3.1.1) and has been observed to migrate during times of rapid surface currents in Southampton Water (Crawford and Purdie 1992). It has been postulated that mechanisms other than irradiance trigger these extensive migrations. Water column stability has been suggested to be a prerequisite for the exceptional blooming of this species. This was observed in August 1998, when a red tide of *M. rubrum* established in Southampton Water after a period of above average freshwater influence (Purdie pers. comm.).

The vertical profiles depicted by the 25 hour study, suggested that during periods of high mixing (i.e. ebb flow and flood phase), the population was well-mixed vertically, and during the stability of the dark high water period, *M. rubrum* behaves in an opposite manner to that seen in *P. trochoideum*, for example. *M. rubrum* positively migrated during the dark high water slack, an observation that links in with the original theory of Crawford and Purdie (1992). This species is not heavily grazed by zooplankton (a reason suggested for the exceptional blooms witnessed during the late 1980's), so would not suffer large population losses throughout the period of positive zooplankton migration. However, this has further implications for the advective losses of the population, as the net transport would be out of the estuary. This may explain the close association with the red water times and the spring-neap tidal cycle described in section 3.1.1, suggesting that as the tidal prism increases, population losses are incurred. Species such as *M. rubrum*, although able to achieve exceptional

concentrations (e.g. 2.2×10^9 cells m^{-2} , Crawford 1989), may be short-lived (i.e. fortnightly) except under conditions of reduced tidal flushing. Species such as *P. trochoideum*, may not reach these intense cell numbers, but will be present in the estuary over a longer timescale.

3.4.4 CONCLUSIONS

The presence of wind-driven stress was able to overcome the usually dominant residual circulation apparent during the high water slack period. This prevented salinity stratification, manifesting in a vertically homogeneous water column. This wind-stress was able to restrict the bottom generated shear, responsible for the re-suspension of sediment and phytoplankton. The residual circulation was established during the high waters of the second tidal cycle, where wind-stress was reduced to a minimum. The patterns of re-suspension, apparent for the benthic diatoms, particularly *Gyrosigma sp.*, suggest further benefits from the increased PAR higher in the water column. Re-suspension of the pelagic diatom community followed the same pattern for four dominant species, and was associated with the periods of increased benthic shear. The motile phytoplankton community exhibited apparent vertical migration (both positive and negative), and for two dinoflagellate species, there was a strong link with the prevailing irradiance field. The phototrophic ciliate, *M. rubrum*, also exhibited vertical migration, but in a contrasting pattern to the dinoflagellate community, with positive migration occurring during the stability of the dark high water stand. Vertical mixing of the *M. rubrum* population was apparent during times of intense turbulence (ebb and flood).

3.5 SPRING-NEAP TIDAL CYCLE: PHYSICAL CONSTRAINTS ON PHYTOPLANKTON GROWTH AND DISTRIBUTION.

3.5.1 INTRODUCTION

Based on the strong link between the timing and intensity of phytoplankton blooms in Southampton Water and the spring-neap cycle, surveys were designed to investigate the tidal constraints on phytoplankton species. The variability of SPM during a spring-neap period and the consequences on depth averaged PAR were also investigated. Four days were chosen to cover a spring and neap period, to determine the longer term effect of the tides on physical and biological parameters. The actual survey days were (Figure 3.24): 8 August 1996 (neap tide; tidal range 1.8m); 15 August 1996 (reduced spring tide; tidal range 2.8m); 22 August 1996 (mean tidal range 2.5m); 30 August 1996 (extreme spring tide; tidal range 4.7m). All surveys were performed at the navigation buoy Netley in Southampton Water during daylight hours.

Table 10. Mean current parameters for 1996

3.5.2 SAMPLING STRATEGY

Two 12 hour surveys were accomplished (8 and 30 August 1996) with two intermediary shorter studies of 7 hours (15 and 22 August 1996). On each date, CTD casts were deployed every 0.5 hour, with water samples collected at 5 depths each hour. ADCP data were collected on 8 August and 30 August 1996, with NBA current meter data from the 15 and 22 August 1996, deployed every 0.5 hr, with current velocity and direction recorded at 0.5 m resolution.

3.5.3 RESULTS

3.5.3.1 CURRENT VELOCITY

Mean current velocities for each survey are shown below in Table 10, clearly highlighting the semidiurnal variability in currents, and the spring-neap forcing.

	TIDAL RANGE (M)	HIGH WATER	EBB	LOW WATER	FLOOD STAND	FLOOD
8 TH AUGUST 1996	1.8 (NEAP)	0.08	0.45	0.10	0.09	0.25
15 TH AUGUST 1996	2.8 (SPRING)	0.14	0.65	-	0.18	0.55
22 ND AUGUST 1996	2.5 (MEAN)	-	0.75	0.30	0.35	0.60
30 TH AUGUST 1996	4.7 (SPRING)	0.15	0.85	0.20	0.15	0.50

Table 10. Mean currents velocities (m s^{-1}) over a spring-neap cycle at varying tidal states.

Figures 3.25 clearly show the dominant residual circulation during high water, especially noticeable during the spring tide (Figure 3.25d₁). These plots describe graphically the velocity profiles over a spring-neap period. Each survey was further divided into four tidal states: high water ₍₁₎, ebb flow ₍₂₎, flood stand ₍₃₎ and the latter flood tide ₍₄₎. Comparisons directly between the extreme cases of the neap and the spring, showed clearly the rapid ebb velocities of the spring tide which double the ebb currents measured during the neap (Table 10). The flood currents of the spring tide were also double the flood currents of the neap. The intermediary days (15 and 22 August 1996) showed expected current velocities between the range of the spring and the neap. The data collected on the intermediary days included near-surface and near-bed current velocities, in contrast to the neap and spring survey days when data were collected using an ADCP (data from the surface and bottom 1.5m were lost due to side-lobing).

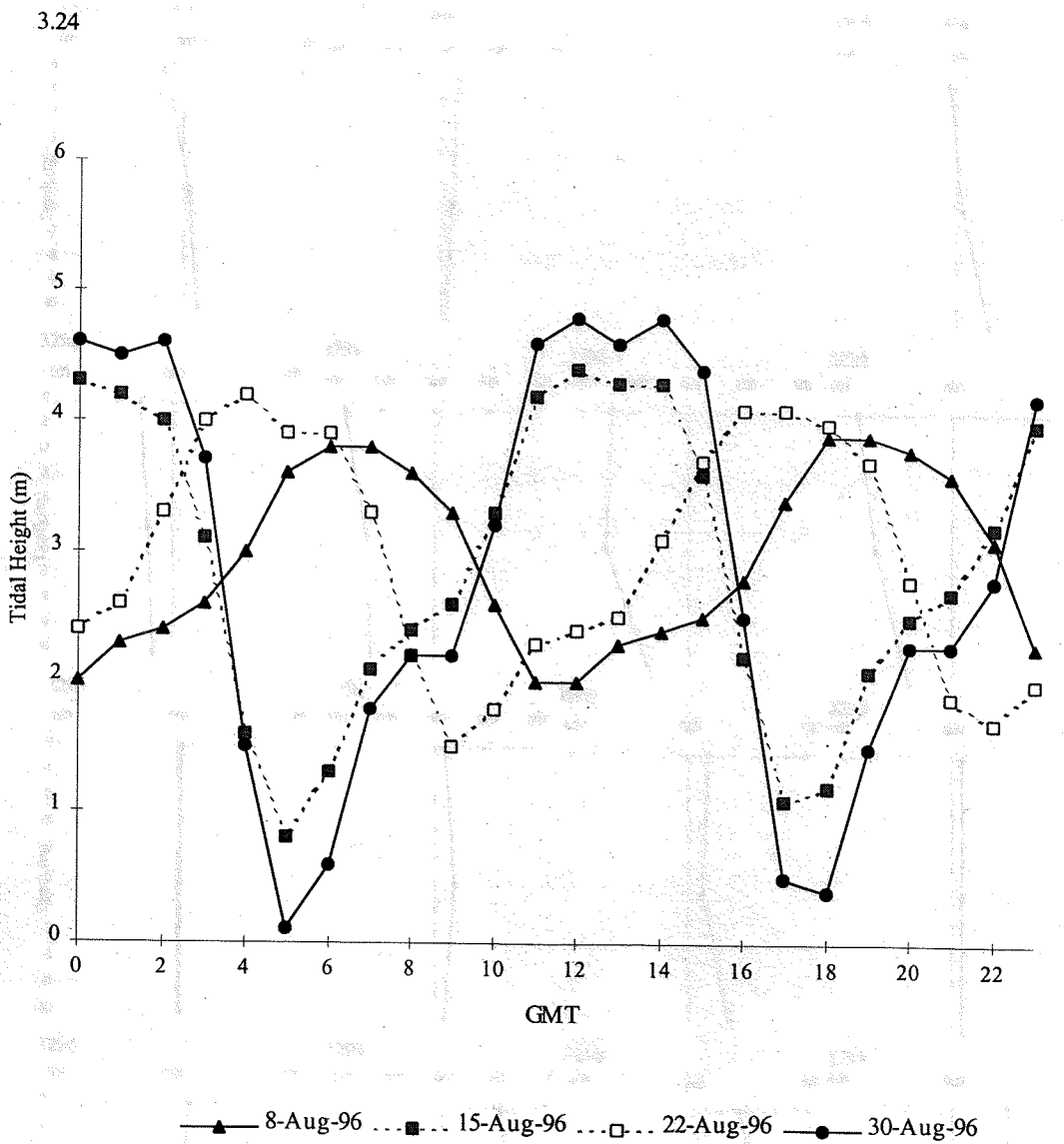


Figure 3.24. Predicted tidal height for the days during the spring-neap tidal survey 1996. Definition of marker styles: solid triangles = 8 Aug 96; solid squares = 15 Aug 96; hollow squares = 22 Aug 96; and solid circles = 30 Aug 96. Solid lines represent 13 hour surveys.

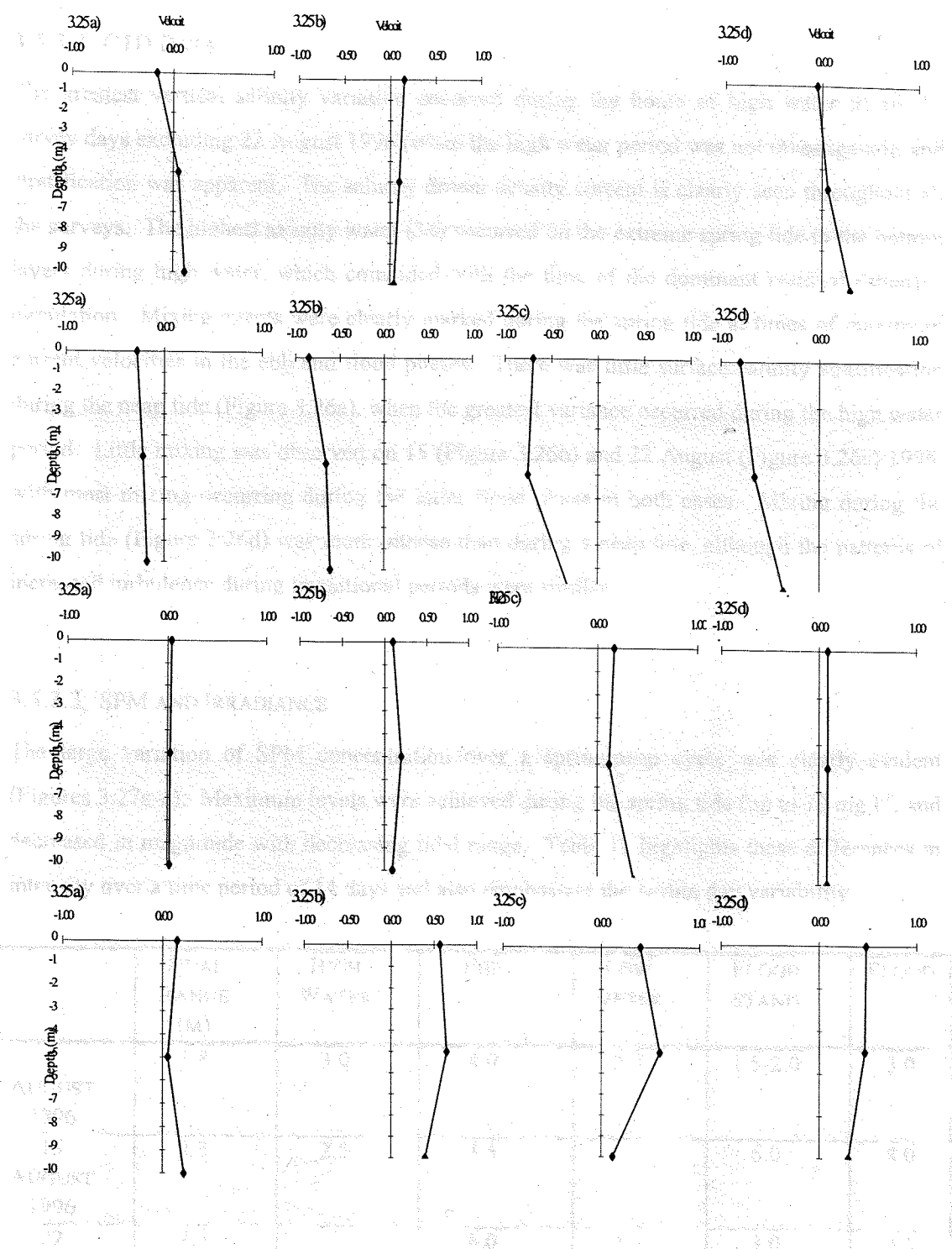


Figure 3.25. Maximum current velocities during varying tidal states. a) neap tide; b) reduced spring tide; c) mid-tidal range; and d) spring tide. Figures 1-4 represent: 1) high water; 2) ebb phase; 3) flood stand; and 4) latter flood phase. All velocities in m s^{-1} .

3.5.3.2 CTD DATA

The greatest vertical salinity variation occurred during the hours of high water in all the survey days excluding 22 August 1996 (when the high water period was not investigated), and stratification was apparent. The salinity driven density current is clearly seen throughout all the surveys. The highest salinity water (34) occurred on the extreme spring tide in the bottom layers during high water, which coincided with the time of the dominant residual estuarine circulation. Mixing events were clearly marked during the spring tide at times of maximum current velocities in the ebb and flood phases. There was little surface salinity stratification during the neap tide (Figure 3.26a), when the greatest variance occurred during the high water period. Little mixing was observed on 15 (Figure 3.26b) and 22 August (Figure 3.26c) 1996, with most mixing occurring during the latter flood phase in both cases. Mixing during the spring tide (Figure 3.26d) was more intense than during a neap tide, although the patterns of increased turbulence during transitional periods were similar.

3.5.3.3 SPM AND IRRADIANCE

The large variation of SPM concentration over a spring-neap cycle was clearly evident (Figures 3.27a-d). Maximum levels were achieved during the spring tide (up to 70 mg l^{-1}) and decreased in magnitude with decreasing tidal range. Table 11 highlights these differences in intensity over a time period of 14 days and also emphasises the within day variability.

	TIDAL RANGE (M)	HIGH WATER	EBB	LOW WATER	FLOOD STAND	FLOOD
8 AUGUST 1996	1.8	3.0	4.0	2.0	1.5-2.0	3.0
15 AUGUST 1996	2.8	2.5	3.5	-	6.0	8.0
22 AUGUST 1996	2.5	-	6.0	4.5	3.0	4.5
30 AUGUST 1996	4.7	15.0	70.0	20.0	20.0	55.0

Table 11. Mean SPM concentrations (mg l^{-1}) over a spring-neap cycle at varying tidal states. Mean values calculated during each tidal period.

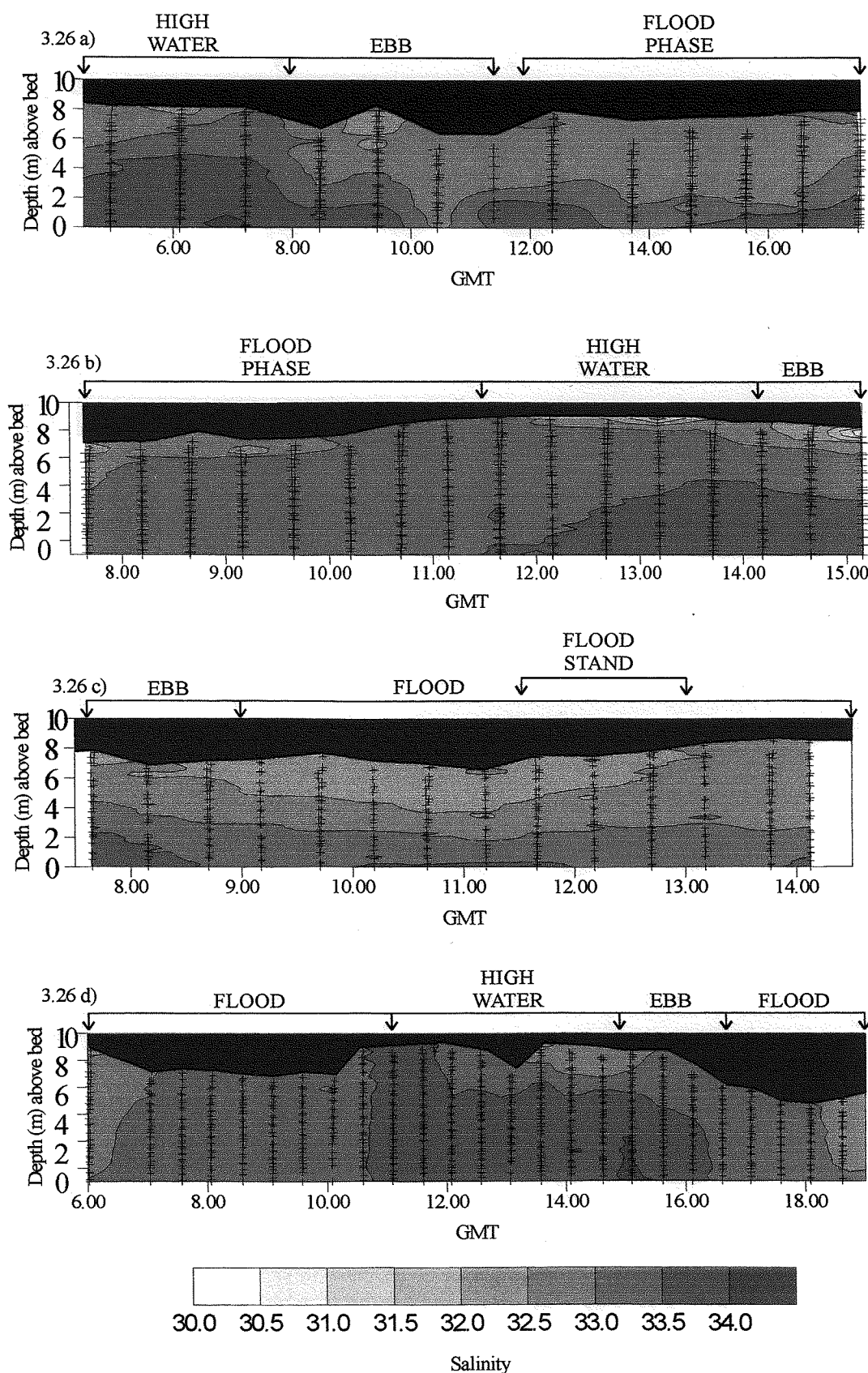


Figure 3.26 a-d. Salinity time series over the spring-neap cycle investigated in August 1996, Southampton Water. a) neap tide; b) reduced spring tide; c) mean tide level; and d) extreme spring tide. Crosses represent CTD casts. Tidal state is annotated.

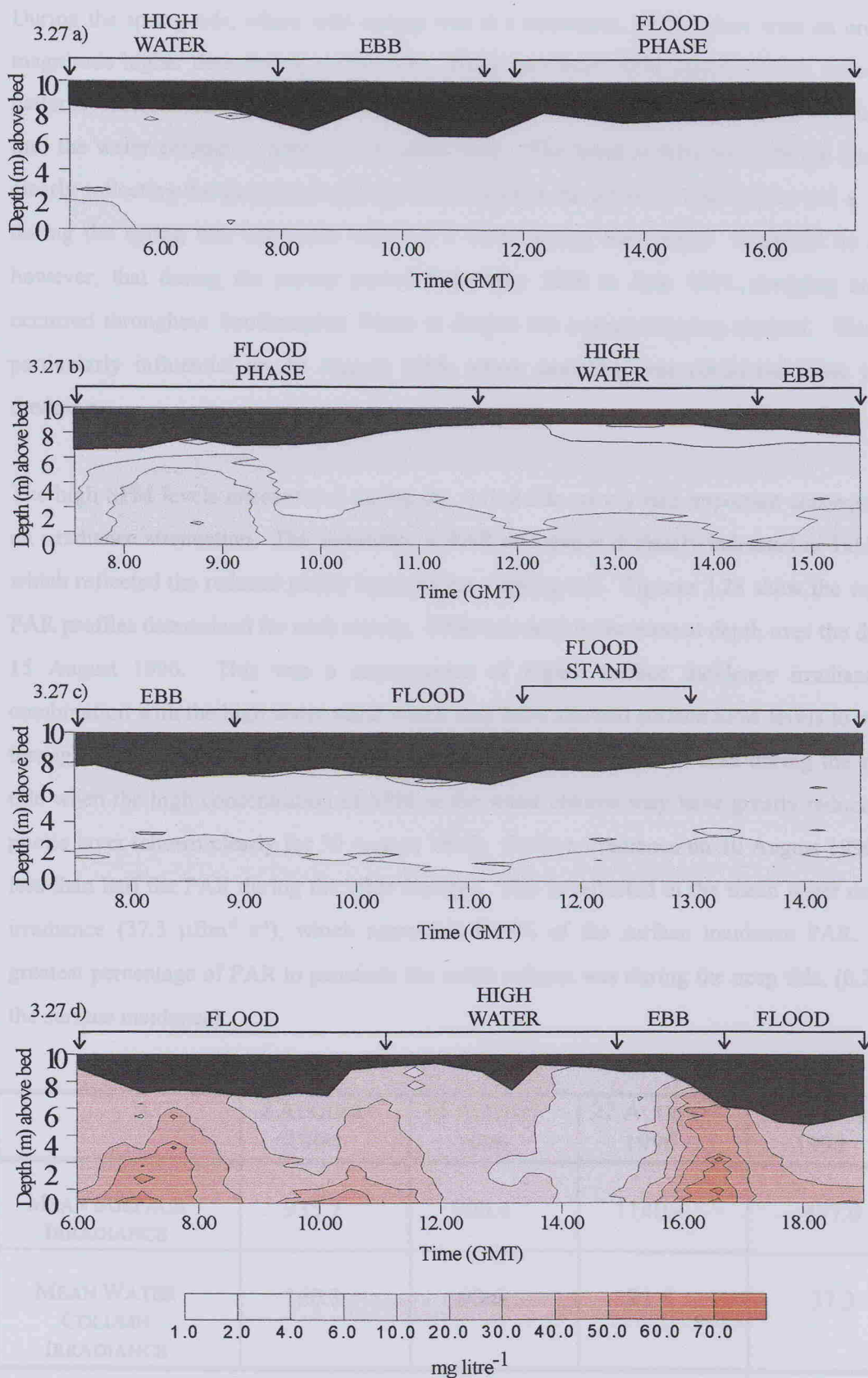


Figure 3.27 a-d. SPM (mg l^{-1}) time series over the spring-neap cycle investigated in August 1996, Southampton Water. a) neap tide; b) reduced spring tide; c) mean tide level; and d) extreme spring tide.

During the spring tide, where tidal energy was at a maximum, SPM values were an order of magnitude higher than during a neap tide. Daily maximum SPM concentrations follow the patterns observed during the earlier preliminary studies, with plumes of sediment entrained into the water column at times of increased TKE. The trend is familiar, with the intensity clearly reflecting the increase in energy resulting from the different tidal prisms ($>1 \times 10^5 \text{ m}^3$ during the spring tide compared with $3.6 \times 10^4 \text{ m}^3$ during the neaps). It should be noted however, that during the survey period from May 1996 to June 1997, dredging activity occurred throughout Southampton Water to deepen the central shipping channel. This was particularly influential on 30 August 1996, where sampling was conducted close to the dredging.

The high SPM levels encountered during the spring tide survey had important consequences on irradiance attenuation. The variability in PAR attenuation is clearly indicated in Table 12, which reflected the reduced photic layer during a spring tide. Figures 3.28 show the vertical PAR profiles determined for each survey. PAR was seen to increase at depth over the day on 15 August 1996. This was a consequence of higher surface incidence irradiance in combination with the high water stand which may have allowed surface SPM levels to reduce through sedimentation. This is in contrast with the vertical patterns seen during the spring tide when the high concentration of SPM in the water column may have greatly reduced the photic layer (shown clearly for 30 August 1996). Surface irradiance on 30 August 1996 was less than half the PAR during the other surveys. This is reflected in the mean water column irradiance ($37.3 \mu\text{E m}^{-2} \text{ s}^{-1}$), which represents 0.08% of the surface incidence PAR. The greatest percentage of PAR to penetrate the water column was during the neap tide, (0.2% of the surface incidence).

	8 AUGUST 1996	15 AUGUST 1996	22 AUGUST 1996	30 AUGUST 1996
MEAN SURFACE IRRADIANCE	935.7	900.4	1140.4	477.0
MEAN WATER COLUMN IRRADIANCE	160.3	98.6	91.5	37.3

Table 12. Average PAR ($\mu\text{E m}^{-2} \text{ s}^{-1}$) over a spring-neap tidal cycle

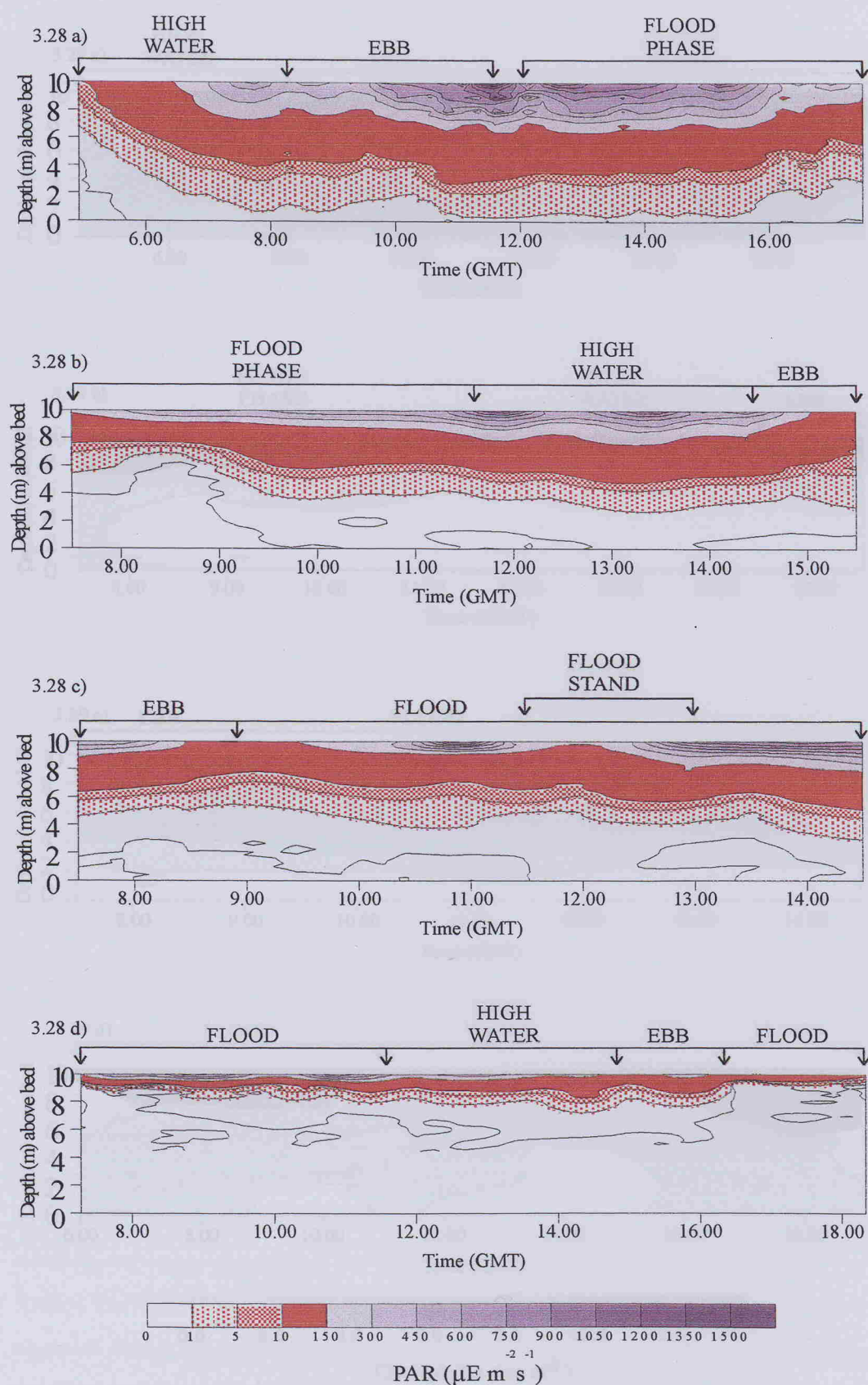


Figure 3.28 a-d. PAR ($\mu\text{E m}^{-2} \text{s}^{-1}$) time series over a spring-neap tidal cycle in Southampton Water, August 1996. a) neap tide; b) reduced spring tide; c) mean tide level; and d) extreme spring tide. The base of the $1\text{ }\mu\text{E m}^{-2} \text{s}^{-1}$ isolume represents the lower limit of the photic zone (Raven 1986). Profiles were taken every 0.5 hr, at 0.5m depth intervals.

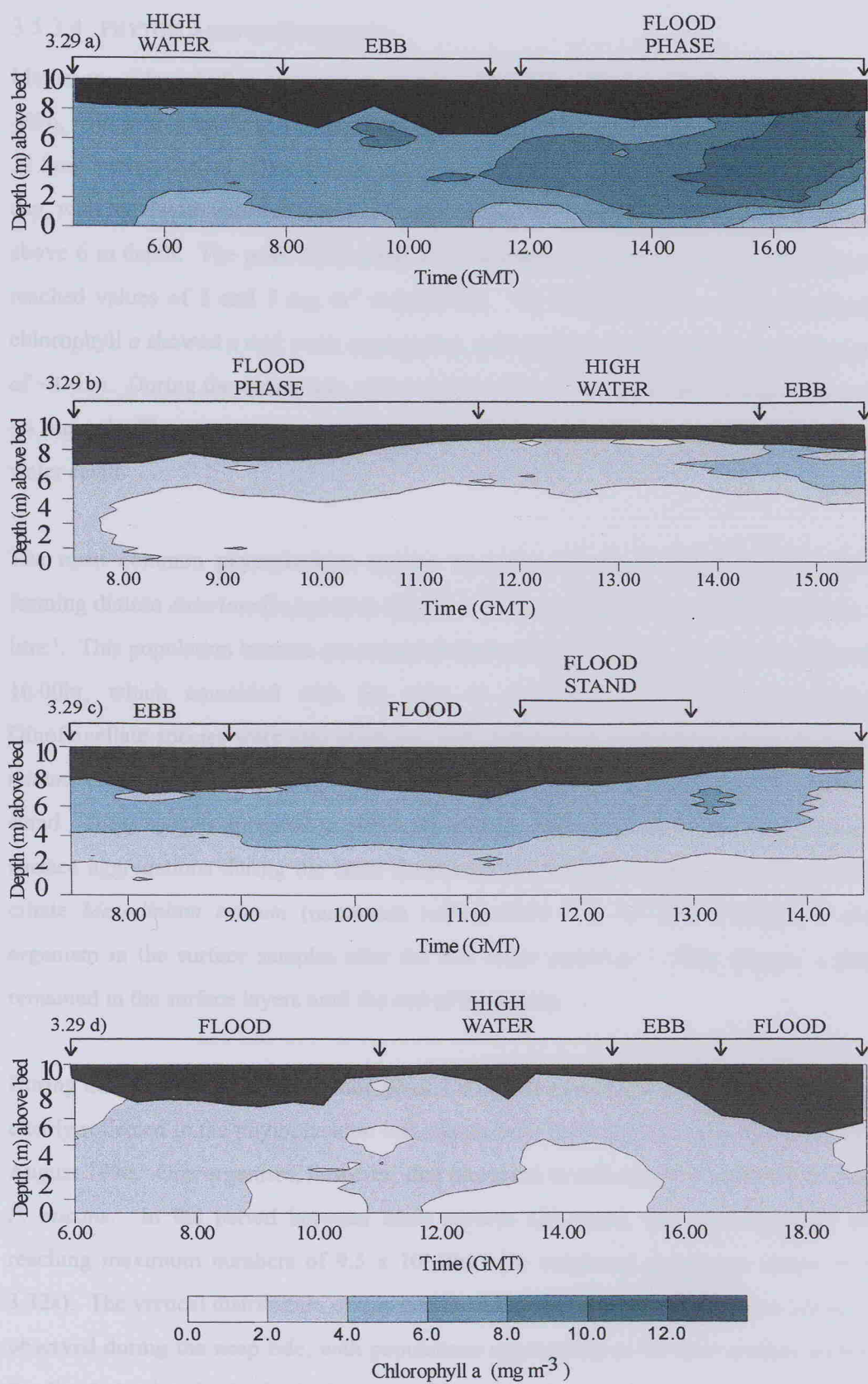


Figure 3.29 a-d. Chlorophyll *a* (mg m^{-3}) time series over the spring-neap tidal cycle survey in Southampton Water, August 1996. a) neap tide; b) reduced spring tide; c) mean tide level; and d) extreme spring tide.

but it gave very similar vertical patterns, which closely followed the physical parameters.

3.5.3.4 PHYTOPLANKTON DYNAMICS

Maximum chlorophyll *a* concentrations were established during the neap tide on 8 August 1996, with values reaching 12 mg m⁻³ (Figure 3.29). The chlorophyll *a* distribution during the 12 hour survey indicated that chlorophyll *a* was vertically well mixed throughout most of the day, with maximum concentrations achieved during the flood and early high water at 16:00 hr above 6 m depth. The peak chlorophyll *a* concentrations during the 15 and 22 August 1996 reached values of 5 and 7 mg m⁻³ respectively. On both days the vertical distribution of chlorophyll *a* showed a mid water aggregation, with highest concentrations forming at a depth of ~4-6 m. During the spring tide, chlorophyll *a* values were reduced to a maximum value of ~4 mg m⁻³. The maximum concentration was measured in the near surface during the high water stand.

The most common phytoplankton species occurring during the neap tide was the chain forming diatom *Asterionella japonica* (Figure 3.30a), with maximum cell numbers of 1.7 x 10⁶ litre⁻¹. This population became concentrated during the latter flood tide, prior to high water at 16:00hr, which coincided with the time of maximum chlorophyll *a* concentrations. Dinoflagellate species were also abundant, and included the dominant species *Prorocentrum micans* (Figure 3.30b) and *Peridinium trochoideum* (Figure 3.30c) during the young flood stand. These species appeared to positively migrate during the slack waters and formed sub-surface aggregations during the latter flood tide and the early high water. The autotrophic ciliate *Mesodinium rubrum* (maximum cell numbers 1 x 10⁵ litre⁻¹) became a common organism in the surface samples after the low water period at 11:00hr (Figure 3.30d), and remained in the surface layers until the end of the survey.

During the extreme spring tide, chlorophyll *a* concentrations were greatly reduced, which was clearly reflected in the phytoplankton cell counts, with most populations in decline from the 8 August 1996. One organism, however, that increased in cell numbers was the dinoflagellate *P. micans*. In the period between these surveys (21 days), the population had doubled reaching maximum numbers of 9.5 x 10⁴ litre⁻¹ (% integrated population shown in Figure 3.32a). The vertical distribution of this dinoflagellate and *P. trochoideum* were similar to that observed during the neap tide, with populations aggregating in the near-surface waters from the flood stand and into the high water. Diatoms such as *A. japonica*, which was the most abundant species during the neap tide, was not identified from the water samples during the spring tide. *Coscinodiscus* sp. was present, again in lower numbers than during the neap tide,

but showed very similar vertical patterns, which closely followed the physical properties of velocity shear at the benthic boundary, where the population became re-suspended into the water column. Many species were present during this day -as it was during the neap tide survey.

Benthic diatoms were also identified during the neap and spring surveys. Species such as *Nitzschia spp.* and *Navicula spp.* were observed in similar numbers during each survey. Figure 3.31 a and b depicts the time series observed for two species of the benthic diatom community during the neap tide. Re-suspension events were evident during times of increased benthic shear, especially during the neap survey, at the time of the ebb (~10:30 hr GMT). *Navicula sp.*, in particular was entrained 4m above the benthos during the ebb of the neap tide. Re-suspension events were also seen during the increased benthic shear of the spring tide survey (Figure 3.33), where clear entrainment of the benthic species (*Nitzschia spp.*) into the water column was apparent. However, during the spring tide survey, these benthic species were observed (in relatively low numbers) throughout the water column at most times during the survey, suggesting intensive mixing and possibly the influence of the dredging activity.

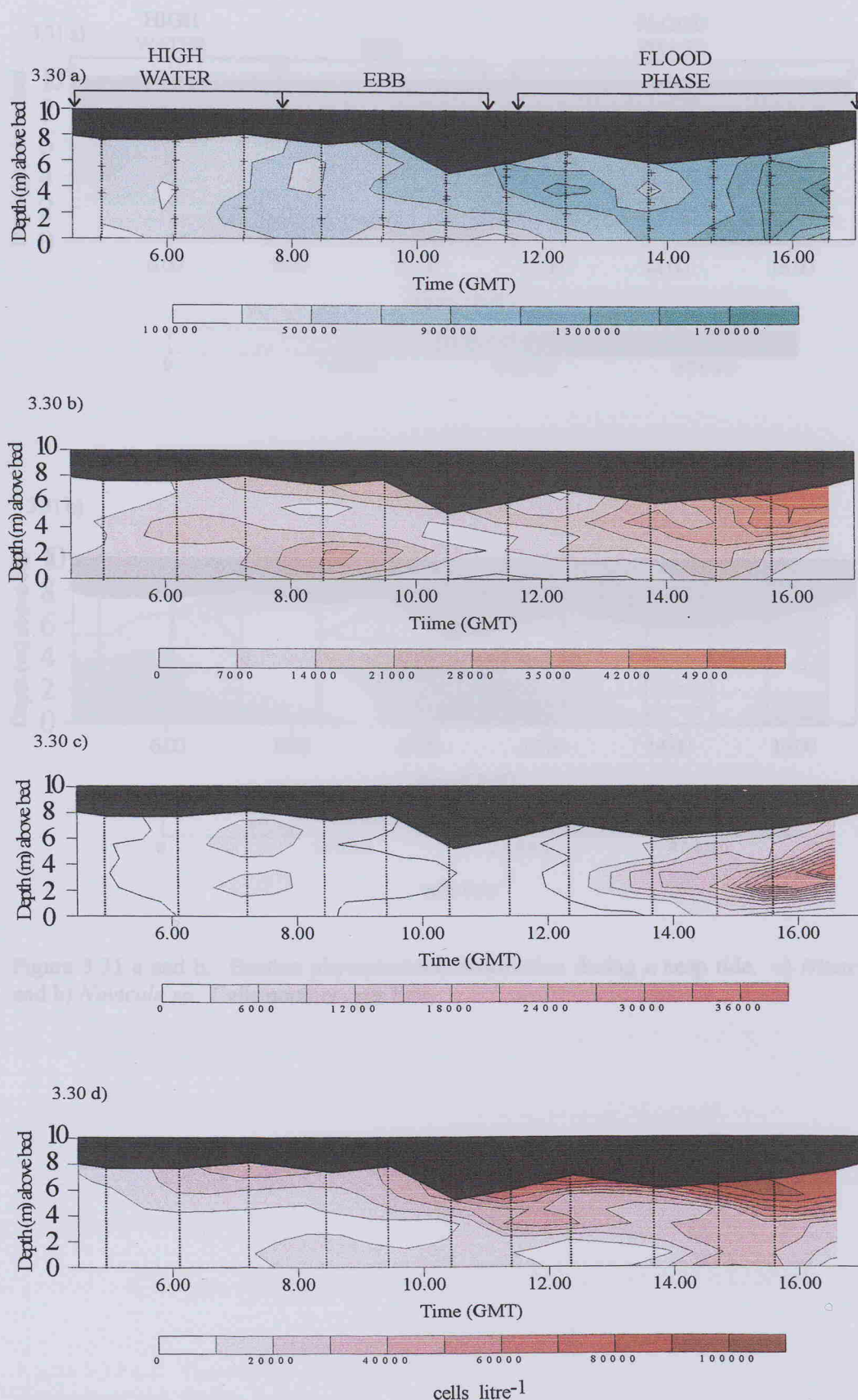


Figure 3.30 a-d. Phytoplankton populations during a neap tide. a) *Asterionella japonica*; b) *Prorocentrum micans*; c) *Peridinium trochoideum*; and d) *Mesodinium rubrum*. Cell numbers per litre, crosses represent water samples.

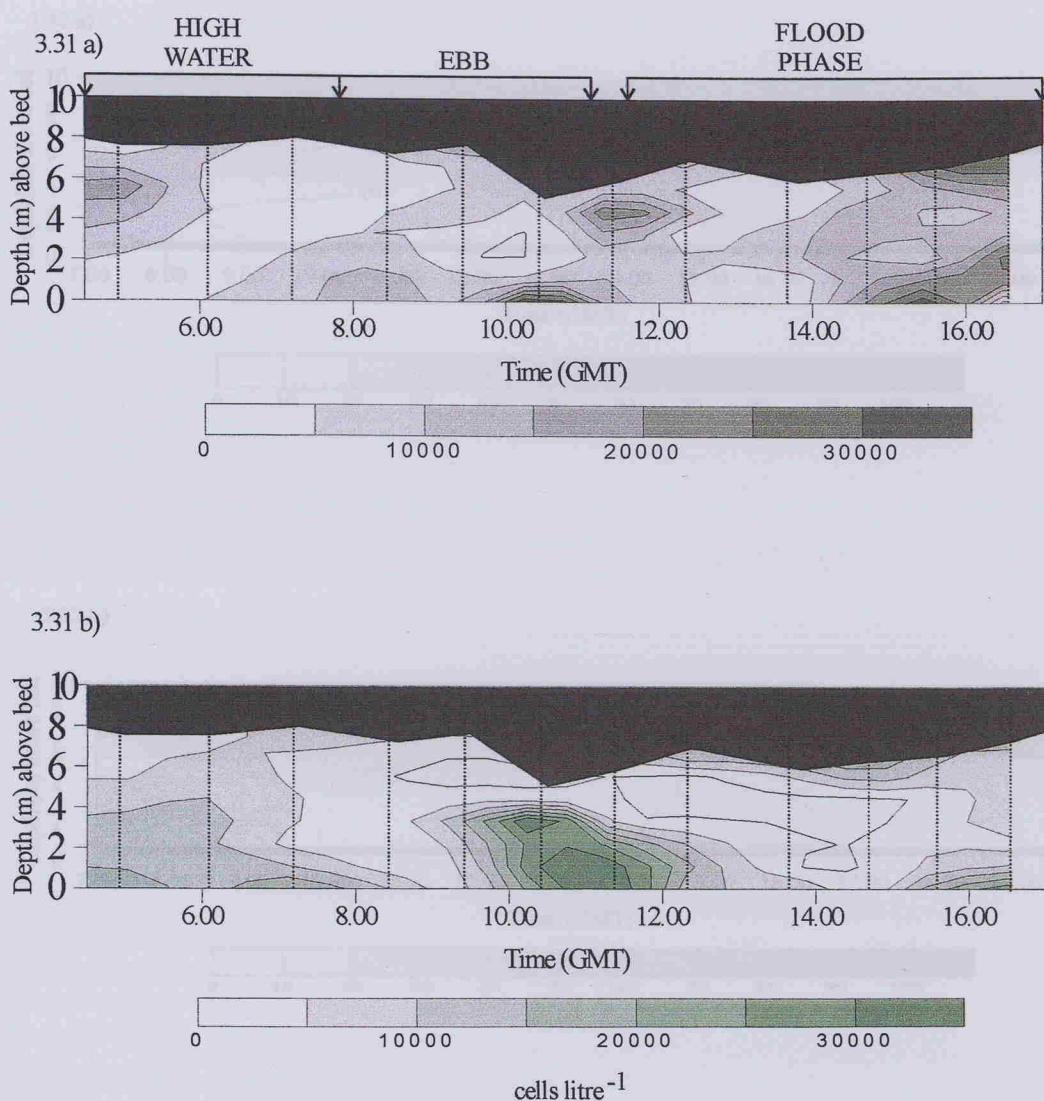
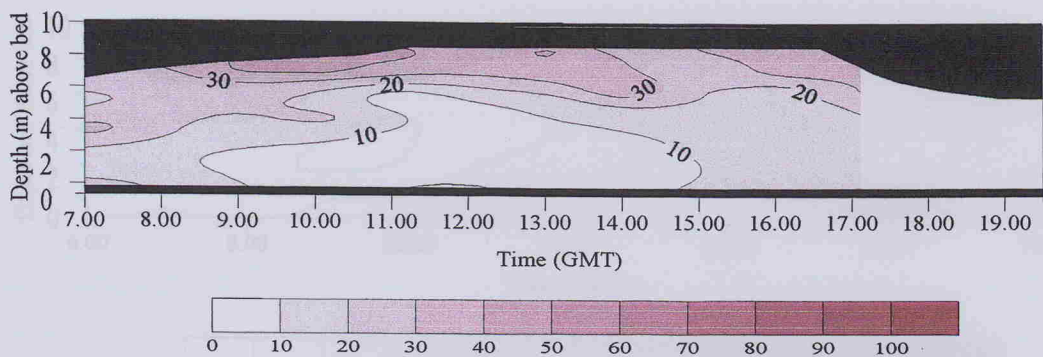


Figure 3.31 a and b. Benthic phytoplankton distribution during a neap tide. a) *Nitzschia* sp.; and b) *Navicula* sp. Cells numbers per litre.

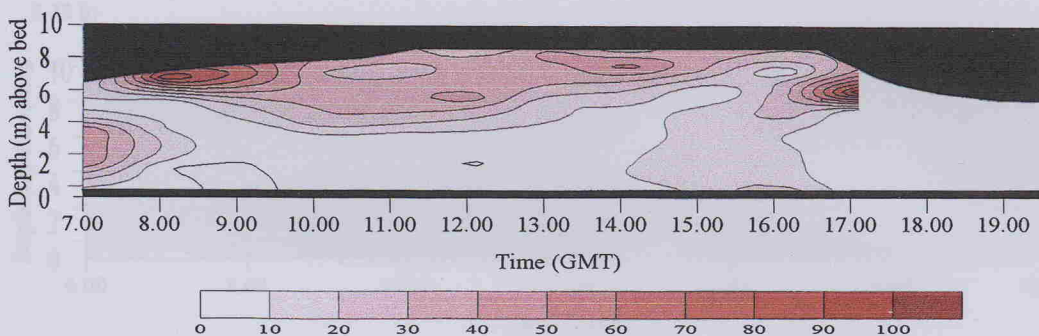


Figure 3.32 a-c. The vertical distribution of various phytoplankton species during a spring tide in Southampton Water, August 1996. a) *Tetraselmis* sp.; b) *Nitzschia* sp.; c) *Phaeocystis* sp. (continued). The vertical axis represents the water column, and the horizontal axis represents the vertically integrated phytoplankton populations (cells Litre⁻¹) at 0.5 m depth intervals. Vertical profiles are taken every 0.5 m.

3.32 a)



3.32 b)



3.32 c)

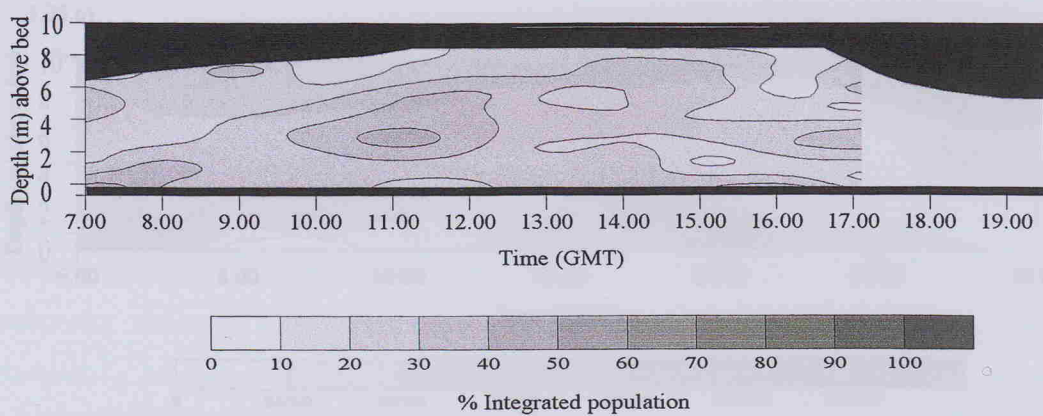
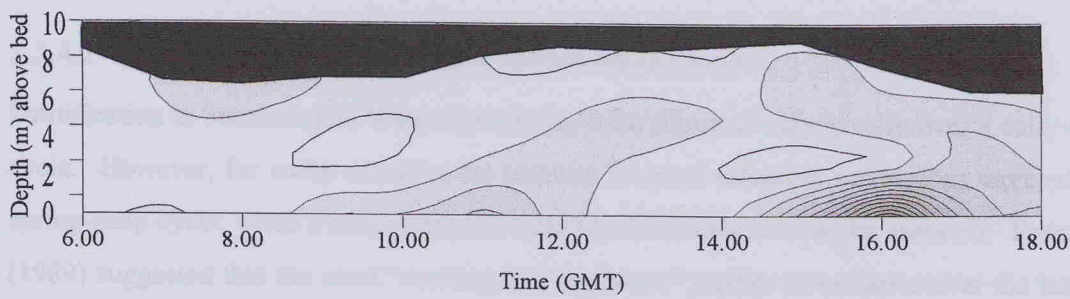
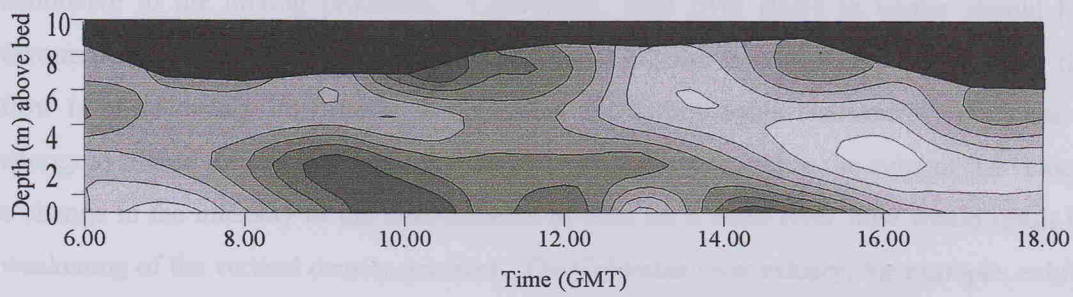


Figure 3.32 a-c. The vertical distribution of various phytoplankton species during a spring tide in Southampton Water, August 1996. a) *Prorocentrum micans*; b) *Peridinium trochoideum*; and c) *Coscinodiscus* sp. Note cell numbers in % vertically integrated phytoplankton population (after Lauria *et al* 1998). 5 whole water samples collected every 0.5 hr.

3.33 a) *Nitzschia* sp.

3.33 b)



3.33 c)

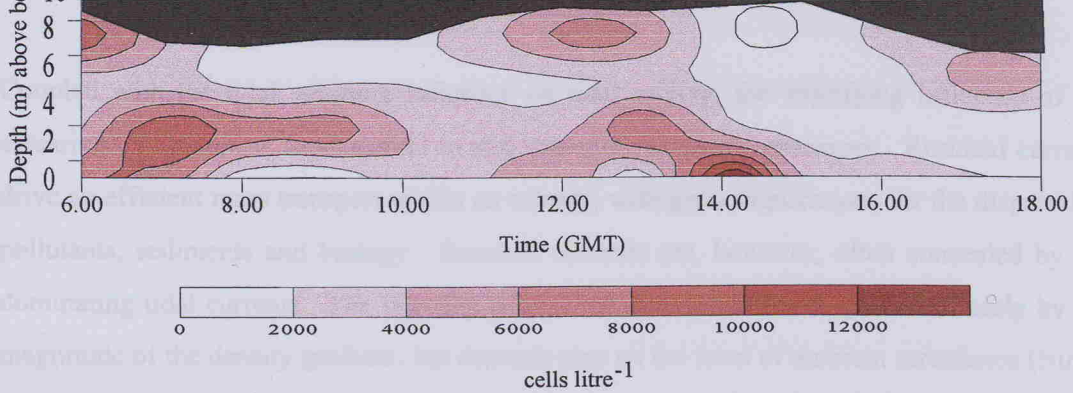


Figure 3.33 a-c. Phytoplankton distribution during a spring tide in Southampton Water, August 1996. a) *Nitzschia* sp; b) *Navicula* sp; and c) *Mesodinium rubrum*. Cells numbers per litre. 5 whole water samples collected every 0.5 hr.

3.5.4 DISCUSSION

3.5.4.1 PHYSICAL CONSEQUENCES OF A SPRING-NEAP CYCLE

Stratification in Southampton Water has already been shown to vary greatly over a daily tidal cycle. However, for many estuaries the primary focus of estuarine mixing has targeted the spring-neap cycle, when a more complete tidal harmonic analysis can be assessed. Pritchard (1989) suggested that the most “*exciting and important*” studies in estuaries over the last 10 years have been the observational and theoretical investigations of the meteorologically forced time variations in the distributions of the residual water surface elevation and the residual currents. Haas (1977) was the first to point out that the sub-estuaries along the western shore of Chesapeake Bay, U.S.A. show a marked spring-neap tidal variation in the intensity of stratification. One site investigated was the York River, Virginia, U.S.A., where low river flow in late summer-early autumn, in conjunction with high spring tides, was conducive to the mixing processes. Conversely, high river flows in winter should have favoured the maintenance of stratified conditions, but the investigations showed that river flow is of secondary importance in regulating the hydrographic characteristics. Since the energy available for mixing from the tidal currents is proportional to the cube of the velocity, a change in the intensity of the tidal currents of 50% for a fixed river flow would result in a weakening of the vertical density gradient. The Columbia river estuary, for example, exhibits an almost uniform horizontal density gradient over 30km from the mouth at the end of the flood period during a spring tide, coupled with weak vertical gradients (Jay and Smith 1988). At the same tidal phase during the neap period, a strong front is formed 25km from the mouth, with a significant vertical density gradient. This re-stratification during the neap cycle is consistent with the baroclinic (residual) circulation observed during low turbulence levels, where potential energy is insufficient to overturn the vertical structure.

Coupled with the tidal straining influence on tidal mixing, the stratifying influence of the estuarine circulation is fundamental to understanding estuarine processes. Residual currents drive an efficient mass transport within an estuary, with great implications for the dispersal of pollutants, sediments and biology. Residual currents are, however, often concealed by the dominating tidal currents. The intensity of residual circulation is not governed solely by the magnitude of the density gradient, but depends also on the level of ambient turbulence (Nunes Vaz *et al.* 1989). In high TKE conditions, the momentum of the residual circulation is diffused vertically, which counteracts the surface residual outflow, slowing the circulation by one to two orders of magnitude in comparison to non-turbulent conditions (Nunes Vaz *et al.*

1989). Turbulence therefore, becomes important in governing flows in estuaries. The preceding chapters have established the intermittency of turbulence in estuaries (e.g. Southampton Water), suggesting that the timescales in which estuarine flows are effected by turbulence may be very short (i.e. semi-diurnal). During spring tides, rapid vertical changes occur, where TKE is maximum creating periods of vertical homogeneity followed by salinity stratification over, for example, a 13 hour time series (30 August 1996). Conversely, during the neap tide (8 August 1996) salinity stratification occurred throughout the period of study.

Linden and Simpson (1988) devised an equation to calculate the time scales involved in the development of stratification in a non-turbulent environment:

$$t_s = \left(\frac{g}{l} \frac{\Delta \rho}{\rho} \right)^{-1} \quad (13)$$

where g is the acceleration due to gravity, ρ is density and l is the mixing length scale.

Using typical estuarine values from Southampton Water, timescales of ~5 minutes have been calculated (Tinton 1997). Significant stratification can therefore be expected within timescales in the order of 10 minutes after tidal turbulence (the main source of mixing in Southampton Water) has ceased, i.e. during periods of slack water. However the intensity of the stratification evolved depends greatly on the spring-neap tidal cycle, with more intense stratification evident during the neap periods, as shown during the survey on 8 August 1996.

Large differences in current velocity were clearly observed between the spring and neap period, with intermediate speeds measured for the surveys conducted during a reduced spring and mean tide. Tidal stirring reduces more significantly than tidal straining from springs to neaps as current velocity (u) reduces, due to the tidal stirring dependence on u^3 and straining on u (Simpson *et al.* 1990). Tidal stirring, therefore, may have an increased influence during the ebb flow, particularly during a spring tide (e.g. 30 August 1996). To establish the effects of these tidal influences, the ADCP data from 30 August 1996 was harmonically analysed to determine the features of the residual flow, particularly at high water (Tinton 1997). The difference between the predicted tidal current from harmonic analysis and the observed value was assumed to be the residual current. Higher tidal harmonics of the M_2 tide are produced in Southampton Water due to the shallow water effects and the proximity of the M_2 degenerate amphidromic point (Pugh 1996). The periods and amplitudes of the tidal harmonics are

shown in Table 13 for the analysed velocity data from two depths (Tinton 1997), these four harmonics were included in the analysis (FORTRAN programme written by Dr J Sharples).

been discussed in the previous section, the following table gives the

HARMONIC	PERIOD		AMPLITUDE	
	1m from surface	2m from surface	1m from surface	2m from surface
M_2	12.4206	12.4206	18.5004	25.6947
M_4	6.2103	6.2103	19.0853	20.9988
M_6	4.14	4.14	28.645	27.9366
M_8	3.105	3.105	3.0074	1.0043

Table 13. The periods and amplitudes of tidal harmonics used to analyse velocity data from two discrete depths (after Tinton 1997).

The analysis showed that surface currents changed direction during the flood stand and on the approach to high water, to a seaward outflow. This was indicative of the surface residual current, and was observed through the velocity magnitude as a surface velocity increase, particularly prominent during the high water stand. The high water stand exhibited a strong oscillating residual current, observed at all depths. The raw residual was calculated to show maximum velocities up to 0.16 m s^{-1} , with direction changing hourly. Unexpectedly, the near-bed residual current was calculated to flow in the same direction as the surface residual. This implies that the entire water column was flowing back and forth during the double high water, with a slight lag between the surface water behind the near-bed zone. Dyer (1982) observed a lateral surface seiching in Southampton Water which led to a lateral internal seiche within the estuary. An along estuarine standing wave (seiche) may exist, which is caused by the rapidly changing pressure gradients produced by the varying current velocities. This seiche would be particularly prominent during an extreme spring tide where rapid current velocities (1.0 m s^{-1}) are interspersed with slack waters over very short timescales.

The highly complex and variable physical regime of Southampton Water is clearly observed through comparisons over a spring-neap cycle, where tidal forcings dominate the residual estuarine circulation. These complexities have an enormous influence on the mass transport properties of the estuary.

3.5.4.2 SPM FLUCTUATIONS OVER A SPRING-NEAP CYCLE

The correlation between re-suspension of SPM and the bottom generated shear has already been discussed in the preceding chapters, where cycles of mixing occurred based on the timing of the ebb and flood currents. The near bed concentrations gradually decreased after the times of maximum currents as vertical mixing could no longer maintain the particles in suspension. These patterns were again observed on each day surveyed in August 1996, but further comparisons were able to be drawn between the longer term variability in conjunction with the spring-neap cycle. The variability of SPM concentration was immediately apparent when comparing the four days surveyed, with concentrations increasing in magnitude from the neap to the spring period.

The main influence of an increase in SPM, within the scope of this thesis, is the consequences on the irradiance field and how this affects phytoplankton populations. Irradiance is exponentially attenuated with depth in the water column due to scattering and absorption of photons by water molecules, suspended particles and by the phytoplankton. Photosynthetic organisms are thus almost exclusively restricted to the photic zone. This is comprised by all layers in the water column in which photoautotrophic production exceeds heterotrophic consumption over the timescale of interest (Tett 1990). Classically, it has been considered as the portion of the water column from the surface down to a depth of 1% surface incident irradiance level. There are indications, however, that this layer can be significantly deeper, with phytoplankton growing at extremely low irradiance, $<1\mu\text{E m}^{-2} \text{ s}^{-1}$ (Raven 1986).

Suspended sediments can become trapped within estuaries by a complexing of factors such as residual circulation, tidal mixing and estuarine morphology. The filtering efficiency is determined by the strength of the residual circulation and by the size of the estuary particularly the length (Schubel and Carter 1984). Once trapped within the residuals, fine particles undergo repeated cycles of deposition and re-suspension prior to permanent accumulation or transport into the sea (Nichols 1984). The timescales involved in these processes will be subject to the flushing time of the estuary and the nature of sediments in question.

The flushing rate for Southampton Water has been estimated as ~17 days (August 1995, chapter 4), based on the fresh water fraction of the estuary, considering an estimated estuarine volume. Mass transport can be calculated by using the measured current velocities at varying water column depths (i.e. surface and bottom), to establish the differential transport of

particles over a tidal cycle. The vertical distribution of SPM varied not only in intensity, but in the propagation of SPM through the water column after re-suspension. The range of vertical re-suspension on the neap survey was 0-2.5m above sea bed, whereas during the spring tide this range had increased to 0-7.0m.

	NEAP TIDE	REDUCED SPRING TIDE	MEAN TIDE	EXTREME SPRING TIDE
EBB	-0.35	-0.80	-0.7	-0.85
HIGH WATER 2	-0.08	-0.05	-0.08 (estimate)	-0.1
FLOOD	0.05	0.18	0.15	0.20
LATTER FLOOD	0.15	0.48	0.4	0.57

Table 14. Maximum Surface (0-5.0 m) current velocities (m s^{-1}) for each survey day over the spring-neap survey. Negative values refer to estuarine outflows. High water during the mean tide was not investigated, therefore value is based on an average of high water velocities measured during the other days.

	NEAP TIDE	REDUCED SPRING TIDE	MEAN TIDE	EXTREME SPRING TIDE
EBB	-0.2	-0.36	-0.3	-0.60
HIGH WATER 2	0.12	0.03	0.08 (estimate)	0.1
FLOOD	0.08	0.14	0.12	0.10
LATTER FLOOD	0.22	0.30	0.30	0.4

Table 15. Maximum Bottom (5-10.0 m) current velocities (m s^{-1}) for each survey day over the spring-neap survey. Negative values refer to estuarine outflows. High water during the mean tide was not investigated, therefore value is based on an average of high water velocities measured during the other days.

Using these calculated velocities (Table 14 and Table 15), the distance travelled in the near surface and bottom zones of the water column were estimated over the spring-neap cycle.

	NEAP TIDE	REDUCED SPRING TIDE	MEAN TIDE	EXTREME SPRING TIDE
SURFACE (km d ⁻¹)	-9.9	-8.2	-9.9	-7.8
BOTTOM (km d ⁻¹)	9.5	4.8	8.6	0
TOTAL DISTANCE (km d ⁻¹)	-0.4	-3.4	-1.3	-7.8

Table 16. Distance travelled (km per day) based on mean current velocities over a spring-neap tidal cycle. Negative values reflected a seaward flow.

In all cases the net daily transport is seaward, and the intensity of this flow increases from a neap to a spring tide. The total distance travelled on the spring tide was 7.8 km d⁻¹, which is twenty times greater than the excursion of the neaps. The vertical propagation of SPM through the water during times of re-suspension, therefore, becomes important in terms of mass transport along estuary. The large vertical range observed during the spring tide (0-7.0m) allows for a proportion of the total re-suspended SPM to travel seaward at a net rate of 7.8 km d⁻¹. In contrast re-suspension of SPM during the neap tide would not only lead to a reduced seaward transport, but also the vertical propagation from the SPM plumes at times of mixing do not entrain into the net seaward, surface current.

This difference in the net transport of the estuary over the spring-neap period has important consequences for the transport of SPM, but also has major implications for the phytoplankton community, particularly those members lacking the ability to migrate vertically.

3.5.4.3 BIOLOGICAL CONSEQUENCES FROM SPRING-NEAP FORCINGS

3.5.4.3.1 DIATOM DYNAMICS

Tidal re-suspension results in the infusion of several types of particulate material back into the water column (Roman and Tenore 1978). The re-suspension of chlorophyll *a* represents both endemic benthic diatoms and phytoplankton that have sedimented out of the water column. The tidal re-suspension of phytoplankton cells, both viable and senescent, reintroduces those cells previously lost from the upper layers. As these populations are moved into different levels of the water column their external environment changes, e.g. faster flowing currents, higher PAR, and higher nutrient levels (NO₃, PO₄ and SiO₃). Benthic diatoms are re-suspended from the sediment, allowing enhanced primary productivity owing to increased

irradiance availability. In order to ascertain the effect of tidal re-suspension on primary production, *in situ* ^{14}C incubations were conducted during tidal cycle studies in Buzzards Bay, Ma., U.S.A. (Roman and Tenore 1978), in 13m of water, over a silt-clay benthos. Over a tidal cycle a 100% increase in the amount of chlorophyll α present in the water was reflected in the change due to tidal re-suspension at 11 m, when the phytoplankton standing crop was high (chlorophyll α $> 4 \text{ mg m}^{-3}$), compared to a 50 % increase when standing crop was low (chlorophyll α $< 2 \text{ mg m}^{-3}$). The microalgae observed in the bottom waters were composed of numerous forms including *Gyrosigma sp.* and *Nitzschia sp.*

The change in primary production in the Buzzards Bay study was compared at 4 and 11m over a tidal cycle. At the start of the ebb tide, chlorophyll was re-suspended from the benthos leading to a 6-fold increase in primary production ($<10 \text{ mg C m}^{-3} \text{ d}^{-1}$ to $65 \text{ mg C m}^{-3} \text{ d}^{-1}$ at the start of the ebb). To determine if irradiance was limiting this enhanced production at 11 m, water samples from 11 m were incubated at 4 m. No significant difference was observed, indicating that there was sufficient PAR in the re-suspension zone to allow enhanced photosynthesis. The phytoplankton observed in the near-bed samples from Southampton Water have a similar species composition to those found in Buzzards Bay, suggesting that the re-suspension of these organisms would allow a periodic enhancement of photosynthesis during times of increased benthic shear. Although primary production was not measured, microscopic examination of live samples from the water samples suggest that the benthic community was viable when collected in the water column., i.e. obvious movement of species such as *Gyrosigma sp.*, *Navicula sp.* and *Nitzschia sp.* when viewed at 200 x magnification.

The vertical propagation of these benthic communities can be compared directly to the plumes observed by the SPM, as these species (*Gyrosigma sp.*, *Navicula sp.* and *Nitzschia sp.*) are unable to actively move in the absence of a hard substrate. The extent, therefore to which these organisms are re-suspended in the water column may depend on the intensity of the boundary shear, due to the near-bed currents. This was particularly apparent during the spring tide survey, where re-suspension of the *Navicula sp.* and *Nitzschia sp.* communities was clearly detected during the latter flood and ebb flows. It is interesting to note that many *Navicula sp.* were re-suspended during the lower shear event caused by the flood tide, whilst *Nitzschia sp.* (although re-suspended during the flood phase) clearly showed the largest increase in cell numbers during the intense bed shear of the ebb tide. *Gyrosigma sp.* was also found in bottom samples, but these data are not shown.

The benthic microalgal community was poorly represented in the neap survey samples, with only *Nitzschia* sp. counted. This population was mainly observed in the bottom samples, showing an increase in cell numbers during the ebb and (to a lesser extent) during the flood flows. It is also interesting to note that although SPM re-suspension on this day was not intense, the *Nitzschia* population was still able to propagate into the water column.

The consequences in estuaries of this entrainment into the water column, not only may potentially enhance photosynthesis (Roman and Tenore 1978), but will also transport these cells with the prevailing current. This would be potentially more important for the population during the spring tide when the intense currents may entraining cells high into the water column where the fastest ebb currents may transport the population ~ 3 km in one hour. The potential photosynthetic enhancement is also an important factor for the benthic population during the spring tide (particularly during 30 August 1996) as the SPM loading was so intense, leading to a highly reduced photic zone (~ 1.2 m = depth of 1% surface PAR). This becomes a vital environmental advantage when PAR levels are highly reduced, especially when phytoplankton have been observed to photosynthesise at PAR values in the order of $10 \mu\text{E m}^{-2} \text{ s}^{-1}$ (growth observed at $1 \mu\text{E m}^{-2} \text{ s}^{-1}$ by Raven (1986)).

As in the case of the spring survey, where PAR was a major limiting factor, re-suspension from the lower waters becomes important for the pelagic diatom community. These organisms, such as *Coscinodiscus* sp. and *Thalassiosira* sp., are reported as being low light adapted where they thrive in a mixed water column, but the PAR values during 30 August 1996, were potentially too low ($<10 \mu\text{E m}^{-2} \text{ s}^{-1}$) to sustain net integrated photosynthesis throughout the water column. The chain forming diatom *Rhizosolenia delicatula* was observed during the neap survey, but by the spring survey this pelagic diatom had been superseded by a dinoflagellate dominated phytoplankton community. However, the *R. delicatula* population followed the same pattern over the survey as that observed in the May 1995 preliminary studies (section 3.3). The community was swept into the upper water column with the high boundary shear, where the increase in PAR may have led to enhanced photosynthesis.

3.5.4.3.2 DINOFLAGELLATE BEHAVIOUR

Using a cost-benefit analysis of dinoflagellate mobility (Raven and Richardson 1984) two important points emerge:

- (1) the energy expended on movements between well-illuminated surface layers and nutrient-rich deeper layers represent a small percentage (~0.1%) of the total energy budget for growth; and,
- (2) the benefits of such migrations are considerable in comparison to a non-migratory behaviour.

They concluded that even in conditions where growth is potentially restricted by both PAR and nutrients, vertical movements at subsurface depths may still enhance growth rates.

Diel migration has been observed for the dinoflagellate *Prorocentrum micans* in Laholm Bay, south-east Kattegat (Edler and Olssen 1985). Salinity gradients of 4-6 did not affect the ascent of *P. micans*, where the mean apparent migration rate was 0.75 m h^{-1} , with an ascent rate (0.85 m h^{-1}) faster than the descent (0.64 m h^{-1}). This data suggested that the optimal PAR level for this dinoflagellate species was $300 \mu\text{E m}^{-2} \text{ s}^{-1}$, based on midday measurements. *P. micans* was not found during the 8 August 1996 survey, and by the end of August a different dinoflagellate species had succeeded the previously dominant *Peridinium trochoideum* dinoflagellate of the neap survey. The population of *P. trochoideum* on the neap survey, i.e. vertically ascending during the flood stand, would lead to an incursion of the community along estuary in association with the prevailing landward currents. This would retain the population within the estuary at times when the tidal excursion was less intense (i.e. during a spring tide). This species has been observed to exhibit relatively slow swimming speeds (0.25 m h^{-1} Taylor 1982), and as the current velocities increase towards the spring tides, these dinoflagellates may be flushed from the system, as no selective retention can occur. Selective retention has been described for many other dinoflagellates (Anderson and Stolzenbach 1985; Garcon and Anderson 1986) where dinoflagellate swimming behaviour restricts advective losses from estuarine embayments.

Although ideas such as the “seedbed” hypothesis (Wall 1975) help to explain the recurrent nature of estuarine dinoflagellate outbreaks, the relatively small size inoculum from germinating cysts each year (Anderson *et al.* 1983) suggests that other factors operate to determine the size of blooms. Motile cells liberated from germinated cysts of *Gonyaulax*

tamarensis, in Perch Pond (Massachusetts, U. S. A.), would be advected from the pond as fast as they could divide, resulting in no net population accumulation even under the best growth conditions (Anderson and Stolzenbach 1985). These authors suggest that population losses would be lowest on sunny days with flood tides during the midday hours, and greatest during periods of low irradiance. The organisms have sufficient motility to maintain a non well-mixed distribution in the presence of efficient tidal mixing. Other studies (Seliger *et al.* 1970) have also shown that without accumulation mechanisms, species such as *Pyrodinium bahamense* in Oyster Bay, Jamaica would be flushed from the area. The vertical distribution of the phototrophic ciliate *Mesodinium rubrum*, has been shown to be influenced by factors other than PAR (Passow 1991), although this organism is strongly phototactic (Smith and Barber 1979). Crawford and Purdie (1992) related the migration of this species to the level of turbulence in the water column, with *M. rubrum* migrating away from the surface waters when faster near-surface ebb currents began - thus also procuring a selective retention within the estuary. The vertical distribution of this highly motile species during the neap survey showed a surface accumulation at all times except during times of intense vertical mixing (i.e. during the ebb and flood currents). Maximum levels re-established in the surface waters during the latter flood tide which would maintain the population within the estuary. By contrast, the distribution of the *M. rubrum* population during the spring tide survey, showed a surface accumulation during the flood stand and the high water period - presumably at times of low TKE, during which the population could migrate into the surface waters. By the time of the extreme spring tide (22 days after the neap survey), the number of *M. rubrum* cells had fallen by an order of magnitude, suggesting flushing losses with the increased flushing rates of the spring tide.

3.5.5 CONCLUSIONS

These longer term investigations have highlighted the variation in physical parameters over a fortnightly period, leading to estimates for mass transport of passive water properties such as SPM and the non-motile phytoplankton community. The daily tidal forcings on re-suspension were again obvious, but when placed in the context of the spring-neap forcings the major re-suspension events are particularly apparent on a spring tide. The bio-physical coupling allowed for calculations of the transport of phytoplankton populations, particularly in terms of benthic species re-suspended during the high TKE events. The migration of dinoflagellate and ciliate species was observed and permitted calculations to be made on phytoplankton population transport over a spring-neap cycle.

3.6 GENERAL CONCLUSIONS FROM SOUTHAMPTON WATER

- There is a clear physical pressure on the phytoplankton community due to the spring-neap tidal cycle. The unique tidal régime in the estuary allows for the persistence of blooms during periods of reduced spring tidal ranges, where flushing rates are reduced.
- The intermittent turbulence that occurs due to the semi-diurnal nature of the tides permits species such as dinoflagellates to actively select a vertical position which will permit maximum PAR. These apparent vertical migrations appear to be triggered by incident irradiance, but ultimately the extent of the migration is governed by the vertical mixing processes.
- During a 25 hour tidal cycle, the influence of wind driven processes became apparent, when the usual salinity stratification during the double high water was suppressed due to the surface wind-shearing processes. Vertical migration of motile phytoplankton species was prevented until a time of water column stability.
- Diatoms show a very close direct coupling to the physical process of velocity shear, and their passive re-suspension patterns follow the same trends as the bottom sediment. However, in many cases the settling rates for diatoms is several hours longer than the settling rates of the re-suspended benthos.
- The autotrophic ciliate, *Mesodinium rubrum*, shows a very similar pattern of migration to that of the dinoflagellates during the daylight hours, however during the dark, *M. rubrum* actively migrates up through the water column during the slack water period, suggesting an external trigger apart from incident irradiance governing its vertical position.

CHAPTER FOUR

NORTH SEA

4. NORTH SEA

4.1 INTRODUCTION

Based on the conclusions from the Southampton Water investigations, the physical constraints on the phytoplankton community were examined within the confines of the shallow coastal environment in the southern North Sea. A Lagrangian experiment was scheduled during which changes in the vertical mixing characteristics would be monitored and coupled to an intensive investigation of the vertical distribution of individual species of phytoplankton.

4.2 GENERAL INTRODUCTION TO THE NORTH SEA

The North Sea is a semi-enclosed continental shelf system in north-west Europe (Figure 4.1). It extends from latitude 51° N to 61° N and longitude 40° W to 9° E. Although shallow, the relatively large surface area (57,500km²) of the North Sea results in a total volume of 3000km³. Atlantic water with a salinity of greater than 35 enters the system through the Strait of Dover in the south and between Shetland and Norway in the north. It is also connected with the Baltic Sea through the Skagerrak, receiving water of reduced salinity. Other minor inflows are from rivers such as the Ems, Elbe, Maas, Humber, Thames and the Rhine. The major outflow from the North Sea is along its northern margin, where waters from the Skagerrak and the northern region entrain some of the Atlantic waters to produce a flux of 63,000km³ yr⁻¹. The region is further divided into defined areas of residual currents (Figure 4.2a). The Shetland Current flows into the North Sea across the broad distance between the north of Scotland and the Shetland Isles. It continues down the east coast of the UK and links with water flowing eastwards through the Dover Strait to form the Southern Bight Drift which moves north and eastwards paralleling the coasts of Belgium, Holland, Germany and Denmark before entering the Baltic Sea. The deep Norwegian Channel Current flows in across the broad continental shelf edge and, at depth, south and eastwards around the coast of Norway. This current appears to predominate during the winter months.

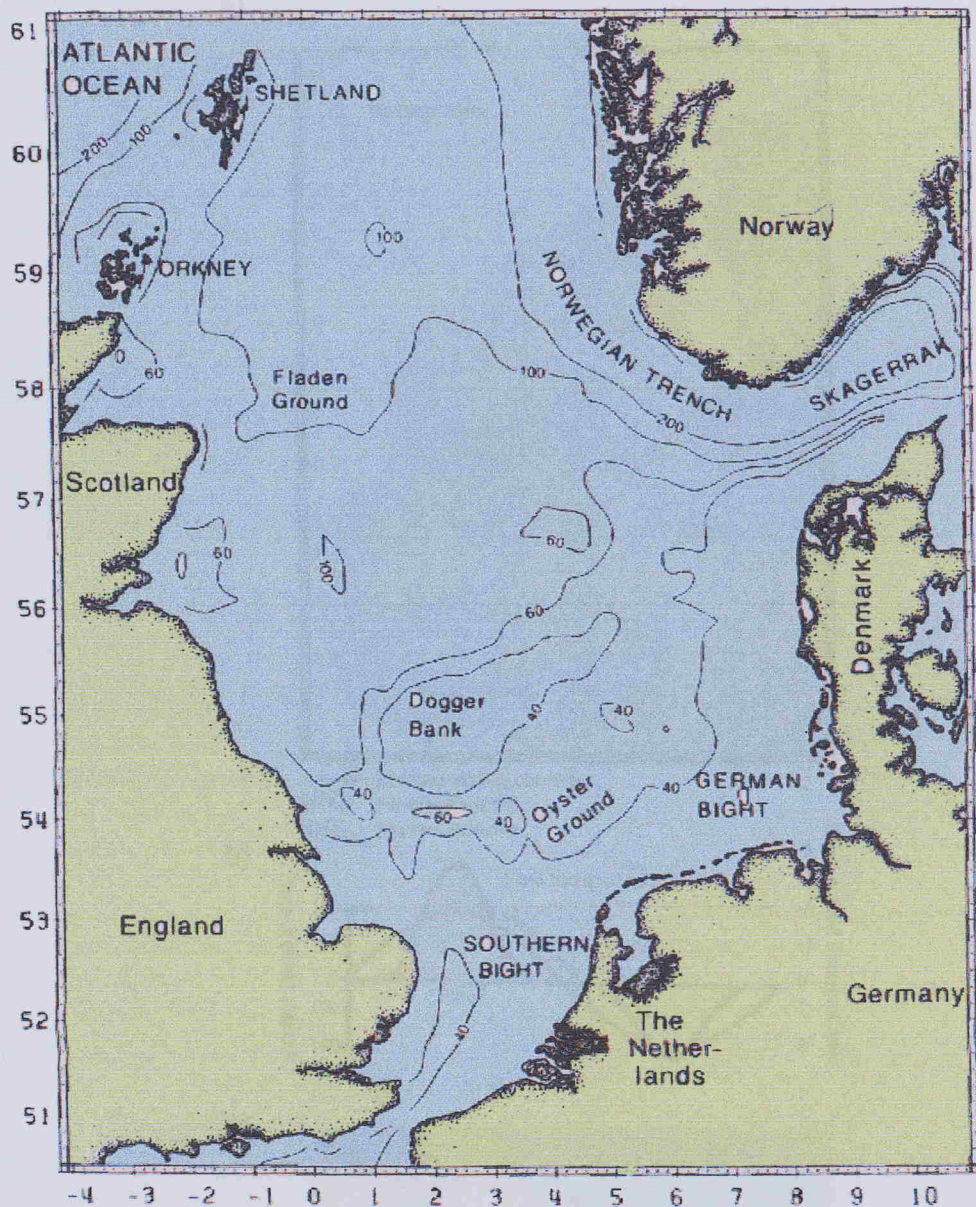
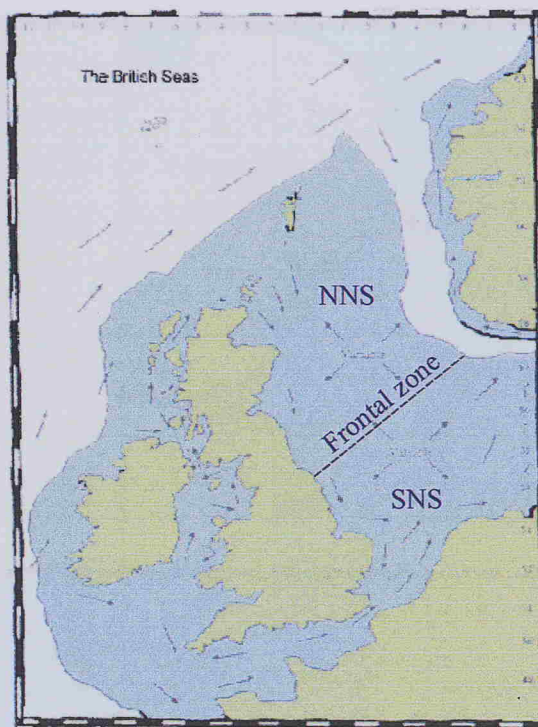


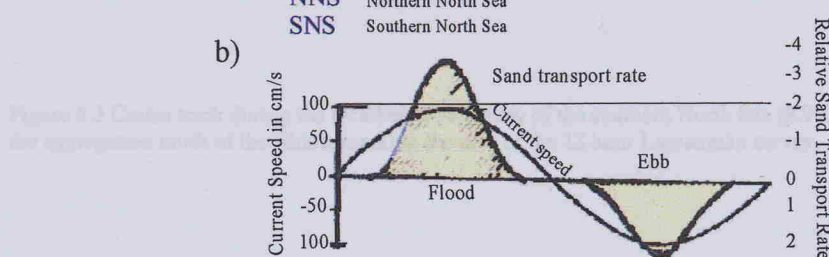
Figure 4.1 Topography of the North Sea (After Sündermann 1994)

Figure 4.2 (a) Residual near-surface circulation, (b) Flow topography, (c) Numerical simulation of maximum flow due to M2 and M4 covariations

a)



b)



c)

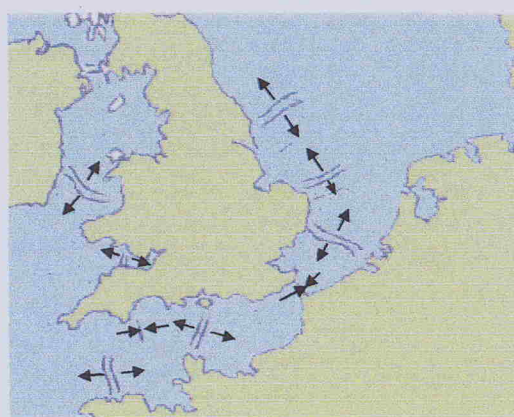


Figure 4.2 a) Residual near surface circulation. b) Flow asymmetry. c) Numerical simulation of maximum flow due to M2 and M4 constituents.

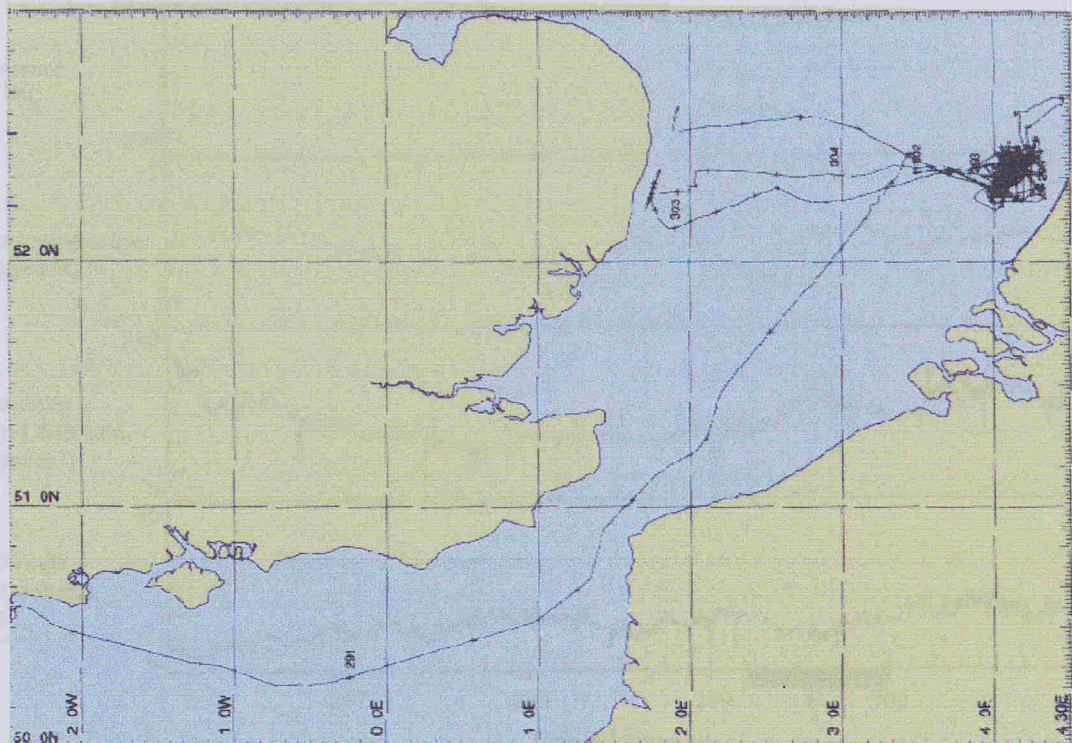


Figure 4.3 Cruise track during the October 1996 survey of the southern North Sea (RV Challenger). Note the aggregation north of the Rhine, marking the area of the 12 hour Lagrangian survey.

Figure 4.4 Intercomparison cruise survey, Challenger 120 cruise in the southern North Sea

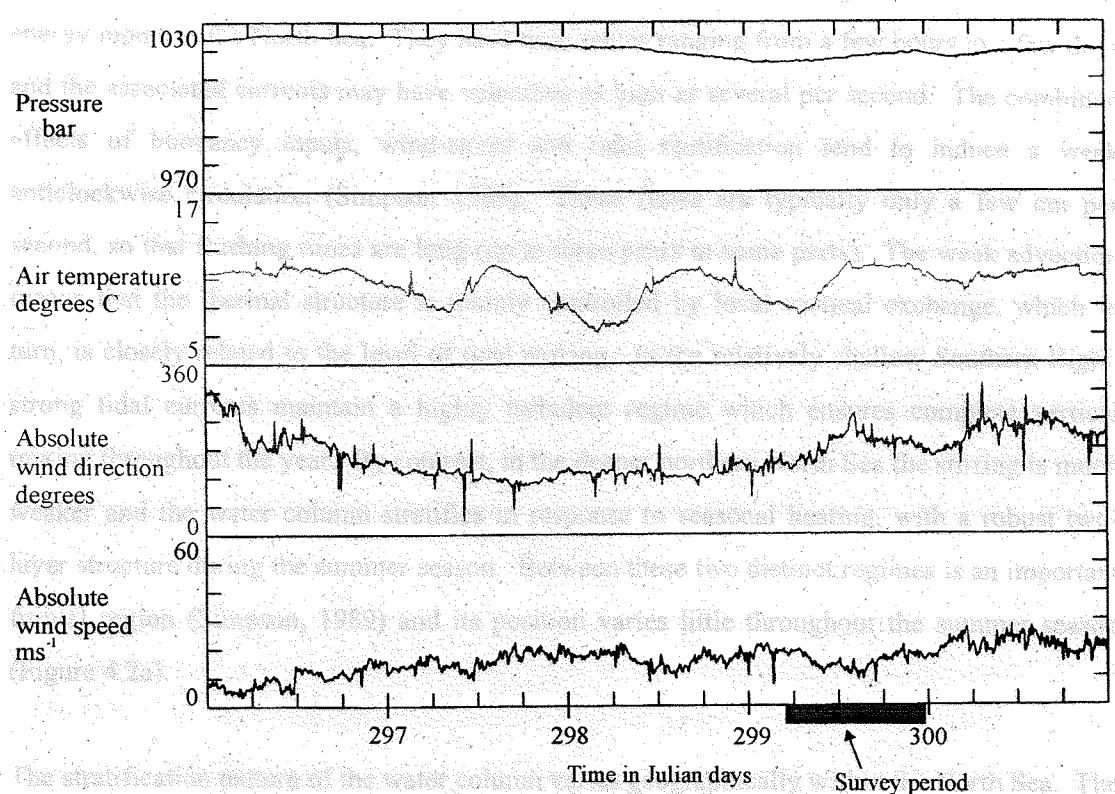


Figure 4.4 Meteorological data during Challenger 129 cruise in the southern North Sea.

4.2 PHYTOPLANKTON DYNAMICS

According to Hartbeck (1987), the phytoplankton biomass in the southern North Sea fluctuated in 1984 and 1985 (Fig. 4.5 & 4.6). This pattern however, differs to that reported in 1984 and 1986 in the English Channel, where there is a reduction in phytoplankton biomass (Fig. 4.7 & 4.8). The following sections will describe the phytoplankton dynamics in the

Mesoscale processes such as tides, wind forced motions and storm surges are the most intense energy inputs to the North Sea. They have time scales ranging from a few hours to a few days and the associated currents may have velocities as high as several per second. The combined effects of buoyancy inputs, wind-stress and tidal rectification tend to induce a weak anticlockwise circulation (Simpson 1989). These flows are typically only a few cm per second, so that flushing times are long (up to three years in some parts). The weak advection means that the thermal structure is mainly controlled by local vertical exchange, which in turn, is closely related to the level of tidal stirring. In the relatively shallow Southern Bight, strong tidal currents maintain a highly turbulent regime which ensures complete vertical mixing throughout the year. By contrast, in the deeper northern North Sea the stirring is much weaker and the water column stratifies in response to seasonal heating, with a robust two-layer structure during the summer season. Between these two distinct regimes is an important frontal region (Simpson, 1989) and its position varies little throughout the summer season (Figure 4.2a).

The stratification pattern of the water column varies geographically within the North Sea. The Southern North Sea and along the British coast is shallow and characterised by strong tidal currents, resulting in a well mixed vertical structure. Surface water temperatures show seasonal variation which is pronounced in the southern areas (ranging from 14 to 15°C), and less marked in the northern areas (0 to 2°C). Bottom temperatures show similar ranges, with little seasonal variation in the thermally stratified northern regions.

Surface salinity is typically ~35 in the northern region and between 34-35 in the central and southern region. Areas of coastal influence, with considerable riverine input, show reduced salinities. Although the main nutrient input into the North Sea is from the Atlantic ($1.7 \times 10^6 \text{ t yr}^{-1} \text{ N}$, after Gerlach (1987)), the southern North Sea riverine inputs contributed 34-35% of the P and N concentrations in 1980. These high river discharges of nutrients and other contaminants, such as toxic chemicals, heavy metals and oil products derived from waste water emissions and sewage sludge dumping, have lead to highly polluted coastal areas.

4.3 PHYTOPLANKTON DYNAMICS

According to Gerlach (1987), the total algal biomass in the southern area increased from $9 \mu\text{g C l}^{-1}$ in 1962 to $37 \mu\text{g C l}^{-1}$ in 1984. This pattern, however, seems to have started to reverse since 1984 in Dutch coastal waters due to a reduction in Rhine river outflow (Reid *et al.*

1990). However, the diatom population, which is a dominant fraction of the net plankton, seems to have remained constant. Perhaps surprisingly this appears to parallel a reduction in available silicate, through a decrease in silicate loading from riverine inputs (Radach and Berg 1986). Flagellates have become important particularly in the microplankton and nanoplankton size fraction and organisms such as the prymnesiophyte *Phaeocystis pouchetti* recurrently form dense blooms (50 mg chl m^{-3}) in some regions of the North Sea. These flagellates occur in two different forms, a motile stage ($3\text{-}10\mu\text{m}$) and a colonial form enclosed in a gelatinous matrix. These colonies may reach several millimeters in diameter. During the 1980's, generally during the second half of June, beaches of the North Sea's Dutch and German coasts were covered with a layer, up to 2m thick of slimy light foam. This phenomenon has been reported for many years, although over the last twenty years nuisance blooms have occurred more frequently and intensively (Lancelot *et al.* 1987).

In Belgian coastal waters the diatoms and *P. pouchetti* contribute greatly to the spring bloom, with flagellates becoming more important during the summer months. Species of *Ceratium* sp. (Dinophyceae) are common bloom-formers in the summer stratified waters of the central and northern North Sea, with blooms of coccolithophorids also observed. *Emiliana huxleyi* is known to bloom in Norwegian coastal waters during summer months and produces milky discolouration of the water (Tangen, 1979) with further consequences on light scattering and attenuation.

4.4 REGIONS OF FRESHWATER INFLUENCE

The physical regime in the vicinity of the Rhine ROFI (Region of Freshwater Influence) has been described in detail by Simpson and Souza (1995). Extensive surveys using CTD/rosette systems, moored instruments with current meters, fluorometers and transmissometers were used to define this highly variable system during September - October 1990. The Rhine ROFI was confirmed to extend north-eastwards along the Dutch coast from its river source, out to approximately 30km from the coast, with a mean flow parallel to the coast and surface speeds of $15\text{-}20\text{cm s}^{-1}$ (Simpson and Souza, 1995).

The discharge of an average of $2200\text{m}^3 \text{s}^{-1}$ of freshwater from the Rhine is an important input of buoyancy into the south-eastern North Sea, which has major implications for water column structure and dynamics. The stratifying effect of the low salinity input competes with the mixing influence of stirring by tidal flow and winds, leading to an alternation of strong

stratification and complete vertical mixing. This alternation is highly influenced by the spring-neap tidal variation, with stratification destroyed at the time of the spring tides. Other variables, such as fluctuating riverine input, and wind and wave conditions introduce random changes to the water column structure. An added complication (Simpson and Souza 1995) is the semi-diurnal oscillations between stable and mixed water columns even during periods of strong 'stratification' shown from 1990 observations. This switching between stratified and mixed conditions has been reflected in the suspended particulate matter (SPM) variations. SPM concentrations were higher during the post-spring period with values of 40-60mg l⁻¹ in the near coast region, contrasting with the neap phase, where surface concentrations had reduced by an order of magnitude (4-6mg l⁻¹).

4.5 BACKGROUND TO NORTH SEA STUDY: TRACER RELEASE

Two experiments during the North Sea project in 1989 were carried out in March and October, which involved the simultaneous release of two inert, non-toxic gaseous tracers sulphur hexafluoride (SF₆) and ³He (Watson *et al.* 1991). The site chosen was a permanently well mixed, flat bottomed and shallow (30m) region of the southern North Sea (Figure 4.3) off the Dutch coast (52°15'-52°30'N; 003°20'-003°40'E). During the autumn cruise, salinity fluctuations were small (34.8-34.9), with a water temperature of approximately 16°C and wind speeds ranging from 7.6 (± 2.4)-12.3 (± 2.6) ms⁻¹ (Daneri 1992). Primary productivity in this region was also monitored with chlorophyll *a* concentrations reaching 2.5 mg m⁻³ in October 1989, and oxygen saturation ranging from 102.4 - 103.9%. This autumn water mass contained a developing bloom of the diatom *Rhizosolenia stolterfothii* (Daneri 1992).

This earlier tracer release study formed the basis of the experiment carried out between 16th October -1st November 1996 in the southern North Sea, Dutch coastal waters, as part of the ASGAMAGE project.

4.5.1 ASGAMAGE

ASGAMAGE is a joint European contribution to the Marine Aerosol and Gas Exchange (MAGE) core science activity. The main aim of this experiment was to measure rates of gas transfer across the air-sea interface as functions of wind speed and associated geophysical variables by the release of volatile and conservative tracers. An independent study during this cruise was established to monitor changes in algal biomass and speciation and to determine their relationship with water column dynamics and the Rhine ROFI. The study area was approximately 20km west of the marine meteorological platform *Meetpost Noordwijk*.

4.5.2 SAMPLING STRATEGY FOR THE NORTH SEA (DUTCH COASTAL WATERS)

Cruise #129 on RRS *Challenger* formed the UK component of the *ASGAMAGE* experiment between 16th October - 1st November 1996, in the southern North Sea. The survey region incorporated the manned meteorological platform (*Meetpost Noordwijk*), 8km off the Dutch coast (52° 17N; 004° 18E), and extended 20km west from the coast (Figure 4.3). Tracers (section 4.5) were released into the water and monitored over a two week period, to compare directly a comprehensive suite of geophysical forcings influencing air-sea gas transfer. As the physical properties of the area were monitored closely, this provided an ideal situation to investigate any changes in algal biomass and phytoplankton species using a Lagrangian approach, in relation to water column mixing and the fresh water Rhine outflow. A vessel mounted ADCP (RD Instruments, 150kHz) collected data every 2 minutes with a depth resolution of 1m. CTD casts were deployed hourly over a 12 hour period during a Lagrangian experiment, in which chlorophyll *a*, total SPM and phytoplankton taxonomy were monitored intensively. The CTD unit had an attached fluorometer, transmissometer and irradiance sensor. Discrete water samples were taken regularly from Niskin bottles to determine chlorophyll *a*, total SPM concentrations and dissolved oxygen (DO). Underway sampling of chlorophyll fluorescence, transmission and DO was achieved from instruments in the non-toxic flow-through supply, from a depth of 5m.

4.5.3 DUAL TRACER RELEASE AND UNDERWAY MONITORING

Tracer preparation occurred ~25km from the target site, to avoid contamination. The tracers used included two volatile gases sulphur hexafluoride (SF₆) and Helium-3 (³He), with the conservative tracers rhodamine-WT, sulpho-G and *Bacillus globigii* spores. The tracer patch was continuously surveyed for SF₆ using gas chromatography, with discrete samples taken for SF₆, ³He, rhodamine and the spores. Continuous underway analysis was used to map the tracer area, where individual chromatograms were matched with time and position co-ordinates. At the patch "centre", vertical CTD profiles were performed (every 12hours) and discrete seawater samples were collected from 3-4 depths using 10 litre stainless steel sprung Niskin bottles, for instrument calibration and phytoplankton analysis.

Results from the longer term experiment will not be discussed here, as little change in the phytoplankton community occurred over the three week period.

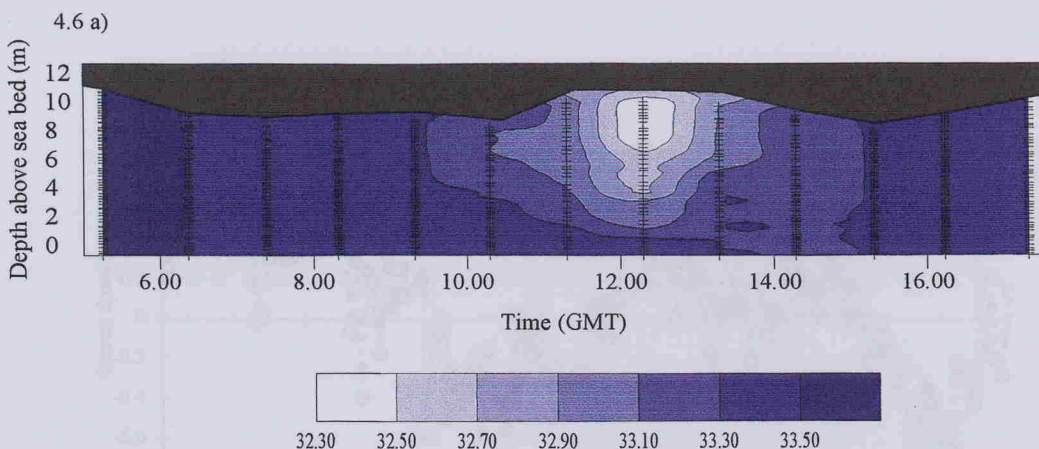


Figure 4.6 b)

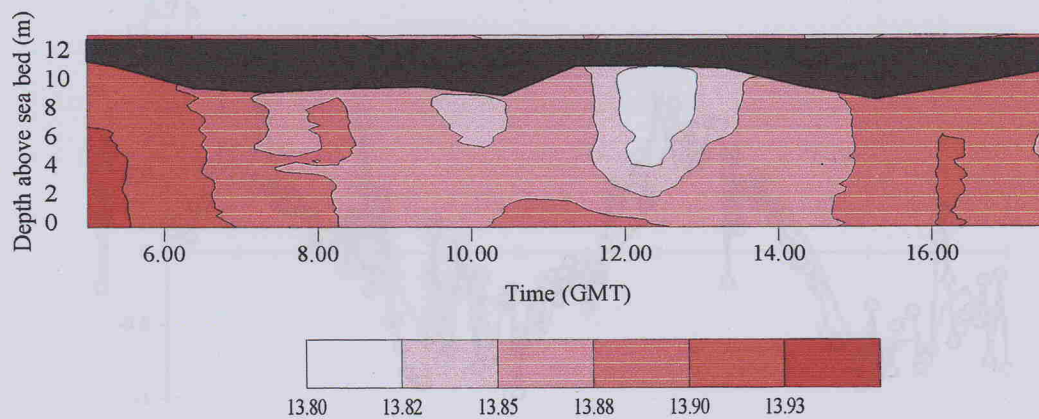
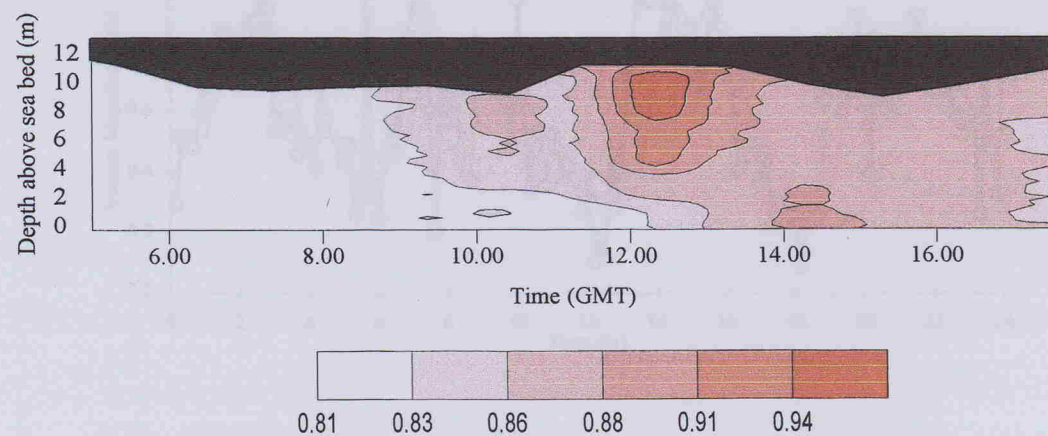


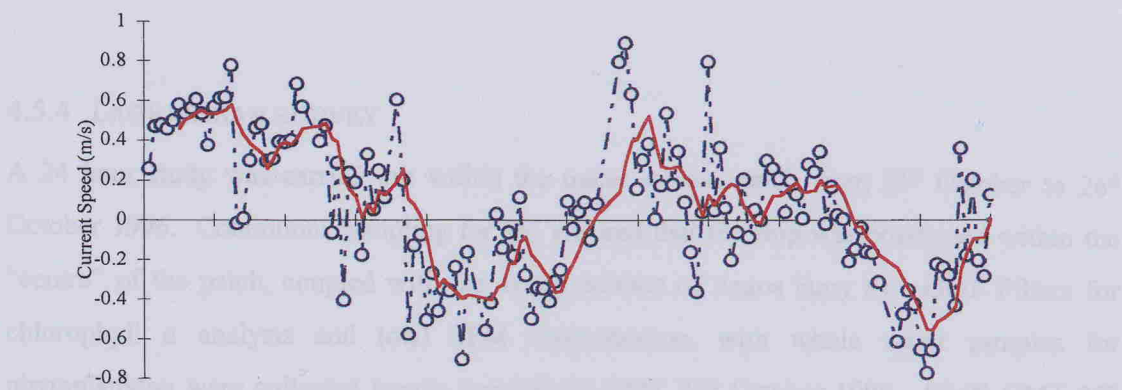
Figure 4.6 c)



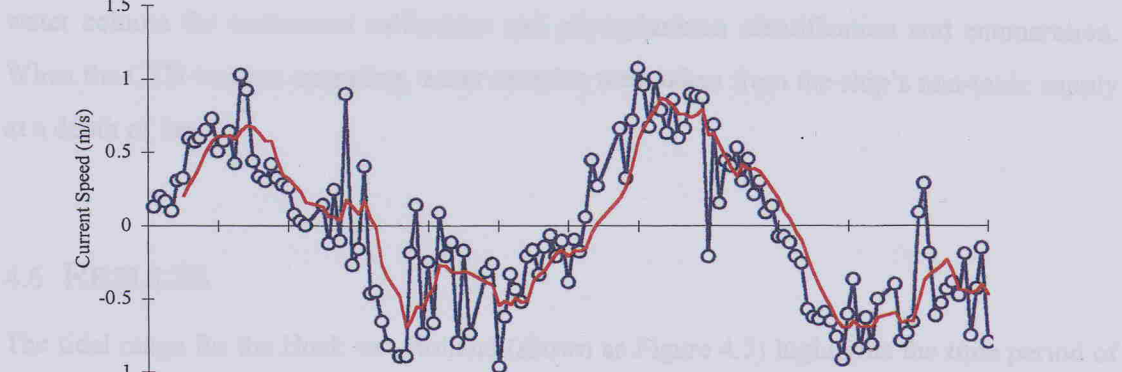
Figures 4.6 a-c. Data collected from hourly CTD casts during the North Sea 12 hour Lagrangian survey 25 October 1996. a) salinity distribution (black vertical lines represent CTD casts); b) temperature distribution ($^{\circ}\text{C}$); c) relative values for SPM, higher values = greater concentration of SPM.

Five dragged, surface drifting buoys were deployed at equal intervals along the transect A-B (Figure 4.6). These were tracked using the Argos satellite network and with downstream tracking receivers.

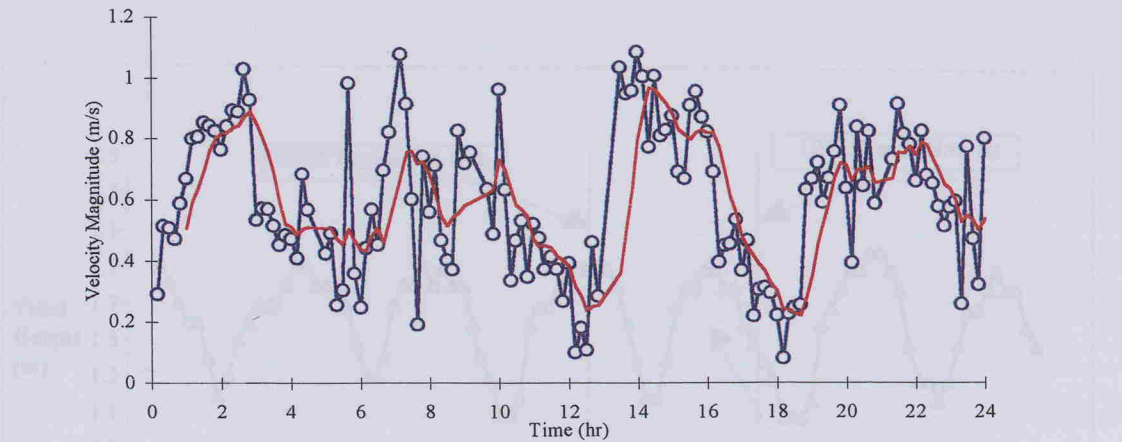
4.7a



4.7 b



4.7c



Figures 4.7 a-c. ADCP data from the southern North Sea. 25-26 October 1996. All figures represent **surface** velocities. a) north-south velocity (+ is north); b) east-west velocity (+ is east); and c) velocity magnitude. The red line represents a moving average trendline (average over 6). Time is in hours. Velocity in m s^{-1} .

Three drogued, surface drifting buoys were deployed at equal intervals along the tracer axis. These were tracked using the Argos satellite network and with direction finding receivers.

4.5.4 LAGRANGIAN SURVEY

A 24 hour study was carried out within the tracer release patch from 25th October to 26th October 1996. Continuous sampling for SF₆ ensured that the ship was positioned within the "centre" of the patch, coupled with the visual contact of Argos buoy #1. GF/F Filters for chlorophyll *a* analysis and total SPM concentration, with whole water samples for phytoplankton were collected hourly from 03:00 GMT 25th October 1996 - 03:00 GMT 26th October 1996. Hourly CTD casts over a 12 hour period began from 05:00 GMT - 17:00 GMT on 25th October 1996. During the CTD casts, water was collected from 3 depths over the 20m water column for instrument calibration and phytoplankton identification and enumeration. When the CTD was not operating, water samples were taken from the ship's non-toxic supply at a depth of 5m.

4.6 RESULTS

The tidal range for the Hoek van Holland (shown as Figure 4.5) highlights the time period of the intensive sampling of phytoplankton and physical parameters. The 12 hour survey was conducted during a spring tide.

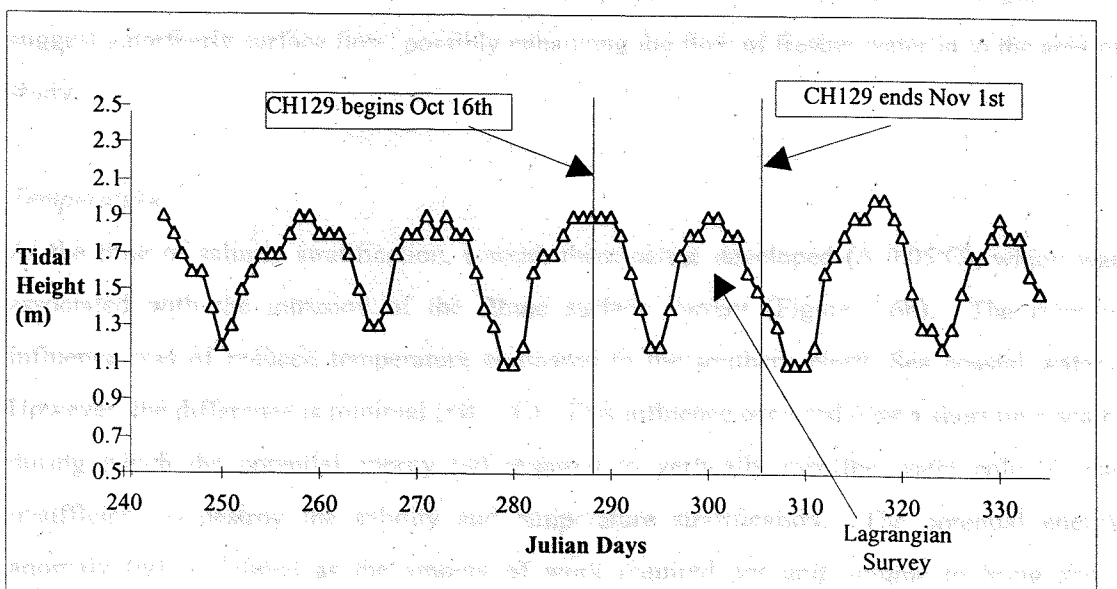


Figure 4.5. Tidal range at the Hoek van Holland during the southern North Sea *ASGAMAGE* cruise.

4.6.1 PHYSICAL PARAMETERS

The course maintained is shown in Figure 4.3, the initial co-ordinates were 52° 22.9N; 004° 11.5 E. The water column was ~20m depth, flat-bottomed and generally remained well mixed throughout the cruise. Meteorological data for the survey (Figure 4.4) indicates little wind stress (~8 m s⁻¹ in a SE direction) during the 12 hour survey, although this period was preceded and followed by stronger winds reaching 15 m s⁻¹. The tidal range for this survey, based on Admiralty tide tables from Hoek van Holland was 1.8 m (Figure 4.5), approaching a spring tide. Mean range for a spring tide in this area is 1.9 m; neap range is 1.5m. Double low waters often occur in this region, with a lower first low water. Low waters on 25 October 1996 were at 08:15 and 17:31 GMT (0.4 and 0.2m respectively). High waters were at 23:54 and 12:17 GMT (2.2 and 2.0m respectively).

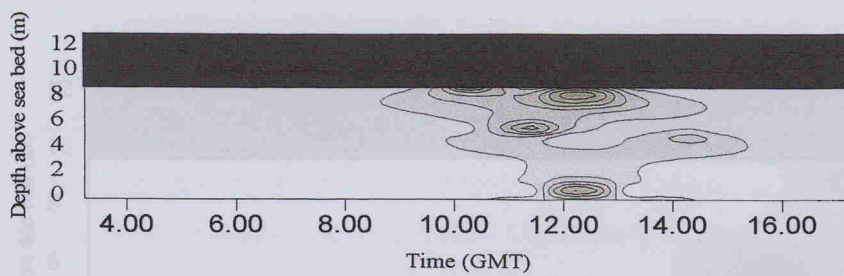
Salinity

The first CTD cast was at 05:15 GMT. Data acquired from the CTD indicated surface intrusion of lower salinity water (Figure 4.6a) during the period of flood tides at Hoek van Holland, creating a weak salinity stratification from ~10:00 GMT ($\Delta 1$). This plume of fresher water was observed for a period of 4.5 hours. The greatest influence of fresher water occurred at 12:30 GMT. The water column became well mixed again at ~14:00 GMT as the lower salinity water retreated, and the tidal influence dominated the ROFI. A period of approximately 2 hours occurred following the intrusion of the Rhine ROFI and the time of high water, showing the greatest influence of surface freshwater at a period approaching high water in Hoek van Holland. Residual currents up to 0.8 m s⁻¹ within this area (Figure 4.7a) suggest a northerly surface flow, possibly enhancing the flow of fresher water in to the area of study.

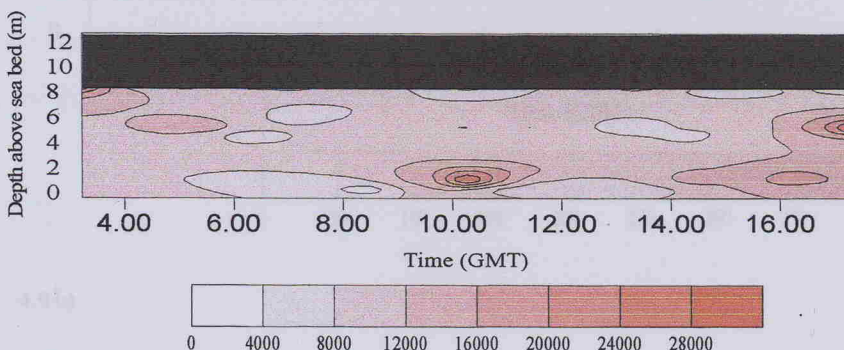
Temperature

At the time of salinity stratification, a weak thermocline developed ($\Delta 0.05^{\circ}\text{C}$), which was associated with the intrusion of the Rhine surface current (Figure 4.6b). The riverine influence was of reduced temperature compared to the southern North Sea coastal waters. However, the difference is minimal ($<0.1^{\circ}\text{C}$). This influence occurred over a short time scale, during which the potential energy (ψ) required to vertically mix the water column was insufficient to destroy the salinity and temperature stratification. The potential energy anomaly (ψ) is defined as the amount of work required per unit volume to bring about complete vertical mixing (see chapter 3).

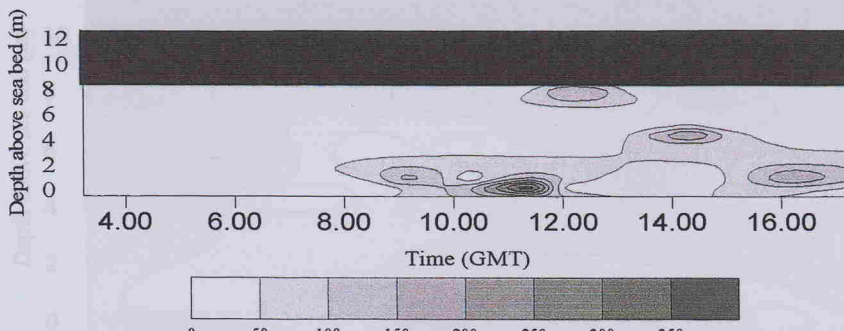
4.8a)



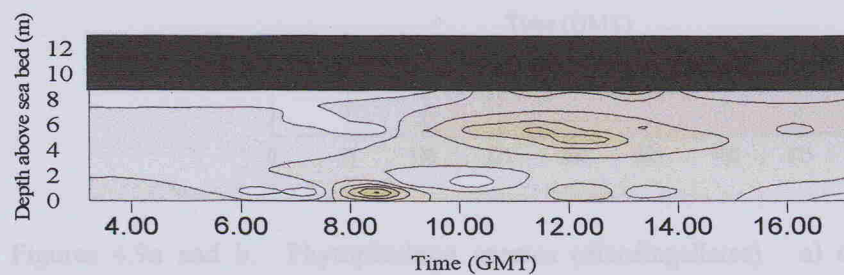
4.8 b)



4.8 c)

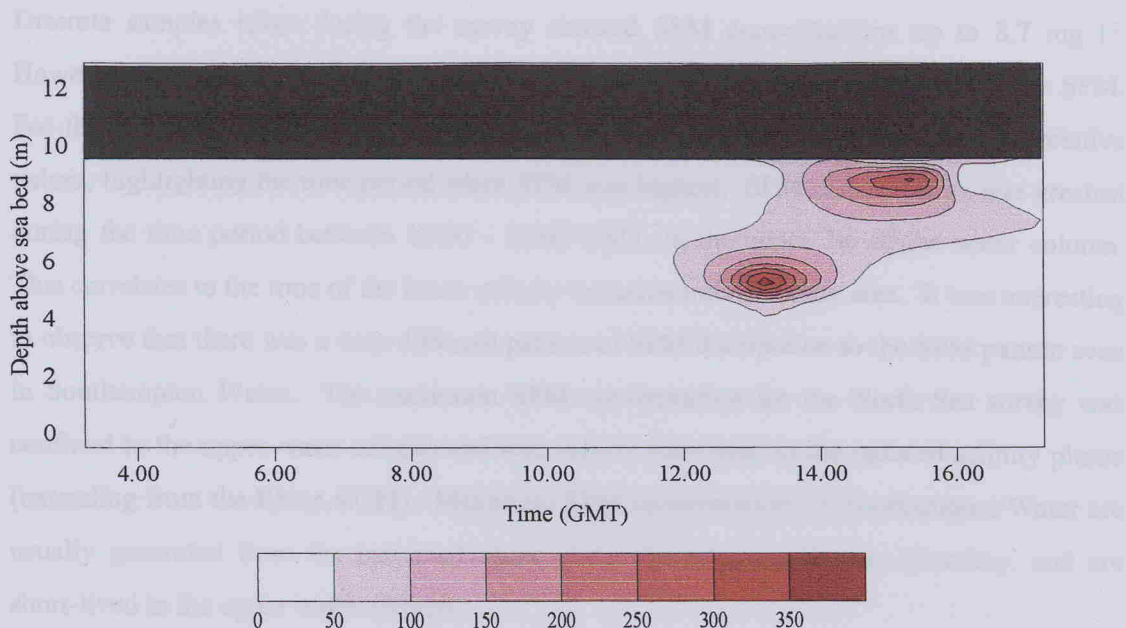


4.8 d)

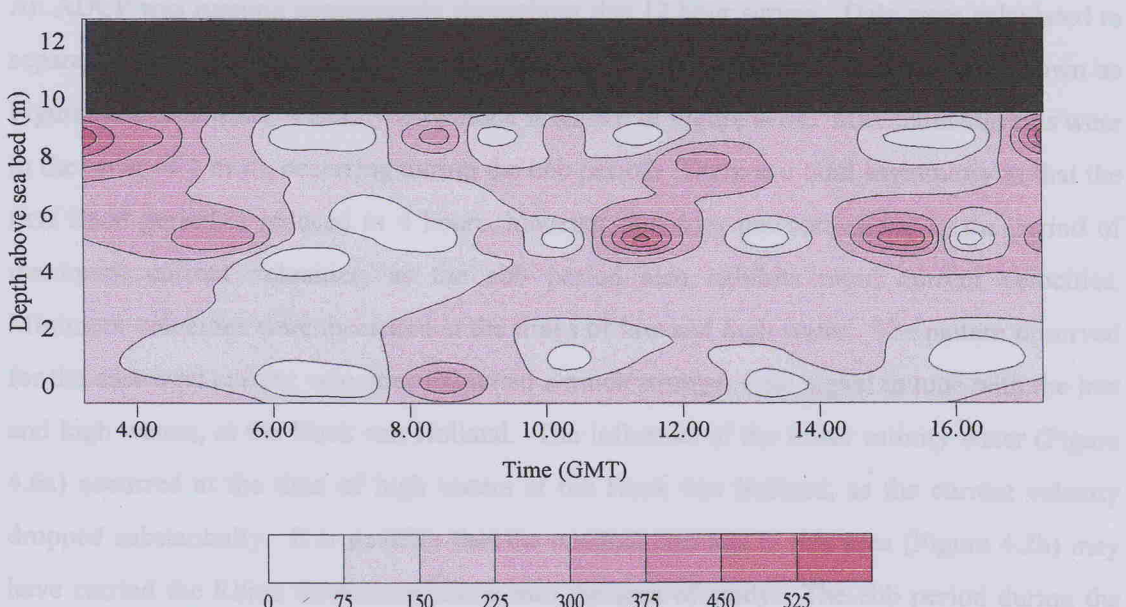


Figures 4.8a and b. The distribution of a) *Conopephora* sp. and b) *Rhizosolenia* sp. in the population of *P. micans* appears to be lower in the population of *P. micans*. Data based on whole water samples from surface mid and bottom depths every hour. Numbers in terms of cells per litre.

Figures 4.8a-d. Phytoplankton species (diatoms) identified during the North Sea survey. 4.8a) *Rhizosolenia styliformis*; b) *Rhizosolenia stolterfothii*; c) *Ditylum brightwelli*; and d) *Biddulphia* sp. Data based on whole water samples from surface mid and bottom depths every hour. Numbers in terms of cells per litre.

4.9 a) *Gonyaulax* sp.

4.9 b)



Figures 4.9a and b. Phytoplankton species (dinoflagellates). a) *Gonyaulax* sp; and b) *Prorocentrum micans*. NB during the hours of 08:00 and 12:00 hr the population of *P. micans* appears to have positively migrated into the surface waters. Data based on whole water samples from surface mid and bottom depths every hour. Numbers in terms of cells per litre.

Current densities are shown as for hourly time 12:00 - 14:00 hr, compared with the timing of the lower tides in the area of the investigation, which reinforces the possibility that this reduced surface salinity was occurring from the Rhine plume.

Suspended Particulate Matter

Discrete samples taken during the survey showed SPM concentrations up to 8.7 mg l^{-1} . However, the calibrated transmissometer values showed very low concentrations for SPM. For the purposes of this thesis, the transmissometer values will only be treated as relative values, highlighting the time period when SPM was highest. SPM concentration was greatest during the time period between 12:00 - 13:00 GMT, in the upper 7m of the water column. This correlates to the time of the lower salinity intrusion into the study area. It was interesting to observe that there was a very different pattern of SPM distribution to the SPM pattern seen in Southampton Water. The maximum SPM concentration for the North Sea survey was confined to the upper water column and was closely correlated to the reduced salinity plume (extending from the Rhine ROFI). Maximum SPM concentrations in Southampton Water are usually generated from the increased shear along the estuarine bottom boundary, and are short-lived in the upper water column.

Tidal Currents

An ADCP was running continuously throughout this 12 hour survey. Data were calculated to separate the ship speed from the bottom tracking feature. u and v velocities are shown as Figures 4.7a and 4.7b. Velocity magnitude is shown in Figure 4.7 c. Maximum currents were in the order of 1 m s^{-1} , occurring during the ebb period. There is a tidal asymmetry in that the first flood period is reduced to 4 hours, however this does not correspond to the period of maximum current velocities, as the ebb period also exhibits rapid current velocities. Minimum velocities were measured at the times of low and high water. The pattern observed for the east-west current velocities exhibited a much stronger tidal signal in tune with the low and high waters, at the Hoek van Holland. The influence of the lower salinity water (Figure 4.6a) occurred at the time of high waters at the Hoek van Holland, as the current velocity dropped substantially. It is possible that the residual currents in this area (Figure 4.2b) may have carried the Rhine freshwater plume into the area of study. The ebb period during the latter part of the survey, showed a definite mid-phase, maximum current peak, similar to that observed in Southampton Water, however the longevity of the two ebb phases is very different (i.e., the ebb phase in the southern North Sea is 2 hours longer than Southampton Water).

Current direction is shown to be northerly from 12:00 - 14:00 hr, associated with the timing of the lower salinity plume in the area of the investigation, which reinforces the probability that this reduced surface salinity was extending from the Rhine ROFI.

4.6.2 BIOLOGICAL PARAMETERS

Chlorophyll *a* was determined regularly throughout this survey, however there was little difference with time or in the vertical distribution through the water column. These data are not shown, so phytoplankton biomass is reported in terms of species abundance. (chlorophyll *a* values = $2\text{mg m}^{-3} \pm 0.1\text{ mg l}^{-1}$).

Table A5 (Appendix IV) lists the phytoplankton species identified and enumerated during the Lagrangian survey. Diatoms formed the highest percentage of species (90.5%), with dinoflagellates accounting for 2.95% and *Phaeocystis pouchettii* forming 0.05% (not shown). Zooplankton represented 6.5% of the total organisms counted in samples during the Lagrangian survey. The chain-forming diatom *Rhizosolenia stolterfothii* (Figure 4.8b) was the most abundant phytoplankton species, with maximum cell densities reaching 3.6×10^3 cells litre $^{-1}$ (62% of total).. At 10:00 GMT this population appeared to aggregate in the near bottom layers between 12-14m depth, however this is based on one data point and may be anomalous. However, this occurred during the time of the temporary salinity stratification, when surface values still remained high ($>1.2 \times 10^3$ cells litre $^{-1}$). An interesting feature of this data set was the arrival of the chain forming diatom *Rhizosolenia styliformis* with the lower salinity influence between 10:00 and 14:00 GMT. This species is commonly found in the southern North Sea. This large diatom, had a maximum chain length of 3 mm. Figure 4.8a indicates its distribution coincident with the lower salinity Rhine ROFI. Although the salinity influence was in the surface 2 m its influence was occurring throughout the depth of the water column. As the water column became well mixed at 14:00 GMT, fewer *Rhizosolenia styliformis* cells were observed and by 15:00 hr no cells were seen. The distribution of *Ditylum brightwelli* is shown in Figure 4.8c. Cell numbers of this organism were low in comparison to the dominating diatoms, with a distribution showing a near-bottom aggregation on either side of high water, while at the time of the lower salinity intrusion reduced concentrations were recorded. This suggests the appearance of a different population of the same species associated with another water mass, possibly due to the mixing at the margins of the fresh water intrusion. Another chain-forming diatom *Biddulphia* sp. (Figure 4.8d) was also abundant (1.6% total). This species was observed throughout the duration of the survey, although longer chains and greater cell volumes were observed during the fresher water intrusion.

Rhizosolenia stolterfothii cells occurring in the water column during periods of lower salinity

related to the ROFI were in greater numbers and present as longer chain (reaching 12 cells per chain, length = 2.5 mm). The mean chain length excluding this lower salinity period was 3 (\pm 2). *Chaetoceros* sp. (data not shown) was another abundant diatom which was present throughout the survey, with numbers intensifying after the ROFI in the surface waters (background concentration = 1.5×10^2 cell litre $^{-1}$, reaching 9×10^3 cell litre $^{-1}$).

Very few dinoflagellates were observed in comparison to the diatom numbers. *Prorocentrum micans* was the most abundant dinoflagellate (Figure 4.9b). Maximum cell numbers were 525 cells litre⁻¹, where >70% was found in the surface water (above 8m). The cell numbers for *P. micans* were relatively low, and yet apparent changes in the vertical distribution of this species seemed to occur. It is difficult to distinguish between the apparent vertical migration of *P. micans* and the concurrent intrusion of the low salinity water, but significant numbers of *P. micans* were observed before and after the plume event suggesting a population residing in the usually well-mixed waters.

The armoured dinoflagellate *Gonyaulax* sp. (Figure 4.9a) was detected during the period of the strongest salinity gradient. This motile phytoplankton was not present during the survey, but aggregated in the surface waters during the temporary water column stability. As the lower salinity plume retracted, and the water column was again vertically homogeneous, this organism was no longer observed.

4.7 DISCUSSION

In the southern section of the North Sea, the water column usually remains well mixed and turbid. As a result, low phytoplankton biomass has been observed (Tett and Mills 1991). This was shown to be the case during the October survey in 1996. It has been argued that this unproductive state would be typical of the entire southern North Sea if it were not for the riverine inputs of freshwater and the mineral nutrients. The explanation provided by Tett and Mills (1991) of plankton dynamics is based on the complex physical processes operating in the region, including the stratifying influence of the Rhine outflow. These temporary zones of reduced vertical mixing coupled with anthropogenic nutrient loading can stimulate phytoplankton growth. The first blooms of the year are reported to be dominated by diatoms, but depletion of silicate quickly reduces their importance. The anthropogenic input of nitrate and phosphate stimulate the growth of flagellates and blooms of *Phaeocystis pouchetti* are common between April and June. By the middle of summer, sufficient silicate may have been regenerated (or input) to support renewed diatom growth (Reid *et al.* 1990).

Semi diurnal variations in water column stability have been previously identified in other ROFI and estuarine régimes (Bowden and Sharaf el Din, 1966; Simpson *et al.*, 1991; Souza and Simpson, 1997), where they were attributed to tidal straining. During spring tidal phases, the water column is well mixed, and only within the immediate region of the Rhine source is any significant stratification seen. This stabilising influence of the lower salinity intrusion was also detected through the October 1996 cruise, leading to behavioural changes in the phytoplankton community during the temporary period of stability. This 12 hour survey occurred during a large tidal range immediately before a spring tide. During a neap period, however, strong stratification exists with ψ up to 20 Jm^{-3} extending out to 30km from the coast and northwards from the Rhine source (Simpson *et al.*, 1991). ψ during a spring phase ranges between $0-4 \text{ Jm}^{-3}$, which explains the temporary nature of the stratification during the October (1996) investigation. CODAR (HF radar) observations for the region have indicated a coherent residual flow to the north which was approximately parallel to the coast and has typical velocities of $15 - 20 \text{ cm s}^{-1}$. With the onset of stratification, the bottom residual current is largely de-coupled from the surface flow (Simpson and Souza, 1995).

SPM distributions were determined from the CTD deployed beam transmissometer. Results are only shown as relative units due to the poor calibration between the gravimetric samples and the attenuation, actual concentrations of SOM are based on gravimetric weights. The

SPM distribution over the time series suggested that the water column was well mixed until the onset of salinity stratification, where the 'fresher' surface waters have a suspended load of up to 9 mg l^{-1} . As the ROFI retreated, the turbid surface waters also disappeared, although the mean water column suspended load was increased after the time of salinity stratification. The SPM range before the freshwater influence was $4\text{--}5 \text{ mg l}^{-1}$, in contrast to the period after the intrusion where the range was $7\text{--}8 \text{ mg l}^{-1}$. This suggests that particulate matter was settling through the halocline coupled with the increased water column turbulence due to the tidal straining.

Tett and Mills (1991) reviewed the pelagic ecosystems of the North Sea and described in detail the results from a mooring station in the southern Dutch coastal waters. At the NERC station (AT) near the mouth of the Scheldt, it was confirmed that phytoplankton can be abundant between March and September in southern regions under the influence of anthropogenic nutrient loading. Their conclusions were that the complex physical processes operating in this region (including the stratifying influence of the Rhine ROFI) gives rise to temporary zones of reduced vertical mixing and increased photic depth, leading on to enhanced primary productivity. This was also confirmed through the October 1996 investigations in which phytoplankton were seen to be larger and more abundant in the water mass associated to the Rhine plume. This enhanced productivity, however, was not observed through the use of chlorophyll α determinations.

Over a tidal cycle, this work has revealed that regular stability occurs through the fresh water intrusion. This follows a lag period from the tidal nodes at the Hoek van Holland. The regularity of the tidal forcings however, is often suppressed due to the unpredictable meteorological conditions, which act to de-stabilise the water column. For example, in this survey the time period before and immediately after the 'Lagrangian' investigation wind speeds reached 60 m s^{-1} , surpassing the stabilising buoyancy forces.

The behavioural patterns of the motile phytoplankton community showed the ability to respond over short timescales to their physical environment. Dinoflagellate species appeared to vertically migrate through the water column during a period of reduced water column mixing which occurred during the time of the theoretical maximum surface irradiance. The population resided in the surface waters of the reduced salinity influence. This population was probably associated with the Rhine ROFI, but did not mix vertically.

Certain components of the diatom community mapped their physical environment, particularly shown by *R. styliformis* which was only detected during the lower salinity intrusion. The use of chlorophyll *a* as an indicator of algal biomass alone, would not have provided the insight into the specific behavioural patterns of the phytoplankton community.

4.8 GENERAL CONCLUSIONS FROM THE NORTH SEA STUDY

The southern North Sea, generally a well-mixed body of water, has intermittent periods of stability resulting from the stabilising forces of the Rhine ROFI. This stability not only changed the physical characteristics of the water column, but showed its influence on the phytoplankton community.

The apparent low algal biomass (chlorophyll *a* concentration $<2 \text{ mg m}^{-3}$) observed during the southern North Sea cruise prevented a detailed examination of phytoplankton community changes with time in terms of bulk parameters. However, the close coupling of the hydrographic features of the region and the biological community were quite clear through the use of microscopic examination. Few motile species were observed, but some evidence suggests that dinoflagellate members were residing in the surfacelayers of the water column. For example *P. micans* occurred during the temporary, more stable period of the low salinity Rhine ROFI in day light hours.

A species of diatom *R. styliformis* was apparently associated with the low salinity ROFI. The vertical distribution of this species followed the physical hydrography of the water mass, where the diatom population was initially associated with the surface waters of the ROFI, but one hour later greater numbers of individual cells were observed in the bottom layers.

In contrast, the armoured, motile dinoflagellate, *Gonyaulax* sp was only observed within the near surface layers of the water column at the time associated with the greatest vertical salinity gradient (suggesting vertical stability). As the water column became vertically mixed, this organism was no longer detected.

CHAPTER FIVE

GENERAL DISCUSSION

5. GENERAL DISCUSSION

The objectives of this research were to investigate how physical mixing processes combine to control the composition of the phytoplankton community and their relative distribution in dynamic temperate, coastal environments. In this final chapter the original hypotheses are addressed in relation to the results obtained.

5.1 SPRING-NEAP TIDAL MIXING

The first two hypothesis to be tested were:-

- *Intermittency of turbulence is fundamental for the proliferation of phytoplankton.*
- *Extended water column stability is not a prerequisite to an abundant phytoplankton community in a partially mixed estuary.*

The highly complex and variable physical regime of Southampton Water was clearly observed through comparisons made during four daylight tidal cycles conducted over a spring-neap cycle (section 3.5) in August 1996. From these surveys it was shown that tidal forcings clearly dominate the residual estuarine circulation and have a large influence on the mass transport properties of Southampton Water. Using calculated velocities from both an ADCP and single point current meters, the distance travelled by the water mass in the near-surface and near-bottom zones of the water column can be estimated over the spring-neap cycle (See Table 16).

	NEAP TIDE	REDUCED SPRING TIDE	MEAN TIDE	EXTREME SPRING TIDE
SURFACE (km d ⁻¹)	-9.9	-8.2	-9.9	-7.8
BOTTOM (km d ⁻¹)	9.5	4.8	8.6	0
TOTAL DISTANCE (km d ⁻¹)	-0.4	-3.4	-1.3	-7.8

Table 16. Distance travelled (km per day) based on mean current velocities over a spring-neap tidal cycle. Negative values reflected a seaward flow.

In all cases the net daily transport is seaward, and the intensity of this flow increases from a neap to a spring tide. The estimated total distance travelled on the spring tide was 7.8 km d^{-1} , which is twenty times greater than the excursion during a neap tide. This difference in the net transport of water in the estuary over the spring-neap period has major implications for the phytoplankton community, permitting residing populations to grow within the estuary (growth $>$ flushing) during periods of reduced seaward transport (i.e. neap tides). During years of exceptional blooms in Southampton Water, particularly dominated by the photoautotrophic ciliate *Mesodinium rubrum*, a closer examination of the tidal phase has revealed the timing of these summer bloom events to be coincident with periods of reduced flushing (i.e. neap tides and reduced spring tides). Ultimately these spring-neap tidal excursions act to control the longevity of phytoplankton blooms within the estuary.

Reviewing the data from the spring-neap investigations, growth rate estimates have been calculated to determine the net daily cell division necessary to balance the population growth and flushing (population removal) within the estuary. For example, high cell concentrations of the chain forming diatom *Asterionella japonica* were observed during a neap tide in August 1996. Maximum cell concentrations were 1.7×10^6 cells per litre. The division rates (per day) of *A. japonica* have been estimated (Table 17) that would be required to balance its net transport out of the estuary, based on the transport rates defined in Table 16. (Calculations are based over a volume of the estuary equal to $6000 \text{ m} \times 15 \text{ m} \times 600 \text{ m}$).

	NEAP TIDE	REDUCED SPRING TIDE	MEAN TIDE	EXTREME SPRING TIDE
DIVISION RATE (PER DAY)	0.07	0.22	0.57	1.31

Table 17. Division rates (per day) for *Asterionella japonica* necessary to balance the transport out of the estuary (Southampton Water).

Reported maximum division rates for this chain-forming diatom where irradiance and nutrients were

unlikely to be achieved in nature. For net growth to occur, daily division rates must be greater than those given in Table 17, suggesting that net growth is only achievable during a neap, reduced spring and a mean tidal cycle.

5.2 DAILY TIDAL INFLUENCES

The third hypothesis to be tested was:-

- *Certain motile phytoplankton species can respond to short lived, intermittent stabilising events and migrations are ultimately constrained by vertical mixing.*

To address this hypothesis, changes in the phytoplankton community were investigated over different tidal phases on a daily basis. The implementation of intensive investigations of the phytoplankton community was necessary to determine the behavioural patterns of different individual species, as the use of chlorophyll *a* alone was shown to mask the behavioural patterns (such as apparent migrations and/or re-suspension events) during these time series. Chlorophyll *a* proved an important tool for assessing the phytoplankton community distribution as a whole, however the use of microscopic enumeration proved necessary to examine the apparent vertical migrations of dinoflagellate species during periods of water column stability in both a partially-mixed estuary and in the southern North Sea. Algal biomass increased to bloom concentrations during the spring months in Southampton Water (May 1995; 1996), suggesting that the stimulation of phytoplankton growth was triggered by greater day length and an increase in water temperature.

In Southampton Water, during a 25 hour tidal survey on 19-20 June 1997, apparent vertical ascent and descent migrations of dinoflagellates and a photoautotrophic ciliate, *M. rubrum* were observed over the light:dark cycle, particularly during periods of intermittent stability (e.g. HW period).

Individual dinoflagellate species, such as *Prorocentrum micans*, appeared to aggregate in the near-surface waters during the first high water period and became more vertically mixed after the period of high shear during the first ebb phase. Throughout the dark period, this species was not detected in water samples, but “re-appeared” at dawn and apparently migrated up into the surface waters during the second flood stand. This species appears to have a strong association with surface irradiance which acts to control its vertical position, however the primary factor governing vertical position was the physical mixing forcings, i.e. vertical migration was only apparently achievable during periods of low turbulence (when Richardson numbers >1.0 , see Figure 5.0c). The vertical distribution of *Peridinium trochoideum*, initially followed a similar pattern to *P. micans*, however its vertical distribution during the dark period was different. An apparent downward migration was observed during the second high water during the dark hours. These negative migrations have been observed for many

dinoflagellate species, with the "normal" autotrophic dinoflagellate diel vertical migration modelled as ascent during daylight and descent at night (Kamykowski, 1974; See section 3.2.3.4).

The 25 hour tidal survey conducted on the 19 - 20 June 1999 marked the first reported observed apparent migratory behaviour of *Mesodinium rubrum*, during dark hours. This follows the earlier studies of Crawford and Purdie (1992), who postulated that mechanisms other than irradiance trigger this organism's extensive migration through the water column. The profiles obtained in this study, suggest that during periods of high mixing (i.e. ebb flow and flood phase), the population of *M. rubrum* becomes well-mixed vertically, but during the dark high water period, *M. rubrum* appeared to positively migrate towards the surface. This species is not believed to be heavily grazed by zooplankton, so would not suffer large population losses throughout the period of positive zooplankton migration which have been shown to occur during dark hours (Kostoloupou pers. comm.). The intensive sampling protocol of the underlying physical features of the estuary coupled with the high resolution phytoplankton sampling, allowed the unexpected difference in the apparent behaviour of various motile phytoplankton species to be detected, highlighting the species-specific nature of phytoplankton dynamics in an estuary, and the close bio-physical coupling.

During a 13 hour daylight tidal survey investigation on 30 August 1996, aggregation of dinoflagellates was observed in surface waters coincident with periods of reduced tidal mixing, during the HW slack. The percentage of cells of the motile dinoflagellate *P. trochoideum* determined in the surface waters, compared to the bottom waters are given in Table 18. In Table 19 a similar comparison is made with the non motile diatom *Coscinodiscus spp.* Both organisms appear to be well mixed during the flood phase, whereas at all other times they show contrasting distributions, with the diatoms generally in higher numbers towards the bottom and the dinoflagellates in higher proportions in the surface waters.

The percentages are calculated using data from all five samples over the entire water column.

	FLOOD	FLOOD STAND	HW1	HW2	EBB
SURFACE	50	80	80	90	70
BOTTOM	50	20	20	10	30

Table 18. Percentage of the population of *Peridinium trochoideum* in the surface and bottom layers of the water column at varying tidal phases.

	FLOOD	FLOOD STAND	HW1	HW2	EBB
SURFACE	40	30	20	30	30
BOTTOM	60	70	80	70	70

Table 19. Percentage of the population of *Coscinodiscus spp.* in the surface and bottom layers of the water column at varying tidal phases.

The contrasting phytoplankton distributions highlight the importance of the asymmetry of tidal current intensity between the flood and the ebb phases in Southampton Water. The asymmetry plays an important role in influencing the temporal development and vertical distribution of different phytoplankton populations. Although estuaries are dynamic systems, the cyclicity seen over a tidal cycle in Southampton Water indicates that during periods of up to 6 hours (total for young flood and high water stands) a relatively stable water column may be established. Table 18 and Table 19 highlight the potential for different phytoplankton populations to coexist by inhabiting different vertical niches (Lauria *et al* 1999) thus supporting the third hypothesis given above.

The gradient Richardson number (Figure 5.0c) has been used to compare the stabilising effect of buoyancy (generated by a density gradient) with the de-stabilising effect of vertical current shear (Figure 5.0b), derived from velocity magnitude (Figure 5.0a). In Southampton Water results from this study have shown that pockets of turbulence are separated in both time and space, with a defined turbulent interface during the high water stand, immediately before the second high water. One feature of this turbulence is that it occurs at the same time as the maximum shear in the mean current. The frictional drag at the sea bed produces a velocity shear at regular intervals over a tidal cycle, which slows down the near bed flow relative to

that higher up in the water column. This cycle of mixing and stability is regular and is governed by the semi-diurnal tidal forcings, whereas the less predictable components are due to meteorological events and changing riverine inputs.

Figure 5.1 (a) examines the data obtained from the 13 hour survey on 30 August 1996. The percentage of the population of different phytoplankton species residing in the surface and the bottom layers were separated and compared to the Richardson (Ri) numbers calculated through time and space. "Surface" values were taken down to a level of 6 m, "bottom" values from 6 m to the sea bed.

The dinoflagellate, *Prorocentrum micans* in the surface waters showed a positive relationship with Ri number up to $Ri = 1.0$ ($r^2=0.99$, $n = 3$, $p<0.07$). However, under conditions of high stability ($Ri>1$) the data suggest that forces other than mixing intensity may influence the vertical distribution (for example, downwelling irradiance). 50-90 % of the integrated dinoflagellate population was found in the surface layers over the time series during day light hours. Conversely, the diatom *Coscinodiscus sp* showed a strong negative relationship with Ri ($r^2=0.88$, $n= 4$, $p<0.07$), suggesting that the vertical position of this passive population is linked with the intense mixing events occurring when $Ri <0.5$, and that factors such as irradiance do not exert a control on their vertical distribution. The percentage of the diatom population observed in the surface layers ranged between 10-25%, with the highest percentage of the population at lower Ri values.

The percentage of the population of these two phytoplankton species observed in the bottom layers of the water column (Figure 5.1b) highlight the bottom aggregation of the diatom, whilst the percentage of the dinoflagellate population reduced greatly (<40%). The population of *P. micans* varied little over the time series (25-35%) in the bottom layers of the water column in terms of water column stability, however a significant negative relationship ($r^2=0.80$, $n = 4$, $p = 0.02$) was again observed between the percentage of the diatom (*Coscinodiscus spp*) population observed in the bottom layers of the water column and the Richardson number. This provides further evidence for the close coupling of the distribution of diatoms becoming entrained and re-suspended during high shear events and again supports the hypothesis given above.

These correlations highlight the close coupling of the diatoms' vertical distribution and the intensity of mixing, whilst the high percentage of the dinoflagellates in the surface waters

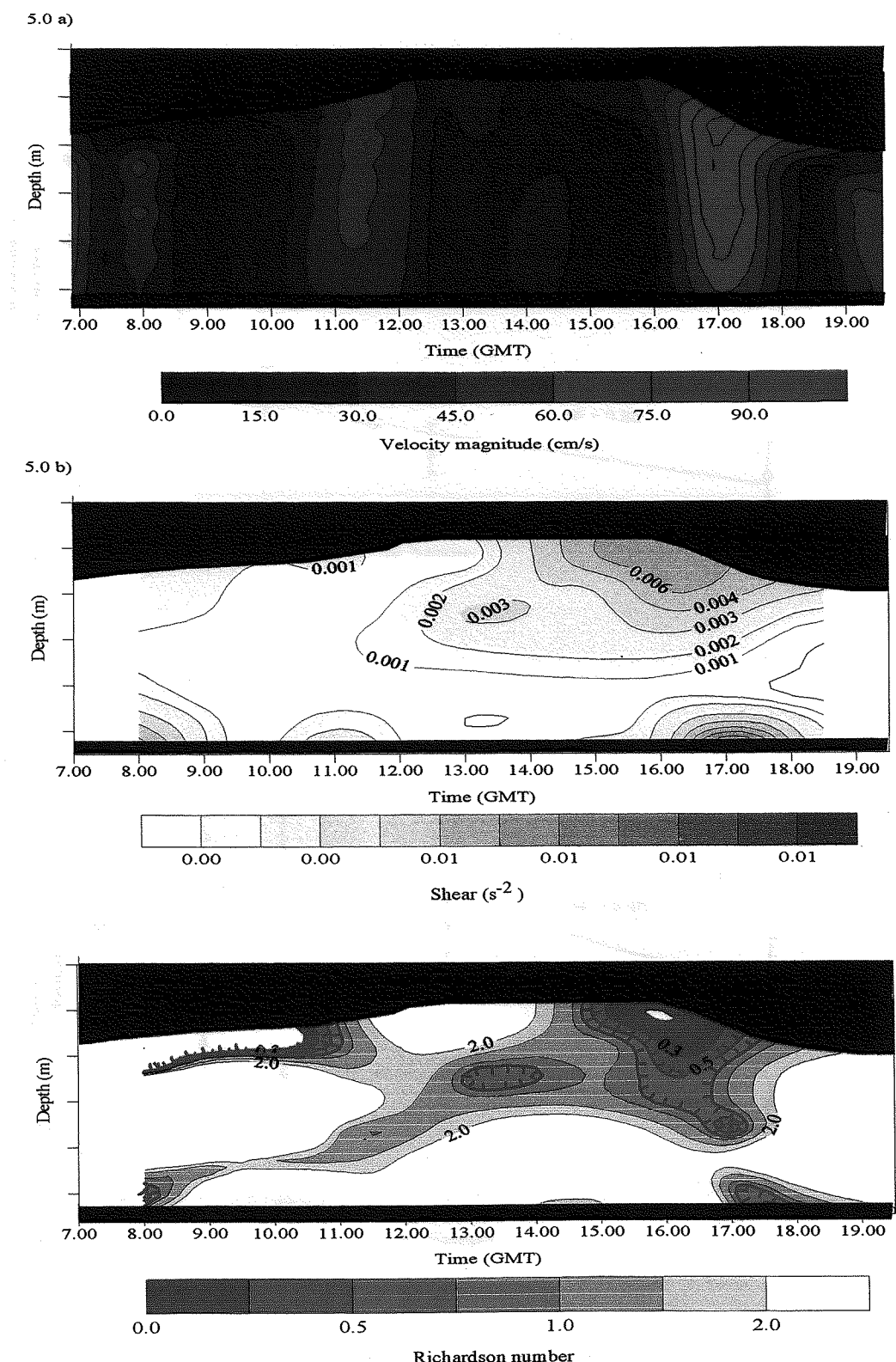
during periods of low mixing, emphasises the inverse relationship between mixing and the surface aggregation of the dinoflagellate community. At Ri numbers of ca. 2, the percentage of dinoflagellates in the surface waters decreased, highlighting the influence of many variables (e.g. surface irradiance) combining to control the vertical position of this motile community.

The intermittency of turbulence over the tidal cycle proves to be an important factor for phytoplankton residence times and their vertical position in a partially-mixed, estuarine environment. The timescales over which the opposing characteristics of mixing and stability occur, may combine in this dynamic estuary to permit the co-existence of different phytoplankton groups that are typically separated in both time and space in more open water environments.

Water Column Stability - Density Influences

The stabilising influence of density was a fundamental physical feature of the southern North Sea investigations, where the stabilising influence of the Rhine ROFI was apparent. Wind stress and strong tidal currents often prevent stratification in the southern North Sea, with strong horizontal gradients of salinity close to the coast. The temporary, short-lived stability coinciding with the fresh water influence highlighted the different phytoplankton communities associated with distinct water masses. Certain members of the diatom community could be used as indicators of the changing physical environment, for example the diatom *Rhizosolenia styliformis*. This species initially appeared in the surface waters, but with time was also observed at depth. The presence of an armoured, motile dinoflagellate, *Gonyaulax sp.*, was also associated with the temporary stability caused by the reduced salinity water mass, however this organism was confined to the surface layers only, and reduced in number as the fresh water plume retracted.

Figure 5.6. Changes in the dinoflagellate community over a 13-hour tide cycle in Southampton Water for August 1974. Estimated by (a) and (c) Ri numbers. Note the upper range of heterotrophic dinoflagellates in the tidal plume compared to the subtropical dinoflagellates.

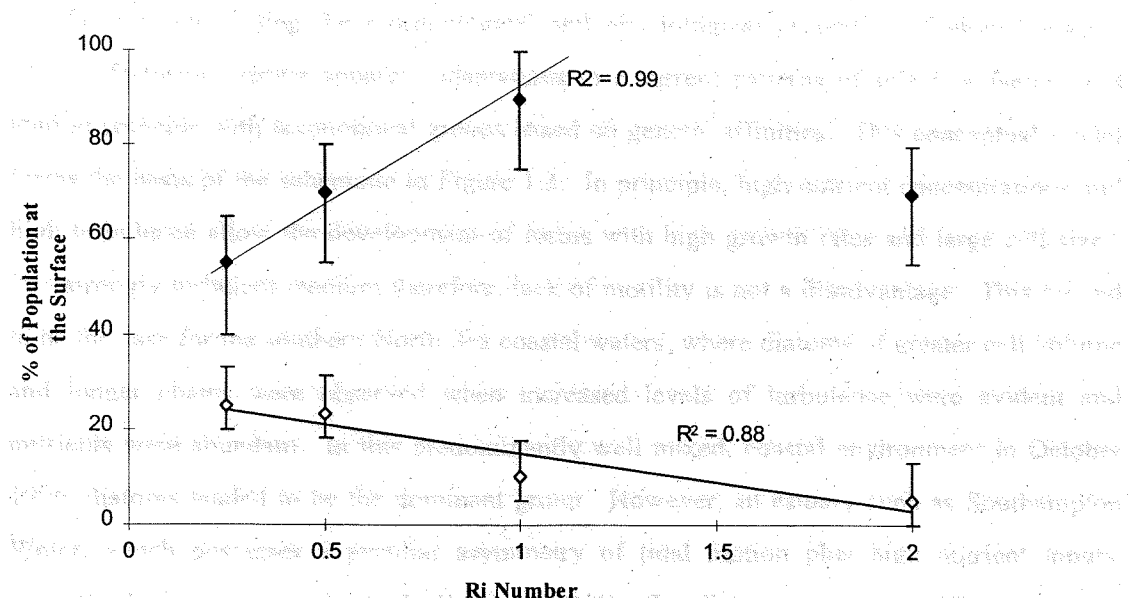


Destabilising Forces dominate

Stabilising (buoyancy) forces dominate

Figure 5.0. Example of the de-stabilising forces during a 13 hour time series in Southampton Water (30 August 1996). a) velocity magnitude; b) shear; and c) Ri number. Note the dominance of boundary shear during the rapid current velocities compared to the turbulent interface during the high water stand.

a)



b)

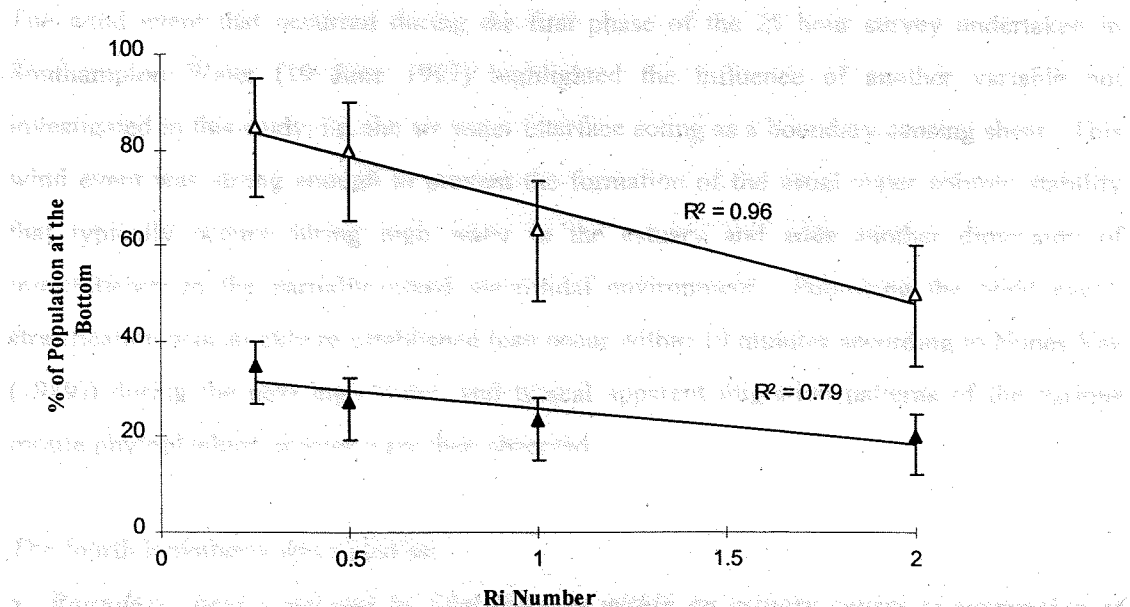


Figure 5.1. Comparison of the Richardson Number and the % population residing in the surface (Figure 5.1a) and the bottom (Figure 5.1b) layers of the water column. Percentages are the average integrated population over 5 sampling points. Filled symbols represent the dinoflagellate *Prorocentrum micans*; open symbols represent the diatom *Coscinodiscus spp.*

Margalef (1978) has suggested that the supply of nutrients and the intensity of turbulence are key factors determining the morphological and physiological properties of phytoplankton. These life-forms express apparent adaptations to recurrent patterns of selective factors and tend to coincide with taxonomical groups based on genetic affinities. This conceptual model forms the basis of the schematic in Figure 1.3. In principle, high nutrient concentrations and high turbulence allow the development of forms with high growth rates and large cell sizes. In a strongly turbulent medium therefore, lack of motility is not a disadvantage. This proved to be the case for the southern North Sea coastal waters, where diatoms of greater cell volume and longer chains were observed when increased levels of turbulence were evident and nutrients were abundant. In this predominantly well mixed, coastal environment in October 1996, diatoms tended to be the dominant group. However, an estuary such as Southampton Water, which possesses a peculiar asymmetry of tidal motion plus high nutrient inputs, presents the opportunity for both diatoms and dinoflagellate species to proliferate, and in some cases to co-exist by taking advantage of the varied hydrography.

Water Column Stability - Other Factors

The wind event that occurred during the first phase of the 25 hour survey undertaken in Southampton Water (19 June 1997) highlighted the influence of another variable not investigated in this study, i.e. the air-water interface acting as a boundary causing shear. This wind event was strong enough to prevent the formation of the usual water column stability that typically occurs during high water in the estuary and adds another dimension of intermittency to the partially-mixed macrotidal environment. Following the wind event, stratification was quickly re-established (can occur within 10 minutes according to Nunes Vaz (1989)) during the next high water, and typical apparent migration patterns of the various motile phytoplankton species were then observed.

The fourth hypothesis was stated as:

- ***Boundary shear generated by tidal forcings within an estuary causes re-suspension of both the bottom sediments and the phytoplankton community, permitting the organisms to be intermittent members of the pelagic microalgal community.***

The daily and spring-neap tidal forcings on the re-suspension of surface sediment were detected during each of the surveys, thus broadly proving this hypothesis. Tidal re-suspension results in the entrainment of particulate material up into the water column, and this will include both recently settled phytoplankton and benthic microalgae. The extent of the vertical

propagation of the benthic algal community can be compared directly to the plumes of SPM. The extent, therefore to which these organisms are re-suspended in the water column depends on the intensity of the benthic boundary shear. This was particularly apparent during the spring-neap survey in August 1996, where re-suspension of the benthic diatoms *Navicula spp* and *Nitzschia spp* was detected during the latter flood period and the ebb flow. An interesting feature of these phytoplankton distributions was the fact that *Navicula spp* were re-suspended during a lower shear event, suggesting that this species is less "sticky" than *Nitzschia spp*. (Kiørboe 1993; Kiørboe *et al* 1990). This contrasting "behaviour" would make an interesting focus for further research, targeting the critical shear necessary to re-suspend different phytoplanktonic species.

The re-suspension of benthic species of microalgae was clearly observed during spring-neap surveys (August 1996), which have shown the distance travelled during the tidal excursions. As well as the pelagic phytoplankton community and the significance for particulate matter, the net transport for the benthic community will be landward (Table 16). The uppermost station sampled during these investigations was at NW Netley. In any future surveys, stations further inland could be sampled to investigate the benthic community composition at the limits of the tidal incursion.

The fourth hypothesis therefore, although investigated as part of the ongoing field program, was not fully examined, primarily due to the sampling problems of determining near-bed currents and the extent of the microbenthic and the pelagic autotrophic communities.

5.3 CONCLUDING REMARKS

Phytoplankton cells are typically smaller than the Kolmogorov length in aquatic environments, so in theory the velocity field around these organisms should be nearly a linear gradient. This suggests that at the scale of the individual, turbulence is not an environmental property of the plankton. However, in the natural environment direct and indirect effects of turbulence on phytoplankton become indistinguishable. The use of laboratory experiments has led to the realisation that there is indeed a direct effect of turbulence on phytoplankton, which extends beyond the interference of the light and nutrient régimes. Laboratory studies have concluded that agitation by means of aeration, paddle wheels, magnetic stirrers or orbital shakers can have detrimental effects on phytoplankton, with dinoflagellates being the most sensitive group. Diatoms, a group often associated with vertically mixed water columns,

seem to have a turbulence threshold, as shown through laboratory experiments. Savidge (1981) reported that cell division times of *Phaeodactylum tricornutum* in the exponential phase decreased with increasing agitation in phosphate-limited cultures, but increased in nitrate-limited cultures. Schöne (1970) showed that the intensity of the motion of the sea surface was inversely related to chain length of several chain forming diatoms, such as *Chaetoceros curvisetus* and *Skeletonema costatum*. The reduction in chain length was apparently due to the mechanical breaking of colonies. Results from some preliminary batch culture experiments conducted during this study, suggested that a turbulent environment is advantageous for the chain forming diatom species (*Rhizosolenia delicatula*). Chain length increased for seven days, after which time there was little difference in the length of chains compared to the non-turbulent condition.

Turbulence is a key environmental property for phytoplankton and plays a central role in controlling or modulating the effects of other factors such as light and nutrients (Estrada and Berdalet 1998) all of which combine to form the fundamental necessities for growth. In partially-mixed estuaries and to a lesser extent, shallow coastal waters, mixing is caused by a combination of internally generated and boundary generated turbulence, and meteorological conditions with their relative magnitudes varying in space and time.

The research presented in this thesis has examined a number of parameters that influence the biological succession of phytoplankton and can lead to the spatial resource partitioning of diatoms and dinoflagellates within the same timescale (Lauria *et al* 1999). The accepted theories which describe dinoflagellates in open water environments where blooms occur under conditions of water column stability are also applicable to more highly dynamic ecosystems like Southampton Water, where phytoplankton populations were shown to respond rapidly to their external environment, and take advantage of the dominant hydrographic features. Diatoms, in contrast, are reported to bloom under conditions of strong vertical mixing where nutrients are abundant and average PAR is reduced. This study has shown that diatoms can also form exceptional blooms in highly dynamic estuaries, where bloom events are often short-lived (e.g. less than two weeks), even under conditions of high nutrients, vertical mixing and adequate PAR levels. The results from this research have explored the intrinsic relationship between these groups of phytoplankton and the tidal forcings which act to ultimately control their distribution and community composition in temperate, shallow coastal environments.

CHAPTER SIX

REFERENCES

REFERENCES

6. REFERENCES

Airy, G.B. (1843). On the laws of individual tides at Southampton and Ipswich. *Philosophical Transactions of the Royal Society*, 133: 45-54.

Alcaraz, M., Saiz, E., Marrasé, C. and Vaqué, D. (1988). Effects of turbulence on the development of phytoplankton biomass and copepod populations in marine microcosms. *Marine Ecology Progress Series*, 49: 117-125.

Alldredge, A.L. and Gotschalk, C. (1989). Direct observations of the flocculation of diatom blooms: Characteristics, settling velocities and formation of diatom aggregates. *Deep-Sea Research II*, 36: 159-171.

Anderson, D.M., Chisholm, S.W. and Watras, C.J. (1983). The importance of life cycle events in the population dynamics of *Gonyaulax tamarensis*. *Marine Biology*, 76: 179-190.

Anderson, D.M., Nosenchuck, D.M., Reynolds, G.T. and Walton, A.J. (1988). Mechanical Stimulation of Bioluminescence in the Dinoflagellate *Gonyaulax polyedra* Stein. *Journal of Experimental Marine Biology and Ecology* 122: 277-288.

Anderson, D.M. and Stolzenbach, K.D. (1985). Selective retention of two dinoflagellates in a well-mixed estuarine embayment: the importance of diel migration and surface avoidance. *Marine Ecology Progress Series*, 25: 39-50.

Anning, T. (1995). The expression of photosynthetic genes in natural populations of marine phytoplankton. *PhD Thesis, University of Southampton*.

Antai, (1989). *PhD Thesis, University of Southampton*.

Barlow, J.P. (1956). Effect of wind on salinity distribution in an estuary. *Journal of Marine Research*, 15: 193-203.

Berdalet, E. (1992). Effects of Turbulence on the marine dinoflagellate *Gymnodinium nelsonii*. *Journal of Phycology*, 28: 267-272.

Berdalet, E. and Estrada, M. (1993). Toxic Phytoplankton Blooms in the Sea. Effects of turbulence on several dinoflagellate species. Elsevier Science Publishers, pp737-740.

Berg, H. and Purcell, E. (1977). Physics of Chemoreception. *Biophysical Journal*, 20: 193-219.

Bowden, K.F. and Fairbairn, L.A. (1952a). A determination for the frictional forces in a tidal current. *Proceedings of the Royal Society of London*, A214: 371-392.

Bowden, K.F. and Fairbairn, L.A. (1956). Measurements of turbulent fluctuations and Reynolds stresses in a tidal current. *Philosophical Transactions of the Royal Society of London*, A244: 335-356.

Bowden, K.F. and Sharaf el Din, S.H. (1966). Circulation and mixing processes in the Liverpool Bay area of the Irish Sea. *Geophysical Journal of the Royal Astronomical Society of London*, 11: 279-292.

Boynton, W.R., Kemp, W.M. and Keefe, C.W. (1982). A Comparative Analysis of Nutrients and other factors influencing Estuarine Phytoplankton production. *Estuarine Comparisons*. Academic Press, 709 pp.

Brand, L.E. (1984). The salinity tolerance of forty-six marine phytoplankton isolates. *Estuarine and Coastal Shelf Science*, 18: 543-556.

Bryan, J.R. (1979). The production and decomposition of organic material in an estuary - Southampton Water. *PhD Thesis, University of Southampton*.

Burkhill, P.H. (1978). Quantitative aspects of the ecology of marine planktonic ciliated protozoans with special reference to *Uronema marinum*, Dujardin. *PhD Thesis, University of Southampton*.

Cloern, J.E. (1987). Turbidity as a control on phytoplankton biomass and productivity in estuaries. *Continental Shelf Research*, 7: 1367-1381.

Cloern, J.E. (1991). Tidal Stirring and Phytoplankton bloom dynamics in an estuary. *Journal of Marine Research*, 49: 203-221.

Cloern, J.E., Powell, T.M. and Huzzey, L.M. (1989). Spatial and temporal variability in South San Francisco Bay. II Temporal changes in salinity, suspended sediments and phytoplankton biomass and productivity over tidal time scales. *Estuarine and Coastal Shelf Science*, 28: 599-613.

Cole, B.E. and Cloern, J.E. (1984). Significance of biomass and light availability to phytoplankton productivity in San Francisco Bay. *Marine Ecology Progress Series*, 15: 15-24.

Costello, J.H., Strickler, J.R., Marrasé, C., Trager, G., Zeller, R. and Freise, A.T. (1990). Grazing in a Turbulent Environment: behavioural response of a Calanoid Copepod, *Centropages hamatus*. *Proceedings of the National Academy of Science USA*, 87: 1648-1652.

Crawford, D. 1989. The physiological ecology of the red water ciliate *Mesodinium rubrum*. *PhD Thesis, University of Southampton*.

Crawford, D. and Lindholm, T. (1997). Some observations on vertical distribution and migration of the phototrophic ciliate *Mesodinium rubrum* (= *Myrionecta rubra*) in a stratified brackish inlet. *Aquatic Microbial Ecology*, 13: 267-274.

Crawford, D. and Purdie, D. (1992). Evidence for the avoidance of flushing from an estuary by a planktonic, phototrophic ciliate. *Marine Ecology Progress Series*, 79: 259-265.

Daneri, G. (1992). Comparison between *in vitro* and *in situ* estimates of primary production within two tracked water bodies. *Arch. Hydrobiol. Beih. Ergebn. Limnol.*, 37: 101-109.

de Oliveria Proenca, L.A. (1994). Phytoplankton biomass, organic matter sedimentation and nutrient remineralisation in a macrotidal estuary - Southampton Water. *PhD Thesis, University of Southampton*.

Demers *et al* (1986).

Dempsey, H.P. (1982). The effect of turbulence on three algae *Skeletonema costatum*, *Gonyaulax tamarensis*, *Heterocapsa triquetra*. S.B. Thesis. Massachusetts Institute of Technology, Cambridge, Ma.

Denman, K.L. and Gargett, A. (1995). Biological-Physical interactions on the upper ocean. The role of vertical and small-scale transport processes. *Annual Review of Fluid Mechanics*, 27: 225-255.

Dickey, T.D. and Mellor, G.L. (1980). Decaying turbulence in neutral and stratified fluids. *Journal of Fluid Mechanics*, 99: 13-31.

Diwan (1978). *PhD Thesis, University of Southampton*.

Drebes, G. (1974). Marines phytoplankton. Eine Auswahl der Helgolander planktonalgen (Diatomeen, Peridineen). Georg Theme Verlag, Stuttgart.

Dyer, K. (1997). Estuaries. A Physical Introduction. John Wiley and Sons, 195 pp.

Edler, L. and Olssen, P. (1985). Observations on diel migration of *Ceratium furca* and *Prorocentrum micans* in a stratified bay on the Swedish west coast. In *Toxic dinoflagellates (3rd conference)* ed. D M Anderson, A W White, D G Baden. Elsevier publications p 195-201.

Eilertson, H. (1993). Spring blooms and stratification. *Nature*, 363(6424): 24.

Eppley, R.W., Koeller, P. and Wallace Jnr, G.T. (1978). Stirring influences the phytoplankton species composition within enclosed columns of coastal sea water. *Journal of Experimental Marine Biology and Ecology*, 32: 219-239.

Eppley, R.W. and Thomas, W. H. (1969). Comparisons of half-saturation constants for growth and nitrate uptake of marine phytoplankton. *Journal of Phycology* 5: 375-379.

Estrada, M., Alcaraz, M. and Marrasé, C. (1987a). Effects of turbulence on the composition of phytoplankton assemblages in marine microcosms. *Marine Ecology Progress Series*, 38: 267-281.

Estrada, M., Alcaraz, M. and Marrasé, C. (1987b). Effect of Reversed Light Gradients on the Phytoplankton Composition in Marine Microcosms, *Inv. Perq.*, 51: 443-458.

Estrada, M. and Berdalet, E. (1997). Phytoplankton in a turbulent world. *Scientia Marina*, 61(S1): 125-140.

Estrada, M. and Berdalet, E. (1998). Effects of turbulence on phytoplankton. NATO ASI. In *Physiological Ecology of Harmful Algal Blooms*. Springer-Verlag (Berlin).

Fogg, G.E. and Than-Tun (1960). Inter-relations of photosynthesis and assimilation of elementary nitrogen in a blue-green alga. *Proceedings of the Royal Society of London*, B153: 111-127.

Forward, R.B. (1976). Light and diurnal vertical migration: photobehaviour and photophysiology of plankton. *Photochemical and Photobiological Reviews*, 1: 157-209.

Garcia, C.A.E., Purdie, D.A. and Robinson, I.S. (1993). Mapping a bloom of the photosynthetic ciliate *Mesodinium rubrum* in an estuary from airborne thematic mapper data. *Estuarine and Coastal Shelf Science*, 37: 287-298.

Garcon, V.C. and Anderson, D.M. (1986). Tidal flushing of an estuarine embayment subject to recurrent dinoflagellate blooms. *Estuaries*, 9: 179-18.

Gardner, G.B. and Smith, J.D. (1978). Turbulent mixing in a salt wedge estuary. In: J. Nihoul (Editor), *Hydrodynamics of estuaries and fjords*. Elsevier, Amsterdam, pp. 79-106.

Gargett, A., 1997. "Theories" and techniques for observing turbulence in the ocean euphotic zone. Lectures on plankton and turbulence. *Scientia Marina*, 61 (1) 25-45 pp.

Gerlach, S.A. (1987). Nutrients- an overview. In: P.J. Nemann and A.R. Agg (Editors), *Environmental Protection of the North Sea*. Heineman Professional Publishing Ltd., pp. 145-175.

Gibson, C.H. and Thomas, W.H. (1995). Effects of turbulence intermittency on growth inhibition of a red tide dinoflagellate, *Gonyaulax polyedra* Stein. *Journal of Geophysical Research*, 100(C12): 24841-24846.

Gran, H.H. and Braarud, T. (1935). A quantitative study of the phytoplankton in the Bay of Fundy and the Gulf of Maine (including observations on hydrography, chemistry and turbidity). *Journal of the Biology Board of Canada*, 1: 279-467.

Gregg, M.C. (1991). The study of mixing in the Ocean. A brief history. *Oceanography*, 4: 39-45.

Haas, L.W. (1977). The effect of the spring-neap tidal cycle on the vertical structure of the James, York and Rappahannock rivers, Virginia, U.S.A. *Estuarine and Coastal Marine Science*, 5: 485-496.

Haas, L.W., Hastings, S.J. and Webb, K.L. (1981). Phytoplankton responses to a stratification-mixing cycle in the York river estuary during late summer. In: B.J. Neilson and L.E. Cronin (Editors), *Estuaries and Nutrients*. Clifton, NJ, Humana, pp. 619-636.

Hand, W.G., Collard, P.A. and Davenport, D. (1965). The effects of temperature and salinity changes on the swimming rates in the dinoflagellates *Gonyaulax* and *Gyrodinium*. *Biological Bulletin*, 128: 90-101.

Harleman, D.R.F. and Ippen, A.T. (1967). Two-dimensional aspects of salinity intrusion in estuaries: analysis of salinity and velocity distributions. *Technical Bulletin, US Army Corps of Engineers*, 13: 55pp.

Hasle, G.R. (1950). Phototactic vertical migrations in marine dinoflagellates. *Oikos*, 2: 162-175.

Hasle, G.R. (1954). More on phototactic diurnal vertical migrations in marine dinoflagellates. *Nyatt. Mag. Bot.*, 2: 139-147.

Hitchcock, G.L. and Smayda, T.J. (1977). The importance of light in the initiation of the 72-73 winter-spring diatom bloom in Narragansett Bay. *Limnology and Oceanography*, 22: 126-131.

Holligan, P. (1987).

Howarth, R.W., Butler, T., Lunde, K., Swaney, D. and Chu, C.R. (1993). Turbulence and planktonic nitrogen fixation: A mesocosm experiment. *Limnology and Oceanography*, 38: 1696-1711.

Ippen, A.T. and Harleman, D.R.F. (1961). One-dimensional model of the seasonal thermocline. II The general theory and its consequences. *Technical Bulletin, US Army Corps of Engineers*.

Iriarte, A. (1992). Picophytoplankton ecology and physiology studies in culture and in natural coastal and estuarine waters. *PhD Thesis, University of Southampton*.

Jay, D.A. and Smith, J.D. (1988). Residual circulation and classification of shallow, stratified estuaries. In: J. Dronkers and W.v. Leussen (Editors), *Physical processes in estuaries*. Springer-Verlag (Berlin), pp. 21-41.

Joint, I.R. and Pomroy, A.J. (1981). Primary Production in a Turbid Estuary. *Estuarine, Coastal and Shelf Science*, 13: 303-316.

Kamykowski, D. (1974). Possible interactions between phytoplankton and semi-diurnal tides. *Journal of Marine Research*, 32: 67-89.

Kamykowski, D. (1987). *Phytoplankton and Diurnal Vertical Migration*. Ph.D. Thesis, University of Southampton.

Kamykowski, D. (1981b). Laboratory experiments on the diurnal vertical migration of marine dinoflagellates through temperature gradients. *Marine Biology*, 62: 81-89.

Kamykowski, D. (1995). Trajectories of autotrophic marine dinoflagellates. *Journal of Phycology*, 31: 200-208.

Kamykowski, D. and McCollum, S.A. (1986). The temperature acclimated swimming speed of selected marine dinoflagellates. *Journal of Plankton Research*, 8: 275-287.

Ketchum, B.H. (1954). Relationship between circulation and planktonic populations in estuaries. *Ecology*, 35: 191-200.

Kiefer, D.A. and Lasker, R. (1975). Two blooms of *Gymnodinium splendens*, an unarmoured dinoflagellate. *Fishery Bulletin, U.S.*, 73: 675-678.

Kifle, D. (1992). Seasonal and spatial variation in species composition, abundance, biomass and primary production of phytoplankton in Southampton Water, U.K. *PhD Thesis, University of Southampton*.

Kifle, D. and Purdie, D. (1993). The Seasonal abundance of the phototrophic ciliate *M. rubrum* in Southampton Water, England. *Journal of Plankton Research*, 15: 823 -833.

Kiørboe, T. (1993). Turbulence, Phytoplankton Cell-Size, and the Structure of Pelagic Food Webs. *Advances in Marine Biology*, 29: 1-72.

Kiørboe, T., Andersen, K. and Dam, H. (1990). Coagulation efficiency and aggregate formation in marine phytoplankton. *Marine Biology*, 107: 235-245.

Kiørboe, T. and Saiz, E. (1995). Planktivorous feeding in calm and turbulent environments, with emphasis on copepods. *Marine Ecology Progress Series*, 122: 135-145.

Kolmogorov, A.N. (1941). The local structure of turbulence in viscous fluid for very large Reynolds numbers. *Dokl. Akad. Nauk SSSR*, 30: 301-305.

Koseff, J.R., Holen, J.K., Monismith, S.G. and Cloern, J.E. (1993). Coupled Effects of Vertical Mixing and Benthic Grazing On Phytoplankton Populations in Shallow, Turbid Estuaries. *Journal of Marine Research*, 51: 843-868.

Kostopoulou, V. (1997). *MSc Thesis, University of Southampton*.

Lakhotia, S. and Papoutsakis, E.T. (1992). Agitation induced cell injury in microcarrier cultures. Protective effect of viscosity is agitation intensity dependent: Experiments and Modelling. *Biotechnology and Bioengineering*, 39: 95-107.

Lancelot, C., Billen, G., Sournia, A., Weisse, T., Coijjn, F., Veldhuis, J.W., Davies, A. and Wassman, P. (1987). *Phaeocystis* blooms and nutrient enrichment in the continental coastal zones of the North Sea. *Ambio*, 16 (1): 38-46.

Latz, M.I., Case, J.F. and Gran, R.L. (1994). Excitation and bioluminescence by laminar fluid shear associated with simple Couette flow. *Limnology and Oceanography*, 39: 1424-1439.

Lauria, M.L., Sharples, J. and Purdie, D.A. (1999). Contrasting phytoplankton distributions controlled by tidal turbulence in an estuary. *Journal of Marine Systems (Accepted)*.

Lazier, J. and Mann, K. (1989). Turbulence and the diffusive layers around small organisms. *Deep-Sea Research*, 36: 1721-1733.

Leakey, R., Burkhill, P. and Sleigh, M. (1992). Abundance and biomass of ciliates determined at Calshot and Netley between June 1986 and June 1987. *Marine Biology*, 114: 67-83.

Leakey, R.J.G. (1989). The ecology of planktonic ciliates in Southampton Water. *PhD Thesis, University of Southampton*.

Levandowsky, M. and Kaneta, P.J. (1987). Behaviour in dinoflagellates. In: F.J.R.Taylor (Editor), *The biology of dinoflagellates*. Blackwell Scientific, Oxford, pp. 360-397.

Linden, P.F. and Simpson, J.E. (1988). Modulated mixing and frontogenesis in shallow seas and estuaries. *Continental Shelf Research*, 8: 1107-1127.

Lindholm, T. (1985). *Mesodinium rubrum*-a unique photosynthetic ciliate. *Advances in Aquatic Microbiology*, 3: 1-48.

Lindsay, P., Balls, P.W. and West, J.R. (1996). Influence of tidal range and river discharge on suspended particulate matter fluxes in the Forth Estuary (Scotland). *Estuarine and Coastal Shelf Science*, 42: 63-82.

Lombardi, E.H. and Capon, B. (1971). Observations on the tidepool ecology and behaviour of *Peridinium gregarium*. *Journal of Phycology*, 7: 188-194.

Lorenzen, C.J. (1967). Vertical distribution of chlorophyll and phaeopigments: Baja California. *Deep-Sea Research*, 14: 735-745.

Malone, T.C. (1977a). Environmental regulations of phytoplankton productivity in the lower Hudson Estuary. *Estuarine, Coastal and Marine Science*, 5: 157-171.

Mann, K. and Lazier, J. (1991). *Dynamics of Marine Ecosystems: Biological-Physical Interactions in the Oceans*. Blackwell Scientific Publications. Boston. 1st Edition.

Mann, K. and Lazier, J. (1996). *Dynamics of Marine Ecosystems: Biological-Physical Interactions in the Oceans*. Blackwell Scientific Publications. Boston. 2nd Edition.

Margalef, R. (1978). Life-forms of phytoplankton as survival alternatives in an unstable environment. *Oceanologica Acta*, 1(4): 493-509.

Margalef, R. (1997). Turbulence and marine life. *Scientia Marina*, 61(S1): 109-123.

Marrasé, C., Costello, J., Granata, T. and Strickler, J.R. (1990). Grazing in a turbulent environment: Energy dissipation, encounter rates and efficacy of feeding currents in *Centropages hamatus*. *Proceedings of the National Academy of Science, USA*, 87: 1653-1657.

Marshall, H.G. and Alden, R.W. (1997). Dynamics of an estuarine ecosystem: The influence of flow patterns on phytoplankton trends in the Chesapeake Bay. *Oceanologica Acta*, 20(1): 109-117.

Munk, W. and Riley, G. (1952). Absorption of nutrients by aquatic plants. *Journal of Marine Research*, 11: 215-240.

Nichols, M.M. (1984). Effects of fine re-suspension in estuaries. In: A.J. Mehta (Editor), *Estuarine Cohesive Sediment Dynamics*. Springer-Verlag, USA, pp. 5-42.

Nunes-Vaz, R.A., Lennon, G.W. and de Silva Samarasinghe, J.R. (1989). The negative role of turbulence in estuarine mass transport. *Estuarine, Coastal and Shelf Science*, 28: 361-377.

Oviatt, C. (1981). Effects of different mixing schedules on phytoplankton, zooplankton and nutrients in marine microcosms. *Marine Ecological Progress Series*, 4: 57-67.

Parsons, T.R., Maita, Y. and Lalli, C.M. (1984). A manual of chemical and biological methods for seawater analysis. Pergamon Press, Oxford, 173 pp.

Passow, U. (1991). Vertical migration of *Gonyaulax catenata* and *Mesodinium rubrum*. *Marine Biology*, 110: 455-463.

Pedley, T. and Kessler, J. (1992). Hydrodynamic phenomena in suspensions of swimming microorganisms. *Annual Review of Fluid Mechanics*, 24: 313.

Peters, F. and Gross, T. (1994). Increased Grazing Rates of Microplankton in Response to Small-Scale Turbulence. *Marine Ecology Progress Series*, 115: 299-307.

Peters, H. (1997). Observations of stratified turbulent mixing in an estuary: Neap to spring variations during high river flow. *Estuarine, Coastal and Shelf Sciences*, 45: 69-88.

Pingree, R. (1975). The advance and retreat of the thermocline on the continental shelf. *Journal of Marine Biological Association UK*, 55: 965-974.

Platt, T., Bird, D. and Sathyendranath, S. (1991). Critical depth and marine primary production. *Proceedings of the Royal Society, London (B)*, 246: 205-217.

Pollinger, U. and Zemel, E. (1981). *In situ* and experimental evidence of the influence of turbulence on cell division processes of *Peridinium cinctum*. *British Journal of Phycology*, 16: 281-287.

Pritchard, D.W. (1956). The dynamic structure of a coastal plain estuary. *Journal of Marine Research*, 15: 33-42.

Pugh, D.T. (1996). Tides, Surges and Mean Sea level: A handbook for engineers and scientists. J. Wiley and Sons.

Radach, G. and Berg, J. (1986). Trends in den konzentrationen der Nahrstoffe in der Helgolande Bucht. *Berlin Biol. Aust. Helgoland*, 2: 1-63.

Radach, G. and Moll, A. (1990). The importance of stratification for the development of phytoplankton blooms. A simulation study. In: W. Michaelis (Editor), *Estuarine Water Quality Management*. Springer-Verlag, Berlin, pp. 389-394.

Randall, J.M. and Day Jnr, J.W. (1987). Effects of river discharge and vertical circulation on aquatic primary production in a turbid Louisiana (USA) estuary. *Netherlands Journal of Sea Research*, 21(3): 231-242.

Raven, J.A. (1986). Physiological consequences of an extremely small size for autotrophic organisms in the sea. In: T. Platt and W.K.W. Li (Editors), *Photosynthetic picoplankton*, *Canadian Bulletin of Fisheries and Aquatic Science*, 214, pp. 1-70.

Raven, J.A. and Richardson, K. (1984). Dinophyte Flagella: Cost-Benefit Analysis. *New Phytologist*, 98: 259-276.

Reid, P.C., Lancelot, C., Gieskes, W.W.C., Hagmeier, E. and Weichert, G. (1990). Phytoplankton of the North Sea and its dynamics: A Review. *Netherlands Journal of Sea Research*, 26(295-331).

Reynolds, C.S. (1994). The Long, the Short and the Stalled - On the Attributes of Phytoplankton Selected By Physical Mixing in Lakes and Rivers. *Hydrobiologia*, 289(1-3): 9-21.

Richardson, T., et al (1996). *Coastal and Shelf Science*, 33: 73-76.

Riley, G.A. (1967). The Plankton of Estuaries. In: G.H. Lauff (Editor), *Estuaries*. American Association for the Advances of Science, Washington, pp. 316-326.

Riley, G.H. (1942). The relationship of vertical turbulence and spring diatom flowering. *Journal of Marine Research*, 5: 67-87.

Roden, C. (1984). The 1980/81 phytoplankton cycle in the coastal waters off Connemara, Ireland. *Coastal Shelf Science*, 18: 485-497.

Roden, C. (1994). Chlorophyll blooms and the spring/neap tidal cycle: Observations at two stations on the coast of Connemara, Ireland. *Marine Biology*, 118: 209-213.

Rohr, J., Losee, O. and Hoyt, J. (1990). Stimulation of Bioluminescence by Turbulent Pipe Flow. *Deep-Sea Research*, 37: 1639-1646.

Roman, M.R. and Tenore, K.R. (1978). Tidal re-suspension in Buzzards Bay, Ma. I. Seasonal changes in the re-suspension of Organic Carbon and chlorophyll *a*. *Estuarine and Coastal Marine Science*, 6: 37-46.

Ryan (1994). MSc. Thesis, University of Southampton.

Saiz, E. and Kiørboe, T. (1995). Predatory and Suspension Feeding of the copepod *Acartia tonsa* in turbulent environments. *Marine Ecology Progress Series*, 122: 147-158.

Savidge, G. (1981). Studies of the effects of Small-Scale Turbulence on Phytoplankton. *Marine Biology Association U.K.*, 61: 477-488.

Schaffer, G.P. and Sullivan, M.J. (1988). Water column productivity attributable to displaced benthic diatoms in well-mixed shallow estuaries. *Journal of Phycology*, 24: 132-140.

Schubel, J.R. and Carter, H.H. (1984). The estuary as a filter for fine-grained sediment. In: V. Kennedy (Editor), *The Estuary as a Filter*. Academic Press, New York, pp. 81-105.

Seliger, H.H., Carpenter, J.H., Loftus, M. and McElroy, W.D. (1970). Mechanisms for the accumulation of high concentrations of dinoflagellates in a bioluminescent Bay. *Limnology and Oceanography*, 15: 234-245.

Sheldon, R.W. (1972). Size separation of marine seston by membrane and glass fibre filters. *Limnology and Oceanography*, 17: 494-498.

Simpson, J.H. (1986). Introduction to the North Sea Project. 1-25.

Simpson, J.H., Brown, J., Matthew, J. and Allen, G. (1990). Tidal straining, density currents and stirring in the control of estuarine stratification. *Estuaries*, 13: 125-132.

Simpson, J.H., Sharples, J. and Rippeth, T. (1991). A prescriptive model of stratification induced by freshwater runoff. *Estuarine, Coastal and Shelf Science*, 33: 23-35.

Simpson, J.H. and Souza, A. (1995). Semi-diurnal switching of stratification in the Rhine ROFI. *Journal of Geophysical Research*, 100(C4): 7037-7044.

Smayda, T.J. (1970). The suspension and sinking of phytoplankton in the sea. *Oceanog. Mar. Biol. Ann. Rev.*, 8: 353-414.

Smith, W.O. and Barber, R.T. (1979). A carbon budget for the autotrophic ciliate *Mesodinium rubrum*. *Journal of Phycology*, 15: 27-33.

Sournia, A. (1982). Form and Function in Marine Phytoplankton. *Biological Review*, 57: 347-394.

Souza, A.J., Simpson, J.H. and Schirmer, F. (1997). Current structure of the Rhine region of freshwater influence. *Journal of Marine Research*, 55: 277-292.

Stein, J.(ed) (1975). Handbook of phycological methods: culture methods and growth measurements. Cambridge University Press. 478pp.

Sündermann, J (ed) (1994). Circulation and Contamination Fluxes in the North Sea. Introduction. p1-9. Springer-Verlag.

Sverdrup, H. (1953). On conditions for the vernal blooming of phytoplankton. *Journal de Conseil International l'Exploration de la Mer*, 18: 287-295.

Tangen, K. (1979). Dinoflagellate blooms in Norwegian water. In: D.L. Taylor and H.H.Seliger (Editors), Toxic dinoflagellate blooms. Elsevier, pp. 79-84.

Taylor, F.J.R. (1982). Symbioses in marine microplankton. *Annales de l'institut Oceanographique. Fascicule supplementaire*, 58: 61-90.

Tennekes, H. and Lumley, J. (1972, 1994). A First Course in Turbulence. MIT Press.

Tett, P. (1990). The photic zone. In: P.J. Herring, A.K. Campbell, M. Whitfield and L.Madoc (Editors), Light and life in the sea. Cambridge University Press, pp. 59-87.

Tett, P. and Mills, D. (1991). The Plankton of the North Sea - Pelagic Ecosystems under Stress? *Ocean & Shoreline Management*, 16: 233-257.

Thomas, W. and Gibson, C. (1990a). Quantified small-scale turbulence inhibits a red tide dinoflagellate, *Gonyaulax polyedra*. *Deep-Sea Research*, 37(10): 1583-1593.

Thomas, W.H. and Gibson, C.H. (1990b). Effects of small-scale turbulence on microalgae. *Journal of Applied Phycology*, 2: 71-77.

Thomas, W.H., Vernet, M. and Gibson, C.H. (1995). Effects of small-scale turbulence on photosynthesis, pigmentation, cell-division, and cell-size in the marine dinoflagellate *Gonyaulax polyedra* (Dinophyceae). *Journal of Phycology*, 31(1): 50-59.

Tinton, E. (1997). An analysis of the physical structure and residual currents of Southampton Water over tidal cycles. *MSc Thesis. University of Southampton*.

Townsend, D. (1992). Spring phytoplankton blooms in the absence of vertical water column stratification. *Nature*, 360(6399): 59-62.

Tyler and Heinbokel (1985). Cycles of red water and encystment of *Gymnodinium pseudopalustre* in the Chesapeake Bay: Effects of hydrography and grazing. In Toxic Dinoflagellates (3rd Conference). Ed. Anderson, White and Baden. Elsevier publications. Pp 213-219.

Villareal, T.A. (1988). Positive buoyancy in the oceanic diatom *Rhizosolenia debyana*. *Deep-Sea Research*, 35(6): 1037-1045.

Wall, D. (1975). Taxonomy and cysts of red tide dinoflagellates. In: V.R. LoCicero (Editor), *Toxic dinoflagellate blooms*. Proceedings of the International Conference (1st). Massachusetts Science and Technology Foundation., pp. 249-256.

Watras, C.J., Chisholm, S.W. and Anderson, D.M. (1982). Regulation of growth in an estuarine clone of *Gonyaulax tamarensis* Lebour. Salinity-dependent temperature responses. *Journal of Experimental Marine Biology and Ecology*, 62: 25-37.

Watson, A.J., Upstill-Goddard R. C., Liss, P.S. (1991). Air-Sea gas exchange in rough and stormy seas measured by a dual-tracer technique. *Nature* 349: 145-147.

Webber, N. (1980). Hydrography and Water circulation in the Solent. In Burton J D (ed.), *The Solent Estuarine System: An Assessment of Present Knowledge*. NERC Publication Series C.

Westwood I. J. and Webber N.B. (1977). A tidal exchange experiment at the entrance to Southampton Water. *Proceedings of the 17th Congress, International Association for Hydrodynamic Research* (Baden-Baden), 3; 85-92.

White, A.W. (1976). Growth Inhibition Caused by Turbulence in the Toxic Marine Dinoflagellate *Gonyaulax excavata*. *Journal of the Fisheries Research Board, Canada*, 33: 2298-2602.

Winter, D., Banse, K. and Anderson, G. (1975). The dynamics of phytoplankton blooms in Puget Sound, a fjord in the Northwestern United States. *Marine Biology*, 29: 139-176.

Wright, P.N., Hydes, D.J., Lauria, M.L., Sharples, J. and Purdie, D.A. (1997). Results from data buoy measurements of processes related to phytoplankton production in a temperate latitude estuary with high nutrient inputs: Southampton Water, U.K. *German Journal of Hydrography*, 49 (2/3) 203-211.

Yin, K.D., Harrison, P.J., Goldblatt, R.H. and Beamish, R.J. (1996). Spring Bloom in the Central Strait of Georgia - Interactions of River Discharge, Winds and Grazing. *Marine Ecology Progress Series*, 138 (1-3): 255-263.

Zinger, I. (1989). Zooplankton community structure in Southampton Water. *PhD Thesis, University of Southampton*.

APPENDIX I

LABORATORY STUDIES

DIRECT TURBULENCE EFFECTS ON PHYTOPLANKTON

ESTABLISHMENT OF MONOCULTURES

Various phytoplankton species were grown in batch cultures in the laboratory, using 200ml volumes, each species in duplicate (see Appendix II, Table A2 for a list of all species). The growth media used was a modified Keller's recipe (Appendix II, Table A1). All containers and tubing used for cultures and media stocks were carefully selected to avoid a potential leaching of toxic compounds. Borosilicate glass and polycarbonate conical flasks were used, with cotton bungs covered with cheesecloth. Sea water was usually collected from Calshot, in Southampton Water and filtered through Whatman GF/F filters. 200ml filtered sea water (FSW) was added to each glass conical flask and sterilised in a Rodwell autoclave. The sterilisation period was 30 minutes at 120°C under a pressure of 2.2 bar. Subculturing occurred every two weeks for all species except *Prorocentrum micans*, which was subcultured every month due to its slow growth rate.

From this culture collection various species were chosen to conduct experiments involving the effect of turbulence on growth rate, comparing not only the effect of turbulent intensity within a monoculture but also between species. In each case turbulence was created by bubbling air into the batch culture.

TURBULENT GROWTH RATE EXPERIMENTS

SMALL BATCH CULTURE TRIALS: *AMPHIDINIUM CARTERAE*

Growth rates were measured for the dinoflagellate *Amphidinium carterae* grown in varying turbulent conditions (Figure A1). 3 x 1litre Duran bottles were autoclaved with 800ml FSW and enriched with full Keller's nutrient recipe (no NH₄Cl). Two bottles simulated a turbulent regime in which air was pumped into the cultures at varying flow rates (i.e. low turbulence, 50-100 cc min⁻¹; high turbulence, 200-300 cc min⁻¹) quantified using a flow gauge. The third culture represented a control with no bubbling, although mixing did occur before each sampling period to ensure a representative sample. A constant temperature (15°C) was maintained with the use of a water bath, and positioned on a light bank providing irradiance of ~100μE m⁻² s⁻¹, on a 16:8hr Light:Dark cycle. Cultures were covered with aluminium foil allowing only the base to be subjected to the light source, providing a constant intensity of light throughout the vessel. Cultures were inoculated to give an initial cell count of 2.6 x 10³ cells l⁻¹. Cell were counted daily using an inverted microscope. Growth rates were calculated

using equation (9) in chapter two. Cell counts continued until the end of the exponential growth phase. Cell density in the culture was measured daily until the stationary phase. Cell counts were conducted daily until the stationary phase.

Daily Irradiance *Temperature* *Control Bottle - no turbulence*

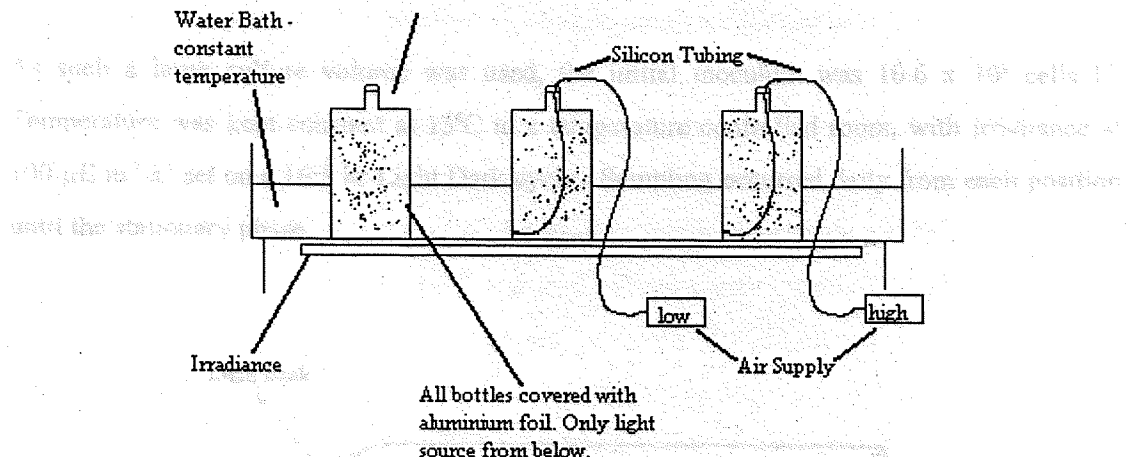


Figure A2. Schematic diagram of the experimental set up for the small batch culture studies.

Small Batch Culture Trials: *Rhizosolenia delicatula*

Growth rates were measured for the chain-forming diatom *Rhizosolenia delicatula* grown under varying turbulent conditions (Figure A3). The experimental design was based on that used for *A. carterae*, with some modifications. Na_2SiO_3 (10 μM) was added along with the usual Keller's nutrients and 5.0 \times 10³ cells l⁻¹ was the initial inoculum. As well as cell numbers, the actual number of cells per chain were counted. Growth rates were calculated using equation (9). Cell and chain counts were conducted daily until the stationary phase.

Large Batch Culture Trials: *Amphidinium carterae*

Using a square tank (internal dimensions 282 x 268 x 339mm) growth rates of *A. carterae* were determined in a 15 litre culture. The structure of the tank prevented sterilisation through the autoclave, so prior to use it was cleaned with a disinfecting solution (Presept tablets ~2.5g sodium dichloroisocyanurate in 2 litres) and rinsed. Autoclaved FSW enriched with Keller's nutrient recipe provided the growth media. This was allowed to equilibrate in the constant temperature room before inoculation. A novel sampling technique (Figure A4) was implemented to prevent any movement (stirring) within the tank, to determine the optimum growth rate achievable in a highly stable environment. Three silicon rubber, narrow bore

tubes were set in a silicon bung and placed through a side wall sampling port being held at different vertical heights within the chamber. Samples were extracted daily to determine the homogeneity within the culture. Before inoculation, a siphoning system was established, so future sampling aliquots flowed freely through the tubes. Sampling in this way prevented daily intrusion into the tank which would create intermittent turbulence within the culture.

As such a large culture volume was used, the initial inoculum was 10.6×10^3 cells l^{-1} . Temperature was kept constant at $15^{\circ}C$ in a temperature controlled room, with irradiance at $100 \mu E m^{-2} s^{-1}$ set on a 16:8 hr Light:Dark cycle. Sampling occurred daily from each position until the stationary phase.

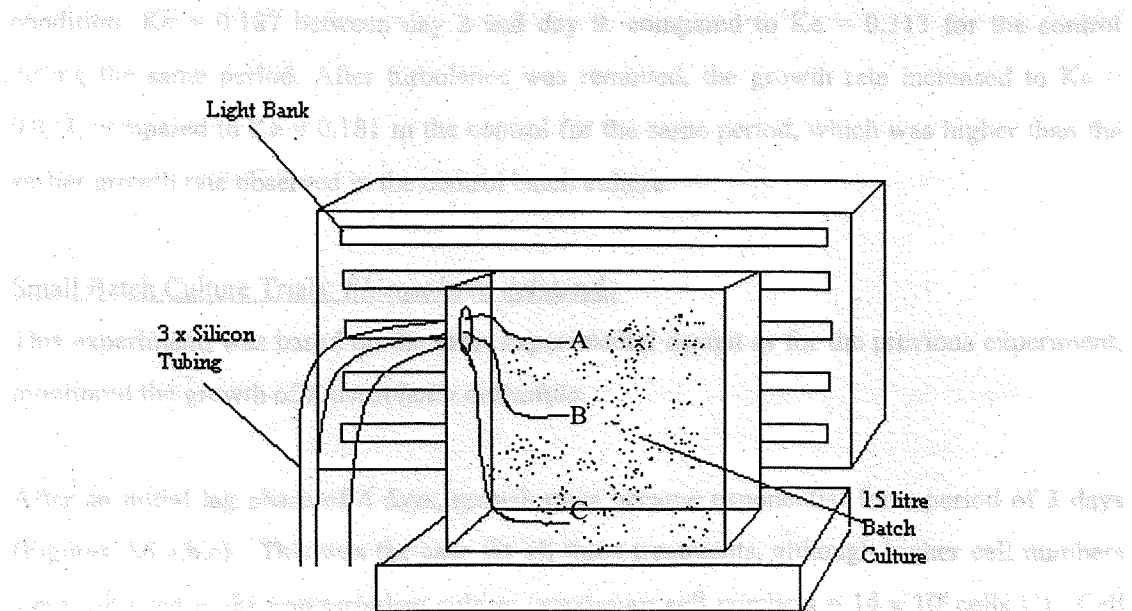


Figure A4. Large culture vessel, with novel sampling port to prevent stirring of medium.

Large Batch Culture Trials: *Rhizosolenia delicatula*

Using the experimental set up as for the previous experiment, growth rates for *Rhizosolenia delicatula* were determined. Two initial trials using *R. delicatula* with this experimental design proved unsuccessful, (using Keller's nutrient recipe with the extra addition of silica). The initial inoculum was 5.3×10^3 cells l^{-1} . Temperature was constant at $15^{\circ}C$, with irradiance at $100 \mu E m^{-2} s^{-1}$ set on a 16:8 hr Light:Dark cycle. Sampling occurred daily from each position until the stationary phase. Chain length was also determined.

LABORATORY RESULTS

Small Batch Culture Trials: *Amphidinium carterae*

Cell counts (Figure A5a) and growth rates (Figure A5b) are shown for *Amphidinium carterae* grown under different turbulent conditions. After an initial lag phase, cell numbers increased. Maximum cell numbers were observed in the 'non-turbulent' culture. By day 12, the control cell numbers had reached 60×10^6 cells l^{-1} , in comparison to the low turbulent vessel 11×10^6 cells l^{-1} and the high turbulent vessel $>5.0 \times 10^6$ cells l^{-1} . Cell numbers in the high turbulent vessel, began to decrease after day 9. On day 12, turbulence was removed from the two vessels. Both cultures showed a marked increase in cell numbers after lag period ~ 1 day. Growth rates (calculated using equation 9) indicated two different rates for the high turbulent condition. $Ke = 0.187$ between day 2 and day 9, compared to $Ke = 0.313$ for the control during the same period. After turbulence was removed, the growth rate increased to $Ke = 0.473$, compared to $Ke = 0.181$ in the control for the same period, which was higher than the earlier growth rate observed in the control batch culture.

Small Batch Culture Trials: *Rhizosolenia delicatula*

This experiment, was based on the same experimental design as for the previous experiment, monitored the growth of *Rhizosolenia delicatula*.

After an initial lag phase of 4 days, growth rates became exponential for a period of 3 days (Figures A6 a,b,c). This was the case for all three treatments, although higher cell numbers were achieved in the non-turbulent culture (maximum cell numbers = 14×10^6 cells l^{-1}). Cell numbers refer to actual cells and not the number of chains per litre. The maximum number of chains was reached on day 11 of the non-turbulent culture, 3 days after the maximum number of cells was reached. The number of cells forming each chain is shown in Figure A6c. In the non-turbulent condition, the number of cells per chain was stable, ranging between 1-4. The high turbulent condition had the maximum number of cells per chain ranging from 1-8, these maximum numbers were reached on day 7, coinciding with the end of the exponential phase.

Large Batch Culture Trials: *Amphidinium carterae*

The dinoflagellate, *Amphidinium carterae* was monitored in a stable environment (Figure A7a), where the vertical variation with depth was also examined. After an initial lag phase, exponential growth continued for 12 days. Little vertical variation was seen between the surface, middle and bottom samples. After exponential phase, many more cells were counted in the bottom samples. A very dense culture occurred, which may have caused an irradiance

gradient within the chamber, as well as self-shading of the organisms. Maximum cell concentrations reached 700×10^6 cells l⁻¹ on day 29. Mean cell numbers, depth averaged, are shown in Figure A7b.

Large Batch Culture Trials: *Rhizosolenia delicatula*

The growth rate and vertical distribution of *Rhizosolenia delicatula* were monitored (Figure A7c). A large vertical gradient was seen in this tank, with maximum cells found at the bottom of the tank. After 3 days, this vertical gradient was visible where a bottom 'mat' of algae formed. Sample A refers to surface, B- middle and C-bottom. Due to the high patchiness within this chamber, it was difficult to determine whether *in situ* growth was occurring, or if cells were simply sinking out of the water column. Surface samples suggested that some cells remained in suspension, with cell counts showing a pattern in vertical distribution, i.e. cell numbers increasing every other day. Chains observed at the surface had a longer chain length (mean = 6.5; n=8) than those at the bottom of the chamber (Mean=4.8; n=9).

DISCUSSION

In recent years, laboratory experiments focusing on a direct effect of turbulence on phytoplankton have increased in number. Direct effects of turbulence prove difficult to distinguish from the indirect effects in nature which cause fluctuating irradiance, temperature and nutrient environments. These experiments were designed to control these variables and focus solely on the biological-physical interaction. The majority of laboratory experiments have centred on predator-prey contact rates in an often unquantified turbulent environment. Few experiments have led to an actual turbulent dissipation rate comparable to the natural environment, and even less have used phytoplankton.

Apart from the problems of quantification, turbulence generation is also questionable. Investigators have used many different methods, each creating a different 'type' of turbulence and in some cases zero turbulence, i.e. homogenous isotropic turbulence - grid generated; heterogeneous vorticity - rotary shakers; laminar shear - Couette device. The method of grid-generated turbulence is the most 'understood' form of turbulence.

AERATION EXPERIMENTS

Although a 'turbulent' environment was created, it was unquantifiable. This is one of the major problems in conducting turbulence experiments. As turbulence by definition is random

and unpredictable, simple models to calculate a dissipation rate do not exist, therefore measurements often remain a relative unit incomparable to real values.

Experiment #1

The method of turbulence generation used was aeration. This not only mixes the culture, but also increases the level of dissolved inorganic carbon to the air-equilibrium value, thus altering the chemical nature. Other physical methods of turbulence generation do not affect the chemical structure, for example, grid turbulence. The results show, however, that 'turbulence' does inhibit the growth rate for *A. carterae*, and that with the removal of this turbulence, growth rate increases to a rate higher than that observed in the control culture (Figure A5a). This growth inhibition has been linked to a cell blockage during cell division (Berdalet 1992) which prevents the final stages of chromosome separation, after the duplication of DNA. In each case, light and temperature were held constant, thus removing the main indirect effect of turbulence in nature - the changing light climate.

Experiment #2

The growth rates for a diatom remained very similar (Figure A6a), which was expected due to the timing and physical conditions usually surrounding a diatom bloom (i.e. high amount of vertical mixing). However, differences were observed in the number of cells per chain for each turbulent condition. Organisms in the high turbulence condition exhibit longer chains (1-8) than those in the control (1-4). This may be advantageous in allowing a greater shear effect along the chains, thus removing any depleted microzones and also may be beneficial in buoyancy terms. Villareal (1988) suggests that diatom cells must be large to float, as cell density increases exponentially as size decreases, and has observed *Rhizosolenia debyana* ascending and accumulating in the surface waters in the Sargasso Sea. In Southampton Water, maximum cell numbers of *R. delicatula* occur in the bottom layers, suggesting a positive advantage for not 'floating'. However, those chains that were in the upper layers had more cells per chain than those in the lower depths.

Experiment #3

The larger scale cultures using square tanks show *A. carterae* to proliferate under still conditions with no mixing at all. Maximum cell numbers reached 7×10^8 cells l^{-1} , with growth continuing for up to 30 days. As this is a motile organism, distribution within the chamber was homogenous, although once stationary phase began, cell numbers increased on the bottom, possibly due to increasing senescence. In nature, dinoflagellate blooms have always

been linked to periods of calm weather, often during a time of strong stratification, nutrient depletion and long daylight hours. It was postulated that, as these organisms are motile, they move down the water column to the nutricline, where nutrient stocks are replenished and then return to the euphotic zone, with the timing of migrations governed by a positive phototaxis. The 'perfectly' still environment created by this experiment proved ideal conditions for cell proliferation, with cell numbers reaching a maximum seven times higher than Experiment #1.

Experiment #4

The vertical distribution of *R. delicatula* shows a distinct increase in the bottom layers where 'mats' formed. Due to the high patchiness within the culture, it was difficult to determine whether growth was occurring, or if cells were simply falling out of the water column. However, cells that were found in the surface samples had a longer chain length than those on the bottom showing agreement to Villareal's (1988) findings on size and buoyancy, although results did not show the level of positive buoyancy as found for *R. debyana*. In nature, diatom blooms are often linked to a period of early stratification, when mixing occurs and nutrient levels are high. As the water becomes calm, diatoms are succeeded by more motile species which then dominate. This experiment suggests that *R. delicatula* requires some mixing to proliferate, although other smaller cultures flourish in the absence of mixing (200 ml cultures). Perhaps the initial inoculum was too small (~200 ml) for the large volume used (15 litres).

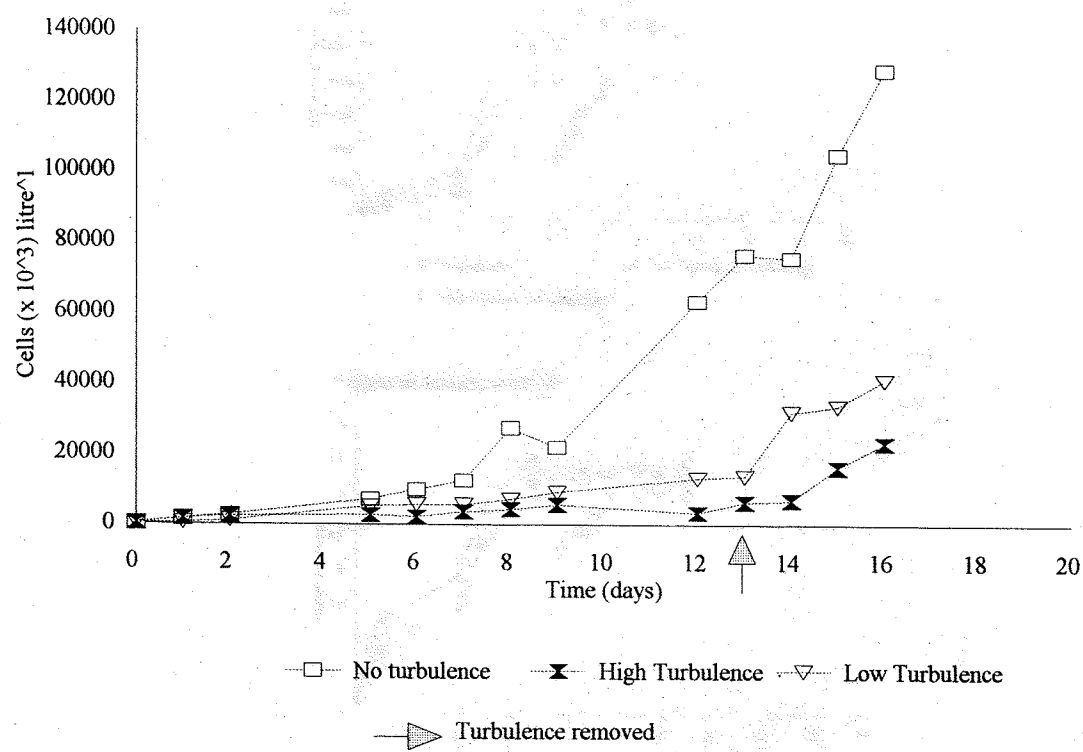
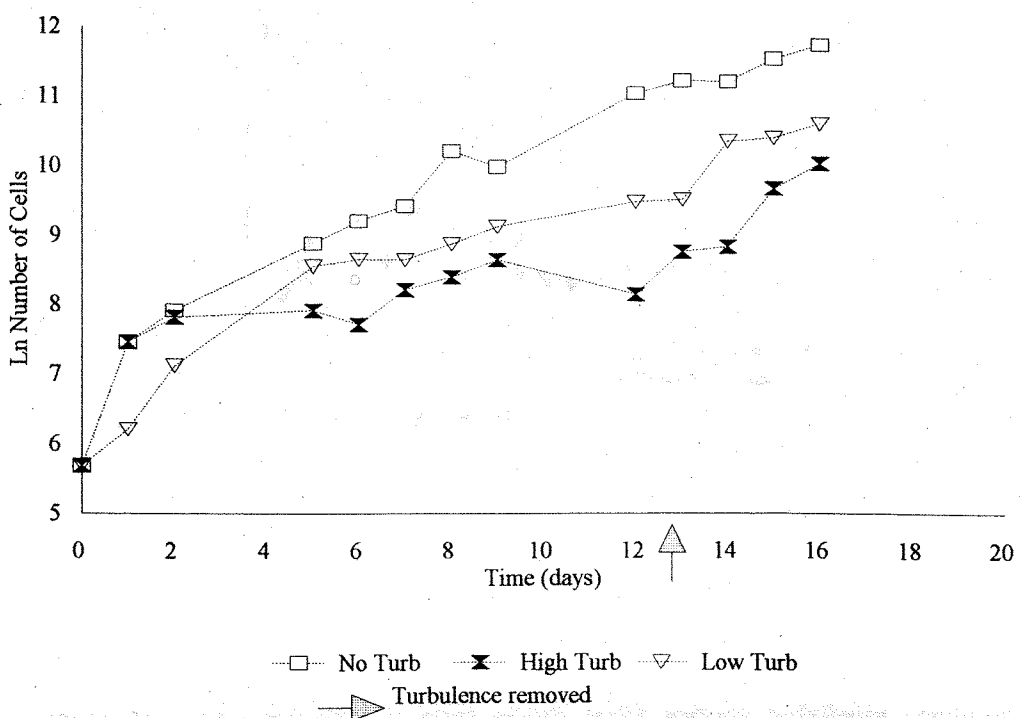
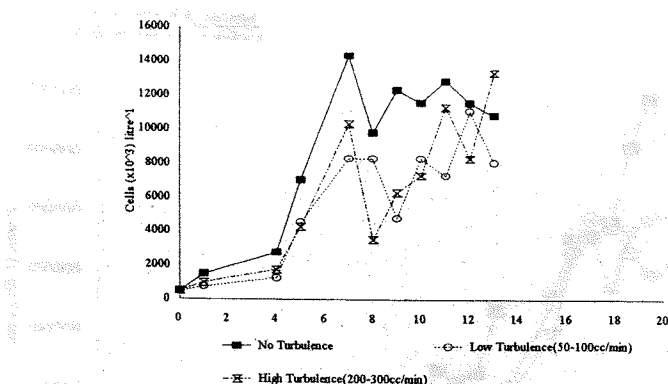
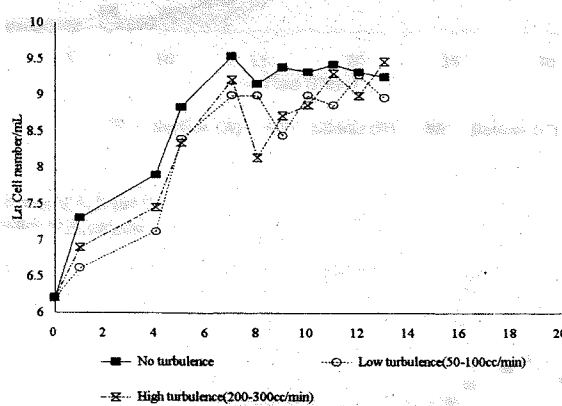
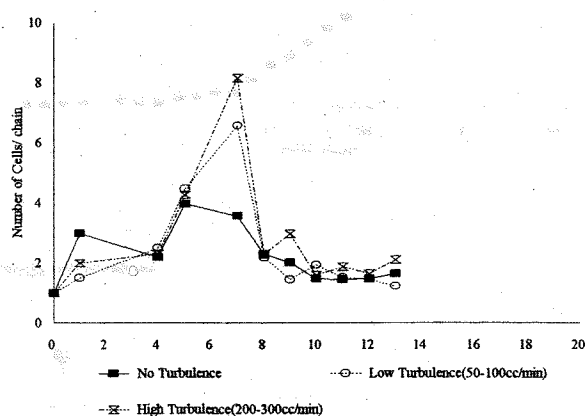
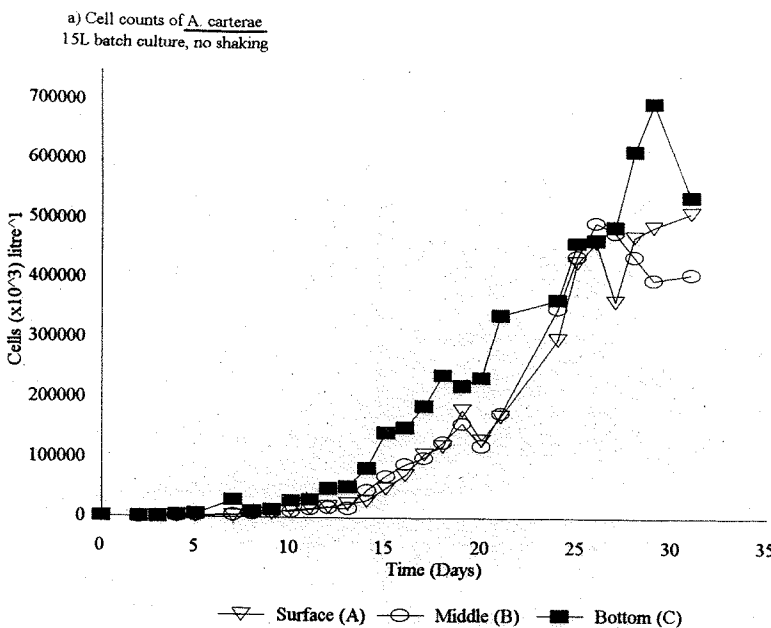
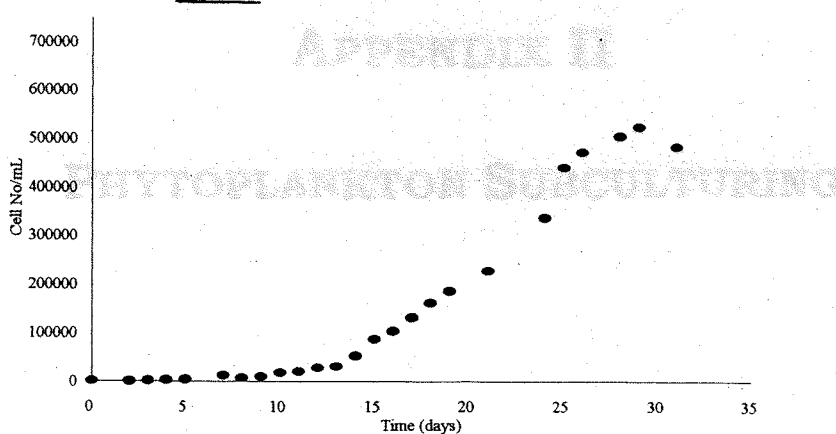
a) Amphidinium carterae cell numbersb) Amphidinium carterae growth rate

Figure A1. *Amphidinium carterae* grown under varying turbulence. a) cell number (per litre); b) growth rate.

a) *Rhizosolenia delicatula* cell numbers.b) *Rhizosolenia delicatula* growth ratec) *Rhizosolenia delicatula* No. cells per chainFigure A3. *Rhizosolenia delicatula* grown under varying turbulence conditions. a) cell numbers (per litre); b) growth rate; and c) number of cells per chain.



b) Mean cell counts of A, B and C
15L batch culture of A. carterae



c) R. delicatula cell numbers

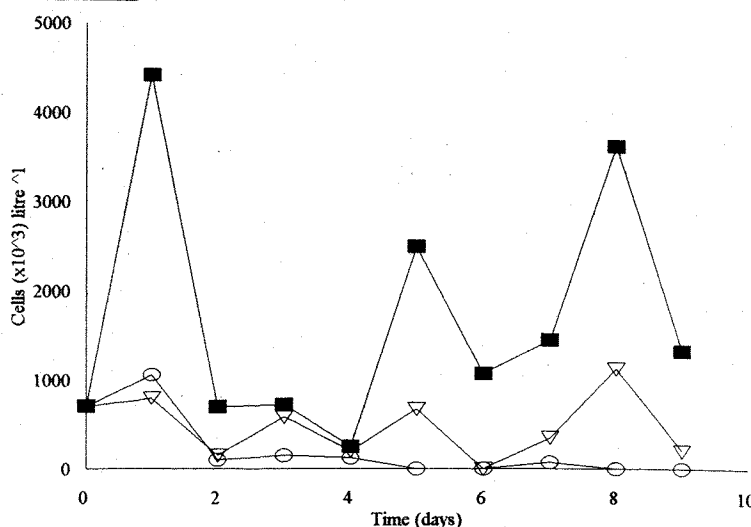


Figure A5. a) *A. carterae* cell counts; b) mean cell counts *A. carterae*; and c) *R. delicatula* cell counts.

APPENDIX II

PHYTOPLANKTON SUBCULTURING

TABLE A1.
KELLER'S MEDIA RECIPE

SALT	WT. REQ. (g)	PRIMARY STOCK VOLUME	VOL. PRIM. STOCK	WT. REQ. (g)	WORKING STOCK VOLUME	VOL. WORK STOCK IN 1LSEA WATER	FINAL CONC.
NaNO ₃	-	-	-	7.5	100ml	1ml	0.88mM
Na ₂ Gly. PO ₄	-	-	-	0.315	100ml	1ml	9.7μM
Vitamins							
Thiamin HCL (B1)	-	-	-	0.01	-	-	0.29μM
Biotin (H)	0.01	100ml	1ml	-	100ml	1ml	2.05nM
B12	0.01	-	-	-	-	-	0.35nM
Tris	-	-	-	12.1	100ml	1ml	0.99mM
NH ₄ Cl	-	-	-	0.054	100ml	1ml	-
H ₂ SeO ₃	0.013	100ml	1ml	-	100ml	1ml	0.01μM
Trace Metals							
MnCl ₂ . 4H ₂ O	1.8	-	-	-	-	-	0.91μM
ZnSO ₄ . 7H ₂ O	0.23	-	-	-	-	-	0.08μM
CoCl ₂ . 7H ₂ O	0.10	100ml	1ml	-	-	-	0.04μM
NaMoO ₄ . 2H ₂ O	0.07	-	-	-	100ml	1ml	0.03μM
CuSO ₄ . 7H ₂ O	0.025	-	-	-	-	-	-
FeNa EDTA				0.429			12μM

TABLE A2.
CULTURE COLLECTION

DATE RECEIVED	SOURCE	ORGANISM	CULTURE CONDITIONS
1991	Southampton Water	<i>Rhizosolenia delicatula</i>	Full K*, ESW*
		<i>Phaeodactylum sp</i>	Full K, ESW
	PML*	<i>Phaeocystis pouchettii</i>	Full K, ESW
	DML*	<i>Synechoccus</i>	Full K, ESW
25.04.95	DML	<i>Isochrysis</i>	Full K, ESW, -Tris
	DML	CCAP 913/3	Full K, ESW, - Tris
	DML	92E	Full K, ESW
	DML	DWN	Full K, ESW
	DML	Lo Calc. <i>Emiliana huxleyi</i>	Full K, ESW, -Tris
	DML	<i>Coccolithus pelagicus</i>	Full K, ESW, -Tris
October 1997	DML	<i>Skeletonema costatum</i>	Full K; ESW
	DML	<i>Amphidinium carterae</i>	Full K, ESW
25.04.95	DML	<i>Prorocentrum micans</i> CCAP 1136/8	Full K, ESW

*ESW = Enriched (filtered) Sea Water

*Full K = Keller's Nutrients (Stein 1975)

*DML = Dunstaffnage Marine Laboratory, Culture Collection

*PML = Plymouth Marine Laboratory

DISCUSSION

The instrument used is very sensitive at low concentrations, but the upper limit of the response is "finite". On some surfaces, differences were greater than the upper limit, and points were taken to be outside the linear range of values containing finite. This led to some variation in the values obtained between SPM and other methods. The results of these points are shown in Table A-1. However, there was no obvious difference in the calibration factor for values outside the linear range.

Spring and summer months were chosen to give a broad range of measured densities. Party lines, which often contain concentrations above 20 mg/l, were also used because other data from specific sites exceeded the upper range.

APPENDIX III

Instrument

INSTRUMENT CALIBRATION

The Appendix contains a brief description of the instrument used. The instrument calibration was performed in the Appendix. Individual points were determined independently after each reading. This will reduce the systematic error due to fluctuations in the object being measured. The use of this instrument minimizes the errors due to a non-linear relationship between SPM and a true biological index (Appendix).

INSTRUMENT CALIBRATION

TABLE A3

TRANSMISSOMETER

The transmissometer used is very sensitive at low turbidities, but the upper limit of linear response is $\sim 25 \text{ mg l}^{-1}$. On some surveys, SPM levels were greater than the upper linear limit, and points were seen to lie outside the main curve at values exceeding 25 mg l^{-1} . This led to some variation in the linear relationship between SPM and Beam attenuation. The regression coefficients are shown in Table A3. However, there was no obvious difference in the calibration curves for water samples of different depths.

Spring and summer values were chosen to give a broad range of estuarine conditions. Early May, where SPM concentrations were below 25 mg l^{-1} , late May and summer where SPM concentrations exceeded the linear range.

FLUOROMETER

The Aquatracka III used for all the Southampton Water surveys, showed a good linear regression when the chlorophyll *a* pigment concentration was greater than 5 mg m^{-3} . Three main calibrations are presented in this Appendix, however, calibrations were completed routinely after each survey. Table A4 shows the regression coefficients for the Fluorometer vs. chlorophyll *a* concentrations during a time of little phytoplankton abundance (i.e. early May), a diatomous bloom (late May) and a dinoflagellate bloom (August).

TABLE A3
TRANSMISSOMETER CALIBRATION

Time	R ²	Constant	X coefficient
Early May	0.544	-1.828	2.457
Late May	0.857	-0.188	2.871
August	0.853	-10.257	4.688

APPENDIX III
NORTH SEA PHYTOPLANKTON SOURCE

APPENDIX IV

NORTH SEA PHYTOPLANKTON SPECIES

TABLE A IV
PHYTOPLANKTON IDENTIFIED DURING THE NORTH SEA SURVEY
(OCTOBER 1996). NUMBER OF CELLS PER LITRE.

Date	Time	Depth (m)	<i>Asterionella</i>	<i>Coscinodiscus</i>	<i>Diatom ladder</i>	<i>Biddulphia</i>	<i>Chaetoceros</i>	<i>Ditylum</i>	<i>Rhizosolenia</i>	<i>Gyrosigma</i>	<i>Navicula</i>	<i>Tabellaria</i>	<i>Thalassiosira</i>	<i>Phaeocystis</i>	<i>Gonyaulax</i>	<i>Procentrum</i>	<i>Proterodinium</i>	<i>Ceratium</i>	<i>Cochliodinium</i>
25.10.96	323	5	0	600	32400	200	0	0	0	0	0	0	0	0	0	600	0	0	0
25.10.96	42	5	0	0	5800	0	400	0	0	0	0	0	0	0	0	400	200	200	0
25.10.96	525	5	0	400	13800	0	400	0	0	0	0	0	0	0	200	0	200	0	0
25.10.96	525	9	0	0	15400	800	1000	0	0	0	0	0	0	0	0	0	400	0	0
25.10.96	525	16	0	800	11600	1200	1800	0	0	0	0	0	0	0	0	0	200	200	0
25.10.96	637	15	0	0	3600	200	400	0	0	0	0	0	0	0	0	0	0	200	200
25.10.96	637	10	0	200	6200	400	0	0	0	0	0	0	0	0	0	0	0	200	0
25.10.96	637	5	0	200	6200	0	0	0	0	0	0	0	0	0	0	0	0	200	0
25.10.96	738	15	0	200	6200	200	200	0	0	0	0	0	0	0	0	0	0	200	200
25.10.96	738	8	3000	200	4200	200	0	0	0	0	0	0	0	0	0	0	600	0	0
25.10.96	738	5	0	200	6200	0	0	0	0	0	0	0	0	0	0	0	200	200	0
25.10.96	83	15	0	200	1400	3200	0	0	0	0	0	0	0	0	0	0	400	200	400
25.10.96	83	9	0	200	11800	0	800	0	0	0	0	0	0	0	0	0	0	200	0
25.10.96	83	5	0	400	15200	0	0	0	0	0	0	0	0	0	0	0	400	0	600
25.10.96	93	14	0	600	12200	400	3600	200	0	0	0	0	0	0	0	0	200	200	200
25.10.96	93	9	0	0	8600	1200	0	0	0	0	0	0	0	0	0	0	200	0	0
25.10.96	93	5	0	200	7600	0	1000	0	0	0	0	0	0	0	0	0	0	200	0
25.10.96	1028	14	0	0	31200	0	1000	0	0	0	0	0	0	0	0	0	200	0	200
25.10.96	1028	9	0	800	7600	1800	0	0	200	0	0	800	0	0	0	0	0	0	200
25.10.96	1028	5	0	0	0	0	800	0	0	3400	0	0	0	0	0	0	200	0	0
25.10.96	113	15	0	1000	5000	1000	200	400	0	0	0	0	0	0	0	0	200	200	0
25.10.96	113	9	0	400	12400	2200	1400	0	2400	0	0	0	0	0	0	600	0	0	400
25.10.96	113	5	0	600	6200	1800	0	0	0	0	0	0	0	0	0	0	0	200	400
25.10.96	1228	15	0	600	3800	1800	0	0	3000	0	0	0	0	0	0	0	200	0	200
25.10.96	1228	10	0	1000	9600	2400	0	0	0	0	0	0	0	0	0	0	200	400	0
25.10.96	1228	6	0	400	12200	1000	0	200	3600	0	200	0	0	0	0	400	200	0	200
25.10.96	1325	15	0	400	4200	600	0	0	0	0	0	0	0	0	0	200	0	0	200
25.10.96	1325	9	1800	400	5200		1200	0	0	0	0	0	0	0	0	0	400	0	0
25.10.96	1325	5	0	400	6600	2800	0	0	0	0	0	400	0	0	0	0	200	0	0
25.10.96	1425	14	1600	400	13400	800	0	0	0	0	0	6600	0	0	0	0	200	200	0
25.10.96	1425	10	0	200	7000	1400	0	200	1000	0	0	0	0	0	0	0	200	200	400
25.10.96	1425	5	0	200	8800		0	0	0	0	0	0	0	0	0	0	200	200	200
25.10.96	1527	4	0	400	16000	800	0	0	0	0	0	0	0	0	0	0	200	200	0
25.10.96	1527	9	0	400	7200	1000	0	0	0	0	0	0	0	0	0	0	600	200	0
25.10.96	1527	5	1600		8800	200	400	0	0	0	0	0	0	0	0	0	400	0	200
25.10.96	1622	14	0	200	18400	800	800	200	0	0	0	0	0	0	0	0	0	200	0
25.10.96	1622	9	6600	200	14600	600	1800	0	0	0	0	0	0	0	0	0	0	0	0
25.10.96	1622	5	0	600	9800	200	0	0	0	0	0	200	0	0	0	0	0	0	0
25.10.96	1728	16	0	200	13200	0	0	0	0	0	0	0	0	0	0	0	200	0	400
25.10.96	1728	9	0	400	28800	1400	0	0	0	0	0	0	0	0	0	0	400	200	0
25.10.96	1728	5	0	200	4600	1000	0	0	0	0	0	200	0	0	0	0	600	0	0